Functional Characterisation of Recombinant $GABA_A$ Receptors

A Thesis submitted for the Degree of Doctor of Philosophy

in the University of London, Faculty of Medicine.

by

Belinda Janine Krishek, B.Pharm., MRPharmS.

Department of Pharmacology
The School of Pharmacy,
29-39 Brunswick Square,
London WC1N 1AX

September 1994

ProQuest Number: U528172

All rights reserved

INFORMATION TO ALL USERS
The quality of this reproduction is dependent upon the quality of the copy submitted.

In the unlikely event that the author did not send a complete manuscript
and there are missing pages, these will be noted. Also, if material had to be removed,
a note will indicate the deletion.

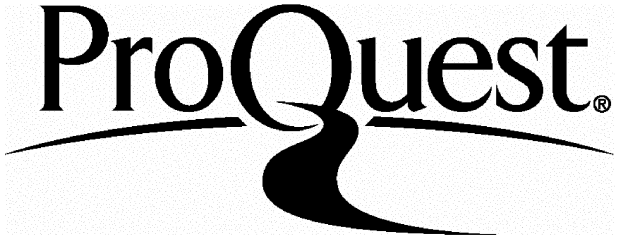

ProQuest U528172

Published by ProQuest LLC(2016). Copyright of the Dissertation is held by the Author.

All rights reserved.
This work is protected against unauthorized copying under Title 17, United States Code.
Microform Edition © ProQuest LLC.

ProQuest LLC
789 East Eisenhower Parkway
P.O. Box 1346
Ann Arbor, MI 48106-1346

ABSTRACT

γ-Aminobutyric acid$_A$ ($GABA_A$) receptors are ligand-gated ion channels that mediate inhibitory synaptic transmission in the central nervous system. Cloning studies have revealed that $GABA_A$ receptors are hetero-oligomeric proteins composed of several distinct subunit proteins (α, β, γ, and δ). The aim of this study was to examine the functional role(s) of some individual subunits within the $GABA_A$ receptor complex using the *Xenopus laevis* oocyte expression system. The physiological and pharmacological properties of expressed $GABA_A$ receptors were characterised using two-microelectrode current and voltage clamp recording techniques.

The functional role(s) of some of the individual subunits were studied by applying a selection of agonists, antagonists and potentiators to $GABA_A$ receptors of differing subunit compositions. Inhibitions of GABA responses by picrotoxin and bicuculline, or enhancements by pentobarbitone and pregnanolone were independent of the subunit composition. In contrast, the modulation of the GABA response by benzodiazepines was dependent on the presence of a γ2 subunit, whereas for zinc-induced inhibition the presence of γ2 and/or δ subunits were influential. The β1 subunit was important in the expression and formation of $GABA_A$ receptors. To further assess the functional properties of the β1 subunit, homomeric murine and bovine β1 receptors were expressed and compared.

The effect of changing the extracellular pH on ion channel function was studied as an alternative method of effecting modulation on $GABA_A$ receptors comprising various subunit compositions. pH also affected the inhibition of the GABA response by zinc.

The role of protein kinase C (PKC) phosphorylation in modulating $GABA_A$ receptor function was ascertained using wild-type receptors of different subunit compositions and receptors incorporating selected site-directed mutants of serine residues involved in known consensus sequences for PKC in the large intracellular domains of the β1 and γ2 subunits.

This study provides evidence of distinct functional role(s) of individual subunits within the $GABA_A$ receptor and indicates for the very first time a novel pharmacology for δ subunit containing receptors. Furthermore, two novel sites on the $GABA_A$ receptor have been uncovered which can modulate receptor function. These sites are sensitive to H^+ or PKC-induced phosphorylation and may be significant in affecting the pharmacological and physiological profile of the $GABA_A$ receptor.

FUNCTIONAL CHARACTERISATION OF RECOMBINANT $GABA_A$ RECEPTORS

LIST OF FIGURES

LIST OF TABLES

CHAPTER ONE

GENERAL INTRODUCTION

GENERAL INTRODUCTION

γ-Aminobutyric acid (GABA) is the major inhibitory neurotransmitter in the vertebrate brain (Bormann, 1988). GABA gates multisubunit channels, termed $GABA_A$ receptors, which are physiologically permeable to chloride and less so to bicarbonate anions (Bormann *et al.*, 1987; Kaila and Voipio, 1987) and inhibited by the competitive GABA antagonist bicuculline (Bormann, 1988). GABA can also activate $GABA_B$ receptors, which are coupled to calcium or potassium channels via second messenger systems and/or a GTP-binding protein (G-protein) and are not inhibited by bicuculline (Bowery, 1993). Recent observations have revealed that in the central visual pathway and the retina responses to GABA were observed that were both insensitive to bicuculline and the $GABA_B$ agonist, baclofen, and permeable to chloride ions (Nistri and Sivilotti, 1985; Polenzani *et al.*, 1991; Sivilotti and Nistri, 1991). Based on the pharmacological criteria noted above, such responses would not be mediated by $GABA_A$ or $GABA_B$ receptors. Since these receptors are sensitive to cis-4-aminocrotonic acid they have been defined as $GABA_C$ (Johnston, 1986). Interestingly, a cloned cDNA receptor subunit, GABA ρ1, whose mRNA is highly expressed in retina was observed to express such receptors after injection in *Xenopus laevis* oocytes (Cutting *et al.*, 1991).

The structure of the $GABA_A$ receptor is of particular interest because it contains a variety of binding sites for many drugs of both clinical and therapeutic relevance which interact allosterically with the GABA agonist site or the receptor channel to modulate receptor function. These drugs include anxiolytic (benzodiazepines), anti-convulsant (barbiturates), anxiogenic (β-carbolines) and convulsant (picrotoxin) agents (Olsen and Venter, 1986; Sivilotti and Nistri, 1991). Traditionally, using pharmacological methods of investigation, receptor subtypes have been defined by their interactions with drugs. Despite the many types of drugs that interact with $GABA_A$ receptors, pharmacological evidence for the subclassification of $GABA_A$ receptors into

multiple subtypes is relatively limited.

1.1 PHARMACOLOGICAL EVIDENCE FOR SUBTYPES

At present, no direct $GABA_A$ receptor agonist or antagonist is known that is able to distinguish between the possible $GABA_A$ receptor subtypes. The benzodiazepines have provided the best basis for division of $GABA_A$ receptors into subtypes. Competition for binding of radioactive benzodiazepines by the non-benzodiazepine, CL 218,872, a triazolopyridazine, appears biphasic in many brain regions (Squires *et al.*, 1979). The sites with higher affinity for CL 218,872, called type I, appear to predominate overall with very high binding in the cerebellum. The sites with a low affinity for CL 218,872, called type II receptors, appear to occur in only a few areas, including the hippocampus, striatum and spinal cord. The differential binding properties of β-carbolines (inverse agonists, which negatively modulate receptor function) in various brain regions have also been used to distinguish two benzodiazepine subtypes, BZ1 and BZ2 (Braestrup and Nielsen, 1981). Interestingly, the ability of GABA to potentiate benzodiazepine binding in different regions of the central nervous system (CNS; Leeb-Lundberg and Olsen, 1983) did not correlate well with either classification indicating that probably more than two subtypes of the $GABA_A$ receptor exist. The existence of distinct $GABA_A$ receptors, as shown by binding data, is supported by a series of biochemical investigations. Photoaffinity labelling of receptors (irradiation with UV light) in the presence of [^{3}H]flunitrazepam, followed by denaturing gel electrophoresis, frequently yielded two (or more) protein bands with similar molecular weights (approximately 55 kDa; Sieghart and Karobath, 1980). The larger band was most predominant in both the hippocampus and striatum (the same regions attributed to Type II benzodiazepine receptors) but was absent in the cerebellum, an area associated with mostly type I benzodiazepine receptors. At that time, the multiple bands were attributed to partial degradation and/or differential

glycosylation. However, it is now known that these bands corresponded to different α subunits (Fuchs *et al.*, 1990; Bureau and Olsen, 1990).

These data are supported by recent results on purified $GABA_A$ receptors. The purified receptor contained two major polypeptides on sodium dodecyl sulphate-polyacrylamide gel electrophoresis (SDS-PAGE; α at 52 kDa and β at 56 kDa; Sigel *et al.*, 1983; Sigel and Barnard, 1984). A hetero-oligomeric complex of approximately 220 kDa (Change and Barnard, 1982; Mohler *et al.*, 1980) to 300 kDa (Schofield *et al.*, 1987) was proposed. The purified receptor was photoaffinity-labelled on the 52 kDa α band with [^{3}H]flunitrazepam, while [^{3}H]muscimol photoaffinity-labelled the 56 kDa β band (Casalotti *et al.*, 1986). In addition, monoclonal antibodies directed exclusively against the α or β subunit of this receptor were able to precipitate both subunits together (Haring *et al.*, 1985; Schoch *et al.*, 1985), indicating that they are probably associated within the intact $GABA_A$/benzodiazepine receptor complex. The application of higher resolution SDS-PAGE revealed that the α and β protein bands each consist of several different proteins with similar molecular weights (Fuchs *et al.*, 1988). Using monoclonal antibodies specific for α or β subunits, it was demonstrated that all the proteins irreversibly labelled by [^{3}H]flunitrazepam are different α subunits of the $GABA_A$ receptor complex (Fuchs *et al.*, 1988). In addition, the existence of several different β subunits was demonstrated. These subunits were specifically and irreversibly labelled by the $GABA_A$ agonist [^{3}H]muscimol and were recognised by a β subunit selective antibody (Fuchs and Sieghart, 1989).

1.2 MOLECULAR BIOLOGY

Our knowledge of the $GABA_A$ receptor structure is growing at a rapid rate. Molecular cloning techniques have expanded on the previous studies and revealed that the $GABA_A$ receptor is a hetero-oligomeric protein composed of several distinct polypeptides. Four different classes of polypeptide subunits

have been defined as; α, β, γ and δ (for review see Olsen and Tobin, 1990; Burt and Kamatchi, 1991; Wisden and Seeburg, 1992). Within these classes there exists multiple variants of subunits namely α1-6, β1-4, γ1-4 and δ which are all expressed in various regions of the CNS (see Table 1.1).
Typically, an alignment of amino acids of members of the same family yields 70 to 80% identity, while different subunit families exhibit only 30 to 40% sequence homology. All the subunits are similar in size, containing about 450 amino acids, and are strongly conserved across species (approximately 95%). Several of the $GABA_A$ receptor subunit mRNAs have been shown to exist in alternatively spliced forms. These include the human, bovine, rat (Whiting *et al.*, 1990) and mouse γ2 (Kofuji *et al.*, 1991) subunits and the chicken β2 (Harvey *et al.*, 1994) and β4 (Bateson *et al.*, 1991b) subunits. This additional level of complexity in the expression of selected receptor subunits represents another mechanism for the generation of $GABA_A$ receptor heterogeneity.

The putative topology of individual $GABA_A$ receptor subunits is shown in Fig. 1.1. The common elements of subunit structure include a long hydrophilic NH_2-terminal extracellular domain containing two to four potential asparagine-glycosylation sites (two in the rat α1 subunit at positions 10 and 110). The function of these carbohydrate moities is unknown but may be involved in functional expression (Sumikawa *et al.*, 1988). Also a conserved cysteine pair is located in this region (shown as a cystine bridge at positions 138 to 152) which are believed to participate in ligand binding (Olsen and Tobin, 1990; Burt and Kamatchi, 1991) although recently this has been shown not be the GABA binding site (Amin *et al.*, 1994). All the published clones encode signal peptide sequences that are presumed to be 'clipped' during the production of the mature polypeptide (Olsen and Tobin, 1990; Burt and Kamatchi, 1991). All the clones are typified by four transmembrane-spanning domains, M1 to M4, the second of which (M2) is thought to line the ion channel (Barnard *et al.*, 1987). The COOH terminus is located at a small extracellular hydrophilic segment following M4.

Table 1.1 Subunits of the $GABA_A$ receptor

SUBUNIT	SELECTED REFERENCES
α1	Schofield *et al.*, 1987 Khrestchatisky *et al.*, 1989 Lolait *et al.*, 1989a Malherbe *et al.*, 1990a Keir *et al.*, 1991 Bateson *et al.*, 1991a
α2	Levitan *et al.*, 1988 Khrestchatisky *et al.*, 1991
α3	Malherbe *et al.*, 1990c
α4	Ymer *et al.*,1989a Wisden *et al.*, 1991
α5	*Khrestchatisky *et al.*, 1989 Pritchett and Seeburg, 1990 Malherbe *et al.*, 1990c
α6	Luddens *et al.*, 1990
β1	Ymer *et al.*, 1989b Malherbe *et al.*, 1990a
β2S, β2L	Ymer *et al.*, 1989b Harvey *et al.*, 1994
β3	Ymer *et al.*, 1989b Bateson *et al.*, 1990
β4S, β4L	Bateson *et al.*, 1991b Lasham *et al.*, 1991
γ1	Ymer *et al.*, 1990
γ2S, γ2L	Shivers *et al.*, 1989 Pritchett *et al.*, 1989 Malherbe *et al.*, 1990b Glencorse *et al.*, 1990 Kofuji *et al.*, 1991
γ3	Wilson-Shaw *et al.*, 1991
γ4	Harvey *et al.*, 1993
δ	Shivers *et al.*, 1989

(* originally published as α4)

Figure 1.1. Putative topology of $GABA_A$ receptor subunits. The NH_2 terminal (labelled N) presumed extracellular domain is shown with the cystine bridge (C-C). Four putative membrane spanning regions, M1-M4, are represented as cylinders in red. The COOH terminus (labelled C) is again extracellular. A large intracellular cytoplasmic loop between M3 and M4 is present.

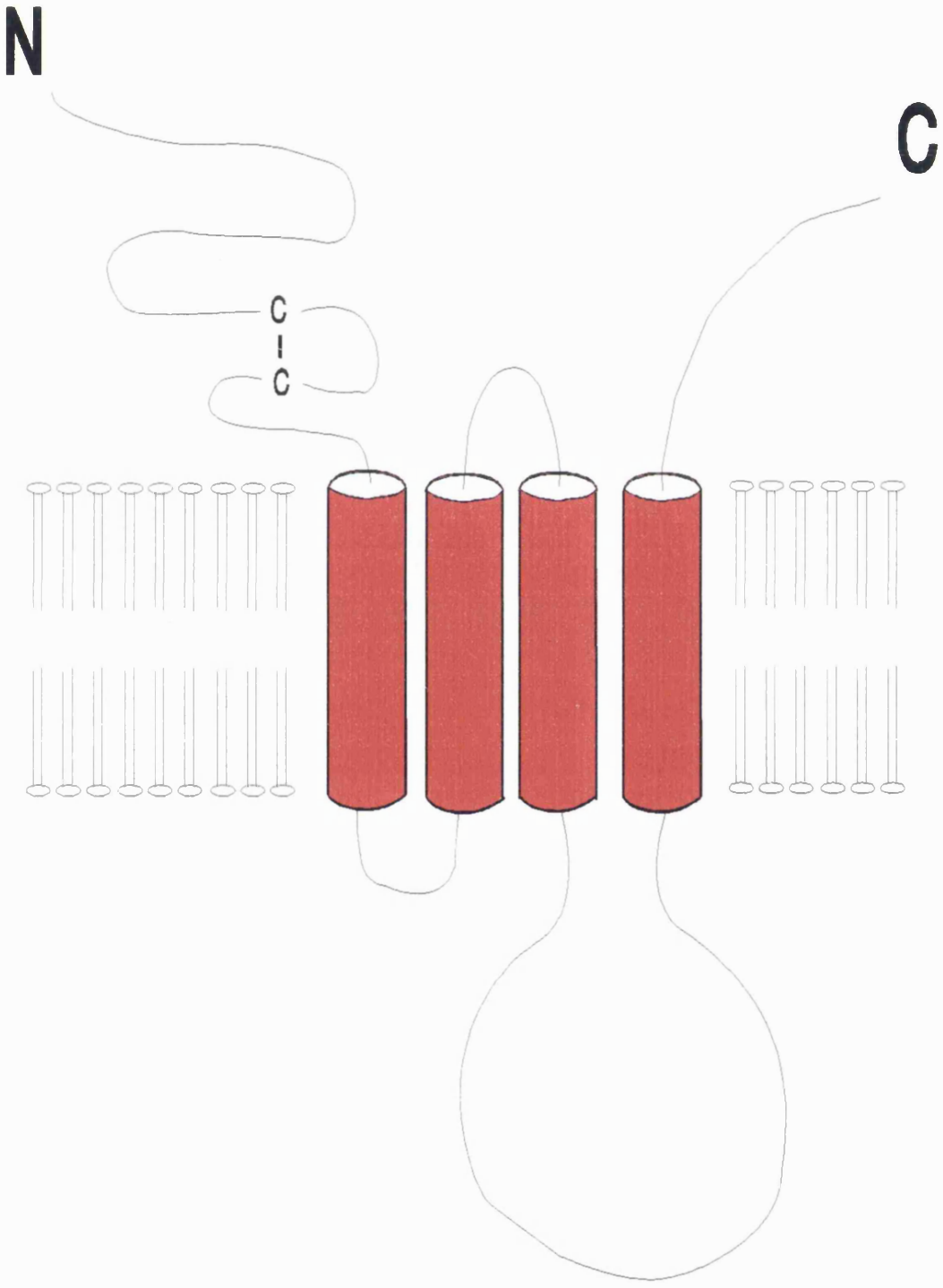
N
C
C
C

The residues conserved among several $GABA_A$ subunit polypeptides include the four transmembrane regions, M1-M4, which are about 40% identical (Barnard *et al.*, 1987). The extracellular NH_2-terminal of approximately 220 residues have considerable sequence identity, including domains of nearly complete homology (Barnard *et al.*, 1987). In contrast, several regions show greater sequence variability among the different subunit classes including the putative cytoplasmic domains (Olsen and Tobin, 1990).

1.2.1 COMPARISON WITH NICOTINIC ACETYLCHOLINE AND GLYCINE RECEPTORS

The proposed domain for transmembrane structure of the $GABA_A$ receptor subunits is remarkably similar to that seen in the various subunits of the nicotinic acetylcholine and glycine receptors (Barnard *et al.*, 1987). All the polypeptides of these receptors are similar in size and contain an identical number and distribution of predicted transmembrane-spanning regions. Furthermore, the $GABA_A$ receptor subunits have sequences in common with both these receptor classes with more than 10% of $GABA_A$ receptor amino acid residues identically positioned in some highly conserved domains, such as the four transmembrane regions, M1-M4, in various nicotinic acetylcholine and glycine receptor cDNAs (Schofield *et al.*, 1987; Boulter *et al.*, 1987; Grenningloh *et al.*, 1987). Moreover, this conservation occurs despite the fact that these receptors bind different neurotransmitter ligands and form channels selective for ions of different charge (cations for acetylcholine, chloride for GABA and glycine). These structural similarities strongly indicate that a super-family of chemically-gated ion channel receptor exists (Barnard *et al.*, 1987; Schofield *et al.*, 1987; Olsen and Tobin, 1990).

1.2.2 MULTIPLE SUBUNITS AND POSSIBLE STOICHIOMETRY

Since the initial cloning of multiple $GABA_A$ receptor subunits (Olsen and Tobin, 1990; Wisden and Seeburg, 1992), it has been demonstrated that functional $GABA_A$ receptors could be assembled from both homomeric and heteromeric subunit combinations (Schofield *et al.*, 1987; Blair *et al.*, 1988; Schofield, 1989; Sigel *et al.*, 1989; Shivers *et al.*, 1989; Sigel *et al.*, 1990). Recently, electron microscopy was applied to $GABA_A$ receptors purified from porcine cortex by benzodiazepine affinity chromatography and revealed that these receptors were probably composed of five subunits with a central ion channel pore (Nayeem *et al.*, 1994). However, the population of $GABA_A$ receptors from the brain cortex contains various combinations of many subunit types (Wisden *et al.*, 1992). The $GABA_A$ receptors isolated by Nayeem and colleagues were only those with a high-affinity site for benzodiazepines. However, although these receptors form the great majority of $GABA_A$ receptors *in situ* a proportion of $GABA_A$ receptors are benzodiazepine insensitive. Therefore, this method did not provide proof that all the permitted combinations of subunits in the native population of $GABA_A$ receptors form pentamers.

At present it is not known whether all the pentameric arrangements actually assemble to form functional receptors that possess different pharmacological properties, or if a preferred configuration(s) exists as seen for the nicotinic acetylcholine (nACh) receptor. The minimum structural requirements for several functional properties of the $GABA_A$ receptor have been studied. Sigel and colleagues, identified the combination $(\alpha1/\alpha3)\alpha5\beta2\gamma2$ as a possible candidate for a native $GABA_A$ receptor channel with the α subunit conferring the cooperativity and high affinity of the channel gated by GABA, the $\beta2$ subunit together with the α subunit for efficient channel formation and the $\gamma2$ subunit responsible for benzodiazepine sensitivity (Sigel *et al.*, 1990). The putative topology of a $GABA_A$ receptor is illustrated in Fig. 1.2. The α, β and

Figure 1.2. A schematic model for the topology of the $GABA_A$ receptor-chloride channel protein. The ligand-gated ion channel is proposed to be a hetero-oligomer composed of five subunits (Nayeem *et al.*, 1994) of the type shown in Fig. 1.1. A member of the α, β and γ subunit family has been represented (Sigel *et al.*, 1990), although the exact subunit composition, stoichiometry, and number of subunits are not known at this time (represented by a blank subunit). Each subunit has four membrane spanning domains (Fig. 1.1), one or more of which contributes to the wall of the central ion channel. Possible phosphorylation consensus sites on the cytoplasmic domain of the β and γ subunits have been indicated by the letter 'P'.

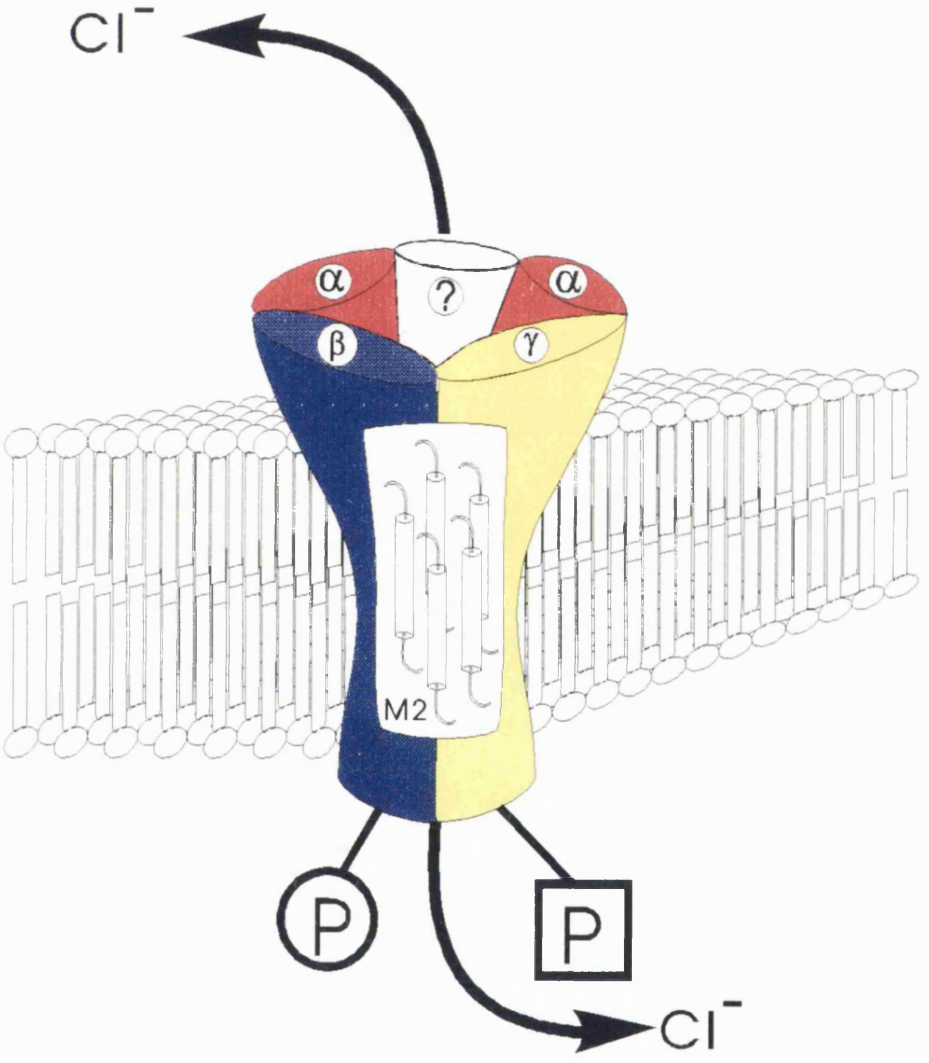
Cl⁻
α
?
α
β
γ
M2
P
P
Cl⁻

γ family have been represented (Sigel *et al.*, 1990), although the inclusion of these subunits is entirely putative as the exact *in vivo* composition of the $GABA_A$ receptor remains unknown.

Recombinant $GABA_A$ receptor channels often fail to exhibit the multiplicity of conductance states often seen in native membranes (Bormann and Clapham, 1985; Bormann *et al.*, 1987; Smith *et al.*, 1989). This could occur due to the examined subunit combinations not matching the $GABA_A$ receptors in native membranes or alternatively each neuron may express numerous subunit combinations, each giving rise to $GABA_A$ receptors with different conductance states. Localization of the mRNA encoding α, β and γ2 subunits by *in situ* hybridization suggests that they are co-localised in some brain regions, such as in the hippocampus and olfactory bulb, and differentially distributed in others, such as in the thalamus and substantia nigra (Wisden *et al.*, 1988; Sequier *et al.*, 1988; Shivers *et al.*, 1989). However, the correlation between the sites of $GABA_A$ receptor subunit expression and possible functional heterogeneity is incomplete. Ultimately, the structure of native $GABA_A$ receptors must be determined with biochemical techniques and/or immunocytochemistry. Furthermore, functional studies are necessary to provide information concerning the functional significance of individual subunits within the $GABA_A$ receptor complex (Verdoorn *et al.*, 1990).

1.3 FUNCTIONAL ROLES OF INDIVIDUAL $GABA_A$ SUBUNITS

The functional role(s) of the different $GABA_A$ subunits are at present being defined mostly by using expression systems.

1.3.1 THE α SUBUNIT

The α subunit class has by far the highest structural diversity among $GABA_A$ receptor subunits. The affinity for benzodiazepine agonists has been shown

to depend on the α subunit expressed within the $GABA_A$ receptor complex. The α1β1γ2 $GABA_A$ receptor has been shown to have the pharmacological profile of type I benzodiazepine receptors and α2β1γ2, α3β1γ2 and α5β1γ2 $GABA_A$ receptors have the properties more typical of type II benzodiazepine receptors (Pritchett *et al.*, 1989). The localisation of α-subunit mRNAs (Levitan *et al.*, 1988; Siegel, 1988; Sequier *et al.*, 1988; Wisden *et al.*, 1988) is also in good agreement with the localisation of the type I and type II benzodiazepine receptors, as determined by ligand binding analysis and by [^{3}H]flunitrazepam photoaffinity labelling (see earlier). The α5 subunit could also be important for high GABA affinity and cooperativity of GABA gating of the channel (Sigel *et al.*, 1990). The functional role(s) of α4 and α6 subunits have not yet been assessed.

1.3.2 THE γ SUBUNIT

The γ2 subunit has been shown to be important in conferring sensitivity upon the $GABA_A$ receptor to modulation by benzodiazepines (Pritchett *et al.*, 1989; cf Malherbe *et al.*, 1990a; Sieghart, 1989; Doble and Martin, 1992). Another consequence of the presence of a γ subunit in recombinant receptors seems to be an insensitivity of the $GABA_A$ receptor to inhibition by zinc ions (Draguhn *et al.*, 1990; Smart *et al.*, 1991). Two differently spliced forms of the γ2 subunit exist, termed short (γ2S) and long (γ2L), which differ by the insertion of 8 amino acids in the intracellular loop between transmembrane domains M3 and M4 (Whiting *et al.*, 1990; Kofuji *et al.*, 1991). Both γ2S and γ2L contain consensus sequences for phosphorylation by protein kinase C (PKC; see chapter 6). The functional role(s) of γ1, γ3 and γ4 subunits have not yet been determined.

1.3.3 THE β and δ SUBUNITS

The roles of the β and δ subunits are less well-defined than that of the α and γ2. Previous studies have implicated the β subunit as an essential structural component of the receptor (Angelotti *et al.*, 1993; Sigel *et al.*, 1990). The absence of a β subunit has been shown to lead to $GABA_A$ receptors with very small current amplitudes in *Xenopus* oocytes (Sigel *et al.*, 1990). In contrast, however, $GABA_A$ receptors composed of rat α1γ2 subunits expressed in human embryonic kidney cells resulted in functional channels with large conductances (Verdoorn *et al.*, 1990; Draguhn *et al.*, 1990). Therefore the β subunits could possibly be an essential structural component of the $GABA_A$ receptor. The functional role of the δ subunit is yet to be determined.

1.4 THE *XENOPUS LAEVIS* OOCYTE AS A MODEL TO STUDY FUNCTIONAL $GABA_A$ RECEPTORS

A large majority of both biochemical and electrophysiological techniques used to study drug- and voltage-operated membrane ion channels have involved the use of brain slices, membrane homogenates and dissociated organotypic tissue culture preparations. However, although these preparations retain the drug receptors and associated ionophores in the native neuronal/glial membrane these receptors were not always ideally placed for study. An alternative method for studying membrane bound receptors has arisen from the use of the *Xenopus laevis* oocyte.

Expression of exogenous proteins in the *Xenopus laevis* oocyte, either following microinjection of mRNA into the cytoplasm (Gurdon *et al.*, 1971) or cDNA into the nucleus (Mertz and Gurdon, 1977) was pioneered by Gurdon and collaborators. The oocyte is ideally suited as a vehicle for such heterologous translation due to the large size of the cell (approximately 1 mm, enabling easy intracellular injections) and the ability of the oocyte to efficiently transcribe and translate injected genetic information, perform

assembly of the protein products and target the nascent polypeptides to the correct subcellular compartment (see Lane, 1983; Colman, 1984; Soreq, 1985, for reviews).

The *Xenopus* oocyte was recognised for the expression of classical neurotransmitters in 1981 by Barnard and colleagues with the nicotinic acetylcholine receptor (Sumikawa *et al.*, 1981; Barnard et al., 1982). Following the discovery of the ability of the oocyte to properly assemble foreign multi-subunit proteins and incorporate them in a functional form into the plasma membrane, the technique was rapidly applied to other ion channels and membrane proteins (Miledi et al., 1982; Smart et al., 1983; Gundersen et al., 1984; Houamed et al., 1984; Smart et al., 1987; Sigel, 1990). These early observations forged a pathway for many investigators to use the *Xenopus* oocyte for the expression of neurotransmitter-gated and voltage-operated channels, and this has been the subject of detailed reviews (Sumikawa et al., 1986; Smart et al., 1987; Dascal, 1987; Snutch, 1988; Sigel, 1990). The oocyte has therefore become an extremely useful model for the study of drug receptors and ion channels. Moreover, it allows a convenient means of studying the molecular construction of membrane proteins which can be modified by injecting different combinations of specified mRNAs or cDNAs (wild-type or mutated) to synthesize various subunit combinations and types of receptor protein. Any functional changes in the protein(s) which gate an ion channel can then be directly monitored using an electrophysiological approach.

The oocyte expression system was therefore used in this study to determine the properties of recombinant $GABA_A$ receptors expressed after the injection of vertebrate CNS cRNAs or cDNAs into *Xenopus laevis* oocytes.

1.5 AIMS OF THE PRESENT INVESTIGATION

The complexity of the study of $GABA_A$ receptors has arisen from the large number of subunits revealed by molecular biology, which has far outdistanced the functional characterisation of all possible receptor subtypes. This study has attempted to unravel some of the functional properties of a number of defined receptor subunits utilising the *Xenopus laevis* oocyte expression system.

The pharmacological properties of $GABA_A$ receptors composed of different subunit combinations were investigated. The pharmacological profile of each receptor was studied using traditional pharmacological tools for the $GABA_A$ receptor complex, including $GABA_A$ receptor agonists, antagonists and allosteric modulators. This pharmacological characterisation confirmed that the oocyte correctly translated the injected cRNAs/cDNAs and assembled the protein products in the plasma membrane in the appropriate orientation. Moreover, the β1 subunit was shown to be crucial for the expression and formation of functional $GABA_A$ receptors. This raised the important question of whether the β1 subunit contained the domain(s) necessary for gating of the channel by GABA. This question was addressed by assessing the functional properties of the homomeric β1 subunit from both the murine and bovine species.

The functional role of the δ subunit has not yet been examined. One aim of this study was to try to determine whether δ subunits were functionally expressed within the $GABA_A$ receptor complex and to ascertain a functional role(s) for this unique subunit. The effect of changing the extracellular pH on ion channel function has been studied as an alternative method of effecting modulation of both nicotinic acetylcholine (Landau *et al.*, 1981; Li and McNamee, 1992) and excitatory amino acid receptors (Tang *et al.*, 1990; Traynelis and Cull-Candy, 1990, 1991). This modulatory tool has been rarely used on the $GABA_A$ receptor. Therefore, the effect of changing the external H^+

on $GABA_A$ receptors comprising of multiple subunits was investigated. This included studying the effect of changing the external pH on the inhibition of the GABA response by zinc on recombinant mammalian $GABA_A$ receptors since zinc and H^+ have been reported to compete for a similar site on an invertebrate muscle GABA receptor.

One further means of regulating the function of ligand-gated ion channels is to modify receptor structure covalently via phosphorylation (Swope *et al.*, 1992; Raymond *et al.*, 1993). The final aim of this study was to determine the modulatory influence of PKC-induced phosphorylation on the $GABA_A$ receptor function and to assess whether the subunit composition of the $GABA_A$ receptor construct could influence this effect.

CHAPTER TWO

MATERIALS AND METHODS

MATERIALS AND METHODS

2.1 PROCUREMENT OF cRNA AND cDNA

All murine cRNAs and cDNAs were kindly supplied by Dr. S. Moss at the IRC Institute for Molecular Cell Biology, University College, London. Bovine cRNAs and cDNAs were obtained from Professor E.A. Barnard and Dr. A. Bateson at the Molecular Neurobiology Unit, Royal Free Hospital School of Medicine, London and the Department of Pharmacology, University of Alberta, Canada respectively.

2.2 HUSBANDRY OF *XENOPUS LAEVIS*

2.2.1 SOURCE AND IDENTIFICATION OF *XENOPUS LAEVIS*

Xenopus laevis are members of the family *Pipidae* and are classified as Anurans (Verhoeff-de Fremery and Griffin, 1987). Wild-type mature females previously imported from South Africa were purchased from Blades Biological, Edenbridge, Kent. Larger frogs of mass 100-200 g were preferentially chosen as they tended to have more oocytes than smaller frogs (<80 g), and of these oocytes, a greater proportion are of developmental stages IV to VI (see section 2.5). The natural breeding season for *Xenopus* is from October to the end of December during which the quality of oocytes are generally very good. To obtain viable oocytes all year round this breeding cycle was interrupted by purchasing new frogs at least 3-6 months before they were required for use and then maintaining them in a constant environment (see sections 2.2.2 and 2.2.3).

Identification of each *Xenopus* was necessary to comply with the Animals (Scientific Procedures) Act 1986 which allowed the donor frog to be used for oocyte extraction only twice. Individual *Xenopus* have a characteristic series of marks on the dark dorsal surface; however, when in a tank of water it was

difficult to use this criterion reliably to identify particular frogs. Therefore *Xenopus* frogs were permanently identified by suturing an electrical cable marker around one of the middle toes of a hind limb. These markers were numbered and coloured and easily visualised under water. The suture formed a loose loop and was made of Nylon so that it did not shrink in water and ulcerate the toe.

2.2.2 HOUSING AND ENVIRONMENT

Xenopus were housed in small colonies of approximately 7-10 in a water tank fabricated from Perspex containing approximately 40 litres of water. One tank was reserved to quarantine newly purchased frogs before mixing with the established colonies. The temperature of the tank-water was maintained by thermostatically controlling the room temperature between 18-22°c and a filter pump kept the water clean from particulate debris. The pump filters were cleaned daily and the tanks 1-2 times per week to remove particles and excreted urea. *Xenopus* skin was quite sensitive to chloride ions and therefore the water used to fill the tanks was first stored in large open tanks for at least 24 hours which allowed the chlorine to evaporate. The frogs were hardy animals with a relatively low annual death rate (approximately 2%) which was maintained in the laboratory by careful husbandry (Verhoeff-de Fremery and Griffin, 1987; Smart and Krishek, 1994).

2.2.3 LIGHTING

The *Xenopus* were kept on an artificial lighting cycle of 12 hours illumination and 12 hours darkness which was maintained throughout the year to help break the natural breeding cycle (Verhoeff-de Fremery and Griffin, 1987). This was simply achieved by placing a timing switch on the main room lights and ensuring that natural light via the windows was excluded.

2.2.4 HANDLING AND FEEDING

As a reaction to any type of stress, the frogs exuded a slippery mucus secretion which made handling difficult. Therefore a small aquarium net sufficient to capture a large frog was used when the animals had to be handled.
Each *Xenopus* colony was fed twice weekly and for new frogs 2-3 times weekly with an alternate combination of fat-free lambs heart and liver. Overfeeding was avoided and any uneaten food was removed manually with a net or by the continuous slow re-circulation in the filtration system.

2.3 REMOVAL OF OVARY TISSUE

A *Xenopus* female contains about 30,000 large diameter (>1 mm) oocytes when fully mature. Since a typical electrophysiological experiment rarely required more than 50-100 oocytes a surgical recovery procedure was used for the limited removal of oocytes under anaesthetic.

A large mature *Xenopus* female was selected and placed into a small tank containing a 0.2% w/v solution of ethyl-m-aminobenzoate (Tricaine), ensuring the frog was completely immersed. The level of anaesthesia was checked every 1-2 minutes and determined by either the loss of the withdrawal reflex whilst pinching the toes of a hind limb or the frog demonstrated the loss of the 'righting-reflex'. Anaesthesia was obtained within 8.5 ± 3 min (n = 50 frogs) after immersion in 0.2% Tricaine. If the frog had been anaesthetized previously, the time period for anaesthesia was usually extended (to 15-20 min).

The *Xenopus* was then transferred and placed dorsal side down on a flat bed of ice to maintain anaesthesia. Throughout the procedure distilled water was frequently sprayed onto the animal to prevent drying of the skin and to keep

the site of surgery clean. A small transverse incision of 3-5 mm was made through the outer layer of the skin on the lateral ventral surface of the frog (Fig. 2.1A). To reach the ovary wall, another incision was made through the connective tissue and subsequently through the muscle sheet in the same manner. The ovary wall and the oocytes were then visible (Fig. 2.1B). Using a fine pair of forceps a section of the ovary containing a sufficient number of oocytes was carefully extracted onto the surface of the frog (about 1-2 cm in length; Fig. 2.1C) and eventually transferred to a petri-dish containing a modified Barth's solution (MBS; Table 2.1) maintained on ice. The skin and muscle layers were then separately sutured using sterile polydioxanone (clear) monofilament suture (Ethicon Ltd, Edinburgh, UK) which degraded gradually over a period of several weeks. Typically the tissues were repaired using up to 4-5 stitches on the inner muscle layer and 4-6 stitches on the outer skin layer (Fig. 2.1D-F). The frog was then washed in warm tap-water to remove any trace of the anaesthetic or exudates. The *Xenopus* was allowed to recover under subdued lighting in shallow water on a slope formed from wet tissue paper to prevent drowning. The *Xenopus* regained consciousness in 42 ± 18 min (n = 50). The rate of recovery depended on the ambient temperature and was significantly accelerated by using warm tap-water (approx. 24°C). The animal was returned to the colony 4-6 hours later and remained under observation over the next 24-48 hours. A 6-8 week recovery period was allowed before selection for possible re-use.

2.4 PREPARATION OF OOCYTES FOR INJECTION

To increase the long term survival of the oocytes the ovary tissue was thoroughly washed in MBS shortly after removal from the frog. This removed any debris and diluted enzymes (from damaged cells). The oocytes were maintained at low temperatures in MBS (approximately 5°C) throughout all subsequent procedures.

2.4.1 SEPARATION OF FOLLICULAR OOCYTES

A clump of oocytes was placed in a 10 cm sterile dish filled with MBS. The outer ovarian epithelial layer (Fig. 2.2A) was carefully removed exposing the underlying oocytes (Fig. 2.2B). After separation from the clump, individual oocytes were contained in a small ovarian sac composed of epithelial cells (inner ovarian epithelium; Fig. 2.3A; Dumont and Brummett, 1978). Separated oocytes were transferred using a blunt and fire-polished Pasteur pipette to a vial or another dish filled with fresh MBS placed on ice.

2.5 SELECTION OF OOCYTES

It is possible to express exogenous cRNA and cDNA in all the different developmental stages of the *Xenopus* oocyte (I-VI; Krafte and Lester, 1989). However, fully grown immature oocytes at stages V and VI (Dumont, 1972; Fig. 2.2B; Table 2.2) were preferred since they were the largest cells frequently enabling the development of large membrane currents and could be injected with up to 100 nl of solution. To separate the various stages of the oocytes, it was necessary to observe some physical characteristics as detailed by Dumont (1972; Fig. 2.2B).

2.5.1 SEPARATION OF STAGE V/VI OOCYTES

Stage V oocytes (diameter 1-1.2 mm) exhibited clear differentiation of animal and vegetal poles with the animal pole appearing lighter in colour compared to oocytes at stage IV. At stage VI, the oocytes reached maturity and had diameters of 1.2-1.3 mm. The differentiated animal and vegetal poles were distinctly separated by an unpigmented equatorial band compared to stage V oocytes (Table 2.2). Oocytes with diameters greater than 1000 µm which had a distinct boundary between the hemispheres were therefore selected. To facilitate this selection the tip of a Pasteur pipette was cut back so that the

orifice was approximately 3 mm wide. The tip was then lightly flame polished. About 10-20 oocytes were drawn up along with 1.5 ml of MBS into the cool Pasteur pipette. The pipette was then held vertically and the larger more dense oocytes were allowed to fall to the bottom and back into the petri-dish. The less dense immature stage oocytes remained in the pipette and were discarded. This procedure was repeated a further two times and then the remaining large oocytes were transferred into a fresh 10 cm dish filled with MBS. Finally each oocyte was examined according to the aforementioned criteria, and included an inspection for any signs of damage e.g. patchy grey membranes, yolk platelet leakage or attached ovarian tissue (Fig. 2.2C). These oocytes were then deemed suitable for microinjection.

2.6 MICROINJECTION OF *XENOPUS* OOCYTES

For the microinjection of oocytes, a number of experimental arrangements have been reported (Gurdon, 1974; Contreras *et al.*, 1981; Burmeister and Soreq, 1984; Colman, 1984; Hitchcock *et al.*, 1987).

A solution of 0.1% v/v diethylpyrocarbonate (DEPC, SIGMA) in distilled water was prepared and sterilised by autoclaving at 121°C for 15 min. This is referred to as DEPC-treated water. Glassware was placed in a fresh solution of 0.1% v/v DEPC in distilled water for 24 hrs to remove all protein traces. The DEPC solution was then discarded and the glassware rinsed with DEPC-treated sterile water prior to sterilisation with dry heat at 220°C for 4 hours to destroy RNases.
To avoid the re-introduction of RNases on injecting cRNAs sterile surgical gloves were worn throughout all subsequent handling of glassware and aseptic techniques were observed.

Each micropipette was manufactured from sterile thin-walled borosilicate glass tubing (outer diameter 1.17 mm, internal diameter 0.68 mm, length

20 cm) using a vertical microelectrode puller (Model 730, David Kopf Instruments, California, USA). The micropipette (12-14 cm long) was then bent by 30° in a small Bunsen flame approximately 3-5 cm from the tip which allowed a vertical positioning of the pipette above the oocyte (Fig. 2.3B,C). The micropipette tip was broken-back producing an enlarged external tip diameter of approximately 20 µm. A fresh micropipette was fabricated before each injection.

cRNA or cDNA solutions were prepared in sterile water and stored at -70°C (cRNA) and -20°C (cDNA). The concentrations used varied; for cRNA and cDNA preparations 1 mg/ml and 0.3-1 mg/ml respectively were routinely used. The cRNA or cDNA solution was allowed to thaw at room temperature and then centrifuged in an Eppendorf microfuge for approximately 20-60 seconds before being stored on ice until required for use. Mineral oil (light white oil, RNase and DNase free, SIGMA) containing a small amount of Sudan IV (Solvent Red 24, SIGMA), an oil soluble dye, was incorporated into the pipette to facilitate the visualisation of the interface between the cRNA or cDNA and the mineral oil. The micropipette was placed fully into a 10 µl digital Drummond microdispenser avoiding the introduction of air bubbles. The Drummond microdispenser was then mounted onto a Prior micromanipulator and secured. Any air bubbles at the tip of the micropipette were then ejected by positive displacement using the microdispenser. A sterile disposable pipette tip was used to place 1-2 µl of cRNA or cDNA onto the middle of a strip of Nescofilm secured to a sterile microscope slide. The cRNA or cDNA sample was taken up into the injection micropipette tip by negative displacement of the digital microdispenser. After back-filling was complete there was a visible boundary between the cRNA/cDNA solution and the sudan IV dyed mineral oil.

2.6.1 CYTOPLASMIC cRNA INJECTION

A number of previously selected oocytes (4-8) were placed on a sterile microscope slide wrapped in Nescofilm. Each oocyte was fully immersed in individual drops of MBS to prevent drying during the injection. Oocytes were manipulated using a sterile pipette tip and held stable whilst the injection micropipette was inserted into the equatorial region of the oocyte. Injection into this area of the oocyte allowed optimal mobility of the cRNA and prevented damage of the nucleus (Colman and Drummond, 1986). Successful impalement of the oocyte was signified by the sudden disappearance of the dimpled membrane surface around the micropipette tip. 50 ± 5 nl of cRNA was then injected into the selected oocyte. 10 nl of cRNA solution was expelled between each injection to ensure that the micropipette tip did not become blocked and to avoid dilution of RNA with intracellular contents from injected oocytes.

2.6.2 NUCLEAR cDNA INJECTION

A number of previously selected oocytes were placed onto a plastic mesh grid fixed to the bottom of a well contained in a Perspex block (Fig. 2.4A). Sufficient MBS was present to keep the oocytes wet without allowing them to float over the grid. The oocytes were manipulated until the animal pole of the oocyte was uppermost. The oocytes were centrifuged in a refrigerated centrifuge (Denley BR 401) at 700-1100 g for 8-12 minutes at 10-15°C. A test spin with a small number of oocytes was used to ascertain the centrifuge settings. Due to differing densities, the germinal vesicles rose to the surface of the oocytes and their position was indicated by a delineated area in the animal pole (Fig. 2.4B,C). Oocytes which had changed their orientation or became damaged during centrifugation were discarded. The microelectrode tip was inserted into the nucleus of the oocyte and up to 20 nl of cDNA was injected (Fig. 2.3B,C). 10 nl of cDNA was ejected between each injection

(cf. Kressmann *et al.*, 1977; Rungger and Turler, 1978; Bertrand *et al.*, 1991; Fig. 2.4D). Oocyte mortality caused by the injection usually became evident in the first 3 days but a survival rate of 70-80 % of injected oocytes for at least 7-14 days was routinely achieved.

The level of receptor/ion channel expression varied considerably amongst different oocytes from different donor frogs and even within oocytes obtained from the same donor. Occasionally, when using cDNAs, expression could be very high and this caused problems when trying to voltage clamp the oocytes with induced membrane currents in excess of 10 μA. Under these circumstances the concentration of cDNA was reduced for subsequent injections (typically from 1 mg/ml to 10 μg/ml). However, this produced only a small reduction in expression efficiency. Greater success was achieved by mixing the receptor/ion channel cDNA with the same vector but lacking the receptor/ion channel DNA.

2.7 CULTURE/INCUBATION OF INJECTED OOCYTES

After injection the oocytes were transferred into sterile glass tubes containing fresh MBS and placed in a small incubator at 18 to 20°C for 24 to 48 hrs (Figure 2.5A). The MBS was replaced every 24 hours with fresh sterile MBS and any damaged or dead oocytes removed. To permit adequate receptor/ion channel expression, oocytes injected with cRNA required incubation for up to 2-5 days. For cDNA injected oocytes, up to 1-2 days was sufficient for expression. Once the oocytes expressed the receptor/ion channel proteins of interest, they were stored at 10°C and the MBS replaced every 3-4 days. The low temperature prolonged the survival of the oocytes such that they could be maintained in a viable state for up to 3-4 weeks. However, the level of protein expression decreased over this period.

2.8 ELECTROPHYSIOLOGICAL RECORDING FROM *XENOPUS* OOCYTES

2.8.1 TWO-ELECTRODE VOLTAGE CLAMP

Oocytes were transferred to the recording bath and immobilised by placement in a circle of shortened insect pins. This arrangement previously positioned in a Sylgard base provided a micro-holder suspending the oocyte just above the base of the bath. The chamber was continuously perfused with frog-Ringer (rate 2.5 to 25 ml/min; Table 2.1) which entered through a gravity feed inlet (approx. 5 mm from the oocyte surface) supplied by one of four reservoirs connected by a 4:1 multiplexer. This system also enabled drug solutions to be bath-applied via the gravity feed. The perfusate was removed by vacuum suction (adjustable bath volume = 0.15 to 1 ml). The bath was placed on a heavy recording table and viewed with a simple compound microscope (magnification 4-20x). The electrical recording apparatus comprised of a conventional two-electrode voltage-clamp Axopatch 2C amplifier, a timer and pulse generator. The data were low pass filtered (0.3 kHz) and recorded permanently on a Gould 2200S chart recorder (Fig. 2.5B).

Glass microelectrodes were fabricated from thin-walled filamented glass (1.5 mm external and 0.86 mm internal diameters; GC150TF-10; Clark's electromedical). Electrodes were pulled on a David Kopf puller (model 730) to give resistances of 0.5 to 2 MΩ. The voltage and current recording electrodes were filled with 3M KCl and 0.6M K_2SO_4 solutions respectively. Connections to the amplifier were made via silver/silver chloride wires. The initial membrane potential after impalement was quite variable between batch's of oocytes (-10 to -50 mV). Following impalement a hyperpolarising current pulse protocol was used (50 nA, 1 s duration, 0.2 Hz) to monitor the membrane resistance as indicated by the amplitude of the electrotonic potential. Gradual disimpalement of the electrodes reduced membrane surface

dimpling followed by sealing of the electrodes which often occurred over a period of 30 mins resulting in a viable oocyte. The gradual improvement in the oocyte after impalement was followed by an increase in the input resistance (from 0.4 ± 0.13 MΩ to 1.4 ± 0.25 MΩ) and hyperpolarization of the membrane potential (typically from -20 ± 5 mV to -50 ± 13 mV; data taken from 25 oocytes). All experiments were performed at room temperature.

The large size of the oocyte, whilst making for easy impalements, carried a significant disadvantage with the amount of membrane that must be charged to voltage clamp the cell. The response time of the voltage clamp amplifier following a voltage command step was a function of $R_e.C_m$ / A, where R_e is the resistance of the current passing electrode, C_m is the membrane capacity and A the gain of the amplifier. Thus low resistance current electrodes and a high gain on the amplifier was adopted for all voltage clamping reducing the time for the clamp to respond. In addition, a further increase in the gain and speed of the amplifier was achieved by placing a grounded shield in between the two electrodes to reduce capacitative coupling (Fig. 2.5B). A constant fluid level was maintained in the bath just above the oocyte which improved visualization under the microscope during the experiment and also reduced microelectrode capacity.

In two-electrode voltage clamp series resistance is a function of the cytoplasm of the oocyte, the bathing solution and the grounding electrode (Jones, 1990; Finkel and Gage, 1985). Series resistance limits both the speed and steady-state accuracy of the clamp. However, to maintain a low series resistance the grounding path was kept at low resistance such that when large currents were passed at the peak of the conductance change, with the resulting decrease in the resistance of the cell (approximately 0.5 MΩ), the series resistance was not more than 1 to 2% of the resistance of the cell. Construction of current-voltage curves revealed a similar reversal potential for each experiment indicating that significant clamp errors were not

introduced at different holding potentials. The small series resistance error was therefore not compensated.

2.8.2 MEASUREMENT OF MEMBRANE POTENTIAL

Two possible sources of error can be encountered while attempting to measure the absolute membrane potential, namely the presence of tip potentials and junction potentials.

The tip potential has been correlated with electrode resistance (Adrian, 1956) and ionic concentration (Agin and Holtzmann, 1966; Agin, 1969). Tip potentials can be determined by measuring the potential change (as seen by the potential beam displacement on the oscilloscope) occurring after the breakage of the electrode tip in solution. The effect of the tip potential is to cause an underestimation of the absolute resting potential (for review see Halliwell and Whitaker, 1987). Generally, the tip potential was < 3 mV for recording electrodes (1-5 MΩ) and the membrane potential was not corrected for this small error.

Liquid junction potentials (E_j) arise from unequal mobilities of cationic and anionic constituents of different salt solutions or two concentrations of the same salt solutions. There will be a liquid junction potential between the microelectrode electrolyte and the oocyte cytoplasm. In this study, experiments involving the complete replacement of ionic constituents were not performed. To maintain a constant E_j, a 3M KCl electrolyte was always used in the voltage electrode. Therefore possible errors introduced due to liquid junction potentials would be minimal.

2.8.3 MEASUREMENT OF MEMBRANE CONDUCTANCE

The membrane conductance change induced by receptor agonists could be determined in current or voltage-clamp. However the latter technique was preferentially used to avoid activation of voltage-gated ion channels on depolarisation of the membrane with the test-agonist. However if the expression of recombinant receptors was sufficiently high, such that the holding potential shifted in voltage-clamp even at high amplifier gain, then the current-clamp mode was adopted. All current clamp experiments were performed around the GABA reversal potential to minimise excursions of the membrane potential and consequent activation of voltage-gated channels. The resting membrane conductance was determined by application of constant current pulses (typically: 1 sec duration, 0.2 Hz) and measuring the resultant electrotonic potential amplitudes. A similar measurement was made during the peak response to the agonist. The resultant conductance induced by the agonist was then simply calculated from subtracting the resting membrane conductance from the conductance measured in the presence of the agonist.

In voltage clamp, the membrane potential was clamped at an appropriate value (-30 to -60 mV). In this case hyperpolarising voltage command steps (10 mV, 1 s duration, 0.2 Hz) were superimposed on the holding potential to monitor membrane conductance. Application of the receptor agonist caused an increase in the amplitude of the leak-current pulse. The agonist-induced conductance was then calculated by subtraction of the resting membrane conductance.

To pool dose-conductance data from more than one oocyte, all conductances induced by different concentrations of GABA were normalised to the conductance produced by 10 μM GABA (defined as 1). The resultant normalised GABA-activated conductance change was termed ΔG_N. The data were fitted with a logistic state function in the form:

$$\Delta G_N = 1 / [1 + (EC_{50} / [A])^n],$$

where ΔG_N represents the normalised agonist-induced conductance at a given concentration. EC_{50} defined the concentration of agonist [A] which induces a 50% of the maximum response and n is the Hill coefficient.

Data used to construct antagonist concentration-inhibition relationships were fitted with an antagonist inhibition model of the form:

$$\Delta G_N' / \Delta G_N = [1 - [B / B + IC_{50}]]$$

where $\Delta G_N'$ and ΔG_N represent the normalised agonist-induced conductance at a given concentration in the presence and absence of antagonist respectively. B represents the antagonist concentration and IC_{50} defines the concentration of antagonist producing a 50% inhibition of the agonist response.

Data used to obtain pA_2 values were fitted with the standard Schild equation (Arunlakshana and Schild, 1959) in the form:

$$\log (DR - 1) = \log [B] - \log [K_B]$$

where DR is the dose ratio, K_B the dissociation constant of the antagonist and [B] is the antagonist concentration. When DR = 2, then:

$$\log [B] = -\log K_B = pA_2$$

Where the pA_2 of a competitive antagonist is defined as the negative logarithm of the molar concentration of an antagonist necessary to produce an agonist DR of 2.

All curves were fitted with Fig. P version 6.0 using Marquardt nonlinear least squares regression.

2.8.4 CURRENT-VOLTAGE RELATIONSHIPS

Current-voltage (I-V) relationships were determined under voltage clamp. The holding potential was stepped to various pre-determined values by application

of depolarising and hyperpolarising voltage command steps (10 mV increments, 1 s duration). In each case the steady-state voltage step achieved and the induced-current were measured. Finally, the agonist I-V was determined by subtracting the control I-V from the I-V relationship determined in the presence of the agonist. The voltage sensitivity of the agonist-induced conductance was analysed by calculating the membrane chord conductance at different membrane potentials according to:

$$\text{Chord } G = I / (V_h - V_{rev}),$$

where chord G and I are the chord conductance and the membrane current evoked by the agonist, V_h represents the holding potential and V_{rev} the agonist response reversal potential.

2.9 DRUGS AND SOLUTIONS

The concentrations of salts present in the MBS and frog-Ringer are shown in Table 2.1. All reagents used in these solutions were of 'Analar' grade and supplied by BDH. The following is a list of all the drugs used in the study and unless otherwise indicated the supply was obtained from Sigma Chemical Co. Ltd.:

(-)-Bicuculline Methobromide, Picrotoxin, Muscimol, Diazepam, Flurazepam, Pentobarbitone, Anthracene-9-Carboxylic Acid (A-9-C), Actinomycin D, Penicillin G, 5β Pregnan-3α-ol-20-one (Pregnanolone), Phorbol 12-Myristate 13-Acetate (PMA), 4α-Phorbol 12,13 Didecanoate (α-PDD).
γ-Aminobutyric acid (GABA) and Zinc chloride ($ZnCl_2$) were supplied by BDH.
Isoguvacine Hydrochloride and 2,6 Diisopropylphenol (Propafol) were obtained from Tocris Neuramin and Aldrich respectively.
Midazolam and Flumazenil were obtained from Hofmann La Roche, Basel, Switzerland.
Methyl-6,7-dimethoxy-4-ethyl-β-carboline-3-carboxylate (DMCM) and Chlormethiazole were a kind gift to Professor Mike Simmonds by Schering,

Berlin, Germany and Astra, England respectively.

Protein kinase C inhibitor (PKCI; 19-36) was supplied by Calbiochem.

A stock solution of each reagent was prepared, in most cases, in distilled water (concentrations ranged 0.1-10 mM) and freshly diluted with frog-Ringer solution to achieve the appropriate final bath concentrations (pH range 7.4-7.5). All stock solutions were frozen and stored at -20°C when not being used. Diazepam, DMCM, Flumazenil, A-9-C, PMA and α-PDD were dissolved in the minimum quantity of 100% ethanol prior to use. Pregnanolone was dissolved in acetone before use. In all cases where solutions contained either ethanol or acetone, control tests with Ringer solutions containing either solvent at the appropriate concentrations were performed.

Figure 2.1. A close-up view of the lateral ventral abdominal surface of a *Xenopus* showing the various stages involved in oocyte extraction (A-C) and subsequent repair (F) by suturing both internal (D) and external (E) tissues. Calibration bar 1 mm.

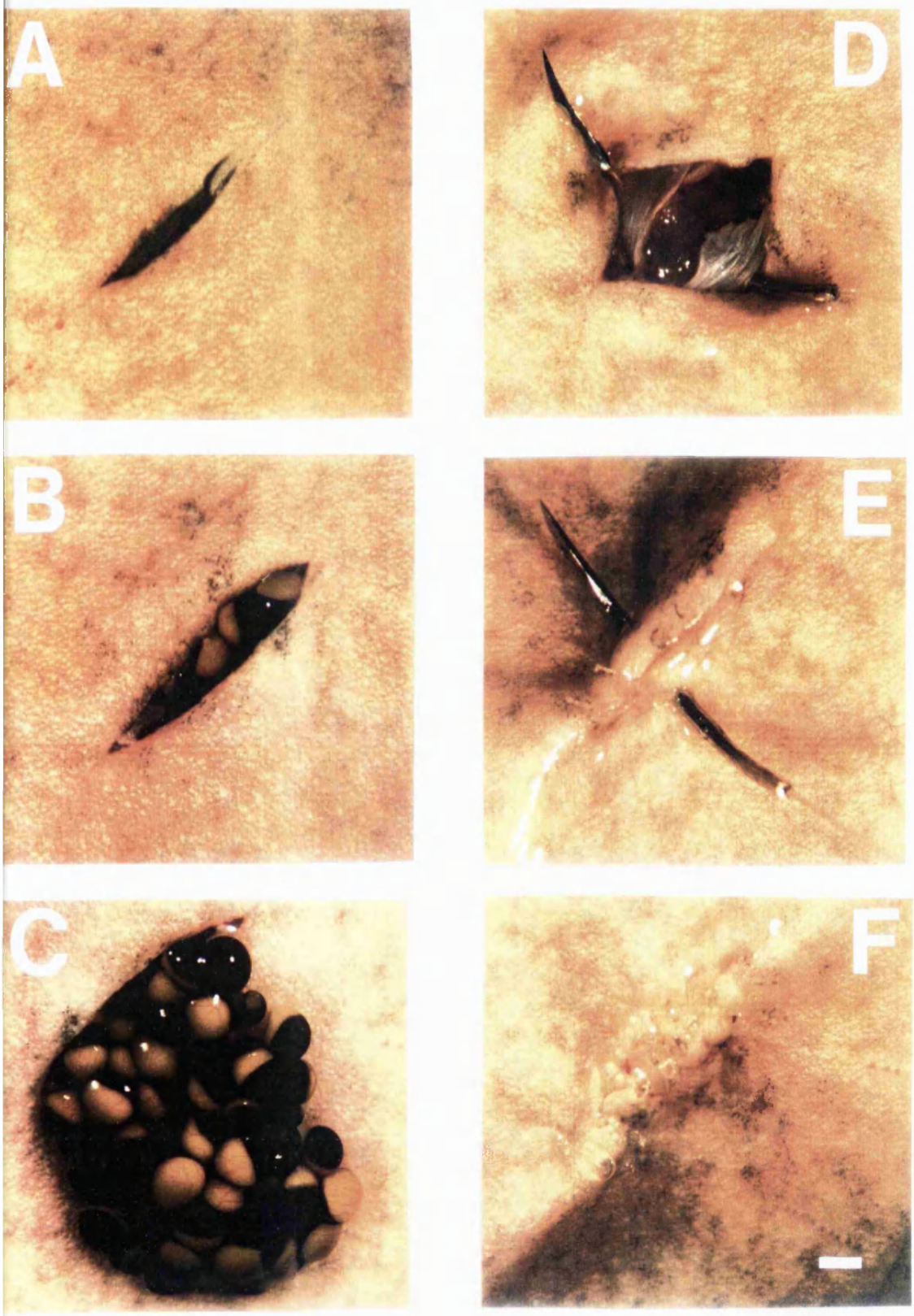
A
D
B
E
C
F

Figure 2.2. A clump of oocytes before (A) and after (B) the removal of the outer ovarian epithelial layer. Various examples of the different developmental stages (I-VI) of the oocytes with their characteristic physical appearance and size are illustrated. The distinctive hemispheres corresponding to the dark animal poles and much lighter vegetal poles in oocytes at stages IV-VI are clearly visible. (C) Characteristic appearance of damaged or poor oocytes. In (A) and (C) calibration bar represents 0.5 mm and in (C) 0.2 mm.

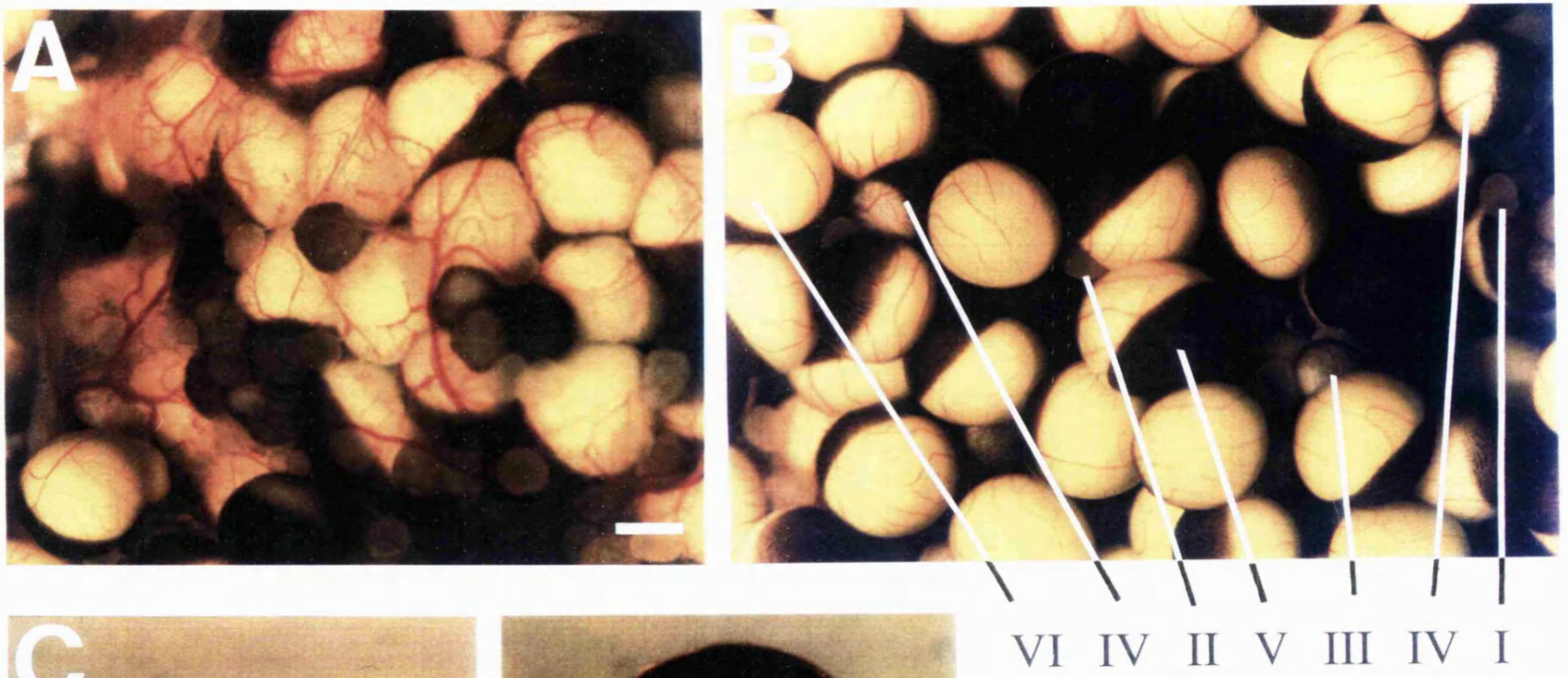
A
B
VI IV II V III IV I
C

Figure 2.3. (A) Schematic diagram of a *Xenopus laevis* oocyte illustrating the various anatomical features including the cell and membrane layers surrounding the oocyte plasma membrane. (B) Schematic diagram illustrating the position of the oocytes on a plastic mesh with respect to the injection micropipette. (C) The position and orientation of the nucleus of a single oocyte prior to injection is shown (white area in the animal pole).

A

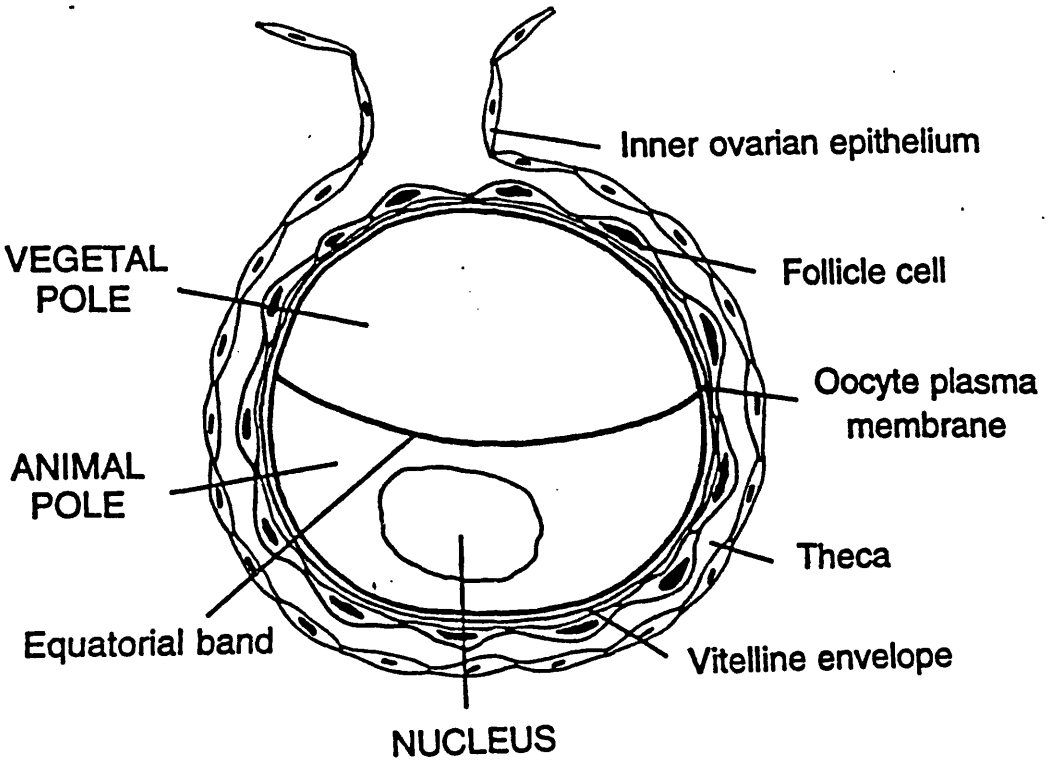
Inner ovarian epithelium
VEGETAL POLE
Follicle cell
Oocyte plasma membrane
ANIMAL POLE
Theca
Equatorial band
Vitelline envelope
NUCLEUS

B

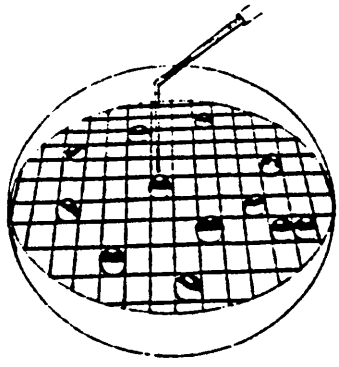

C

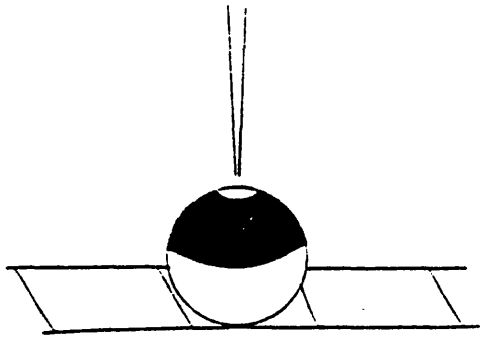

Figure 2.4. Stage V oocytes placed in a plastic mesh and shown before (A) and after (B) centrifugation. The appearance of the nuclei in (B) is illustrated for one oocyte magnified in (C). After injection healthy oocytes had the appearance of the example in (D). Note the central spot indicating the position of impalement by the injection micropipette. In (A) and (B) the calibration bar indicates 0.5 mm and in (C) and (D) 0.15 mm.

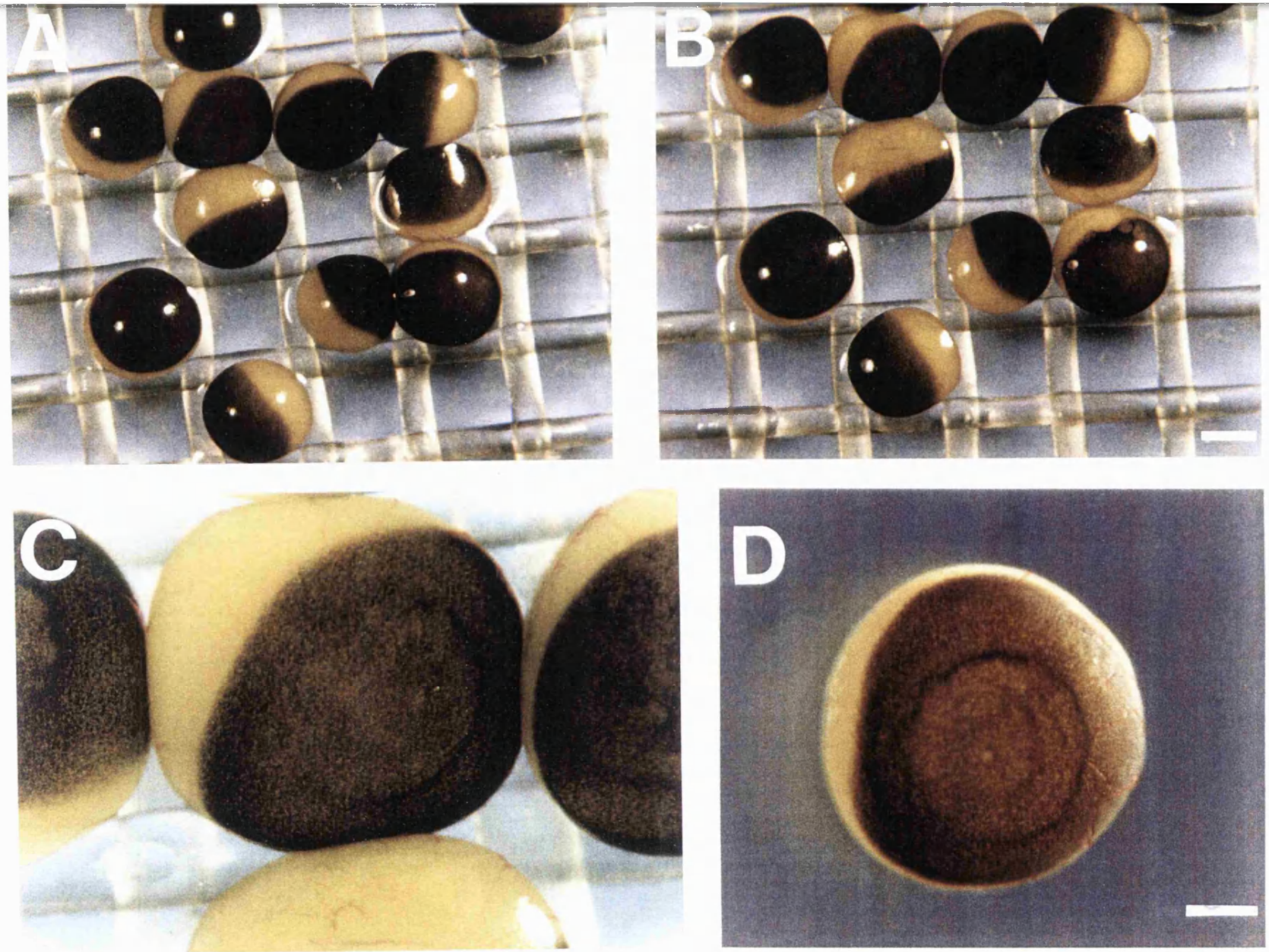
A
B
C
D

Figure 2.5. (A) Equipment used to incubate the injected oocytes on the laboratory bench. This consisted of a temperature controller (Peltier device) which controlled the water temperature in a small bath utilising a paddle stirrer to provide a constant circulation of water. (B) Recording arrangement for two-electrode voltage clamp experiments on *Xenopus laevis* oocytes showing a Prior and a Leitz micromanipulator, the recording chamber and four plastic funnels for bath application of solutions. The position of the recording microelectrodes and the intervening aluminium shield is also shown.

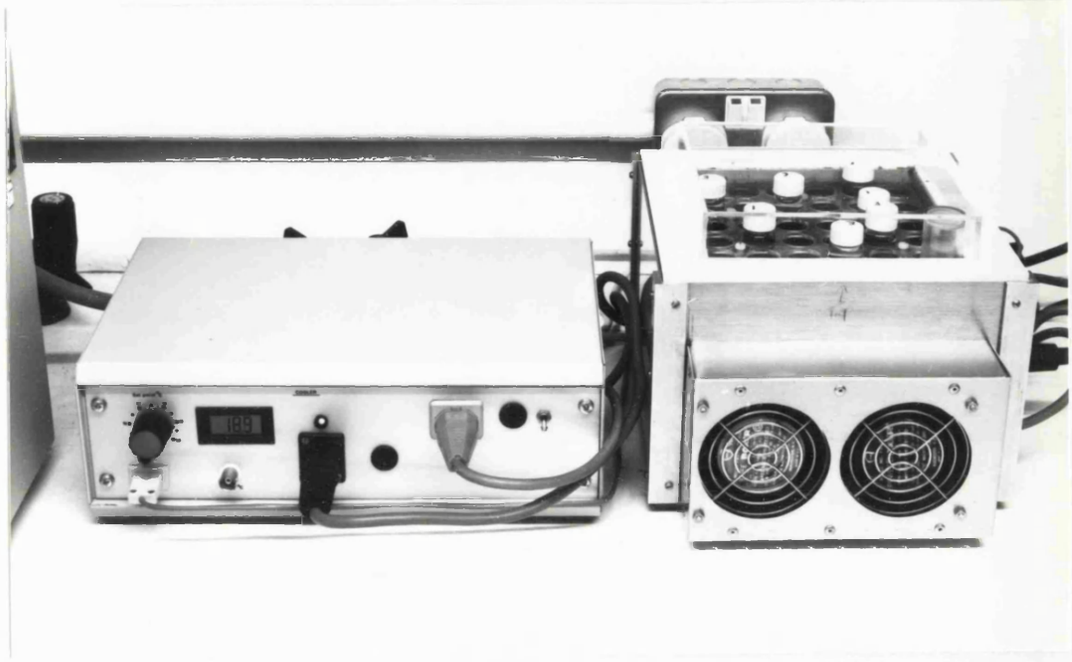

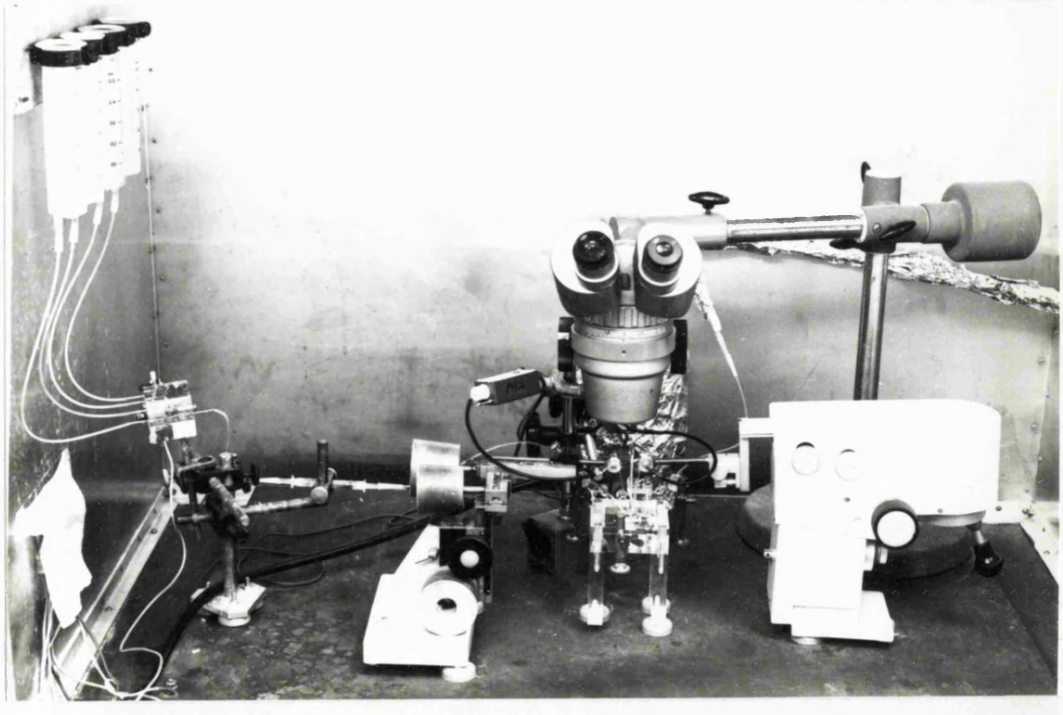

TABLE 2.1

COMPOSITION OF PHYSIOLOGICAL SOLUTIONS

Modified Barth's Solution

NaCl	110 mM
KCl	1 mM
$NaHCO_3$	2.4 mM
Tris/HCl	7.5 mM
$Ca(NO_3)_2$	0.33 mM
$CaCl_2$	0.41 mM
$MgSO_4$	0.82 mM
pH	7.6
gentamycin	50 mg/l

Frog-Ringer Solution

NaCl	110 mM
KCl	2 mM
HEPES	5 mM
$CaCl_2$	1.8 mM
pH	7.4 - 7.5

The constituents of both solutions were added and dissolved in the sequence shown. Modified Barth's solution was sterilised by autoclaving before addition of the gentamycin and $NaHCO_3$. The antibiotic and $NaHCO_3$ were sterilsed by filtration through a 0.22μm pore filter (Millipore) and added aseptically to the sterile Modified Barth's solution.

TABLE 2.2

DEVELOPMENTAL STAGES OF *XENOPUS* OOCYTES

Stage of oocyte	Diameter	Typical Characteristics
I	50 - 300 μm	Translucent with no animal or vegetal pole but with a clear nucleus
II	300 - 450 μm	A white cytoplasm towards the end of this stage of development, but no clear polar differentiation
III	450 - 600 μm	A blackish-brown patchy colouration, some polarity just becoming evident
IV	600 - 1000 μm	Separation into animal and vegetal poles
V	1 - 1.2 mm	Clear differentiation of animal and vegetal poles with the animal pole appearing lighter in colour compared to oocytes at stage IV
VI	1.2 - 1.3 mm	Differentiated animal and vegetal poles were distinctly separated by an unpigmented equatorial band compared to stage V oocytes

CHAPTER THREE

RECEPTOR CHARACTERISATION: FUNCTIONAL PROPERTIES OF RECOMBINANT $GABA_A$ RECEPTORS

RECEPTOR CHARACTERISATION: FUNCTIONAL PROPERTIES OF RECOMBINANT $GABA_A$ RECEPTORS

3.1 INTRODUCTION

Since the initial cloning of multiple $GABA_A$ receptor subunit cDNAs (for review see Olsen and Tobin, 1990; Wisden and Seeburg, 1992), it has been demonstrated using expression studies that functional $GABA_A$ receptors could be assembled from both homomeric and heteromeric receptors. Moreover, these various receptor subtypes express different pharmacological properties (Schofield *et al.*, 1987; Blair *et al.*, 1988; Sigel *et al.*, 1989; Shivers *et al.*, 1989; Sigel *et al.*, 1990). Burt and Kamatchi (1991) assumed that if a random pentameric arrangement of receptor subunits formed the ion channel, then a possible 151,887 different combinations could be assembled from the 15 known receptor subunits. Recently, Nayeem and colleagues have revealed that the $GABA_A$ receptor is likely to be composed of the assumed five subunits with a central ion-conducting pore (Nayeem *et al.*, 1994). However, at present it is not known whether all the possible pentameric arrangements suggested by Burt and Kamatchi actually assemble *in vivo* to form functional receptors possessing different pharmacological properties, or if only a few preferred configurations exist.

Homologous and heterologous expression of various $GABA_A$ receptor subunits have been utilised previously to determine the specific pharmacological properties of receptors formed by different subunits (Blair *et al.*, 1988; Levitan *et al.*, 1988; Sigel *et al.*, 1990; Verdoorn *et al.*, 1990; Smart *et al.*, 1991). Interestingly, it has been shown that recombinant $GABA_A$ receptors of the composition $\alpha1\beta1\gamma2S$ were preferentially expressed over $GABA_A$ receptors consisting of $\alpha1\beta1$ subunits when all three cDNAs were incorporated into L929 cells (Angelotti *et al.*, 1993). These results suggest that assembly of $GABA_A$ receptors from constituent subunits did not proceed along a random pathway, but that certain subunit assemblies were distinctly preferred.

Furthermore, there is a precedent in the ligand-gated ion channel superfamily for preferential subunit assembly, notably with the nicotinic acetylcholine (nACh) receptor, which is composed of α, β, γ or ε, and δ subunits. These subunits could randomly assemble into 208 different pentameric configurations, but preference appears to be given to two pentameric structures, α2βδγ or α2βδε (Toyoshima and Unwin, 1990).

The *Xenopus* oocyte has been used as a reliable experimental tool for the expression of plasma membrane proteins (for reviews see Sigel, 1990; Smart and Krishek, 1994). However, with regard to nACh receptors, there is some evidence for endogenous expression from the *Xenopus* oocyte's own genome of nACh receptor α subunit mRNA that, when translated, can be co-assembled with subunits derived from exogenous cRNAs to form functional receptors (Buller and White, 1989). Therefore, this study attempted to address whether the $GABA_A$ receptors expressed in the *Xenopus* oocytes were solely produced from the injection of exogenous cRNAs or cDNAs. The pharmacological properties of $GABA_A$ receptors consisting of different subunit combinations were investigated using traditional pharmacological agents known to bind to the $GABA_A$ receptor complex. These experiments were undertaken to try and identify that the correct translational products were formed following cRNAs/cDNAs injection. This study provides evidence for the functional roles of some of the different subunits.

3.2 RESULTS

3.2.1 EXPRESSION AND AGONIST PHARMACOLOGY OF MURINE RECOMBINANT $GABA_A$ RECEPTORS

The relative potency of $GABA_A$ receptor agonists, GABA, isoguvacine and muscimol revealed by concentration-response curves, have previously been identified in brain slice preparations such as the rat hippocampal brain slice

(Kemp *et al.*, 1986) and the rat cuneate nucleus (Pickles and Simmonds, 1980). However, the potency of GABA in these preparations is likely to be substantially influenced by uptake processes that reduce the free concentration of GABA in the extracellular space. Therefore, the relative potencies of GABA receptor agonists depended on their susceptibilities to uptake and the anatomical arrangement and density of uptake sites in relation to $GABA_A$ receptors in the tissue under study. In contrast, it has been previously shown that there are no GABA uptake sites present on the *Xenopus* oocyte (Houamed, 1988). Therefore, expression of $GABA_A$ receptors in these cells offers an ideal opportunity to accurately determine the relative potencies of some $GABA_A$ receptor agonists.

Heteromeric $GABA_A$ receptors incorporating combinations of murine α1, β1, γ2S, γ2L and δ subunits were expressed in *Xenopus* oocytes. Recording from single *Xenopus* oocytes expressing α1β1, α1β1γ2S, α1βγ2L, α1β1δ and α1β1γ2Sδ receptor subunits, membrane currents evoked by bath-applied GABA were monitored. At holding potentials of -40 to -60 mV under voltage-clamp the GABA-activated responses had membrane currents which were maintained over recording periods of up to 8 hours. To minimise variations in responses among oocytes, drug effects were studied on individual oocytes and routinely normalised to the conductance change induced by 10 μM GABA in control Ringer obtained from the same oocyte.

Under voltage clamp at a holding potential of -40 mV, oocytes injected with α1β1 $GABA_A$ receptor constructs responded to GABA (10 μM), isoguvacine (50 μM) and muscimol (1 μM) with large consistent membrane currents and conductances (Fig. 3.1A). The responses induced by GABA, isoguvacine and muscimol were dose-dependent as demonstrated by constructing equilibrium dose-response curves for the three agonists. These curves revealed EC_{50} values of 5.87 ± 0.7, 34.0 ± 2.3 and 0.63 ± 0.05 μM and Hill coefficients of 0.95 ± 0.09, 1.03 ± 0.06 and 1.16 ± 0.08 for GABA, isoguvacine and muscimol

respectively (Fig. 3.1B; Table 3.1). Overall, the rank order of agonist potency determined from the EC_{50}s for the α1β1 receptor construct was: muscimol > GABA > isoguvacine with a nine fold increase in relative potency for muscimol and a 6 fold decrease in relative potency for isoguvacine compared to GABA. Interestingly, the maximal response produced by each agonist was apparently similar indicating that GABA, isoguvacine and muscimol are full agonists on this recombinant $GABA_A$ receptor (Jenkinson and Abbott, 1990).

$GABA_A$ receptors composed of α1β1γ2L subunits revealed a similar agonist sensitivity to the α1β1 receptor construct. GABA (10 μM), isoguvacine (75 μM) and muscimol (2.5 μM) induced large inward currents and increases in the membrane conductances (Fig. 3.2A). Equilibrium response curves for GABA, isoguvacine and muscimol revealed EC_{50} values of 10.2 ± 0.5, 76.87 ± 4.5 and 2.6 ± 0.32 μM and Hill coefficient values of 1.22 ± 0.05, 1.19 ± 0.06 and 1.13 ± 0.1 respectively (Fig. 3.2B; Table 3.1). Overall, the rank order of agonist potency for the α1β1γ2L receptor construct was the same as the α1β1 $GABA_A$ receptor complex: muscimol > GABA > isoguvacine with a four fold increase in potency for muscimol and a 7.5 fold decrease in potency for isoguvacine compared to GABA. The agonists maximal response were similar on this receptor construct indicating that, as for the α1β1 receptor, GABA, isoguvacine and muscimol are full agonists on α1β1γ2L $GABA_A$ receptors (Jenkinson and Abbott, 1990).

Oocytes expressing α1β1γ2S $GABA_A$ receptor subunits also revealed a similar agonist sensitivity with 2.5 μM muscimol inducing a similar inward current and conductance increase as 10 μM GABA and 75 μM isoguvacine (Fig. 3.3A). Construction of a dose-response curve for GABA led to a EC_{50} and Hill coefficient value of 10.03 ± 0.2 μM and 1.29 ± 0.03 respectively (Fig. 3.3B; Table 3.1).

Conversely, oocytes injected with α1γ2S $GABA_A$ receptor subunits failed to respond to 1 mM GABA, 1 mM isoguvacine or 500 μM muscimol (Fig. 3.4A). Expression of this receptor construct was attempted on several occasions with no success indicating a possible role for the β subunit in the construction of functional $GABA_A$ receptors. Furthermore, Blair and colleagues revealed that GABA-sensitive chloride channels were formed after the expression of bovine homomeric "β" $GABA_A$ subunits (Blair *et al.*, 1988). Conversely, expression of the rat β1 subunit alone produced an anion-selective channel which lacked GABA-gated properties (Sigel *et al.*, 1989). Therefore, the β subunit could contain domains which are crucial for gating of the ion channel by GABA.

Interestingly, addition of the δ subunit to either the α1β1 or α1βγ2S receptor constructs, yielding α1β1δ or α1β1γ2Sδ $GABA_A$ receptors, had little effect on the GABA sensitivity (0.1 to 1000 μM). Construction of equilibrium dose-response curves for GABA for the α1β1δ and α1β1γ2Sδ receptor constructs revealed EC_{50} values of 4.9 ± 0.4 and 27.7 ± 1 μM and Hill coefficient values of 0.85 ± 0.05 and 1.44 ± 0.06 respectively (Fig. 3.4B; Table 3.1).

3.2.2 ANTAGONIST PHARMACOLOGY OF MURINE $GABA_A$ RECEPTORS

Three murine $GABA_A$ receptor subunit constructs, α1β1, α1β1γ2S and α1β1γ2L were initially employed to assess the functional roles of the individual receptor subunits in the antagonism of the GABA response by the traditional $GABA_A$ antagonist, picrotoxin (Olsen, 1982). GABA-induced conductances mediated by receptors comprising α1β1 subunits were inhibited by picrotoxin in a dose-dependent manner (0.05 to 50 μM). The response to 10 μM GABA in the absence and presence of increasing concentrations of picrotoxin was measured. The inhibition of the GABA response by picrotoxin was calculated as a percentage of the response induced by the agonist in the absence of picrotoxin and plotted against the picrotoxin concentration. The resultant picrotoxin inhibition curve led to the determination of the IC_{50} for

picrotoxin as 1.3 ± 0.15 μM (Fig. 3.5; Table 3.2). GABA concentration response curve analysis revealed that in the presence of 1 μM picrotoxin there was a slight lateral shift as well as a depression of the maximum response (Fig. 3.5). A higher picrotoxin concentration (10 μM) gave virtually a complete suppression of the GABA concentration-response curve (Fig. 3.5). A lateral shift to the right of the control curve in the presence of an antagonist is indicative of a competitive mode of antagonism with a decrease in the maximal response also indicating non-competitive antagonism. Therefore picrotoxin appeared to shift the dose-response curve and decrease the maximum response suggesting a complex mode of antagonism for picrotoxin which is consistent with 'mixed inhibition' (Fig 3.5; Smart and Constanti, 1986). There was a small increase in both the EC_{50}s and Hill coefficients for GABA in the presence of picrotoxin (Table 3.2).

To determine whether the γ2 subunit affected the antagonism of the GABA-induced responses by picrotoxin cDNAs were injected into oocytes encoding α1β1γ2S or α1β1γ2L $GABA_A$ receptor subunits. GABA-induced conductances mediated by receptors comprising α1β1γ2S or α1β1γ2L subunits were also inhibited by picrotoxin (0.01 to 100 μM). The construction of picrotoxin inhibition curves for α1β1γ2S and α1β1γ2L $GABA_A$ receptors led to the determination of IC_{50} values for picrotoxin as 2.65 ± 0.2 μM and 0.99 ± 0.22 μM respectively (Fig. 3.6/3.7; Table 3.2). GABA concentration-response curve analysis for each receptor construct revealed that in the presence of picrotoxin (2.5 to 5 μM) there was again a small lateral shift with a depression in the maximum (Fig. 3.6/3.7). This is consistent with a mixed/non-competitive type of inhibition. There was also a small increase seen in the EC_{50}s and Hill coefficients for GABA in the presence of picrotoxin (Table 3.2).

To further ascertain the functional roles of the individual $GABA_A$ receptor subunits, the affinity of bicuculline was investigated in receptors consisting

of α1β1, α1β1γ2S and α1β1γ2L subunits. Equilibrium dose-response curves were constructed revealing rightward shifts in a parallel manner with increasing bicuculline concentration. Moreover, the equilibrium response curves did not exhibited any depression in the maximum response, compatible with a competitive mode of antagonism (Fig. 3.8/3.9/3.10). For the receptor constructs α1β1, α1β1γ2S and α1β1γ2L there were occasional significant increases in the Hill coefficients and large increases in the EC_{50} values for GABA in the presence of bicuculline (Table 3.3). From the dose-response relationships the GABA concentrations giving approximately 50% of the maximal conductance were ascertained on the control curve and for the curves in the presence of bicuculline. The concentrations of GABA in the presence of bicuculline were then used to calculate the dose ratio (DR) for each bicuculline concentration. Schild plots of log. agonist (DR-1) against log. antagonist concentration were then constructed for the three receptor constructs (see methods; Fig. 3.8/3.9/3.10; Arunlakshana and Schild, 1959). The lower left hand plots show least square regression lines fitted to the data without slope constraints and with 95% confidence limits. Derived pA_2 values with 95% confidence limits and the slope of each generated line are given in Table 3.4. The lower right hand plots indicate least square regression lines for the same data with the slopes constrained to unity yielding pA_2 values for α1β1, α1β1γ2S and α1β1γ2L of 5.87, 5.83 and 5.86 respectively (Table 3.4; Jenkinson, 1991; see methods).

In order to ascertain the functional role of the δ subunit in the $GABA_A$ receptor construct two further $GABA_A$ receptors consisting of α1β1δ and α1β1γ2Sδ subunits were expressed in *Xenopus* oocytes. For both receptors GABA-induced an inward current and conductance increase which was antagonised by bicuculline (10 μM) and picrotoxin (10 μM; Fig. 3.11A,B). Zinc has previously been shown to be an antagonist on cultured embryonic neuronal $GABA_A$ receptors (Westbrook and Mayer, 1987; Smart and Constanti, 1990). Application of 250 μM zinc to α1β1δ $GABA_A$ receptor

constructs completely blocked the GABA-induced current and conductance change (Fig. 3.11A). Conversely, bath applied zinc (100 μM) had little effect on $GABA_A$ receptors composed of $\alpha1\beta1\gamma2\delta$ subunits (Fig. 3.11B).

3.2.3 POSITIVE MODULATORS OF THE $GABA_A$ RECEPTOR

The enhancement of the GABA-induced response by benzodiazepines has previously been shown to depend on the composition of the $GABA_A$ receptors, with the benzodiazepine enhancement of GABA-induced responses only occurring in heteromeric constructs containing a γ subunit (Pritchett *et al.*, 1989; cf Malherbe *et al.*, 1990a; for review see Sieghart, 1989; Doble and Martin, 1992). In order to determine the effect of subunit composition on the modulation of the GABA response by benzodiazepines and other drugs acting at the barbiturate and neurosteroid binding site(s) five murine $GABA_A$ receptor subunit constructs were assembled, $\alpha1\beta1$, $\alpha1\beta1\gamma2S$, $\alpha1\beta1\gamma2L$, $\alpha1\beta1\delta$, and $\alpha1\beta1\gamma2S\delta$.

Bath-application of 1 μM flurazepam had no effect on the GABA-induced current and conductance increase in oocytes expressing $\alpha1\beta1$ $GABA_A$ receptors (Fig. 3.12A). Conversely, application of pentobarbitone (25 μM) to this receptor construct potentiated the GABA-evoked response (Fig. 3.12A). The degree of potentiation of the GABA-induced response produced by different concentrations of pentobarbitone was examined by repeatedly exposing the oocytes to a fixed dose of GABA together with different concentrations of pentobarbitone. The resultant pentobarbitone potentiation curve of the GABA-evoked conductance increase revealed an EC_{50} value for pentobarbitone of 56 ± 2.4 μM with the maximal increase in the GABA response induced by 500 μM pentobarbitone of 708.7 ± 15% (Fig. 3.12B; Table 3.5). Equilibrium dose-response curves for GABA (0.01 to 500 μM) revealed that flurazepam (1 μM) had no effect on the dose-response curve; however pentobarbitone (50 μM) shifted the curve to the left with an increase in the maximum

response (Fig. 3.12B). The EC_{50} values and Hill coefficients remained relatively unaffected by flurazepam, whilst pentobarbitone decreased the EC_{50} and increased the Hill coefficient for GABA (Table 3.6).

As expected, the addition of the γ2S subunit to this receptor complex yielding receptors with α1β1γ2S subunit constructs revealed a sensitivity to the benzodiazepines which appeared to be absent in α1β1 $GABA_A$ receptor complexes (Levitan *et al.*, 1988; Pritchett *et al.*, 1989; Horne *et al.*, 1993). Application of 1 μM flurazepam potentiated the GABA-induced current and conductance change (Fig. 3.13A). Pentobarbitone (50 μM) and pregnanolone (500 nM) also potentiated the GABA-induced response (Fig. 3.13A). The potentiation produced by diazepam, flurazepam and pentobarbitone on the GABA-induced response was dependent on the concentration of each drug applied. As the concentration of each drug was raised the conductance change evoked by 10 μM GABA increased along a sigmoidal curve with the maximal increases in the GABA response induced by flurazepam, diazepam and pentobarbitone being: 52.2 ± 2.4% (2.5 μM), 57.1 ± 1.6% (0.25 μM) and 190 ± 4.9% (500 μM) respectively (Fig. 3.13B; Table 3.5). The EC_{50} values for the potentiation induced by diazepam, flurazepam and pentobarbitone of the GABA-induced responses are 0.05 ± 0.003, 0.17 ± 0.02 and 21.97 ± 1.9 μM respectively (Table 3.5). Construction of equilibrium dose-response curves for GABA revealed a shift to the left in the presence of 1 μM flurazepam and 50 μM pentobarbitone with an increase in the maximum only in the presence of the barbiturate (Fig. 3.13B). The Hill coefficient values remained relatively unaffected with a decrease in the EC_{50} values for GABA in the presence of flurazepam and pentobarbitone (Table 3.6).

A similar picture to the α1β1γ2S $GABA_A$ receptor complex was seen for the α1β1γ2L subunit receptor construct. Flurazepam (1 μM) and pentobarbitone (25 μM) potentiated the GABA-induced current and conductance increase (Fig. 3.14A). The potentiation of the response to a fixed dose of GABA (10 μM)

by flurazepam and pentobarbitone was concentration dependent (Fig. 3.14B). The maximal increase of the GABA-induced response for flurazepam and pentobarbitone was 51.4 ± 1.3% (2.5 μM) and 239.8 ± 7.6% (500 μM) with EC_{50} values for the potentiation of 0.17 ± 0.01 and 28.23 ± 2.8 μM respectively (Table 3.5). Construction of equilibrium dose response curves for GABA again revealed similarities with the α1β1γ2S receptors with a shift to the left in the presence of 1 μM flurazepam and 50 μM pentobarbitone and an increase in the maximum in the presence of the barbiturate (Fig. 3.14B). The Hill coefficient values remained relatively unaffected with a decrease in the EC_{50} values for GABA in the presence of flurazepam and pentobarbitone (Table 3.6).

The addition of a γ2 subunit, γ2S or γ2L, to the α1β1 $GABA_A$ receptor was shown to confer a sensitivity of the resulting receptor construct to the benzodiazepines. Therefore, it was interesting to ascertain whether or not the δ subunit could also modulate the benzodiazepine sensitivity of $GABA_A$ receptors. Oocytes were injected with cDNAs encoding murine α1β1δ $GABA_A$ subunits. These receptor constructs revealed a similar sensitivity to benzodiazepines and barbiturates to the α1β1 $GABA_A$ receptor construct. Application of 1 μM flurazepam and 1 μM diazepam failed to potentiate the GABA-induced response indicating that the presence of the δ subunit did not induce the same benzodiazepine sensitivity as the γ2 subunits in the $GABA_A$ receptor (Fig. 3.15A). Conversely, application of 50 μM pentobarbitone potentiated the GABA response (Fig. 3.15A). Interestingly, murine α1β1γ2Sδ $GABA_A$ receptors revealed a similar sensitivity to the positive modulators of the $GABA_A$ receptor as the α1β1γ2S receptor constructs. The GABA-induced current and conductance increase was potentiated by the application of flurazepam (1 μM), diazepam (1 μM), pentobarbitone (50 μM) and pregnanolone (500 nM). As for the α1β1γ2S receptor construct, 1 μM diazepam appeared to be more potent in potentiating the GABA-induced response than 1 μM flurazepam in this receptor complex. Interestingly, the

addition of the δ subunit to either α1β1 or α1β1γ2S receptor constructs yielding receptors with the subunit composition α1β1δ and α1β1γ2Sδ seemingly had little or no effect on the sensitivity of the $GABA_A$ receptor to positive modulators.

3.2.4 COMPARISON OF $GABA_A$ RECEPTORS FROM TWO DIFFERENT SPECIES

To ascertain whether the pharmacological profile of $GABA_A$ receptor constructs was dependent on the species used the pharmacological properties of the murine receptor constructs α1β1 and α1β1γ2S were compared to the equivalent bovine $GABA_A$ receptor subunits. Oocytes expressing bovine α1β1 and α1β1γ2S $GABA_A$ receptor subunits responded to GABA (10 μM), isoguvacine (10 μM) and muscimol (10 μM) with large consistent membrane currents and conductances (Fig. 3.16A/3.17A). For the bovine α1β1 receptor the benzodiazepine, flurazepam (1 μM) failed to potentiate the GABA-induced response (Fig. 3.16A). Conversely, pentobarbitone (50 μM) potentiated the GABA-evoked current and conductance change (Fig. 3.16A). The positive potentiators of the $GABA_A$ receptor therefore appeared to have the same effect on both the α1β1 receptor constructs from murine and bovine species. As expected, both flurazepam (1 μM) and pentobarbitone (25 μM) potentiated the GABA-evoked response as for the murine α1β1γ2S $GABA_A$ receptor construct (Fig. 3.17A). Furthermore, for both receptor constructs bicuculline (10 μM) and picrotoxin (10 μM) antagonised the GABA-induced responses (Fig. 3.16B/3.17B).

Therefore, both bovine α1β1 and α1β1γ2S $GABA_A$ receptor constructs appeared to have similar pharmacological profiles to the equivalent murine $GABA_A$ receptors.

3.3 DISCUSSION

Functional $GABA_A$ receptors were expressed after microinjection with cRNAs or cDNAs and the pharmacological profile appeared to depend on the exact subunit composition. Interestingly, functional $GABA_A$ receptors comprising $\alpha1\beta1$ subunits were expressed in *Xenopus* oocytes. This demonstrated that not all the subunits identified for the $GABA_A$ receptor are required to be microinjected for the formation of functional $GABA_A$ receptors suggesting that at least some of the subunits share some functional homology.

3.3.1 THE EFFECT OF SUBUNIT COMPOSITION ON $GABA_A$ RECEPTOR FUNCTION

3.3.1.1 EXPRESSION AND AGONIST PHARMACOLOGY

Xenopus oocytes expressing murine $\alpha1\beta1$, $\alpha1\beta1\gamma2S$, $\alpha1\beta1\gamma2L$, $\alpha1\beta1\delta$ and $\alpha1\beta1\gamma2\delta$ subunits produced functional $GABA_A$ receptors. Previous studies have revealed that $GABA_A$ receptors composed of rat $\alpha1\gamma2$ subunits expressed in human embryonic kidney cells resulted in functional channels with large whole-cell conductances (Verdoorn et al., 1990; Draguhn *et al.*, 1990). However, Angelotti and colleagues cotransfected $\alpha1\beta1$, $\alpha1\beta1\gamma2S$ and $\alpha1\gamma2S$ subunit combinations in mammalian cell lines with only the two former $GABA_A$ receptor combinations producing functional channels (Angelotti *et al.*, 1993). The results in *Xenopus* oocytes would agree with this study where the expression of functional $GABA_A$ receptors required the presence of $\beta1$ subunits. The absence of a β subunit was also shown to lead to GABA receptors mediating very small current amplitudes in *Xenopus* oocytes (Sigel *et al.*, 1990). Furthermore, a recent study indicated that the $GABA_A$ receptor required two domains present in the β-subunit for activation by GABA (Amin and Weiss, 1993). The importance of the β subunit in the functional expression of $GABA_A$ receptors and receptor pharmacology has been studied

in greater detail in chapter 4.

There have been relatively few attempts to quantify the potencies of $GABA_A$ receptor agonists. Relative potencies have been studied in spinal cord and brain slice preparations but the results in these cases depend on the susceptibilities of the agonists to uptake and also the anatomical arrangement and density of uptake sites in relation to receptors in the tissue. Therefore, from measuring induced depolarisations or inhibition of action potential firing, the potency of muscimol, which is slowly taken up (Johnston *et al.*, 1978), is greater than that of GABA by a factor of 5 in spinal root fibres (Allan *et al.*, 1980) and rat sympathetic ganglia (Bowery *et al.*, 1978); by a factor of 35 for dorsal funiculus depolarisations in rat cuneate nucleus (Pickles and Simmonds, 1980); and by a factor of 833 in rat hemisected spinal cord preparations (Allan *et al.*, 1980). Furthermore, Kemp *et al* (1986), by measuring the inhibition of population spikes, revealed muscimol to be approximately 7.5 fold more potent on $GABA_A$ receptors than isoguvacine in the rat hippocampal slice preparation. These results are in broad agreement with the potency order of agonists seen in this study. In *Xenopus* oocytes, where no GABA uptake sites are present (Houamed, 1988), muscimol was approximately four times more potent than GABA on $GABA_A$ receptors expressed from chick brain mRNA (Smart *et al.*, 1987). The present study revealed that muscimol was also approximately four times more potent than GABA on recombinant $\alpha1\beta1\gamma2L$ $GABA_A$ receptors and nine times more potent on $\alpha1\beta1$ $GABA_A$ receptors. It is possible that the $GABA_A$ receptors expressed from chick brain mRNA contained $\alpha1\beta1\gamma2$ subunits leading to the similarity of the agonist potency ratio to the $\alpha1\beta1\gamma2L$ $GABA_A$ receptors. Interestingly, in the present study each agonist appeared to have a greater affinity for the $\alpha1\beta1$ receptor compared to the $\alpha1\beta1\gamma2L$ $GABA_A$ receptor construct with an approximate two fold increase in affinity for GABA and isoguvacine and four fold increase for muscimol on the former receptor construct (Table 3.1). Addition of the δ subunit to the $\alpha1\beta1$ receptor construct yielding $\alpha1\beta1\delta$

$GABA_A$ receptors had little effect on the apparent GABA affinity. Interestingly, the addition of the δ subunit to the α1β1γ2S receptor construct forming α1β1γ2Sδ $GABA_A$ receptors appeared to decrease the GABA affinity for the receptor by approximately two and a half fold. The ability of the δ subunit to lower the affinity of GABA for the receptor in α1β1γ2S compared to α1β1 receptors is intriguing. It could be possible that the actual quaternary structure of the two receptors is different so that the δ subunit has more influence on the affinity of GABA on the α1β1γ2S receptor compared to the α1β1 $GABA_A$ receptor.

The maximal response induced by GABA also depended on the subunit composition of the $GABA_A$ receptor (Fig. 3.1B/3.2B/3.3B/3.4B). The rank order of maximal response for GABA on the various $GABA_A$ receptors was:

$$\alpha1\beta1\gamma2S\delta >> \alpha1\beta1\gamma2S = \alpha1\beta1\gamma2L > \alpha1\beta1 = \alpha1\beta1\delta.$$

In agreement with these results, Moss and colleagues revealed that α1β1 $GABA_A$ receptors expressed in cultured hamster ovary cells had a smaller main conductance state (19 pS) and mean apparent open time (1.7 ms) compared to $GABA_A$ receptor channels recorded from mouse spinal cord neurones (main conductance state of 27 pS and mean open time of 6 ms; Moss *et al.*, 1990). Furthermore, Angelotti and colleagues revealed that the maximum amplitude of α1β1γ2S $GABA_A$ receptor single-channel currents were larger than α1β1 $GABA_A$ receptor currents when expressed in L929 cells (Angelotti and Macdonald, 1993; Angelotti *et al.*, 1993).

A number of previous studies have ascertained EC_{50} values and Hill coefficients for GABA on recombinant $GABA_A$ receptors. Sigel and colleagues revealed that oocytes expressing rat α1β1 and α1β1γ2 $GABA_A$ receptors displayed no cooperativity for GABA-dependent gating of the channel, with Hill coefficients around unity (Sigel *et al.*, 1990). In agreement a further study revealed rat α1β1γ2 $GABA_A$ receptors expressed in *Xenopus* oocytes also had a similar Hill coefficient of 1.03 (Malherbe *et al.*, 1990b). This lack of

cooperativity for GABA-gating was also observed in *Xenopus* oocytes expressing bovine α1β1 $GABA_A$ receptors (Levitan *et al.*, 1988) and in mammalian cell lines expressing human α1β1 and α1β1γ2 $GABA_A$ receptors (Pritchett *et al.*, 1989). This study revealed a Hill coefficient of 0.95 ± 0.09 for murine α1β1 $GABA_A$ receptors indicating a similar lack of cooperativity of GABA-dependent gating of the channel. The addition of a γ2 subunit slightly increased the Hill coefficients and α1β1γ2Sδ $GABA_A$ receptors possessed the largest cooperativity. A similar increase in Hill coefficients in $GABA_A$ receptors containing γ2 subunits was seen for α1β1γ2L (1.66 ± 0.019) compared to α1β1 (1.45 ± 0.019) bovine $GABA_A$ receptors (Horne *et al.*, 1993). Hadingham and colleagues reported that cell lines transfected with bovine α1β1γ2L $GABA_A$ receptors had quite high cooperativity with a Hill coefficient of 1.9 ± 0.2 (Hadingham *et al.*, 1992) which is closer to Hill slopes established from native neuronal $GABA_A$ receptors (Akaike *et al.*, 1986). These previous results indicate that the Hill coefficient of the same recombinant $GABA_A$ receptors even when expressed in the same system can give a significant degree of variability. This variability in results was also seen for the EC_{50} value obtained for GABA from different studies. *Xenopus* oocytes expressing rat α1β1 receptors had an EC_{50} value of 13 ± 7 μM and for α1β1γ2 74 ± 13 μM (Sigel *et al.*, 1990; Malherbe *et al.*, 1990b). For bovine α1β1 $GABA_A$ receptors EC_{50} values of 12 ± 1 μM (Levitan *et al.*, 1988) and 5.6 ± 0.02 μM (Horne *et al.*, 1993) have been reported. For $GABA_A$ receptors composed of bovine α1β1γ2L subunits, EC_{50} values were reported as 5.2 ± 0.1 μM (Hadingham *et al.*, 1992), 41 ± 7.3 μM (Wafford *et al.*, 1992) and 5.2 ± 0.09 μM (Horne *et al.*, 1993). This study determined EC_{50} values for GABA of 5.87 ± 0.7 μM for α1β1 receptors and approximately 10 μM for receptors containing γ2 subunits. A number of explanations could account for these variations. The stoichiometry of receptor subunits within the $GABA_A$ receptor, following expression of the same cRNAs or cDNAs, could be changeable leading to variabilities in Hill coefficients and EC_{50} values. Another possibility is that the values could be calculated from a limited agonist dose response curve, where the maximum

response may not be clear, leading to inaccuracies in determining both Hill coefficients and EC_{50} values. The different degrees of phosphorylation of the $GABA_A$ receptors could also affect Hill coefficients and EC_{50} values (for review see Stelzer, 1992; also see chapter 6). A further interesting possibility is that receptor density could modify the agonist response on $GABA_A$ receptors giving rise to variations in the EC_{50} and Hill coefficients. This has been observed for human glycine receptors where the affinity of agonists increased at high receptor densities (Taleb and Betz, 1994). The glycine receptor subunits, α and β, share a common transmembrane topology and significant sequence homology to the $GABA_A$ receptor subunits. Therefore the intriguing possibility remains that the $GABA_A$ receptor pharmacology may be affected by the phenomenon of receptor clustering/density, which if proven to be true could have important consequences for neurotransmitter efficacy at the geometrically compact inhibitory synapse.

3.3.1.2 ANTAGONIST PHARMACOLOGY

To further characterise the pharmacological profile of the $GABA_A$ receptor constructs and determine the role(s) of the individual subunits of the receptor the antagonist profiles of murine α1β1, α1β1γ2S, α1β1γ2L, α1β1δ and α1β1γ2δ subunits were studied. Interestingly, $GABA_A$ receptors comprising of α1β1γ2S subunits appeared to be less sensitive to blockade by picrotoxin than either α1β1 or α1β1γ2L receptors (Table 3.2). It could be possible that the γ2S subunit confers a decreased sensitivity by altering the quaternary structure of the receptor. Verdoorn and colleagues revealed that α1β2γ2 $GABA_A$ receptors, when expressed in human embryonic kidney cells, displayed a unique profile with respect to single-channel conductance and concentration-response relationship, compared to α1β2 $GABA_A$ receptors (Verdoorn *et al.*, 1990). Intriguingly, the additional eight amino acids present in the γ2L subunit compared to the γ2S subunit seemingly had the ability to increase the sensitivity of the receptor to picrotoxin, such that both the α1β1 and

$\alpha1\beta1\gamma2L$ receptors had similar IC_{50} values for picrotoxin. It could be possible that these extra amino acids alters the quaternary structure of the resulting $GABA_A$ receptor such that the picrotoxin binding site on $\alpha1\beta1\gamma2L$ receptors is similar to that of $\alpha1\beta1$ receptors. In comparison picrotoxin IC_{50} values have previously been revealed for chick brain mRNA injected *Xenopus* oocytes of approximately 0.6 μM (Sigel and Baur, 1988) and for rat $\alpha1\beta1\gamma2$, $\alpha5\beta2\gamma2$, $\alpha1\beta2\gamma2$ and $\beta2\gamma2$ $GABA_A$ receptors of approximately 1 μM (Sigel *et al.*, 1990). Therefore, from these previous studies the binding site for picrotoxin seems to be relatively non-specific in terms of subunit isoform requirements. Interestingly, the β1 subunit alone is sufficient to form a picrotoxin binding site (Sigel *et al.*, 1989; Blair *et al.*, 1988; see chapter 4), but the β subunit may not to be an essential component for the formation of a picrotoxin binding site since $\alpha3\alpha5\gamma2$ $GABA_A$ receptors retain a sensitivity towards picrotoxin (Sigel *et al.*, 1990).

Ffrench-Constant and colleagues revealed that one amino acid change, a point mutation of alanine to serine within the second membrane spanning domain (Rdl), conferred high levels of resistance to picrotoxin of GABA responses in the fruit fly, *Drosophila melanogaster* (Ffrench-Constant *et al.*, 1993). It will be of interest to determine, using a point-mutational study, whether or not this domain is important in conferring picrotoxin sensitivity to mammalian $GABA_A$ receptors.

Schild analysis of the dose-response curves in the presence of bicuculline determined pA_2 values for $\alpha1\beta1$, $\alpha1\beta1\gamma2S$ and $\alpha1\beta1\gamma2L$ $GABA_A$ receptors of 5.87, 5.83 and 5.86 respectively These apparent pA_2 values suggested that the affinity of the antagonist appears to be relatively unaffected by the subunit isoforms present within the $GABA_A$ receptor construct. One previous study on bovine $\alpha1\beta1\gamma2L$ $GABA_A$ receptor revealed a similar pA_2 value for bicuculline of 6.4 (Horne *et al.*, 1992). In comparison to the recombinant $GABA_A$ receptors, native neuronal $GABA_A$ receptors revealed a pA_2 value for bicuculline on the rat cuneate nucleus slice of 5.93 (Simmonds, 1982).

Furthermore, bicuculline antagonised the isoguvacine and muscimol induced inhibition of hippocampal population spikes with pA_2 values of 6.24 and 6.10 respectively (Kemp *et al.*, 1986). The similarity in the pA_2 values for bicuculline on native neuronal $GABA_A$ receptors, which probably represents a heterogenous population of $GABA_A$ receptors, to the pA_2's ascertained from recombinant $GABA_A$ receptors in this study, would be expected as the antagonism by bicuculline is probably independent of the subunit composition.

Interestingly, zinc was shown to antagonise the GABA-induced responses at murine $\alpha1\beta1\delta$ $GABA_A$ receptors but not $\alpha1\beta1\gamma2\delta$ receptor constructs. Previous studies have revealed the importance of the composition of the $GABA_A$ receptor for the inhibition of GABA-induced responses by zinc. Smart *et al.* (1991) reported that $GABA_A$ receptors which lacked the $\gamma2$ subunit were inhibited by zinc in mouse $\alpha1\beta1$ $GABA_A$ receptors expressed in human embryonic kidney cells. The addition of a $\gamma2$ subunit revealed a relative insensitivity to inhibition by zinc ions (Draguhn *et al.*, 1990; Smart *et al.*, 1991). These results are consistent with the zinc inhibition profile seen in $\alpha1\beta1\delta$ and $\alpha1\beta1\gamma2S\delta$ $GABA_A$ receptors used in this study. The antagonistic profile of zinc on recombinant $GABA_A$ receptors and the effect of subunit composition is discussed in further detail in chapter 5.

3.3.1.3 POSITIVE MODULATORS

Pentobarbitone potentiated the responses to GABA in oocytes expressing murine $\alpha1\beta1$, $\alpha1\beta1\gamma2S$, $\alpha1\beta1\gamma2L$, $\alpha1\beta1\delta$ and $\alpha1\beta1\gamma2\delta$ $GABA_A$ receptors. Therefore, the ability of pentobarbitone to enhance the GABA-induced responses appears to be relatively independent of the subunit composition of the $GABA_A$ receptor complex. Previous studies have revealed that pentobarbitone potentiates GABA-induced responses in $GABA_A$ receptors composed of different subunits (Levitan *et al.*, 1988; Sigel *et al.*, 1990; Hadingham *et al.*, 1992; Horne *et al.*, 1993). These results are consistent with

suggestions that the Cl^- channel itself is the site of action of the barbiturates. Moreover, direct gating of the $GABA_A$ channel has been shown to occur by pentobarbitone in the absence of GABA in a number of studies (Parker *et al.*, 1986; Levitan *et al.*, 1988; Sigel *et al.*, 1990; Malherbe *et al.*, 1990b). The present study revealed that the degree of potentiation of the GABA response depended on the concentration of pentobarbitone applied and the composition of the subunits present in the $GABA_A$ receptor. The maximal percentage increase in GABA-evoked responses by pentobarbitone was largest in $\alpha1\beta1$ receptors compared to when a $\gamma2$ subunit was present. Conversely, the EC_{50} for pentobarbitone revealed that the barbiturate had a greater affinity for the $\alpha1\beta1\gamma2S$ and $\alpha1\beta1\gamma2L$ receptors compared to $\alpha1\beta1$ $GABA_A$ receptor constructs. In addition, dose response curves for GABA showed that 50 μM pentobarbitone increased the affinity of GABA by approximately ten fold for $\alpha1\beta1\gamma2S$ and $\alpha1\beta1\gamma2L$ receptors compared to five fold for $\alpha1\beta1$ $GABA_A$ receptors; however, pentobarbitone did not appear to alter the cooperativity of the $GABA_A$ receptors.

In contrast to pentobarbitone, the ability of benzodiazepines to potentiate the GABA-induced responses was dependent on the subunit composition. The coexpression of a $\gamma2$ subunit was found to be essential for modulation by benzodiazepines as reported previously (Pritchett *et al.*, 1989; cf Malherbe *et al.*, 1990a; Sieghart, 1989; Doble and Martin, 1992). Previous studies on expressed $GABA_A$ receptors of the composition $\alpha1\beta1$ subunits revealed a lack of potentiation by benzodiazepines (Levitan *et al.*, 1988; Pritchett *et al.*, 1989; Horne *et al.*, 1993). Substitution of the δ subunit for the $\gamma2$ subunit did not render the $GABA_A$ receptor sensitive to benzodiazepines (Shivers *et al.*, 1989). Interestingly, the present study also revealed that the potentiation by benzodiazepines of the GABA-induced response on murine $\alpha1\beta1\gamma2S$ and $\alpha1\beta1\gamma2L$ $GABA_A$ receptors was characterised by a Hill coefficient for GABA of about 1 indicating that the addition of benzodiazepines to these receptors did not enhance the cooperativity of these $GABA_A$ receptor constructs. Similar

observations have previously been made for chick brain mRNA expressed in *Xenopus* oocytes (Sigel and Baur, 1988). Interestingly, the maximal degree of potentiation by flurazepam of the GABA-induced response on oocytes expressing murine α1β1γ2L or α1β1γ2S receptor constructs was very similar. Moreover, the affinity of flurazepam for the α1β1γ2S and α1β1γ2L $GABA_A$ receptor also appeared to be similar, but diazepam had a greater affinity for the α1β1γ2S. The affinity of GABA increased approximately three times in the presence of 1 μM flurazepam for α1β1γ2S and α1β1γ2L $GABA_A$ receptor constructs.

Interestingly, the neurosteroid pregnanolone potentiated the GABA-induced response on murine α1β1γ2S $GABA_A$ receptors. Previous studies indicate that the steroid modulation of the $GABA_A$ receptor was strongly influenced by the presence of both the α and the γ subunits (Shingai *et al.*, 1991; Zamin *et al.*, 1992). The influence of the δ subunit on the modulatory effect of pregnanolone was also studied on α1β1γ2δ $GABA_A$ receptors. There was no clear difference in the ability of pregnanolone to potentiate the GABA-evoked response between $GABA_A$ receptors with and without the δ subunit. However, a more detailed analysis of the effect of the δ subunit should be completed before the effect of this subunit with neurosteroids can be clearly defined.

3.3.2 SUBUNIT ROLES: IS THE EXISTENCE OF 151,887 $GABA_A$ RECEPTORS A VIABLE PROPOSITION?

The evidence reviewed in this chapter shows that the modulation of recombinant $GABA_A$ receptors by extracellularly applied ligands is dependent on the subunit composition of the $GABA_A$ receptor. The challenge that now remains is to ascribe the exact function of particular subunits within the native receptor, to determine the stoichiometry and composition of native receptors and to determine the physiological significance of the functional properties of individual subunits.

While it is clearly evident that the precise subunit composition of $GABA_A$ receptors has major effects on the pharmacological sensitivity of these complexes it is not yet clear whether this functional variety, when expressed *in vivo*, gives rise to multiple, physiologically distinct types of $GABA_A$ receptors. It is probable that subunit diversity evolved as a means for physiologically diverse types of receptor, the distribution of which could occur throughout the central nervous system in an adaptive manner. Evidence for this is already accruing with results from various studies, such as *in situ* hybridization and western blotting, of specific areas of the central nervous system indicating the expression of a limited number of subunits in contrast to a random combination of possible subunits (Wisden *et al.*, 1988; Schofield *et al.*, 1989; Shivers *et al.*, 1989; Benke *et al.*, 1991; Araki *et al.*, 1992; Bovolin *et al.*, 1992; Laurie *et al.*, 1992; Valerio *et al.*, 1992; Poulter *et al.*, 1993; Mertens *et al.*, 1993).

Furthermore, it has been demonstrated that assembly of $GABA_A$ receptor channels from $\alpha 1$, $\beta 1$ and $\gamma 2S$ subunits did not proceed randomly since not all combinations of subunits produced functional ion channels. Though the stoichiometry of the different subunits in a single native or recombinant $GABA_A$ receptor has not yet been determined, the subunits probably assemble into a pentameric structure (Nayeem *et al.*, 1994). It was calculated that 51 different configurations of a $GABA_A$ receptor with three subunits ($\alpha 1$, $\beta 1$ and $\gamma 2S$) were possible, assuming this pentameric arrangement (Burt and Kamatchi, 1991). One configuration of the $GABA_A$ receptor may have the same complement of subunits but may be arranged into different pentameric constructs. Of these, 3 would be single-subunit configurations, 18 would be two-subunit configurations (six per pair of subunits) and the remaining 30 contained all three subunits. Of the 18 two-subunit configurations, 12 were potentially $\alpha 1\gamma 2S$ and $\beta 1\gamma 2S$ $GABA_A$ configurations. These latter configurations have not been found universally to express functional $GABA_A$ receptors in the oocyte or mammalian cell lines (cf Verdoorn *et al.*, 1990;

Draguhn *et al.*, 1990). Thus, 39 different $GABA_A$ receptor configurations could exist. Of these receptor constructs, only those composed of all three subunits formed functional $GABA_A$ receptors which were sensitive to benzodiazepines. A potential candidate for a native $GABA_A$ receptor could be: $\alpha1\beta1\gamma2$ subunit construct. Therefore, it would be expected that this isoform would be selectively expressed over other subunit isoforms of the $GABA_A$ receptor, that the subunits are co-localised in specific regions of the brain and that $GABA_A$ receptors in such regions would have pharmacological profiles equivalent to that seen for these recombinant receptors. Interestingly, Angelotti and colleagues have revealed that the $\alpha1\beta1\gamma2S$ $GABA_A$ receptors appeared to be favoured over the $\alpha1\beta1$ $GABA_A$ receptor configuration, since only after increasing the $\beta1$ subunit level fourfold within a cell, relative to the $\alpha1$ and $\gamma2S$ subunits, were any diazepam-insensitive $GABA_A$ receptor currents recorded (Angelotti *et al.*, 1993). Furthermore, Mertens and colleagues revealed that the δ subunit was found to be associated with the $\alpha1$, $\alpha3$, $\beta2/3$ and $\gamma2S$ subunits using immunoaffinity chromatography (Mertens *et al.*, 1993). Therefore, this suggests that both $\gamma2S$ and δ subunit can co-localise within $GABA_A$ receptors, with the former subunit conveying a benzodiazepine sensitivity to the receptor construct. The demonstration that there exists a final preferred configuration(s) of the $GABA_A$ receptor must ultimately be confirmed using biochemical or immunocytochemical techniques. By repeating and combining the data from this and other studies on recombinant $GABA_A$ receptors composed of all possible combinations of the different subunits, it should be possible to produce a unique pharmacological signature for each conformation of the recombinant receptors for comparison to native $GABA_A$ receptors. By combining this information with the expression patterns of receptor subunit mRNAs (Laurie *et al.*, 1992), it may be possible in the future to determine the exact $GABA_A$ receptors expressed in various brain regions and ultimately determine the underlying architecture of inhibitory synaptic transmission.

Figure 3.1. Agonist sensitivity of mouse α1β1 $GABA_A$ receptors expressed in *Xenopus* oocytes. (A) Similar membrane current and conductance changes evoked by GABA (10 μM), isoguvacine (50 μM) and muscimol (1 μM). In this and all subsequent recordings the membrane conductance was monitored throughout by repetitively applying brief hyperpolarizing voltage command steps (-10mV; 1s, 0.2Hz). The solid line in each case represents the duration of drug application. Holding potential for all oocytes, -40mV. (B) Equilibrium concentration response curves for GABA, isoguvacine and muscimol which are normalised with respect to 10 μM GABA. The points represent means ± s.e.m recorded from 3 to 5 oocytes. In this and subsequent dose-response curves the data were fitted according to the logistic model (see methods).

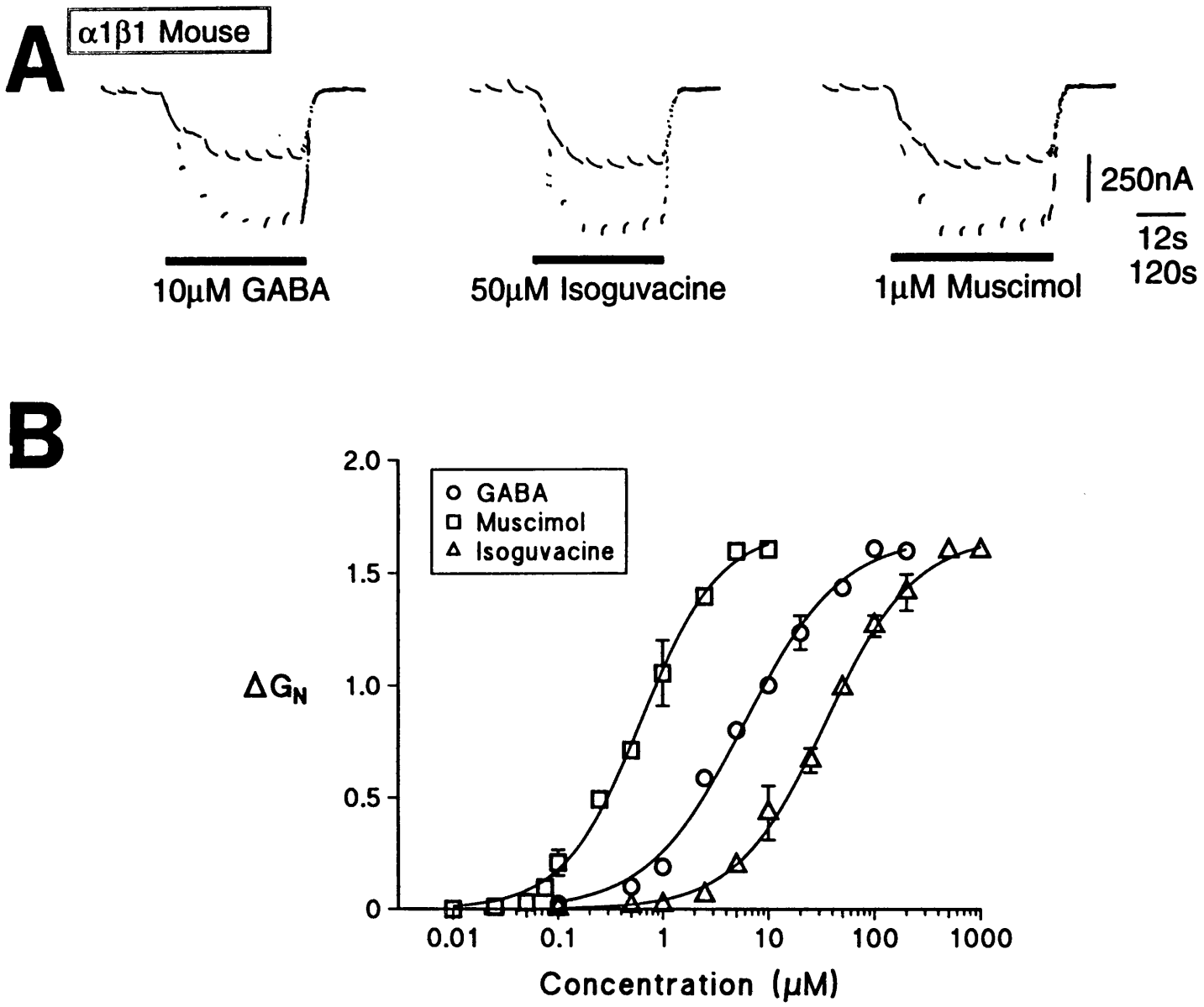
A
α1β1 Mouse
250nA
12s
120s
10μM GABA
50μM Isoguvacine
1μM Muscimol
B
GABA
Muscimol
Isoguvacine
ΔG_N
2.0
1.5
1.0
0.5
0
0.01
0.1
1
10
100
1000
Concentration (μM)

Figure 3.2. Agonist sensitivity of mouse $\alpha 1\beta 1\gamma 2L$ $GABA_A$ receptors.
(A) Membrane responses induced by GABA (10 μM), isoguvacine (75 μM) and muscimol (2.5 μM). (B) Equilibrium concentration response curves for GABA, isoguvacine and muscimol which have been normalised with respect to 10 μM GABA. The points represent means ± s.e.m recorded from 3 to 5 oocytes.

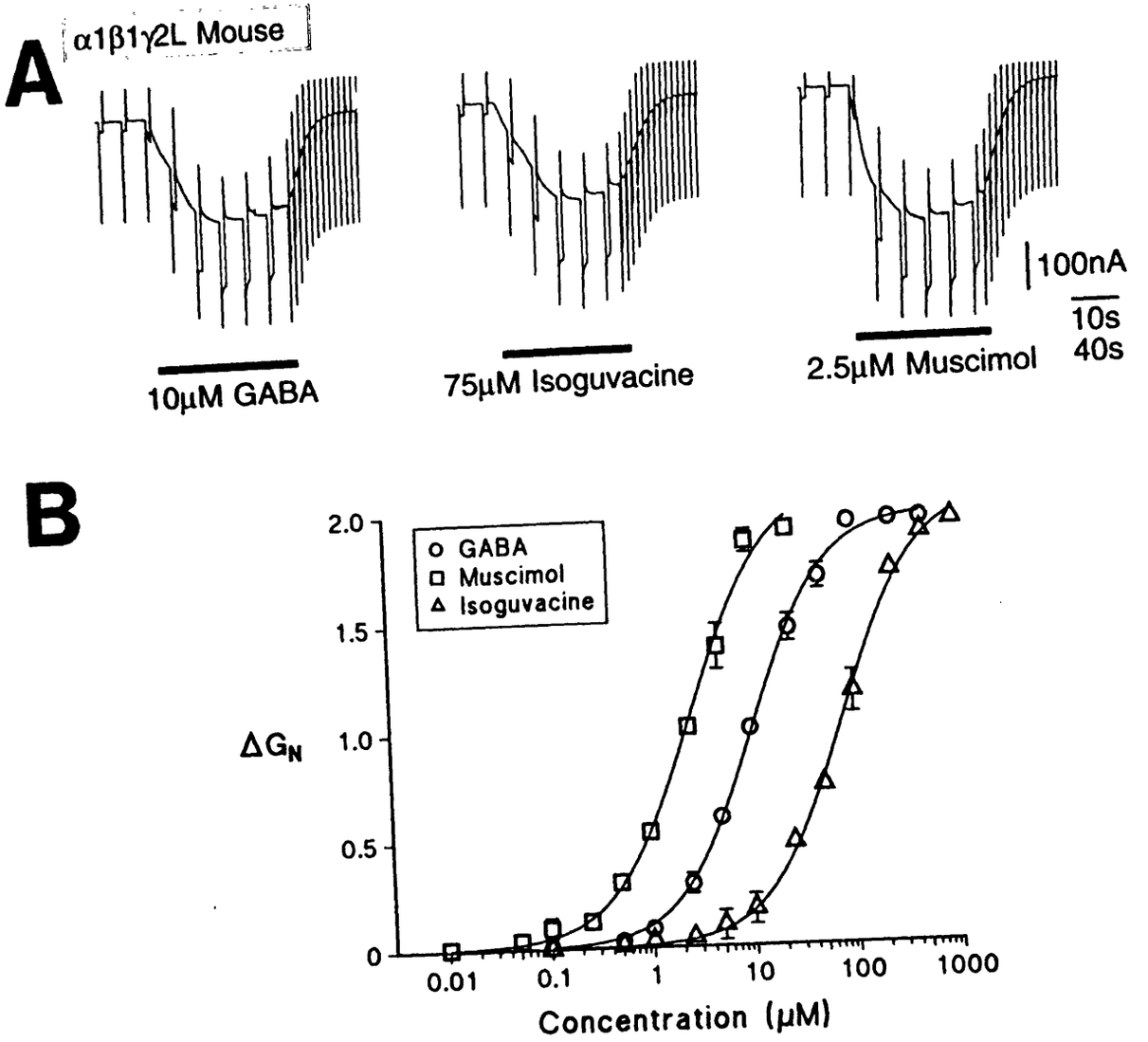
A
α1β1γ2L Mouse
100nA
10s
40s
10μM GABA
75μM Isoguvacine
2.5μM Muscimol
B
GABA
Muscimol
Isoguvacine
ΔG_N
2.0
1.5
1.0
0.5
0
0.01
0.1
1
10
100
1000
Concentration (μM)

Figure 3.3. Agonist sensitivity of mouse α1β1γ2S $GABA_A$ receptors expressed in *Xenopus* oocytes. (A) Membrane current and conductance changes evoked by GABA (10 μM), isoguvacine (75 μM) and muscimol (2.5 μM).
(B) Equilibrium concentration response curves for GABA, isoguvacine and muscimol which have been normalised with respect to 10 μM GABA. The points represent means ± s.e.m recorded from 3 to 5 oocytes.

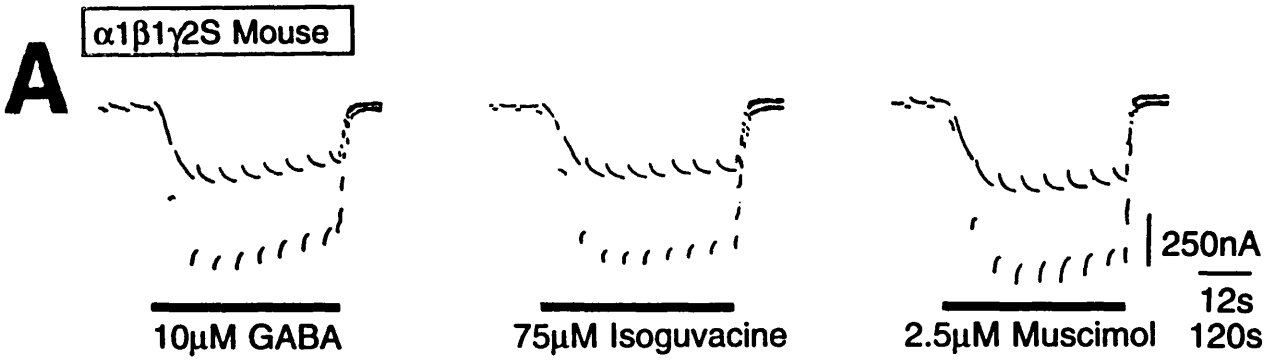
A
α1β1γ2S Mouse
250nA
12s
120s
10μM GABA
75μM Isoguvacine
2.5μM Muscimol

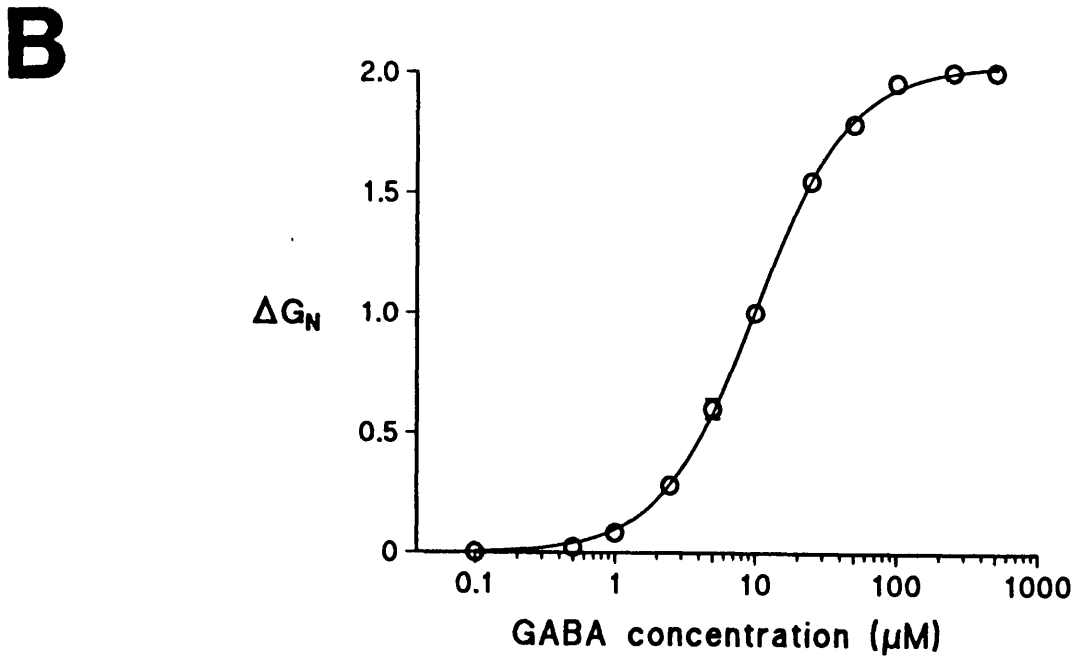
B
2.0
1.5
1.0
0.5
0
ΔG_N
0.1
1
10
100
1000
GABA concentration (μM)

Figure 3.4. Agonist sensitivity of mouse α1γ2S, α1β1δ and α1β1γ2Sδ $GABA_A$ receptors. (A) Application of 1 mM GABA, 1 mM isoguvacine and 500 μM muscimol to oocytes microinjected with α1 and γ2S $GABA_A$ cDNAs.
(B,C) GABA dose-response curves for α1β1δ (left hand plot) and α1β1γ2Sδ (right hand plot) which have been normalised with respect to 10 μM GABA. The points represent means ± s.e.m recorded from 3 to 5 oocytes.

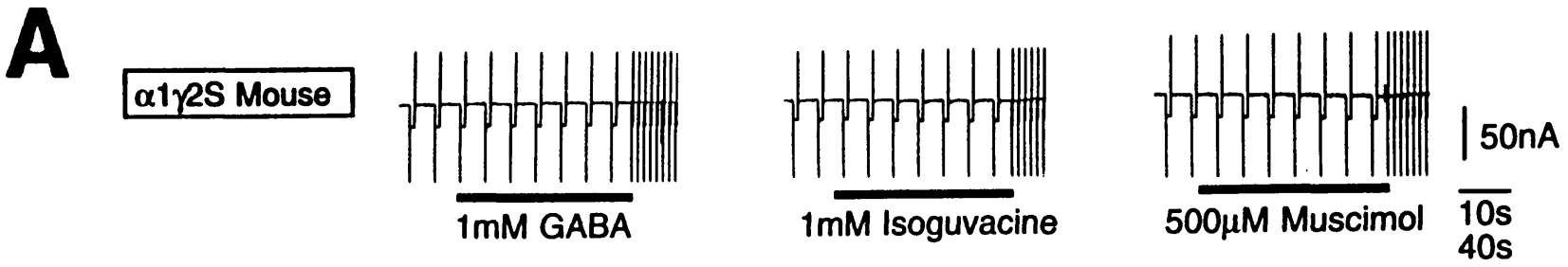
A
α1γ2S Mouse
1mM GABA
1mM Isoguvacine
500μM Muscimol
50nA
10s
40s

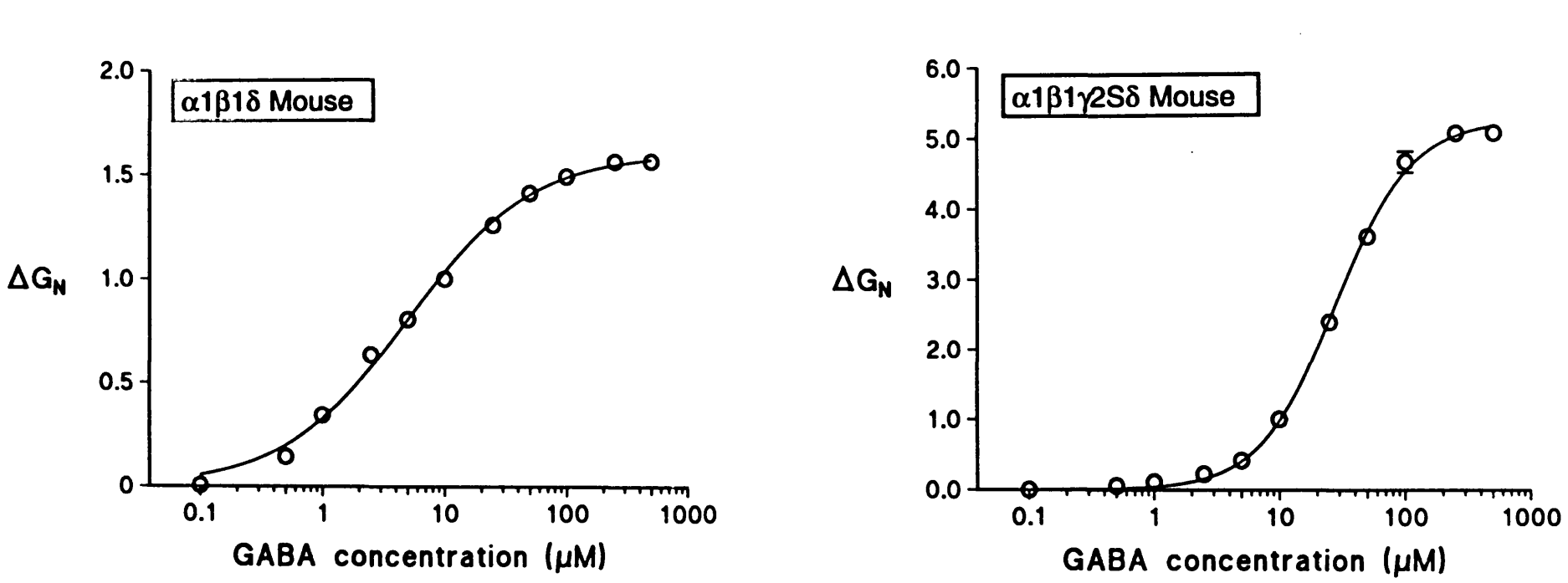
B
α1β1δ Mouse
ΔG_N
2.0
1.5
1.0
0.5
0
0.1
1
10
100
1000
GABA concentration (μM)
α1β1γ2Sδ Mouse
ΔG_N
6.0
5.0
4.0
3.0
2.0
1.0
0.0
0.1
1
10
100
1000
GABA concentration (μM)

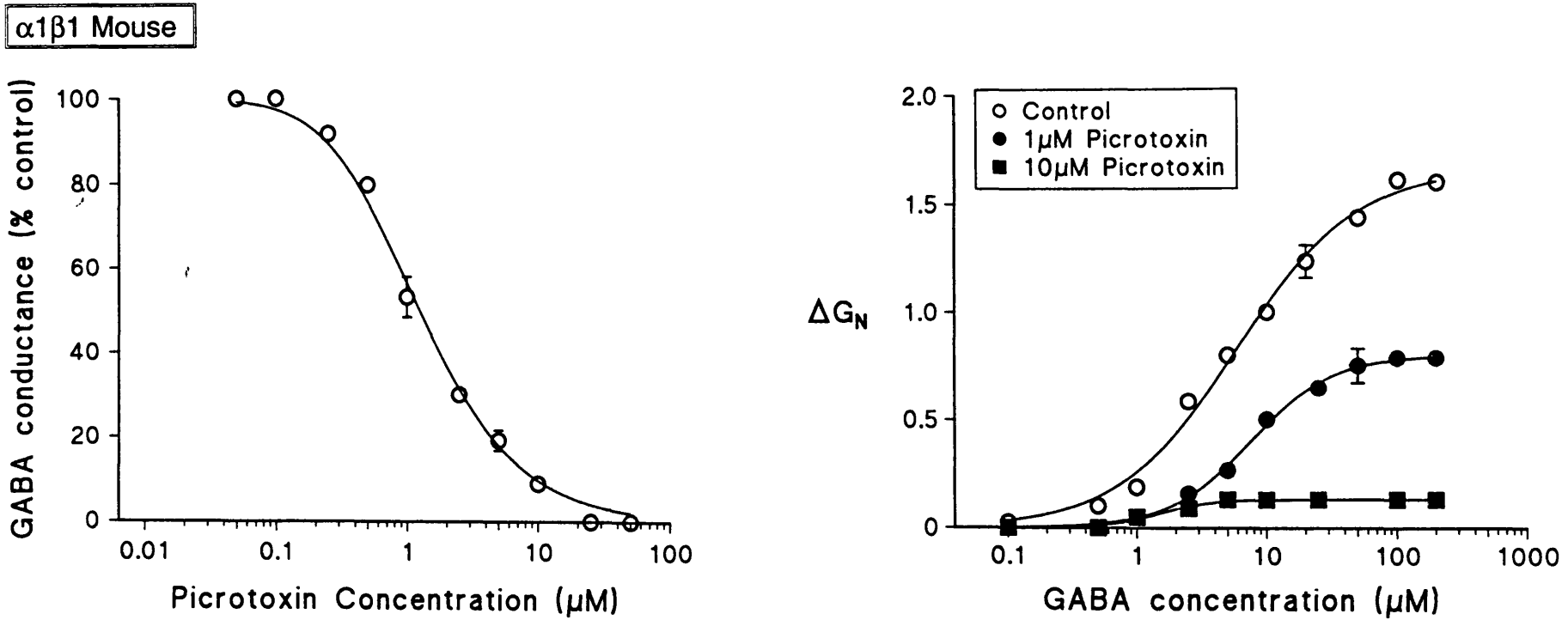

Figure 3.5. Inhibition of the GABA-induced conductance change by picrotoxin on oocytes expressing murine α1β1 $GABA_A$ receptors. The left hand plot indicates a picrotoxin inhibition curve. GABA (10 μM) was applied to the oocyte, first alone and then in combination with increasing concentrations of picrotoxin. In this and all subsequent picrotoxin inhibition curves the conductance increase evoked by 10 μM GABA in the absence of picrotoxin was taken as 100% and the curve fitted according to the antagonist inhibition model (see methods). The right hand plot indicates GABA concentration conductance curves constructed in the absence and presence of 1 and 10 μM picrotoxin and fitted according to the logistic model (see methods).

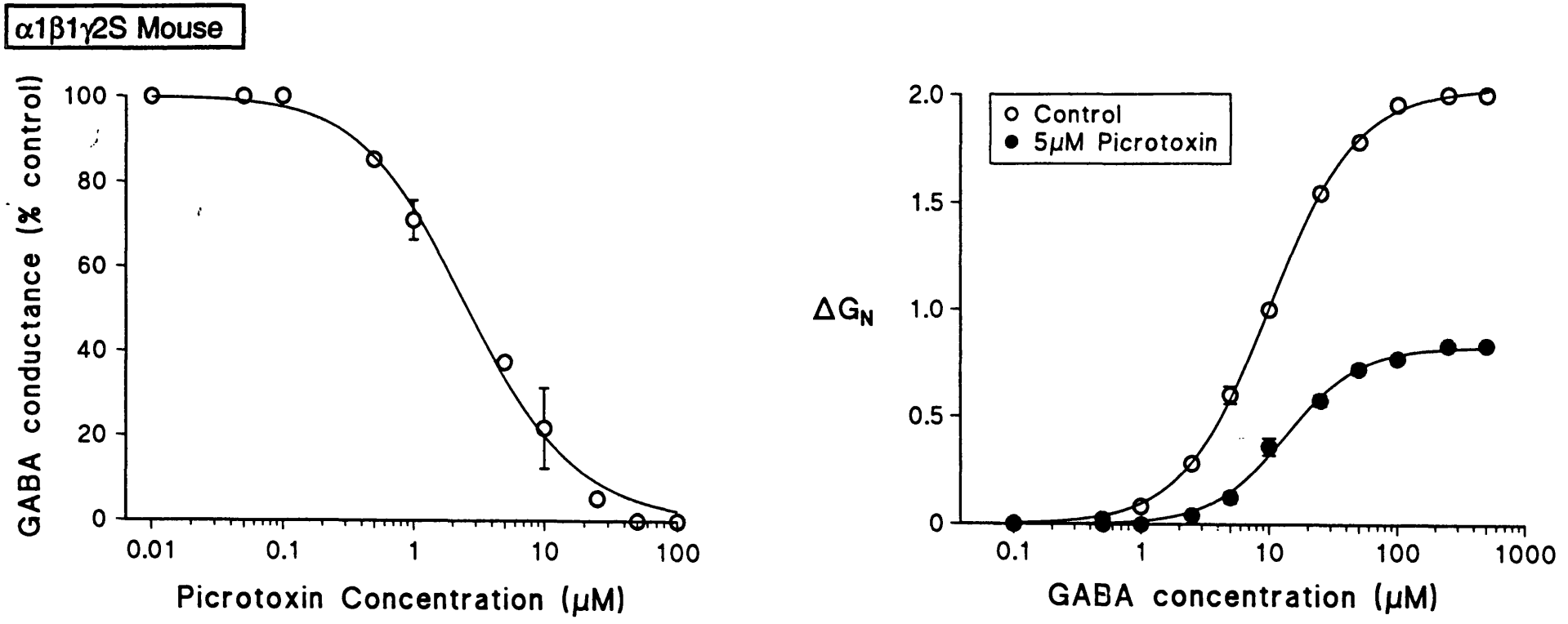

Figure 3.6. Inhibition of the GABA-induced conductance change by picrotoxin on oocytes expressing murine α1β1γ2S $GABA_A$ receptors. The left hand plot indicates a picrotoxin inhibition curve. The conductance change evoked by application of 10 μM GABA alone and following addition of different concentrations of picrotoxin was determined. The right hand plot indicates GABA concentration conductance curves constructed in the absence and presence of 5 μM picrotoxin.

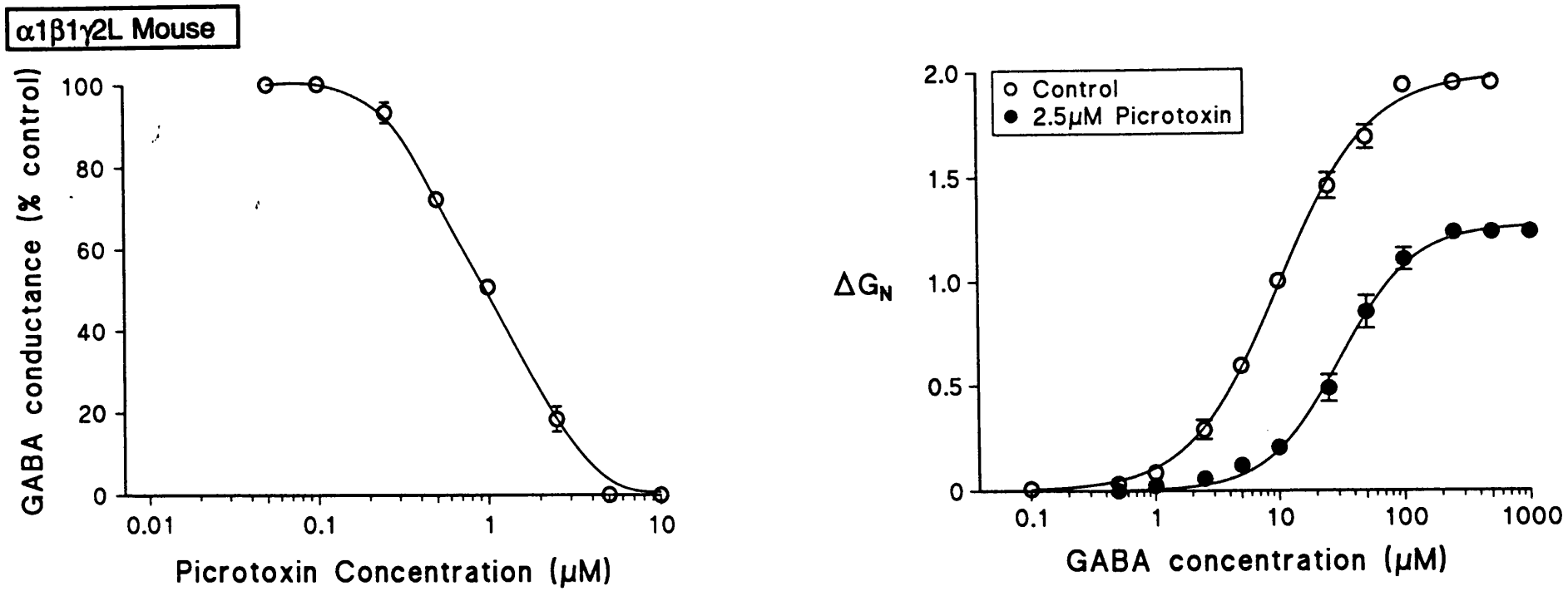

Figure 3.7. Inhibition of the GABA-induced conductance change by picrotoxin on oocytes expressing murine α1β1γ2L $GABA_A$ receptors. The left hand plot indicates a picrotoxin inhibition curve. GABA (10 μM) was applied to the oocyte, first alone and then in combination with increasing concentrations of picrotoxin. The right hand plot indicates GABA concentration conductance curves constructed in the absence and presence of 2.5 μM picrotoxin.

Figure 3.8. Antagonism of the GABA-induced conductance change by bicuculline in murine α1β1 $GABA_A$ receptors. The top plot indicates GABA concentration conductance curves constructed in the absence and presence of 5, 50 and 100 μM bicuculline. The left hand bottom plot indicates a Schild plot of log (dose ratio - 1) against - (log molar) bicuculline concentration for the antagonism of the GABA-induced response by bicuculline. The fitted line is determined by least squares regression for unweighted data (without slope constraint), with 95% confidence limits of the calculated regression. On the right, the same Schild analysis has been shown with the regression line constrained to unity (see methods). Calculated data from the regression lines are given in Table 3.4.

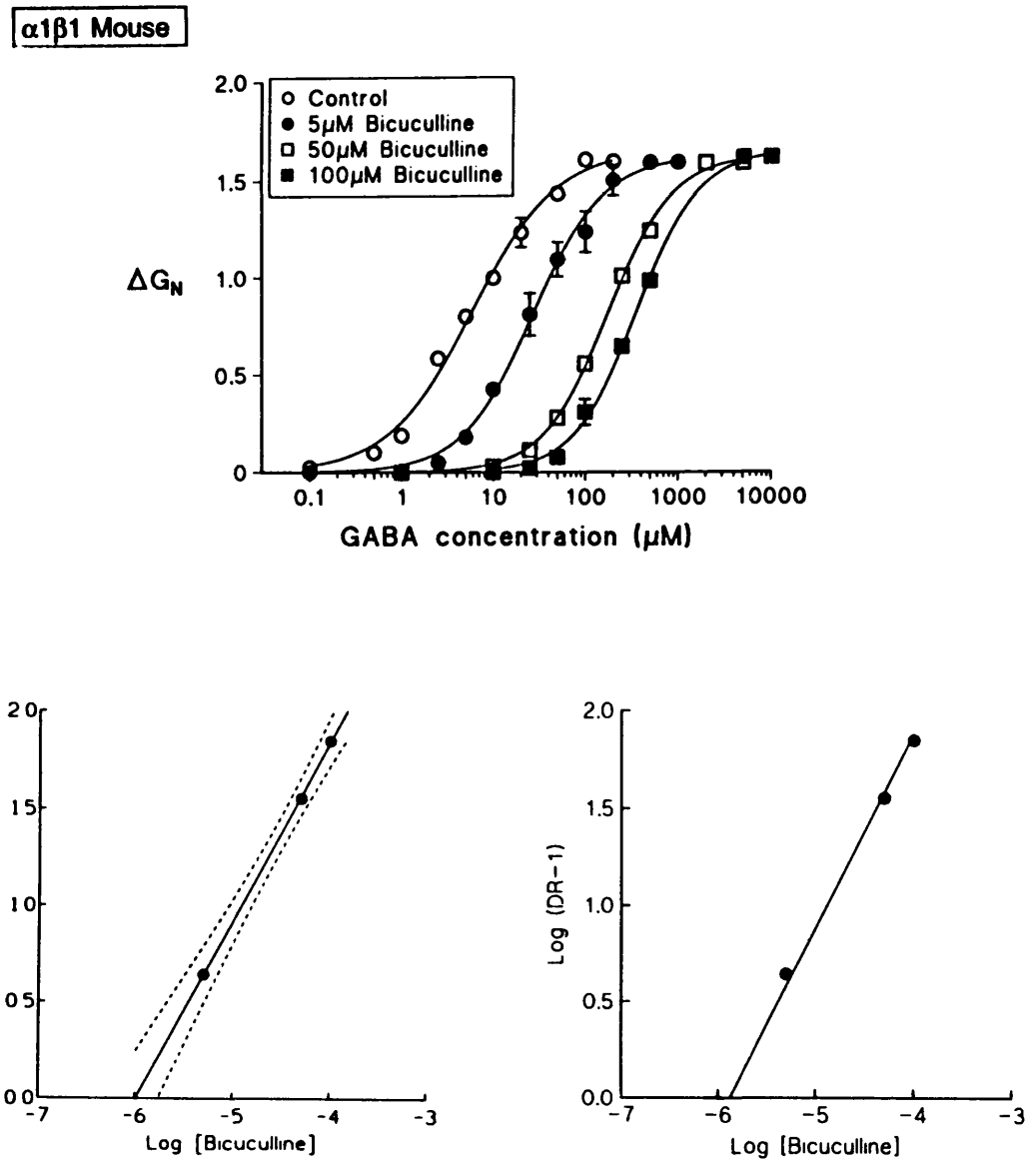
α1β1 Mouse
Control
5μM Bicuculline
50μM Bicuculline
100μM Bicuculline
ΔG_N
GABA concentration (μM)
Log (DR-1)
Log [Bicuculline]
Log (DR-1)
Log [Bicuculline]

Figure 3.9. Antagonism of the GABA-induced conductance change by bicuculline in murine $\alpha 1\beta 1\gamma 2S$ $GABA_A$ receptors. The top plot indicates GABA concentration conductance curves constructed in the absence and presence of 5, 10, 25, 50 and 100 μM bicuculline. The bottom left hand plot indicates a Schild plot of log (dose ratio - 1) against - (log molar) bicuculline concentration for the antagonism of the GABA-induced response by bicuculline. The line is a least squares regression line for unweighted data (without slope constraint), with 95% confidence limits of the calculated regression. On the right, the same Schild analysis has been shown with the regression line constrained to unity (see methods). Calculated data from the regression lines are given in Table 3.4.

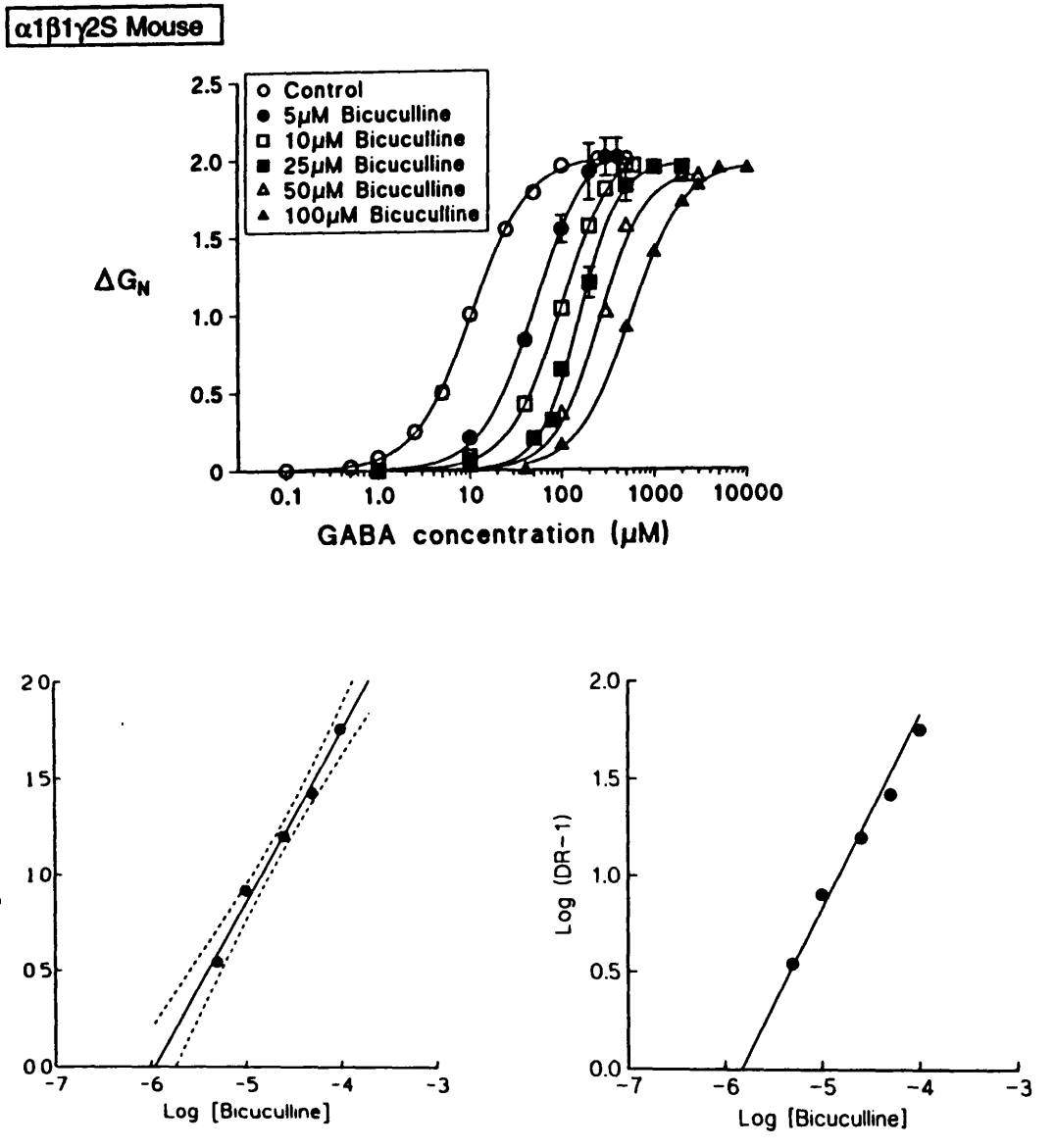
α1β1γ2S Mouse
Control
5μM Bicuculline
10μM Bicuculline
25μM Bicuculline
50μM Bicuculline
100μM Bicuculline
ΔG_N
GABA concentration (μM)
Log (DR-1)
Log [Bicuculline]
Log (DR-1)
Log [Bicuculline]

Figure 3.10. Antagonism of the GABA-induced conductance change by bicuculline in murine α1β1γ2L $GABA_A$ receptors. The top hand plot indicates GABA concentration conductance curves constructed in the absence and presence of 1, 10, and 50 μM bicuculline. The bottom left hand plot indicates a Schild plot of log (dose ratio - 1) against - (log molar) bicuculline concentration for the antagonism of the GABA-induced response by bicuculline. The line is a least squares regression line for unweighted data (without slope constraint), with 95% confidence limits of the calculated regression. On the right, the same Schild analysis has been shown with the regression line constrained to unity (see methods). Calculated data from the regression lines are given in Table 3.4.

α1β1γ2L Mouse

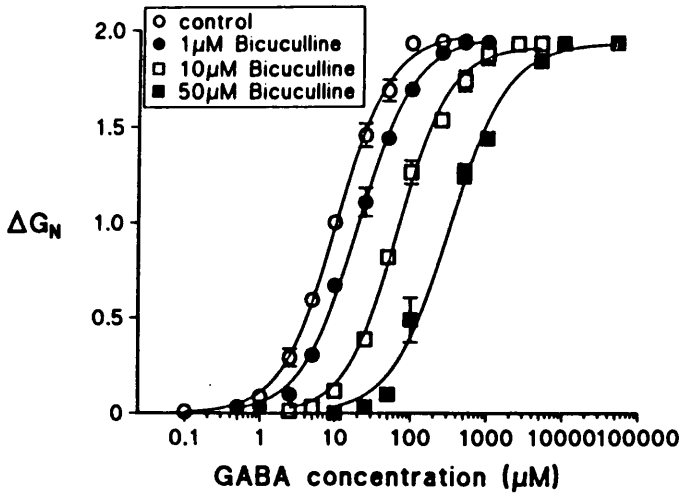

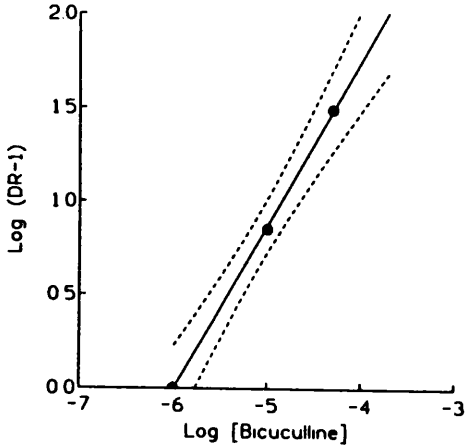

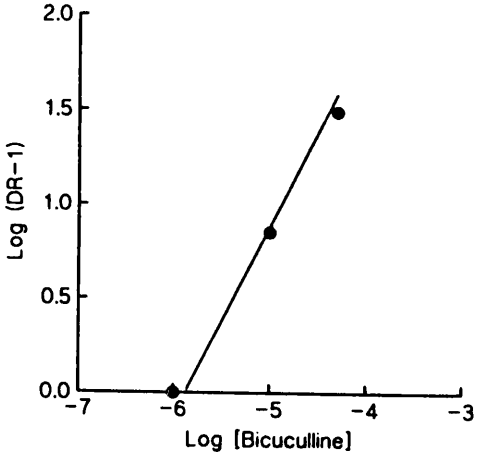

Figure 3.11. Antagonist profile of murine α1β1δ and α1β1γ2Sδ $GABA_A$ receptors. (A) Membrane current and conductance change evoked by GABA (10 μM) in the absence and presence of bicuculline (10 μM), picrotoxin (10 μM) and zinc (250 μM) in oocytes expressing α1β1δ $GABA_A$ receptors. (B) Effect of bicuculline (10 μM), picrotoxin (10 μM) and zinc (100 μM) on the response induced by 10 μM GABA in oocytes expressing α1β1γ2Sδ $GABA_A$ receptors. Recovery responses were obtained to 10 μM GABA in between exposures to the antagonist (not shown).

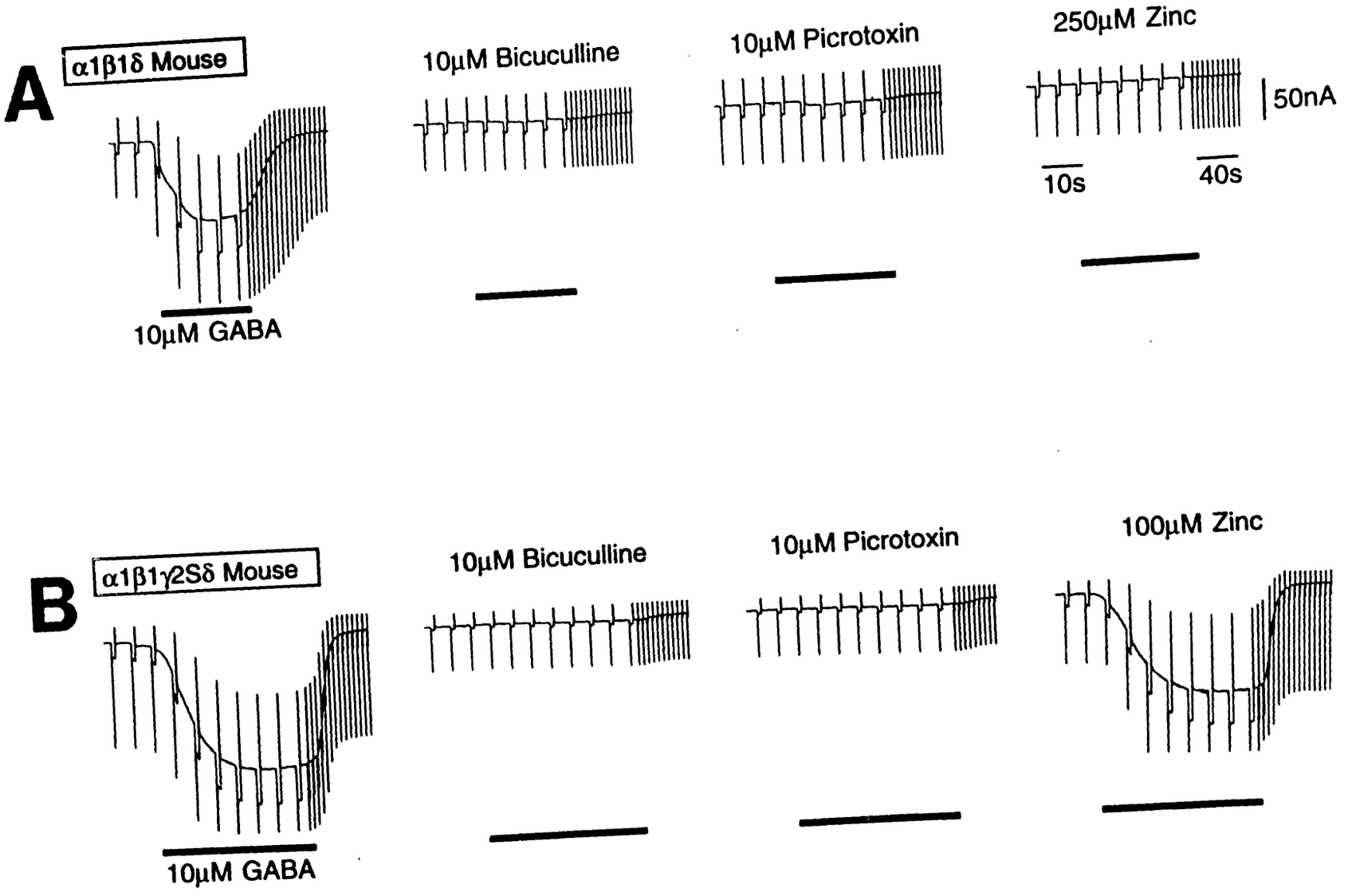
A
α1β1δ Mouse
10μM GABA
10μM Bicuculline
10μM Picrotoxin
250μM Zinc
50nA
10s
40s
B
α1β1γ2Sδ Mouse
10μM GABA
10μM Bicuculline
10μM Picrotoxin
100μM Zinc

Figure 3.12. Benzodiazepine and barbiturate modulation of the GABA-induced response in murine $\alpha 1\beta 1$ $GABA_A$ receptors. (A) Membrane current and conductance changes evoked by GABA (10 μM) in the absence and presence of flurazepam (1 μM) and pentobarbitone (25 μM). (B) Left hand plot indicates the potentiation of the response elicited by 10 μM GABA by different concentrations of pentobarbitone. The right hand plot shows GABA dose-response curves constructed in the absence and presence of 1 μM flurazepam and 50 μM pentobarbitone.

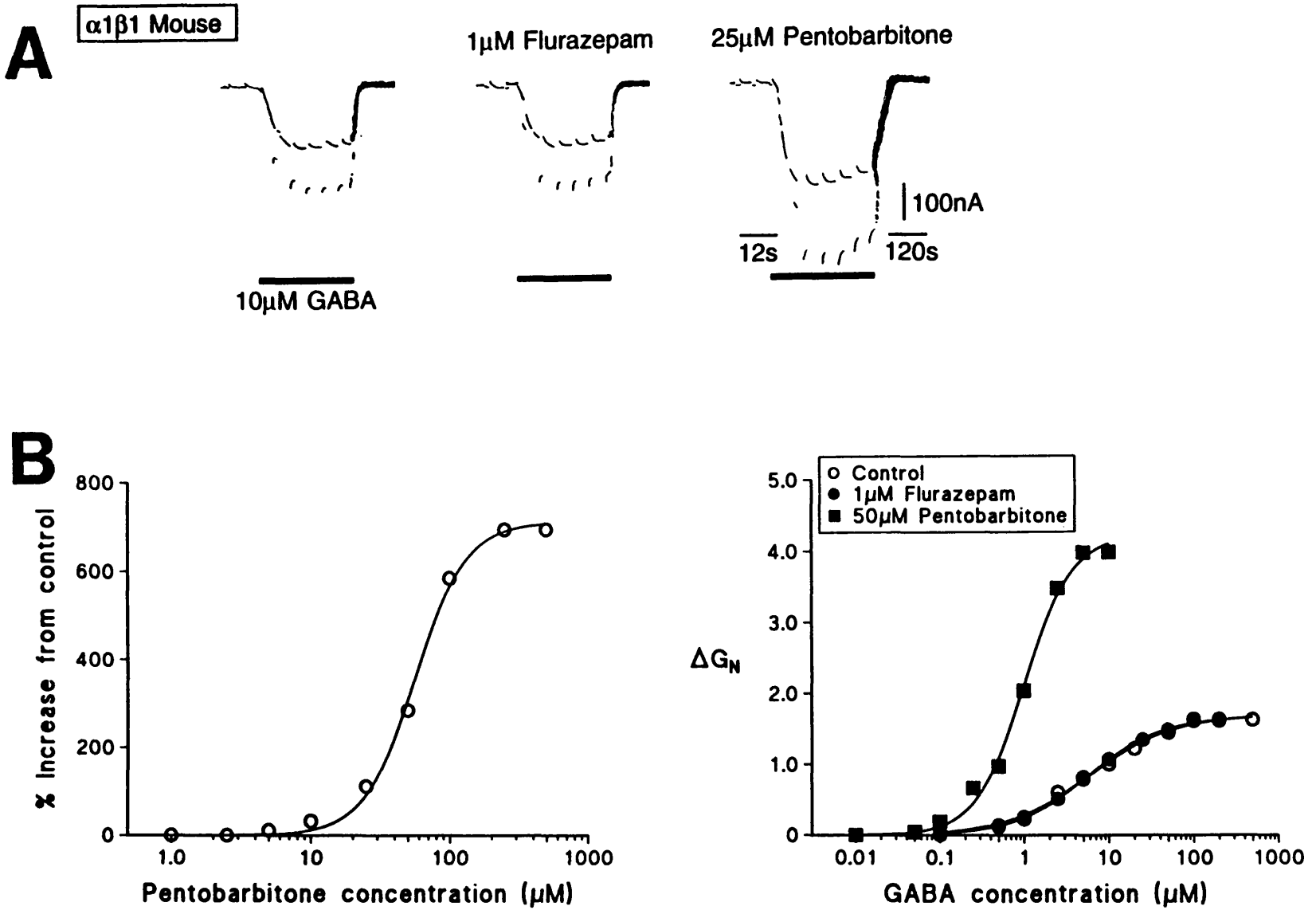
A
α1β1 Mouse
1μM Flurazepam
25μM Pentobarbitone
100nA
12s
120s
10μM GABA
B
% Increase from control
800
600
400
200
0
1.0
10
100
1000
Pentobarbitone concentration (μM)
Control
1μM Flurazepam
50μM Pentobarbitone
ΔG_N
5.0
4.0
3.0
2.0
1.0
0
0.01
0.1
1
10
100
1000
GABA concentration (μM)

Figure 3.13. Potentiation of GABA-evoked membrane currents and conductances on oocytes expressing murine α1β1γ2S $GABA_A$ receptors by different positive modulators of the GABA channel. (A) Membrane current and conductance change evoked by GABA (10 μM) in the absence and presence of flurazepam (1 μM), pentobarbitone (50 μM) and pregnanolone (500 nM). (B) Left hand plot indicates the potentiation of the response elicited by 10 μM GABA by different concentrations of pentobarbitone, flurazepam and diazepam. The right hand plot shows GABA dose-response curves constructed in the absence and presence of 1 μM flurazepam and 50 μM pentobarbitone.

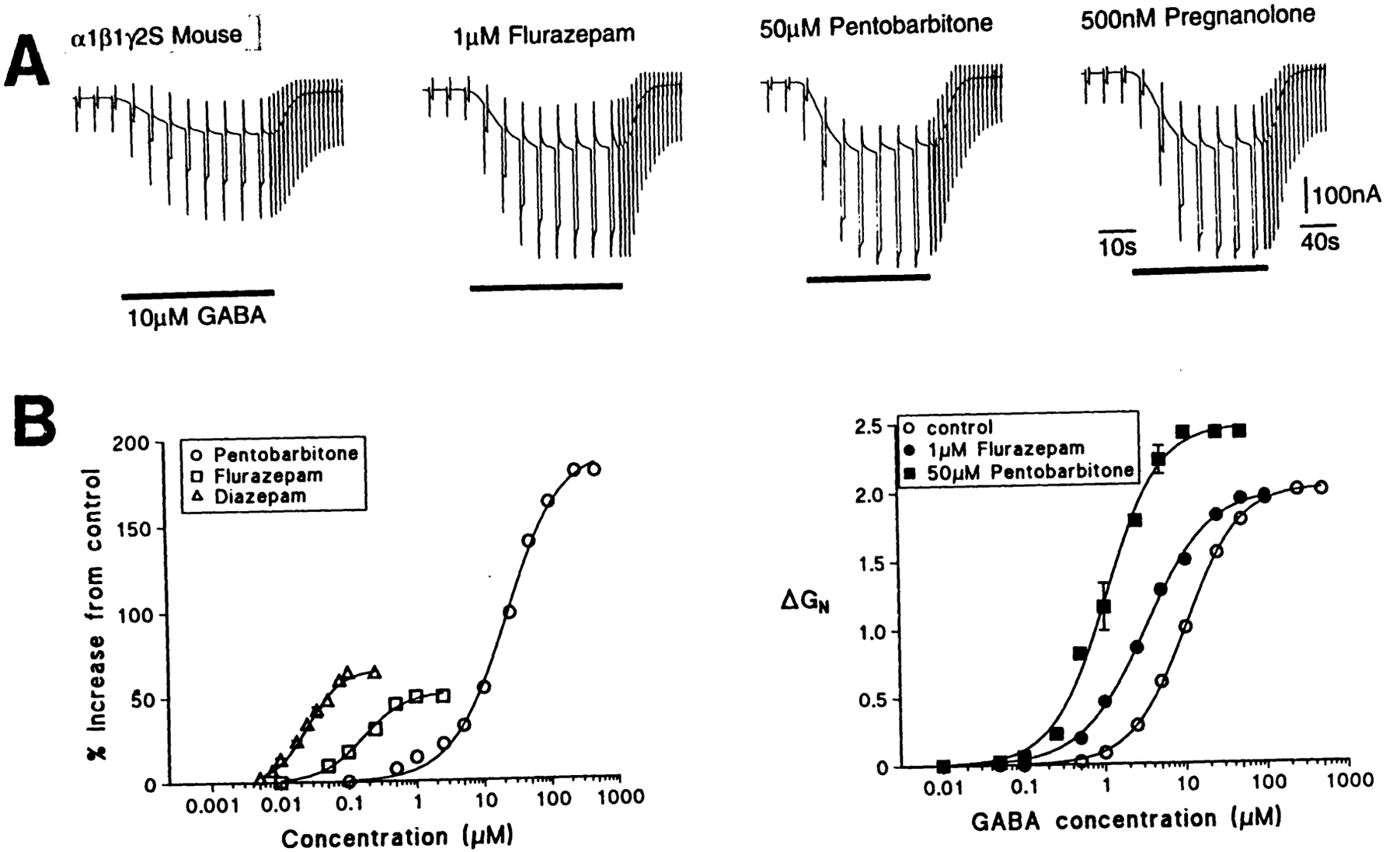
A
α1β1γ2S Mouse
1μM Flurazepam
50μM Pentobarbitone
500nM Pregnanolone
100nA
10s
40s
10μM GABA
B
Pentobarbitone
Flurazepam
Diazepam
% Increase from control
Concentration (μM)
control
1μM Flurazepam
50μM Pentobarbitone
ΔG_N
GABA concentration (μM)

Figure 3.14. Potentiation of GABA-evoked membrane currents and conductances on oocytes expressing murine α1β1γ2L $GABA_A$ receptors by benzodiazepines and barbiturates. (A) Effect on the 10 μM GABA-induced membrane current and conductance change evoked by the application of flurazepam (1 μM) and pentobarbitone (25μM). (B) Left hand plot indicates the potentiation of the response elicited by 10 μM GABA by different concentrations of pentobarbitone and flurazepam. The right hand plot shows GABA dose-response curves constructed in the absence and presence of 1 μM flurazepam and 50 μM pentobarbitone.

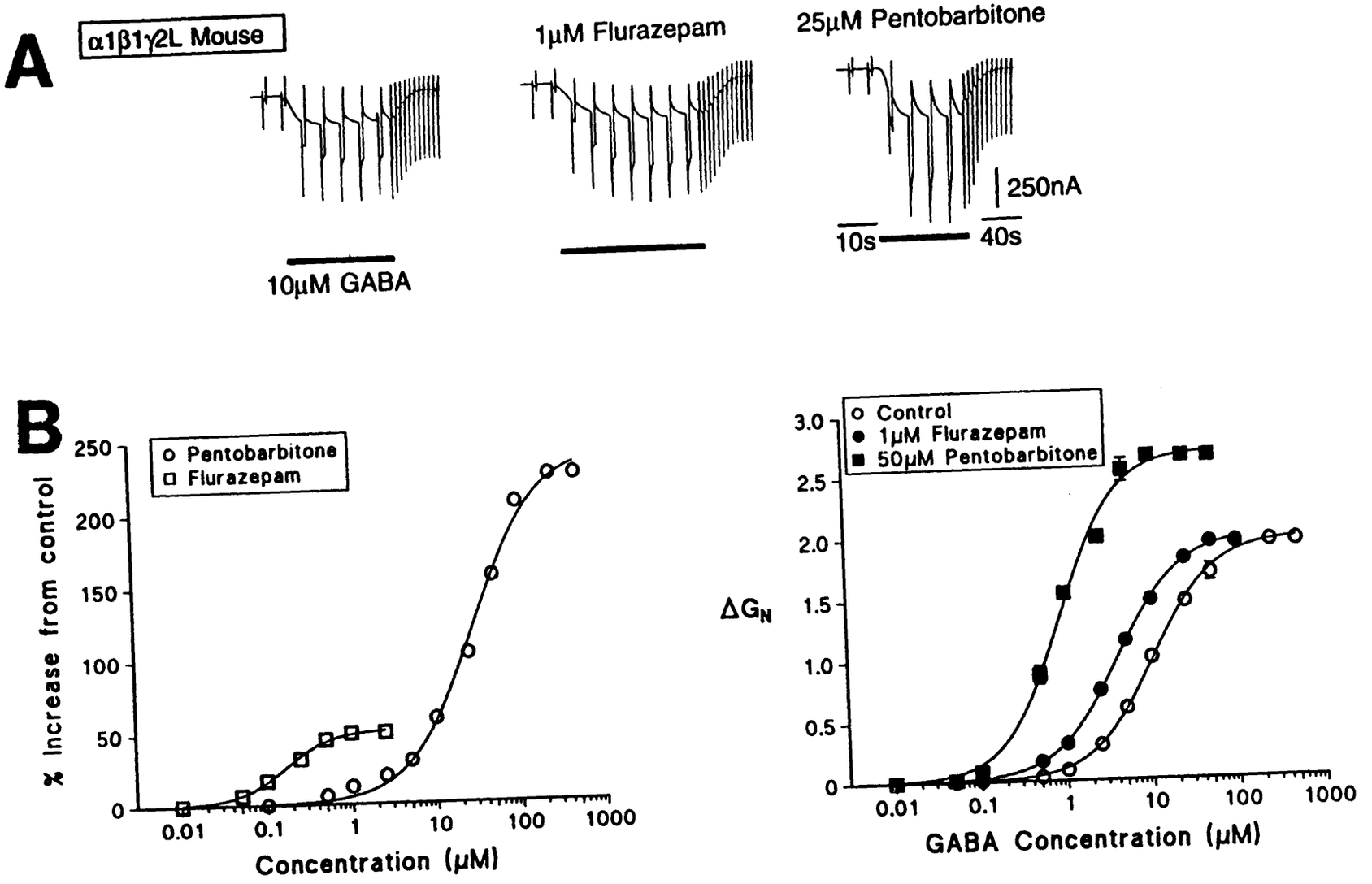
A
α1β1γ2L Mouse
1μM Flurazepam
25μM Pentobarbitone
250nA
10s
40s
10μM GABA
B
Pentobarbitone
Flurazepam
% Increase from control
Concentration (μM)
Control
1μM Flurazepam
50μM Pentobarbitone
ΔG_N
GABA Concentration (μM)

Figure 3.15. Effect of different positive modulators on the GABA-evoked response on oocytes expressing murine α1β1δ (A) and α1β1γ2Sδ (B) $GABA_A$ receptors. Membrane current and conductance changes were evoked by GABA (10 μM) in the absence and presence of flurazepam (1 μM), diazepam (1 μM), pentobarbitone (50 μM) and pregnanolone (500 nM). Note, for both receptor constructs, controls obtained before each modulator application are not shown but a 'representative' control response induced by 10 μM GABA is indicated.

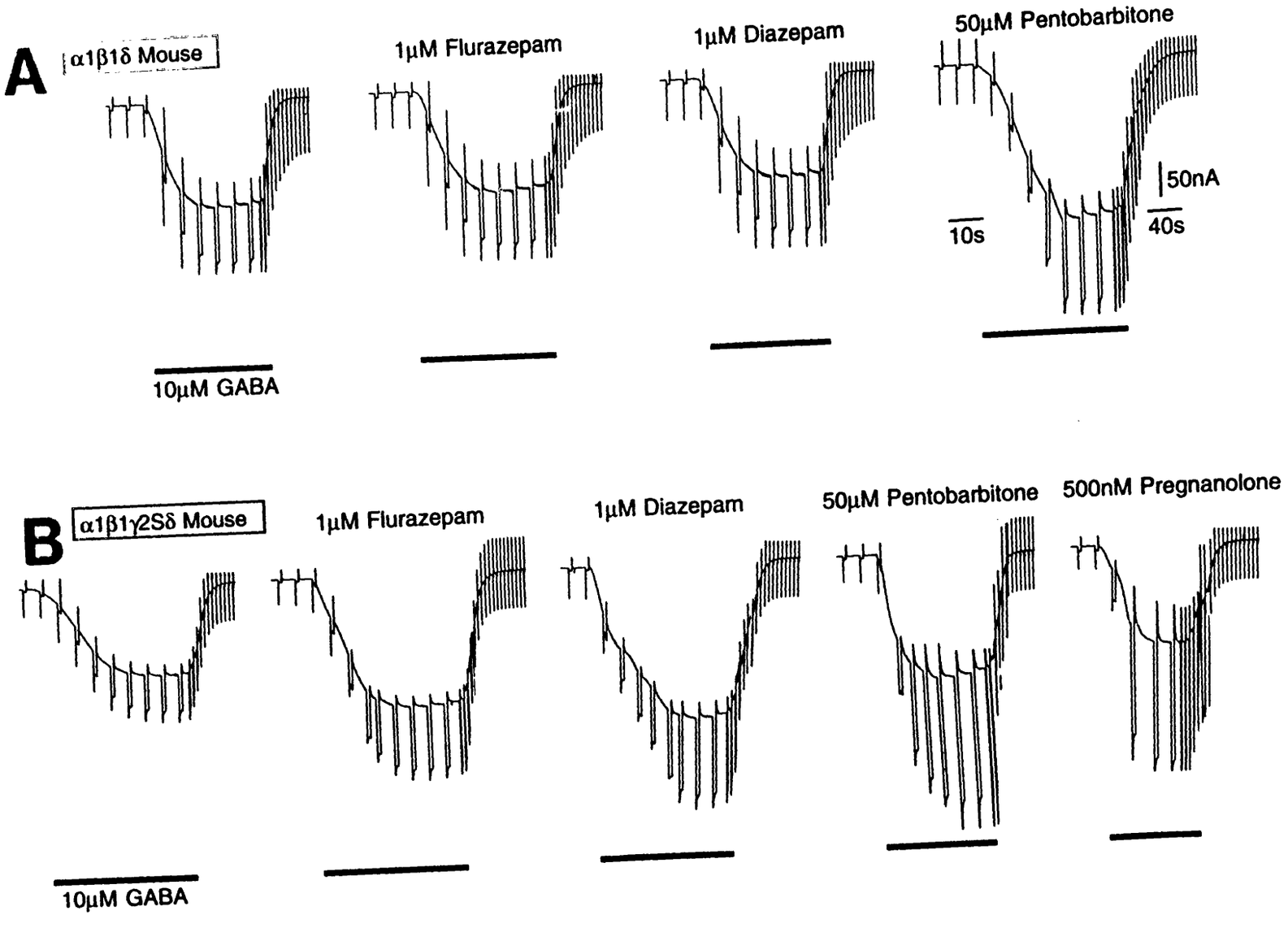
A
α1β1δ Mouse
1μM Flurazepam
1μM Diazepam
50μM Pentobarbitone
50nA
10s
40s
10μM GABA
B
α1β1γ2Sδ Mouse
1μM Flurazepam
1μM Diazepam
50μM Pentobarbitone
500nM Pregnanolone
10μM GABA

Figure 3.16. Pharmacological profile of bovine α1β1 $GABA_A$ receptors.
(A) Membrane current and conductance changes evoked by GABA (10 μM), isoguvacine (10 μM) and muscimol (10 μM). Effect of the $GABA_A$ receptor modulators flurazepam (1 μM) and pentobarbitone (50 μM) on the GABA-induced responses. (B) Inhibition of the membrane current and conductance changes evoked by GABA (10 μM) using bicuculline (10 μM) or picrotoxin (10 μM).

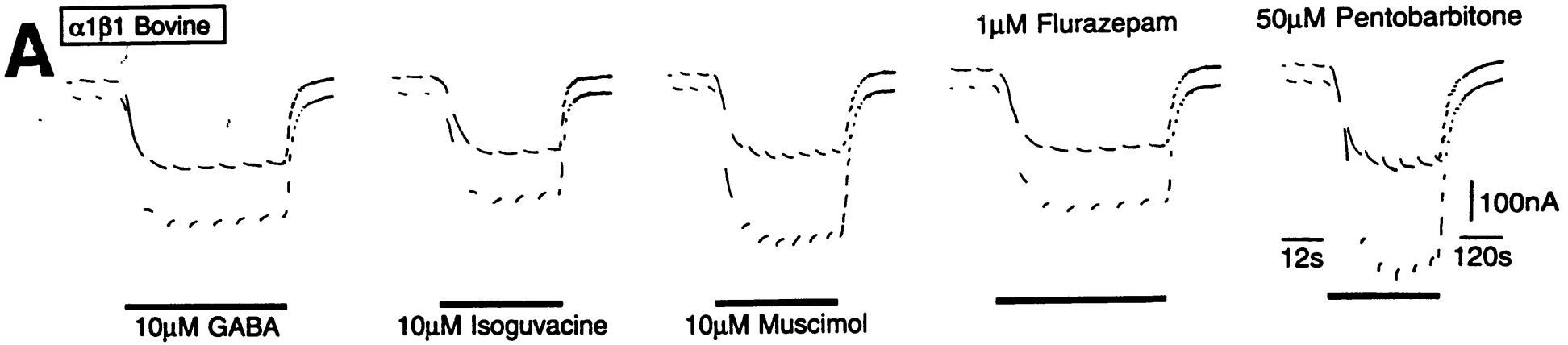
A
α1β1 Bovine
1μM Flurazepam
50μM Pentobarbitone
100nA
12s
120s
10μM GABA
10μM Isoguvacine
10μM Muscimol

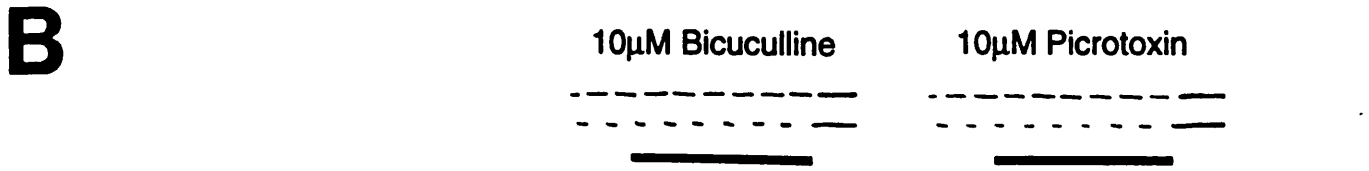
B
10μM Bicuculline
10μM Picrotoxin

Figure 3.17. Pharmacological profile of bovine α1β1γ2S $GABA_A$ receptors. (A) Membrane current and conductance changes evoked by GABA (10 μM), isoguvacine (10 μM) and muscimol (10 μM). Effect of the $GABA_A$ receptor modulators flurazepam (1 μM) and pentobarbitone (25 μM) on the GABA-induced responses. (B) Inhibition of the membrane current and conductance changes evoked by GABA (10 μM) after bicuculline (10 μM) or picrotoxin (10 μM).

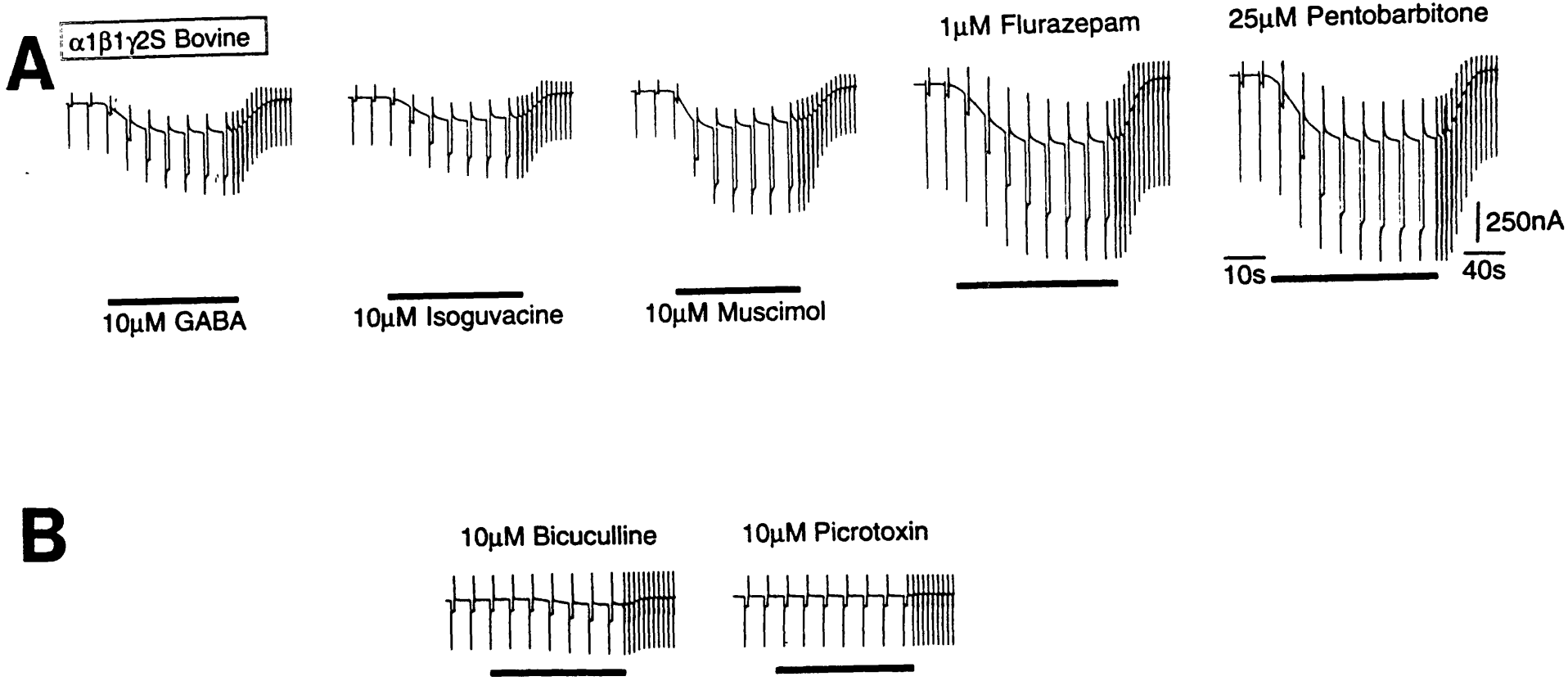
A
α1β1γ2S Bovine
10μM GABA
10μM Isoguvacine
10μM Muscimol
1μM Flurazepam
25μM Pentobarbitone
250nA
10s
40s
B
10μM Bicuculline
10μM Picrotoxin

Table 3.1

Subunit Composition	EC_{50} (μM)			Hill Coefficient		
	GABA	Isoguvacine	Muscimol	GABA	Isoguvacine	Muscimol
α1β1	5.87 ± 0.7	34.0 ± 2.3	0.63 ± 0.05	0.95 ± 0.09	1.03 ± 0.06	1.16 ± 0.08
α1β1γ2L	10.2 ± 0.5	76.87 ± 4.5	2.6 ± 0.32	1.22 ± 0.05	1.19 ± 0.06	1.13 ± 0.1
α1β1γ2S	10.03 ± 0.2	-	-	1.29 ± 0.03	-	-
α1β1δ	4.9 ± 0.4	-	-	0.85 ± 0.05	-	-
α1β1γ2Sδ	27.7 ± 1	-	-	1.44 ± 0.06	-	-

Analysis of the equilibrium concentration response curves for GABA, isoguvacine and muscimol recorded from expressed $GABA_A$ receptor constructs. The EC_{50} and Hill coefficient data were determined from fitting the logistic model to the normalised curves (see methods) with all values mean ± s.e.m.

Table 3.2

Subunit Composition	IC_{50} (μM)	EC_{50} (μM)		Hill Coefficient	
		Control	+ Picrotoxin	Control	+ Picrotoxin
α1β1	1.3 ± 0.15	5.87 ± 0.7	(1)* 7.5 ± 0.45	0.95 ± 0.09	(1)* 1.37 ± 0.1
α1β1γ2S	2.65 ± 0.2	10.03 ± 0.2	(5)* 13.5 ± 0.8	1.3 ± 0.03	(5)* 1.5 ± 0.1
α1β1γ2L	0.99 ± 0.22	10.2 ± 0.5	(2.5)* 31.2 ± 1.6	1.22 ± 0.06	(2.5)* 1.5 ± 0.1

Analysis of the picrotoxin inhibition plots for GABA in *Xenopus laevis* oocytes injected with $GABA_A$ receptor cDNAs. The IC_{50} values were obtained from fitting the antagonist inhibition model to the normalised curves (see methods) with all values mean ± s.e.m. Analysis of the equilibrium concentration response curves for GABA was completed in the absence and presence of picrotoxin. EC_{50} and Hill coefficient data were determined from fitting the logistic model to the normalised curves (see methods) with all values mean ± s.e.m. Numbers in parentheses indicate the picrotoxin concentration (μM); * represents a significant change from control $P < 0.05$.

Table 3.3

Subunit Composition	EC_{50} (μM)		Hill Coefficient	
	Control	+ Bicuculline	Control	+ Bicuculline
α1β1	5.87 ± 0.7	(5)* 26.9 ± 2.2 (50)* 174.6 ± 8.2 (100)* 356.3 ± 20.8	0.96 ± 0.09	(5) 1.13 ± 0.08 (50)* 1.25 ± 0.06 (100)* 1.29 ± 0.09
α1β1γ2S	10.03 ± 0.2	(5)* 52.6 ± 2.8 (10)* 100 ± 3.5 (25)*156.4 ± 8.1 (50)* 256.7 ± 21.8 (100)* 554.1 ± 16.4	1.3 ± 0.03	(5) 1.43 ± 0.1 (10)* 1.5 ± 0.07 (25)* 1.6 ± 0.09 (50)* 1.55 ± 0.06 (100)* 1.5 ± 0.07
α1β1γ2L	10.2 ± 0.5	(1)* 19.9 ± 0.97 (10)* 66.4 ± 4.1 (50)* 319.6 ± 38	1.22 ± 0.06	(1) 1.2 ± 0.05 (10) 1.3 ± 0.09 (50) 1.2 ± 0.1

Analysis of the equilibrium concentration response curves for GABA in the absence and presence of bicuculline in *Xenopus laevis* oocytes injected with $GABA_A$ receptor cDNAs. EC_{50} and Hill coefficient data were determined in the absence and presence of bicuculline from fitting the logistic model to the normalised curves (see methods) with all values mean ± s.e.m. Numbers in parentheses indicate the bicuculline concentration (μM); * represents a significant change from control $P < 0.05$.

Table 3.4

Subunit Composition	Unconstrained Slope	pA_2 (unconstrained slope)	pA_2 (constrained slope)	K_B (μM) (unconstrained slope)	K_B (μM) (constrained slope)
α1β1	0.76 to 1.08	5.75 to 6.25	5.87	0.56 to 1.78	1.35
α1β1γ2S	0.72 to 1.04	5.69 to 6.24	5.83	0.75 to 2.04	1.48
α1β1γ2L	0.67 to 1.08	5.77 to 6.22	5.86	0.60 to 1.70	1.38

Analysis of bicuculline antagonism of the GABA-induced response in recombinant $GABA_A$ receptors. Values are derived from the Schild plots of pooled data shown in Figures 3.8, 3.9 and 3.10. Data were subjected to linear regression analysis and the slope constrained to unity. 95% confidence limits of the calculated regressions were determined for lines generated without slope constraint. K_B was determined according to the equation $pA_2 = - \log K_B$.

Table 3.5

Subunit Composition	Modulator EC_{50} (μM)			% Maximum Potentiation		
	Pentobarbitone	Flurazepam	Diazepam	Pentobarbitone	Flurazepam	Diazepam
α1β1	56 ± 2.4	-	-	(500) 708.7 ± 15.1	-	-
α1β1γ2S	21.97 ± 1.9	0.17 ± 0.02	0.05 ± 0.003	(500) 190 ± 4.9	(2.5) 52.2 ± 2.4	(0.25) 57.1 ± 1.6
α1β1γ2L	28.23 ± 2.8	0.17 ± 0.01	-	(500) 239.8 ± 7.6	(2.5) 51.4 ± 1.3	-

Analysis of the equilibrium concentration response curves for the potentiation of a fixed dose of GABA by increasing concentrations of pentobarbitone, flurazepam and diazepam recorded from $GABA_A$ receptor constructs. The EC_{50} and % maximum potentiation data were determined from fitting the logistic model to the normalised curves (see methods) with all values mean ± s.e.m. Numbers in parentheses indicate the concentration of drug in μM.

Table 3.6

Subunit Composition	GABA EC_{50} (μM)			Hill Coefficient		
	Control	+ Pentobarbitone	+ Flurazepam	Control	+ Pentobarbitone	+ Flurazepam
α1β1	5.87 ± 0.6	* 1.0 ± 0.09	5.6 ± 0.23	0.9 ± 0.07	* 1.4 ± 0.15	1.02 ± 0.05
α1β1γ2S	10.0 ± 0.2	* 1.06 ± 0.09	* 3.2 ± 0.17	1.3 ± 0.03	1.3 ± 0.1	1.2 ± 0.07
α1β1γ2L	10.2 ± 0.5	* 0.87 ± 0.07	* 4.0 ± 0.1	1.2 ± 0.06	1.3 ± 0.13	1.2 ± 0.03

Analysis of the equilibrium concentration response curves for GABA in the absence and presence of pentobarbitone and flurazepam recorded from $GABA_A$ receptor constructs. The EC_{50} and Hill coefficient data were determined from fitting the logistic model to the normalised curves (see methods) with all values mean ± s.e.m. Pentobarbitone and flurazepam were bath-applied at 50 and 1 μM respectively; * represents a significant change from control $P < 0.05$.

CHAPTER FOUR

THE β1 SUBUNIT: AN IMPORTANT SITE FOR GABA BINDING?

THE β1 SUBUNIT: AN IMPORTANT SITE FOR GABA BINDING?

4.1 INTRODUCTION

The functional role of the β subunit within the $GABA_A$ receptor complex remains unclear. Previous studies have implicated this subunit as an essential structural component of the receptor which is important for the expression of functional channels (Angelotti *et al.*, 1993; Sigel *et al.*, 1990). The absence of a β subunit was also shown to lead to $GABA_A$ receptors with very small current amplitudes in *Xenopus* oocytes (Sigel *et al.*, 1990). In agreement with these results, it was shown in the previous chapter that expression of $GABA_A$ receptors was not possible without the presence of a β subunit indicating the importance of this subunit in the reconstitution of a functional $GABA_A$ receptor. In contrast, however, $GABA_A$ receptors composed of rat α1γ2 subunits expressed in human embryonic kidney cells resulted in functional channels with large conductances (Verdoorn *et al.*, 1990; Draguhn *et al.*, 1990).

There has been little information available on the domains which are important for activation of the $GABA_A$ receptor. However, a recent study indicated that the $GABA_A$ receptor required two domains present in the β2-subunit for activation by GABA (Amin and Weiss, 1993). Both domains of the β2 subunit were shown to occur in the N-terminal region of the subunit. However, it could be possible that domains from neighbouring subunits (α, γ and δ) may contribute to the binding site because an amino acid of the α1 subunit has been identified that when mutated (F64L), impairs activation of the GABA channel (Sigel *et al.*, 1992). These results suggest the possibility that the N-terminal portions of the extracellular regions of all the subunits could be involved with the gating of the channel.

In order to determine the exact function of the β subunit, electrophysiological and pharmacological analysis have been performed on *Xenopus* oocytes expressing homomeric, or single subunit, β subunits. The expression of bovine homomeric "β" subunits was quite poor but revealed a GABA-sensitive chloride channel which was potentiated by pentobarbitone and inhibited by picrotoxin (Blair *et al.*, 1988). Conversely, expression of the rat β1 subunit alone produced an anion-selective channel which lacked GABA-gated properties (Sigel *et al.*, 1989). These channels appeared to be open in the absence of GABA and could be shut by picrotoxin (Sigel *et al.*, 1989). Interestingly, a similar current was observed in oocytes expressing rat α1β1γ2 $GABA_A$ receptors. Application of picrotoxin, applied in the absence of GABA, induced a small shift in the holding current in the opposite direction to the current elicited by GABA (Malherbe *et al.*, 1990b). The small shift amounted to less than 0.5% of the maximum current obtained with GABA and presumably indicates the possibility of a minor fraction of channels open in the absence of added GABA. It could also be possible that these open channels could represent the expression of a small amount of homomeric β1 $GABA_A$ receptors.

This study investigates the pharmacological properties of the β1 homomeric $GABA_A$ receptor from two different species and reveals for the first time that GABA and other compounds known to interact with the $GABA_A$ receptor may have separate binding sites. Moreover, very little change in the amino acid sequence of the β1 subunit can apparently lead to homomeric receptors with very different pharmacological and physiological properties.

4.2 RESULTS

4.2.1 PHARMACOLOGICAL CHARACTERISATION OF THE MURINE β1 SUBUNIT: A NOVEL $GABA_A$ RECEPTOR

Two to five days after injection of murine cDNAs encoding for β1 mouse subunits, the oocytes were screened for expression of $GABA_A$ receptors by the bath-application of GABA (0.1 μM to 1 mM). Under voltage clamp at a holding potential of -40 mV no change in the membrane currents and conductances were evoked even by high concentrations of GABA (1 mM; Fig. 4.1A). Interestingly, the resting membrane resistance was lower (0.05 to 0.25 MΩ) than normally seen with oocytes expressing heteromeric $GABA_A$ receptors (0.5 to 2.5 MΩ). There were no visible morphological differences between the batches of oocytes indicating that structural damage induced by the expression of homomeric β1 subunit receptors was unlikely. Application of the competitive $GABA_A$ receptor antagonist, bicuculline at high concentrations (50 μM), also had no effect on the resting membrane currents and conductances (Fig. 4.1A). However, bath application of low concentrations of both zinc (1 μM) or picrotoxin (10 μM) restored the normal membrane resistance in these oocytes (Fig. 4.1A). Zinc has been shown to be a non-competitive antagonist at the $GABA_A$ receptor (Smart and Constanti, 1990; Smart, 1990). Zinc induced an outward current and conductance decrease which was also seen with the GABA-channel blocker, picrotoxin. Picrotoxin and zinc-inhibition curves were constructed for the decrease in the conductance induced by these antagonists (Fig. 4.2A,B). The IC_{50} for picrotoxin and zinc were estimated as 2.11 ± 0.6 and 0.23 ± 0.03 μM respectively indicating that zinc has a greater affinity for this β1 receptor subunit compared to picrotoxin. To establish the identity of the conductance being reduced by these inhibitors current-voltage relations were constructed. The I-V relationships for the unusual ion channel formed by the β1 subunit displayed a slight degree of outward rectification with reversal potentials

estimated as -27.1 and -24.7 mV respectively which are close to the Cl^- reversal potential in these cells (Fig. 4.2A,B; Barish, 1983; Dascal, 1987).

The β1 homomeric channels were not affected by some other $GABA_A$ receptor agonists under study. GABA (500 μM), muscimol (500 μM) and isoguvacine (500 μM) failed to induce any change in the membrane potential or current suggesting that the binding site for these agonists is either occluded or not adopting the correct conformation in this homomeric receptor (Fig. 4.3A). Interestingly, the barbiturate, pentobarbitone, did induce an inward current associated with a conductance increase (Fig 4.3A). These results indicate that the binding site for GABA and barbiturates are clearly different with only the barbiturate site existing in these homomeric β1 subunits. Construction of an equilibrium dose-response curve for pentobarbitone produced a Hill coefficient and EC_{50} value of 1.9 ± 0.26 and 6.0 ± 0.34 μM respectively (Fig. 4.3B). The current-voltage relation for the pentobarbitone-induced conductance revealed a reversal potential of -15.5 mV which is again similar to the Cl^- reversal potential in these cells (Fig. 4.3B).

Heteromeric $GABA_A$ receptors contain a number of allosteric binding sites (for review see Burt and Kamatchi, 1991; Olsen and Tobin, 1990). To establish whether such binding sites also existed on the homomeric β1 subunit, a number of $GABA_A$ receptor allosteric modulators were applied to this receptor. Initially, both positive modulators, including the benzodiazepines and neurosteroids and negative modulators such as inverse agonists were tested. The unusual ion current was not affected by the benzodiazepines, flurazepam (10 μM) and midazolam (10 μM) or the negative allosteric modulator methyl-6,7-dimethoxy-4-ethyl-β-carboline-3-carboxylate (DMCM; 10 μM; Fig. 4.4A). Neither the benzodiazepine antagonist, flumazenil (Ro 15-1788; 10 μM; Fig. 4.4A), nor the neurosteroid pregnanolone (500 nM) had any effect on the current (Fig. 4.4B). Chlormethiazole has been previously shown to be a positive allosteric modulator of the $GABA_A$ receptor (Harrison and

Simmonds, 1983; Hales and Lambert, 1992). Application of chlormethiazole (100 μM) had no effect on the current formed by the homomeric β1 subunit (Fig. 4.4B). Propofol is a novel general anaesthetic which has been previously shown to be a potent enhancer of GABA responses (Hales and Lambert, 1991; Prince and Simmonds, 1992). Interestingly, propofol (100 μM) potentiated the membrane conductance which could be inhibited by the co-application of picrotoxin (10 μM; Fig 4.4B). Penicillin has been observed to reduce GABA-evoked chloride currents (Chow and Mathers, 1986; Twyman *et al.*, 1992; Katayama *et al.*, 1992). Application of 1 mM penicillin G induced an outward current and conductance decrease which could be further accentuated by the co-application of picrotoxin (1 μM) in an additive manner (Fig. 4.4C). This provided evidence that penicillin G and picrotoxin were acting on the same unusual ion current formed by the homomeric β1 subunit. Anthracene-9-carboxylic acid (A-9-C) has been previously shown to be a chloride channel blocker (Bowie and Smart, 1993). Bath-application of A-9-C (1 mM) had no effect on the membrane current or conductance (Fig. 4.4C).

Xenopus oocytes have been shown to express an endogenous gene for the acetylcholine receptor α subunit which was thought to be able to co-assemble with acetylcholine receptor subunit proteins, synthesised after cRNA injection, to yield functional acetylcholine receptors (Buller and White, 1989). It was therefore conceivable that the homomeric β1 subunits could also co-assemble with a transcription product from the oocyte's own genome, producing the novel ion current formed by the β1 subunit. Therefore many control experiments were performed to determine that the novel current seen in this study was a product solely of the β1 subunit expression including:
(i) injection of an unrelated reporter gene (Lac Z) to determine whether an injection of cDNA will produce the unusual ion current and (ii) the utilisation of actinomycin D which prevents any transcription of the host cells genome. To ascertain the effectiveness of actinomycin D on the prevention of transcribing DNA to mRNA, a control experiment was performed using cDNA

injections of α1β1 subunits in the presence and absence of actinomycin D.

Thus the first approach was to inject the Lac Z gene into the *Xenopus* oocyte which encodes for the β-galactosidase protein (Bassford *et al.*, 1978). This ensured the unusual ion current was not a product of expression from the oocyte's own genome which was somehow induced to be expressed after injection of a volume (15 nl) of cDNA into the nucleus. Two to five days after the injection of the Lac Z gene the oocytes exhibited normal resting membrane resistances and bath-application of GABA (1 mM), zinc (10 μM), picrotoxin (50 μM) or pentobarbitone (50 μM) had no effect on the resting membrane current or conductance (Fig. 4.5A). It is therefore improbable that the injection of cDNAs *per se* activates an endogenous gene within the oocyte which could be expressing the protein for the novel ion channel seen in this study. To further ascertain that the expression of the ion channel was only from the injected β1 subunit, oocytes were incubated in the presence of 50 μg/ml actinomycin D after injection with cRNA encoding for mouse β1 subunits or cDNAs encoding for α1β1 $GABA_A$ receptors. As actinomycin D blocks transcription of DNA to mRNA, injection and subsequent expression of the products of cRNA should be unaffected by actinomycin D but expression of injected cDNA should be prevented. After two to five days incubation in actinomycin D, the cRNA injection of β1 subunits expressed to give receptors with the same ion channel properties as those seen for cDNA injections of the β1 subunit. GABA (500 μM) failed to affect the ion channel properties with both zinc (1 μM) and picrotoxin (50 μM) inducing an outward current and conductance decrease (Fig. 4.5B). Moreover, pentobarbitone (10 μM) induced an inward current and conductance increase (Fig. 4.5B). To ensure that actinomycin D was preventing transcription at this concentration, oocytes injected with α1β1 cDNAs were also bathed in actinomycin D. Expression of α1β1 subunits was not seen after incubation in actinomycin D for two to five days. GABA (10 to 500 μM) and picrotoxin (50 μM) failed to elicit any response (Fig. 4.5C). To ascertain that this lack of expression was

due to the effects of actinomycin D and not due to poor expression of the cDNAs, oocytes from the same experiment were also incubated in the absence of actinomycin D. In this case, the injection of α1β1 subunits for the $GABA_A$ receptor led to the efficient formation of GABA-gated anion channels. GABA (10 and 100 μM) induced large inward currents and conductance increases (Fig. 4.5D). Application of 10 μM picrotoxin inhibited the response induced by GABA (10 μM; Fig. 4.5D). From these control experiments it is very likely that the currents seen in this study arose from only the expression of homomeric mouse β1 subunits and not from a product of the expression of the oocyte's own genome.

4.2.2 COMPARISON OF HOMOMERIC β1 SUBUNIT $GABA_A$ RECEPTORS FROM TWO DIFFERENT SPECIES

The unusual ionic current seen with expressed mouse β1 homomeric $GABA_A$ receptors is intriguing. Whether such an effect is related specifically to this mouse $GABA_A$ subunit was studied by comparison with expressed homomeric bovine β1 $GABA_A$ receptor subunits.

Bath-application of GABA (100 μM) or muscimol (100 μM) induced a small inward current (Fig. 4.6A). The bovine β1 homomeric receptors therefore appeared to have GABA-gating properties which were lacking in the mouse β1 $GABA_A$ subunit. The GABA response was unaffected by the benzodiazepine midazolam (50 μM) but was enhanced by 50 μM pentobarbitone (Fig. 4.6A). The GABA-induced response was completely inhibited by the $GABA_A$ receptor antagonists bicuculline (10 μM), picrotoxin (10 μM) and zinc (10 μM; Fig. 4.6B). Addition of the chloride channel blocker A-9-C had no effect on the GABA-induced response (Fig. 4.6B). The responses induced by GABA on this homomeric bovine β1 $GABA_A$ receptor were shown to be dose-dependent with the application of increasing concentrations of GABA inducing larger responses (Fig. 4.6C). Construction of an equilibrium response curve revealed

a Hill coefficient and EC_{50} value of 0.8 ± 0.08 and 29.34 ± 5.1 μM respectively (Fig. 4.7). Current-voltage relations for GABA revealed a reversal potential of -21.35 mV which is close to the Cl^- reversal potential in these cells (Fig. 4.7; Barish, 1983; Dascal, 1987). Interestingly, the I-V relationships for this $GABA_A$ receptor revealed a saturation of the GABA-induced current at positive potentials possibly indicating a very inefficient expression of these single bovine subunits. Alternatively the expression could be efficient but the channels may have a small single channel conductance or possibly a relatively low channel opening frequency and/or short mean open or long mean closed times at depolarised membrane potentials.

4.3 DISCUSSION

This study represents an examination of the functional properties of homomeric β1 $GABA_A$ receptors and the apparent ability of a small number of amino acid residues to change the pharmacological profile of the same subunit from different species.

4.3.1 SPECIES DEPENDENCE OF THE PHARMACOLOGICAL PROFILE FOR HOMOMERIC β1 $GABA_A$ RECEPTORS

Xenopus oocytes injected with mouse β1 homomeric $GABA_A$ subunits resulted in the expression of homomeric anion selective channels. This channel, however, was not gated by GABA since it is apparently open in the absence of this agonist. This was indicated by a low resting membrane resistance which was restored to the normal membrane resistance by the application of $GABA_A$ receptor antagonists picrotoxin or zinc. Moreover, muscimol and isoguvacine both failed to elicit any response on this channel. In comparison, bovine β1 $GABA_A$ receptors were sensitive to both GABA and muscimol with the agonists inducing a small inward current. However, these responses were small even at high GABA and muscimol concentrations. This could possibly

indicate an inefficient functional expression of these homomeric receptors. However, it is also possible that the single channel kinetics, such as opening frequency, burst duration, mean open time and single channel conductance, could be responsible for the small responses observed with the expression of these homomeric channels being relatively efficient. Interestingly, Blair and colleagues observed bursts of channel activity followed by long periods of no openings from patches exposed to 100 μM GABA in oocytes expressing bovine "β" subunit $GABA_A$ receptors (Blair *et al.*, 1988). Therefore it is conceivable that a low frequency of channel openings could also be responsible for the small responses to the test agonists seen in this study. Construction of a current-voltage relation for GABA revealed that the channel formed from the expression of bovine β1 subunits was either not able to conduct large currents leading to the rectification seen (Fig. 4.7) or the channel activity was strongly voltage-dependent. Previous experiments observed a strong voltage-dependence, with outward rectification of the single channel currents at depolarising potentials, for bovine homomeric "β" $GABA_A$ receptors (Blair *et al.*, 1988). Construction of a dose-response curve for GABA produced an EC_{50} value of 29.34 ± 5.1 μM which is approximately five fold higher than the EC_{50} value of 5.87 ± 0.6 μM for the heteromeric α1β1 $GABA_A$ receptor construct. Similar GABA-sensitive chloride channels were detected after injection of bovine "β" RNA in *Xenopus* oocytes (Blair *et al.*, 1988). Human β1 homomeric $GABA_A$ receptors expressed in human embryonic kidney cells have also been shown to be gated by GABA although again only small currents were detected (Pritchett *et al.*, 1988). Moreover, these cells once transfected with cDNAs encoding the single subunit, synthesized the respective mRNA in amounts similar to cDNAs encoding α1β1 $GABA_A$ receptors (Pritchett *et al.*, 1988). Thus it could be possible that the low currents obtained by expression of the human β1 $GABA_A$ receptor was either due to the reduced efficiencies of receptor assembly or that there was an efficient expression of these homomeric channels but the channel kinetics were such that only small currents were obtained (see earlier).

The mouse β1 receptor current was not sensitive to the competitive $GABA_A$ receptor antagonist bicuculline. It is possible that both GABA and bicuculline share a common binding site which is not present on the mouse β1 $GABA_A$ receptor or the site(s) at which these compounds bind is obscured. Conversely, on bovine β1 $GABA_A$ receptors bicuculline was found to block the GABA-induced current.

Both zinc and picrotoxin have the ability to antagonise the channel present in the mouse β1 receptors. Interestingly, zinc has a greater affinity for this receptor compared to picrotoxin with IC_{50} values of 0.23 ± 0.03 and 2.11 ± 0.6 μM respectively. Previous studies have determined the IC_{50} value for zinc on rat and mouse α1β1 $GABA_A$ receptors as approximately 1 μM (Draguhn *et al.*, 1990; Smart *et al.*, 1991). It could be possible that the conformation of the quaternary structure of the heteromeric and homomeric receptors are different leading to an altered affinity of the zinc binding site. There could also be a zinc binding site(s) on the α1 subunit as well as on the β1 subunit. An extra binding site(s) on the α1 subunit could alone or in combination with the β1 subunit influence the binding of zinc to the heteromeric $GABA_A$ receptor producing the decreased affinity of zinc for these receptors in comparison to the homomeric β1 subunit. Sigel and colleagues have previously shown that expression of the rat β1 induced a similar picrotoxin-sensitive channel lacking GABA-gating properties (Sigel *et al.*, 1989). Khrestchatisky and colleagues revealed application of picrotoxin to oocytes expressing rat "β" $GABA_A$ receptors elicited an outward current (Khrestchatisky *et al.*, 1989). Rather surprisingly, picrotoxin-induced currents were also observed in heteromeric $GABA_A$ receptors expressed in oocytes injected with either α5 (originally defined incorrectly as α4; for α4 see Ymer *et al.*, 1989a) and "β" RNAs or α1 and "β" RNAs (Khrestchatisky *et al.*, 1989). Furthermore, a similar current was observed in oocytes expressing rat α1β1γ2 $GABA_A$ receptors. Application of picrotoxin, applied in the absence of GABA, induced a small shift in the holding current in the opposite direction to the current elicited by GABA (Malherbe *et al.*, 1990b). It is possible that

this picrotoxin sensitive current seen in heteromeric GABA receptors could possibly be due to a minor fraction of channels open in the absence of added GABA or that these open channels could represent the expression of a small amount of homomeric β1 $GABA_A$ receptors. In bovine β1 $GABA_A$ receptors both zinc and picrotoxin completely abolished the GABA-induced current. Construction of current-voltage relations for zinc and picrotoxin on mouse β1 receptors and GABA on bovine β1 receptors revealed that both species of β1 homomeric $GABA_A$ receptors had a reversal potential near to the Cl^- equilibrium potential in these cells indicating that the channels are probably chloride-selective (Barish, 1983; Dascal, 1987).

The channel present in mouse β1 receptors was enhanced by pentobarbitone indicating physiologically for the first time that GABA and barbiturates bind to different sites within the $GABA_A$ receptor. In agreement with these results, a previous study identified two domains on the β2 subunit necessary for the activation of GABA but not pentobarbitone in $GABA_A$ receptors composed of rat α1β2γ2 subunits (Amin and Weiss, 1993). Moreover, the Hill coefficient revealed for pentobarbitone of 1.9 ± 0.26 indicates that there may be two binding sites for pentobarbitone on the homomeric murine β1 subunit. The GABA-induced current in the bovine β1 receptor was also enhanced by pentobarbitone. Conversely, the benzodiazepines appear to have no binding sites on either mouse or bovine β1 $GABA_A$ receptors. These results are in agreement with previous studies where the benzodiazepine enhancement of GABA-induced responses on $GABA_A$ receptors occurs only in heteromeric constructs containing a γ subunit with the selectivity for the benzodiazepines determined by the α subunit present. (Pritchett *et al.*, 1989; cf Malherbe *et al.*, 1990a; Doble and Martin, 1992).

The neurosteroid pregnanolone showed no sensitivity for the mouse β1 $GABA_A$ receptor. These results are in agreement with previous studies where it was shown that the steroid modification of the $GABA_A$ receptor was

strongly influenced by the presence of both the α and the γ but not the β subunits (Shingai *et al.*, 1991; Zamin *et al.*, 1992). Interestingly, propofol potentiated the ion channel conductance of this homomeric receptor demonstrating a potential binding site for this general anaesthetic on the β1 subunit. Thus propofol has a separate binding site from GABA and the benzodiazepines on this homomeric murine β1 subunit; however it is unclear whether propofol has a novel binding site in this β1 subunit or whether both propofol and pentobarbitone share a common binding site. Propofol has been previously shown to act as a positive allosteric modulator at $GABA_A$ receptors although no firm conclusions were drawn as to the site of propofol interactions with the receptor or the relative importance of the action of propofol at the $GABA_A$ receptor for anaesthesia (Hales and Lambert, 1991; Prince and Simmonds, 1992).

Penicillin G induced an outward current and decrease in the conductance of the ion channel present in the mouse β1 receptor. Previous studies have demonstrated that penicillin induces an open channel blockade of $GABA_A$ channels from mouse spinal cord neurones in culture (Twyman *et al.*, 1992; Katayama *et al.*, 1992). The convulsant action of the drug *in vivo* may occur through this inhibition of the $GABA_A$ receptor (Chow and Mathers, 1986). This study indicates that the ion channel formed by β1 receptor subunits may still accommodate the binding site for penicillin G.

The chloride channel blocker A-9-C was shown to have very little effect on both the ion channel present in the mouse β1 receptors and on the GABA-induced response in the bovine homomeric β1 $GABA_A$ receptor. A-9-C has been reported to block endogenous calcium-activated chloride currents in *Xenopus laevis* oocytes (Bowie and Smart, 1993). The lack of effect of A-9-C on the mouse homomeric β1 $GABA_A$ receptors provides further evidence that the ion channel present is the product of expression of the β1 $GABA_A$ receptor subunit.

4.3.2 EFFECT OF THE AMINO ACID SEQUENCE ON THE $GABA_A$ RECEPTOR PHARMACOLOGY

Extensive studies have previously revealed that replacement of a single amino acid in a variety of receptors changes the pharmacology of the mutant receptor. A profound effect of point mutation was seen on the pharmacological profile of the glycine receptor when residues in the α1 subunit, phenylalanine at position 159 and tyrosine at position 161, were exchanged. GABA which does not activate wild type glycine receptors formed from α1 subunits now gated the mutant channel with an EC_{50} value of approximately 600 μM (Schmeiden *et al.*, 1993). Moreover, the introduction of three amino acids, proline at position 236 and alanine and threonine at positions 237 and 251 respectively from the transmembrane domain M2 of the glycine or $GABA_A$ receptor into the M2 segment of the α7 nicotinic receptor was sufficient to convert the cationic-selective ion channel in this receptor into an anionic-selective channel gated by acetylcholine (Galzi *et al.*, 1992).

A physiological effect of a single mutation has been identified where an arginine has been mutated to a glutamine residue in the N-terminal region at position 100 in the α6 subunit in the cerebellar region of alcohol-non-tolerant (ANT) rat line. This mutation incurs a diazepam sensitivity not normally present in the cerebellum of 'wild-type' alcohol-tolerant rat $GABA_A$ receptors and renders the ANT rats highly susceptible to impairment of postural reflexes by benzodiazepine agonists (Korpi *et al.*, 1993). Furthermore, Sigel and colleagues demonstrated that a single amino acid substitution in the rat α1 subunit (leucine for phenylalanine at position 64) decreased the GABA affinity of the mutant receptor when expressed with β2 and γ2 subunits (Sigel *et al.*, 1992). These results suggest the involvement of N-terminal portions of the extracellular domains of subunits in the gating of the channel. Moreover, a recent study identified domains on the rat β2 subunit which were necessary for the activation of the receptor by GABA. Four amino

acid residues located in the β2 subunit, tyrosine at position 157, threonine at position 160, threonine at 202 and tyrosine at position 205, were identified as some of the key residues for the activation of the $GABA_A$ receptor by GABA (Amin and Weiss, 1993). These key residues are however conserved in the mouse, bovine, rat and human β1 subunits and could not therefore underlie the changes in pharmacological profiles seen in this study between the homomeric β1 receptors from mouse and bovine (Fig. 4.8). It could be possible that these residues play an important role in the GABA channel sensitivity to activation by GABA when the β subunit is expressed with the other $GABA_A$ receptor subunits α1 and γ2, but these amino acid residues may have little influence on the GABA binding in the homomeric β1 receptor (Amin and Weiss, 1993). Another possibility is that these sites are somehow occluded in the mouse β1 homomeric receptor but are present and accessible in the equivalent bovine $GABA_A$ receptor.

The β1 mouse amino acid sequence is approximately 97% identical to the amino acid sequence of the bovine β1 polypeptide (Fig. 4.8). One amino acid residue in the N-terminal region differs between these two species, a serine is present in the mouse at residue 3 which corresponds to an alanine at the identical position in the bovine (Fig. 4.8). All other differences between the amino acid sequences of the mouse and bovine β1 subunit occur in the large intracellular loop between transmembrane domains M3 and M4 (Fig. 4.8). Interestingly, the rat β1 subunit, which has been previously shown to have the pharmacological profile of that seen in this study with the mouse β1 subunit (Sigel *et al.*, 1989), contains a serine residue at position 3 which corresponds to that of the mouse β1 subunit (Fig. 4.8). It will be interesting to ascertain in the future whether this single amino acid change is responsible for the difference in the gating properties between the expressed mouse and bovine β1 homomeric $GABA_A$ receptors. It is also possible that the numerous changes in the residues between mouse and bovine in the large intracellular loop could incur different quaternary structures of the mouse

and bovine β1 subunits which could produce some of the variations seen between the pharmacological profile of these two species (Fig. 4.8). Furthermore, similar residues are located in this region for the rat β1 as that in the mouse β1 subunit which again could lead to the similarities in the pharmacology of these two species (Fig. 4.8). Moreover, Pritchett and colleagues demonstrated the human homomeric β1 subunit receptor to be gated by GABA in a way analogous to the bovine β1 $GABA_A$ receptor (Pritchett *et al.*, 1988). Interestingly, the residues located in this large intracellular loop for the human β1 subunit resemble more closely those of the bovine β1 subunit than the mouse β1 $GABA_A$ subunit (Fig. 4.8). A chimeric or point mutation study of these key residues will be required to determine their influence on the $GABA_A$ receptor function.

This study has shown a pharmacological variation between species homologues of the same receptor indicating that caution should be given when extrapolating the properties of a given receptor across species without independent validation, even when there is a high interspecies sequence identity. This has important implications for the design and therapeutic use of receptor-selective drugs of the future when these are based on measurements of affinity, selectivity and efficacy in non-human species.

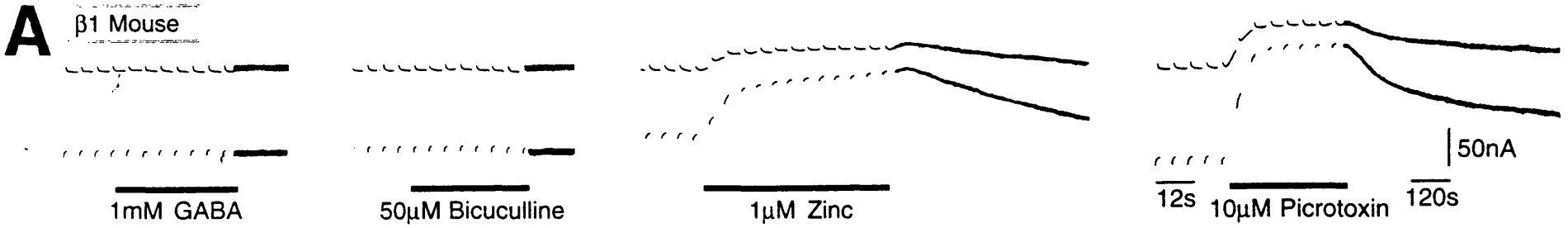

Figure 4.1. Pharmacological profile of mouse β1 homomeric $GABA_A$ receptors expressed in *Xenopus* oocytes. (A) Application of 1 mM GABA, 50 μM Bicuculline, 1 μM zinc and 10 μM picrotoxin to the mouse β1 homomeric receptor. The solid line in each case represents the duration of drug application. In this and all subsequent recordings the membrane conductance was monitored throughout by repetitively applying brief hyperpolarizing voltage command steps (-10mV; 1s, 0.2Hz). Holding potential for all oocytes, -40mV.

Figure 4.2. Inhibition plots and current-voltage relations for picrotoxin and zinc on the mouse β1 homomeric $GABA_A$ receptor. (A,B) Picrotoxin and zinc inhibition curves were constructed for the picrotoxin- and zinc-sensitive conductance (left hand plots). In this and all subsequent inhibition curves the resting conductance was taken as being 100 % before the addition of the antagonist and the solid line was generated according to the antagonist inhibition model (see methods). The right hand plots indicate the current-voltage relations for picrotoxin and zinc. The solid lines were constructed using 2^{nd} order polynomials and the reversal potentials of the picrotoxin- and zinc-sensitive component were determined.

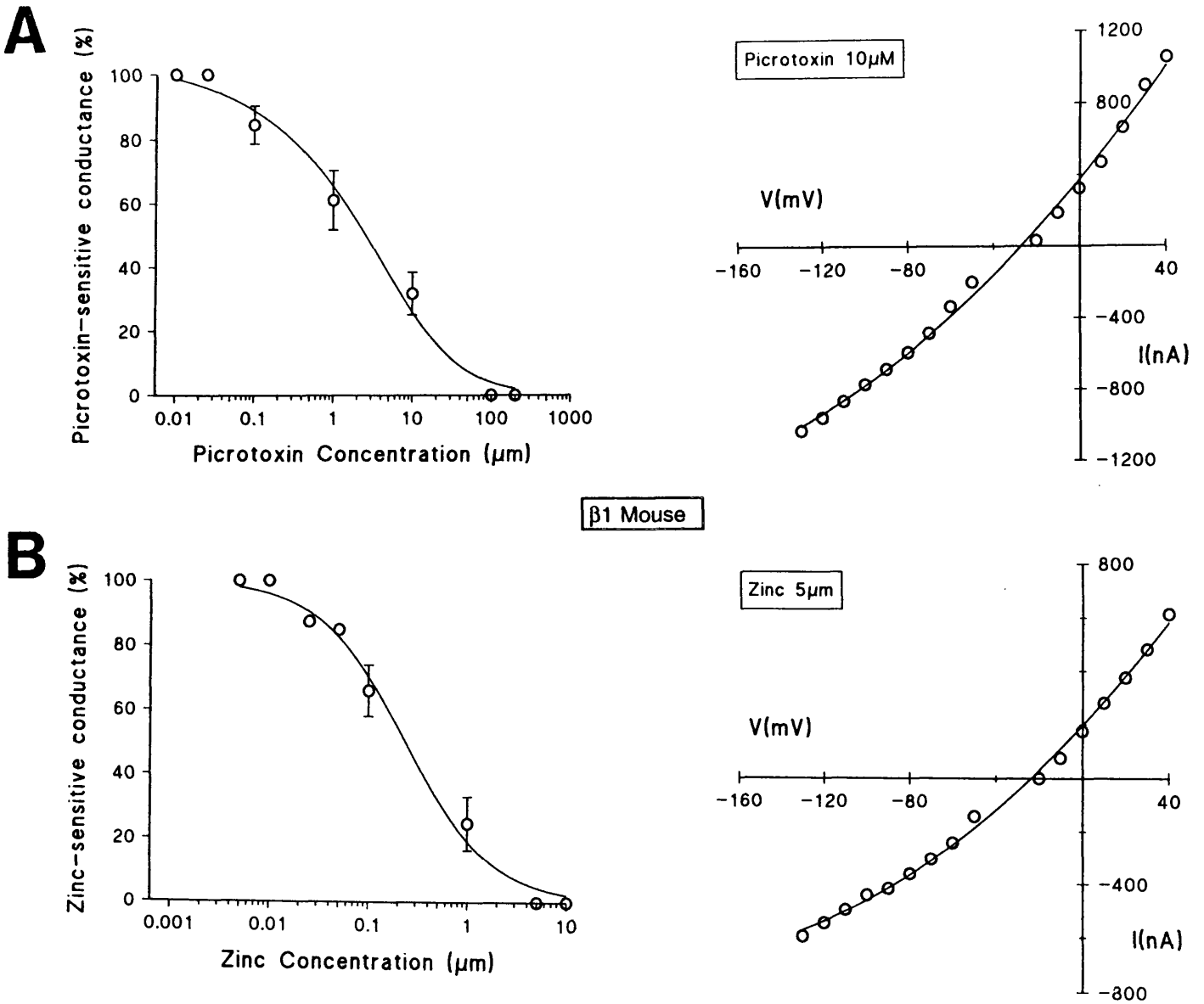
A
Picrotoxin-sensitive conductance (%)
100
80
60
40
20
0
0.01
0.1
1
10
100
1000
Picrotoxin Concentration (μm)
Picrotoxin 10μM
1200
800
V(mV)
-160
-120
-80
40
-400
I(nA)
-800
-1200
β1 Mouse
B
Zinc-sensitive conductance (%)
100
80
60
40
20
0
0.001
0.01
0.1
1
10
Zinc Concentration (μm)
Zinc 5μm
800
V(mV)
-160
-120
-80
40
-400
I(nA)
-800

Figure 4.3. Sensitivity of $GABA_A$ receptor agonists and pentobarbitone on the mouse β1 homomeric receptor. (A) Bath-application of 500 μM GABA, 500 μM muscimol, 500 μM isoguvacine and 50 μM pentobarbitone are indicated by the solid lines. (B) The left hand plot shows the pentobarbitone equilibrium concentration curve which was normalised with respect to 10 μM pentobarbitone with the conductance in the absence of pentobarbitone taken as the base line. The points represent means ± s.e.m recorded from 3 oocytes. The curve was fitted according to the logistic model (see methods). The right hand plot indicates the current-voltage relation for pentobarbitone from which the reversal potential of the pentobarbitone-sensitive component was determined.

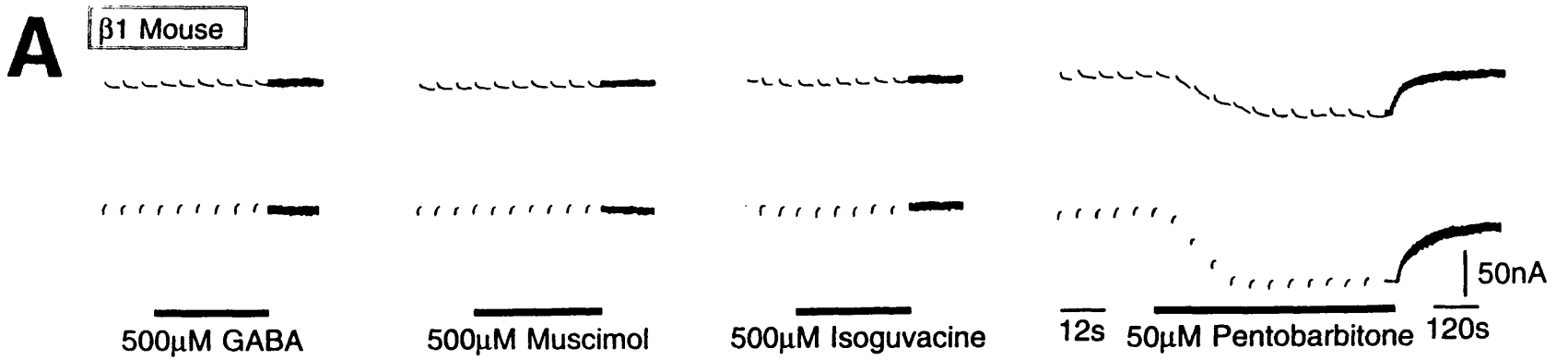
A
β1 Mouse
50nA
500μM GABA
500μM Muscimol
500μM Isoguvacine
12s
50μM Pentobarbitone
120s

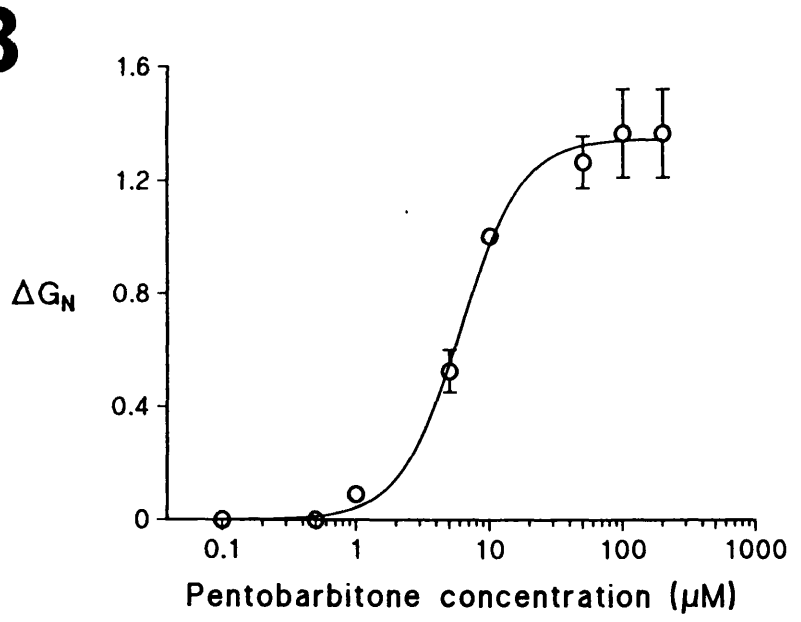
B
1.6
1.2
0.8
0.4
0
ΔG_N
0.1
1
10
100
1000
Pentobarbitone concentration (μM)

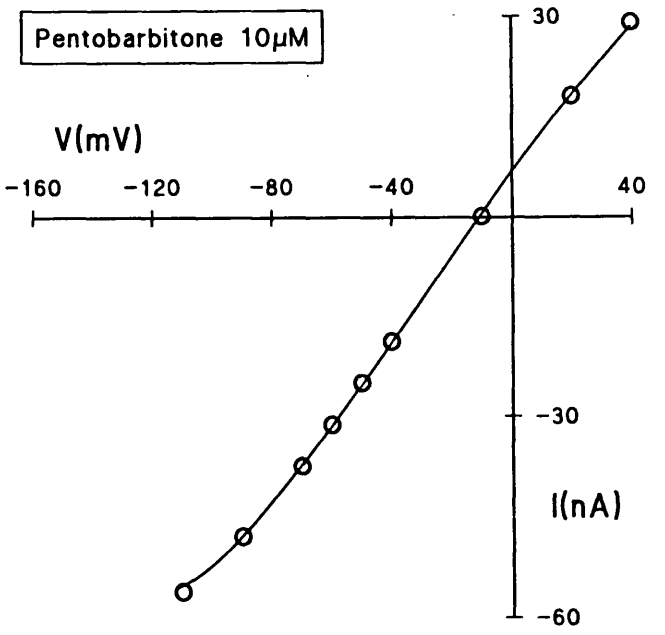
Pentobarbitone 10μM
V(mV)
-160
-120
-80
-40
40
30
-30
-60
I(nA)

Figure 4.4. Effect of $GABA_A$ receptor allosteric modulators on the homomeric mouse β1 receptor expressed in *Xenopus* oocytes. (A) Application of 10 μM flurazepam; 10 μM midazolam; 10 μM DMCM; and 10 μM flumazenil are indicated by the solid line. (B) Application of 500 nM pregnanolone; 100 μM chlormethiazole and 100 μM propofol in the absence and presence of 10 μM picrotoxin. (C) The effect of 1 mM penicillin G and 1 μM picrotoxin are indicated by the arrows and A-9-C application is shown by the solid line.

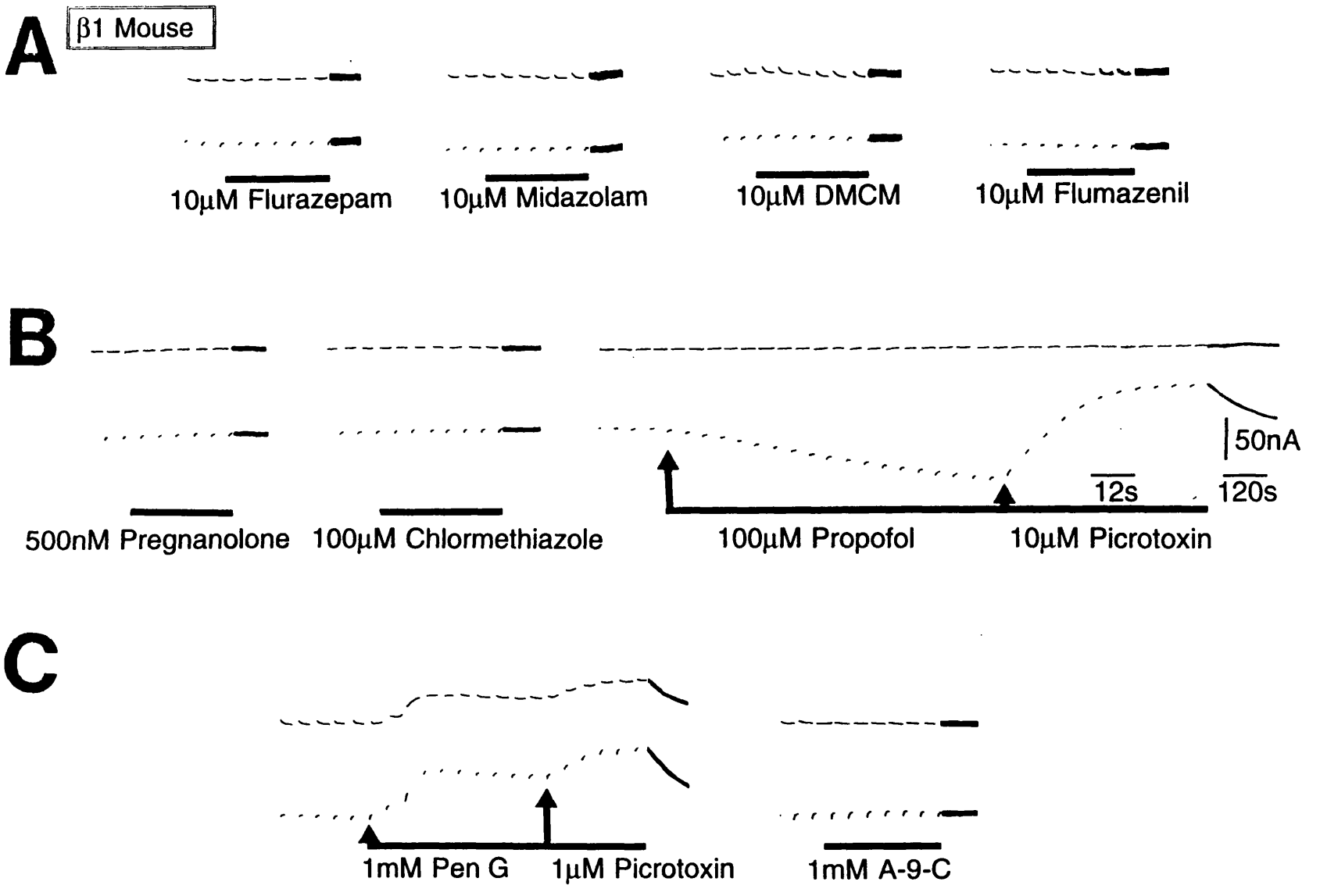
A
β1 Mouse
10μM Flurazepam
10μM Midazolam
10μM DMCM
10μM Flumazenil
B
50nA
12s
120s
500nM Pregnanolone
100μM Chlormethiazole
100μM Propofol
10μM Picrotoxin
C
1mM Pen G
1μM Picrotoxin
1mM A-9-C

Figure 4.5. Control experiments performed to ascertain the source of the unusual ion channels present after injection of mouse β1 subunits.
(A) Injection of the Lac Z gene encoding for β-galactosidase. Application of 1 mM GABA, 10 μM zinc, 50 μM picrotoxin and 50 μM pentobarbitone are indicated. (B) Injection of cRNA corresponding to the mouse β1 subunit. Oocytes were incubated in 50 μg/ml actinomycin D for two-five days prior to recording. Application of 500 μM GABA, 1 μM zinc, 50 μM picrotoxin and 10 μM pentobarbitone are shown. (C) Injection of cDNAs corresponding to α1β1 $GABA_A$ subunits. After incubation conditions as in (B) 10 and 500 μM GABA and 50 μM picrotoxin were bath-applied. (D) Injection of cDNAs corresponding to α1β1 $GABA_A$ subunits into oocytes in the absence of actinomycin D. Bath-application of 10 and 100 μM GABA and the antagonism of the response evoked by 10 μM GABA by picrotoxin (10 μM) are shown.

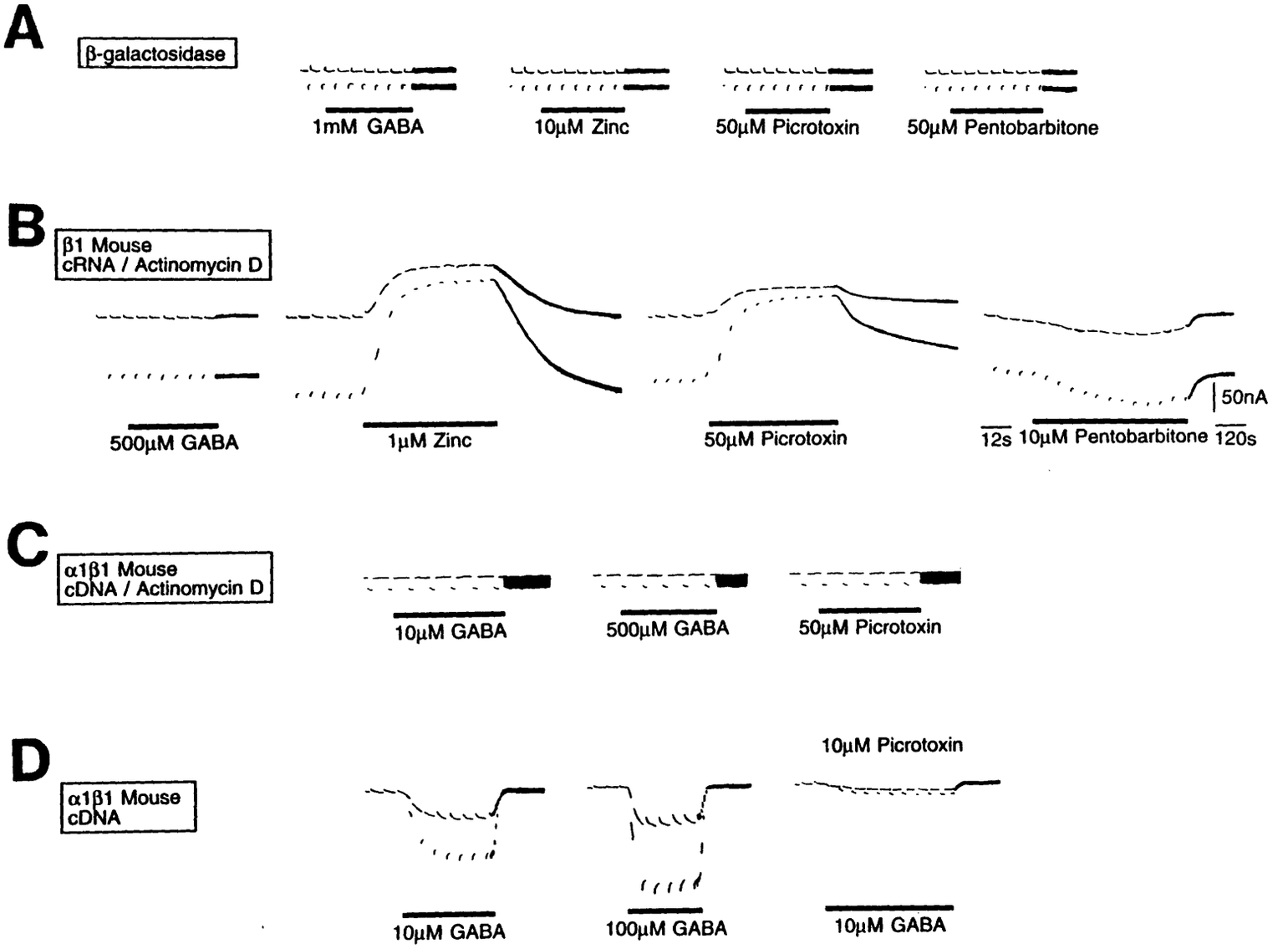
A
β-galactosidase
1mM GABA
10μM Zinc
50μM Picrotoxin
50μM Pentobarbitone
B
β1 Mouse
cRNA / Actinomycin D
500μM GABA
1μM Zinc
50μM Picrotoxin
50nA
12s
10μM Pentobarbitone
120s
C
α1β1 Mouse
cDNA / Actinomycin D
10μM GABA
500μM GABA
50μM Picrotoxin
D
α1β1 Mouse
cDNA
10μM Picrotoxin
10μM GABA
100μM GABA
10μM GABA

Figure 4.6. Pharmacological profile of bovine β1 homomeric receptors.
(A) Membrane current responses to 100 μM GABA and 100 μM muscimol are shown. All subsequent solid lines indicate the application of 100 μM GABA. The affect of 50 μM midazolam and 50 μM pentobarbitone on this GABA-induced response are indicated. (B) The β1 receptor was exposed to the $GABA_A$ receptor antagonists bicuculline (10 μM), picrotoxin (10 μM) and zinc (10 μM). The effect of the chloride channel blocker A-9-C on this GABA-induced current is also shown. (C) Membrane current and conductance change evoked by 5, 10, 100 and 1000 μM GABA.

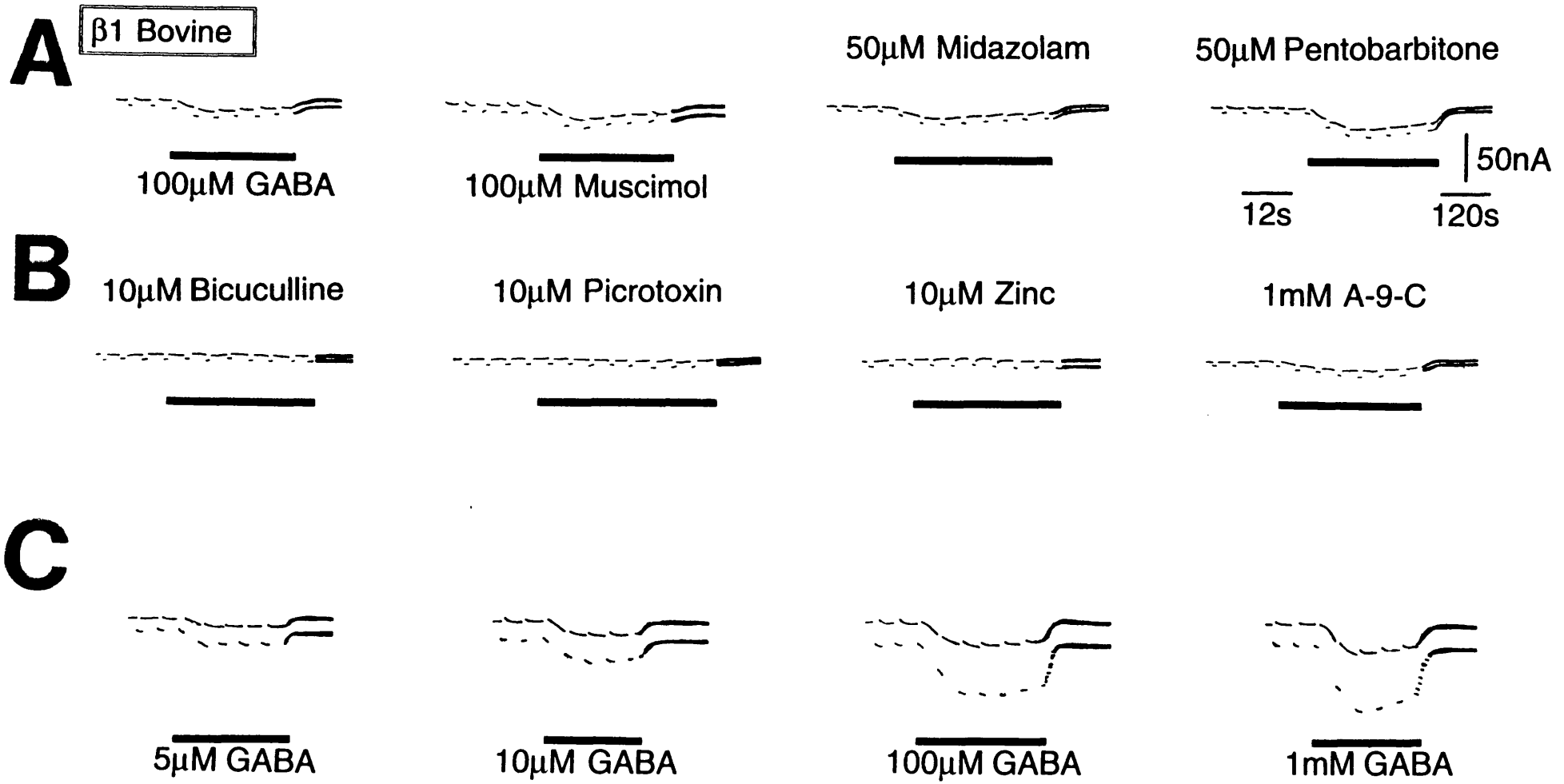
A
β1 Bovine
100μM GABA
100μM Muscimol
50μM Midazolam
50μM Pentobarbitone
50nA
12s
120s
B
10μM Bicuculline
10μM Picrotoxin
10μM Zinc
1mM A-9-C
C
5μM GABA
10μM GABA
100μM GABA
1mM GABA

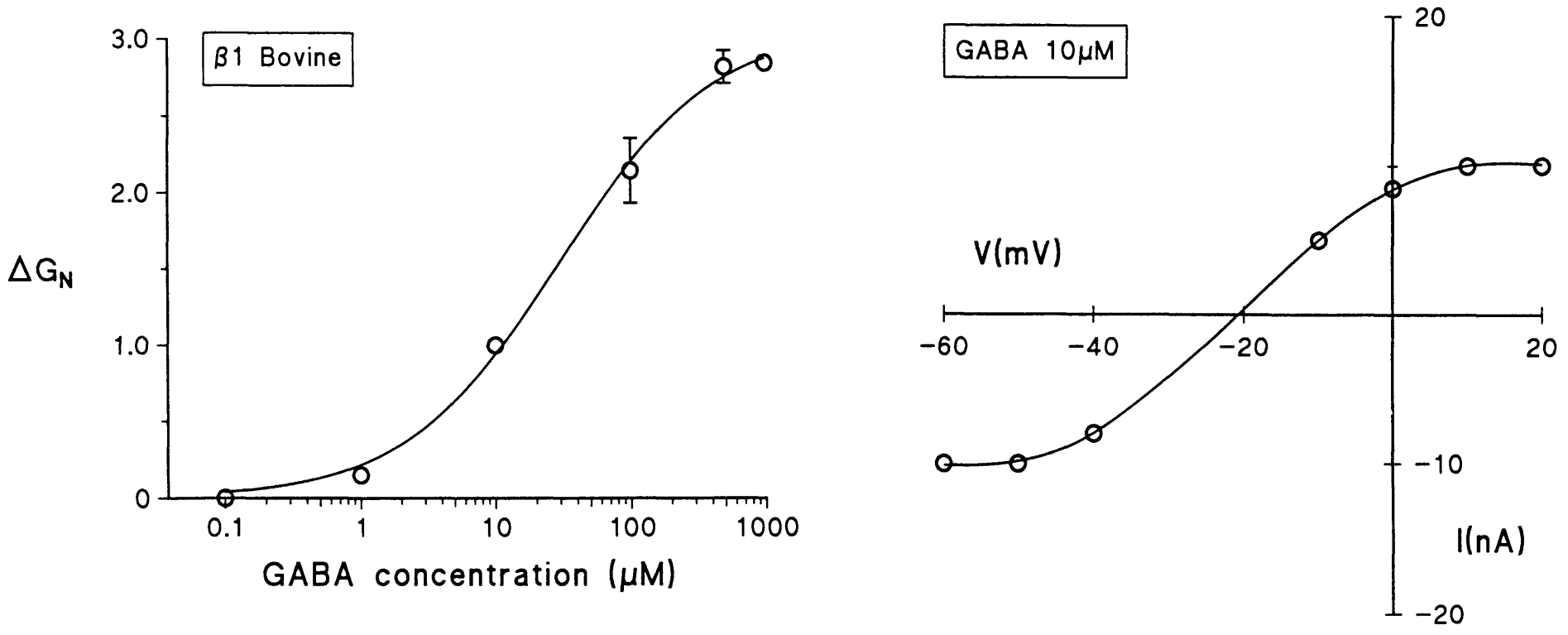

Figure 4.7. Characterisation of the GABA-induced current and conductance in oocytes expressing bovine β1 homomeric receptors. The left hand plot shows the GABA equilibrium concentration curve which was normalised with respect to 10 μM GABA. The points represent means ± s.e.m recorded from 3 oocytes. Curves were fitted according to the logistic model (see methods). The right hand plot indicates the current-voltage relation for GABA. Note the saturation of the current at positive potentials.

Figure 4.8. Homologies of the predicted amino acid sequences for mouse, rat, human and bovine $GABA_A$ β1 subunits. The vertical arrow indicates the proposed end of the signal sequence and the start of the mature protein, which is also where numbering starts. Numbers on the right denote amino-acid residues. Identical residues are shown by asterisks (*), a conservative change in an amino acid is indicated by a dot (.) and a non-conservative change by a space ( ). The overall sequence identity between the $GABA_A$ β1 subunits is 96.6%. The proposed membrane-spanning hydrophobic sequences (M1-M4) are indicated by the solid bars and some proposed key residues for GABA binding are boxed (Amin and Weiss, 1993). Sequences were obtained from Ymer *et al.*, 1989b (rat and bovine), Schofield *et al.*, 1989 (human) and Dr. D. Burt, University of Maryland, Baltimore, personal communication (mouse) and aligned using PC/GENE version 6.6.

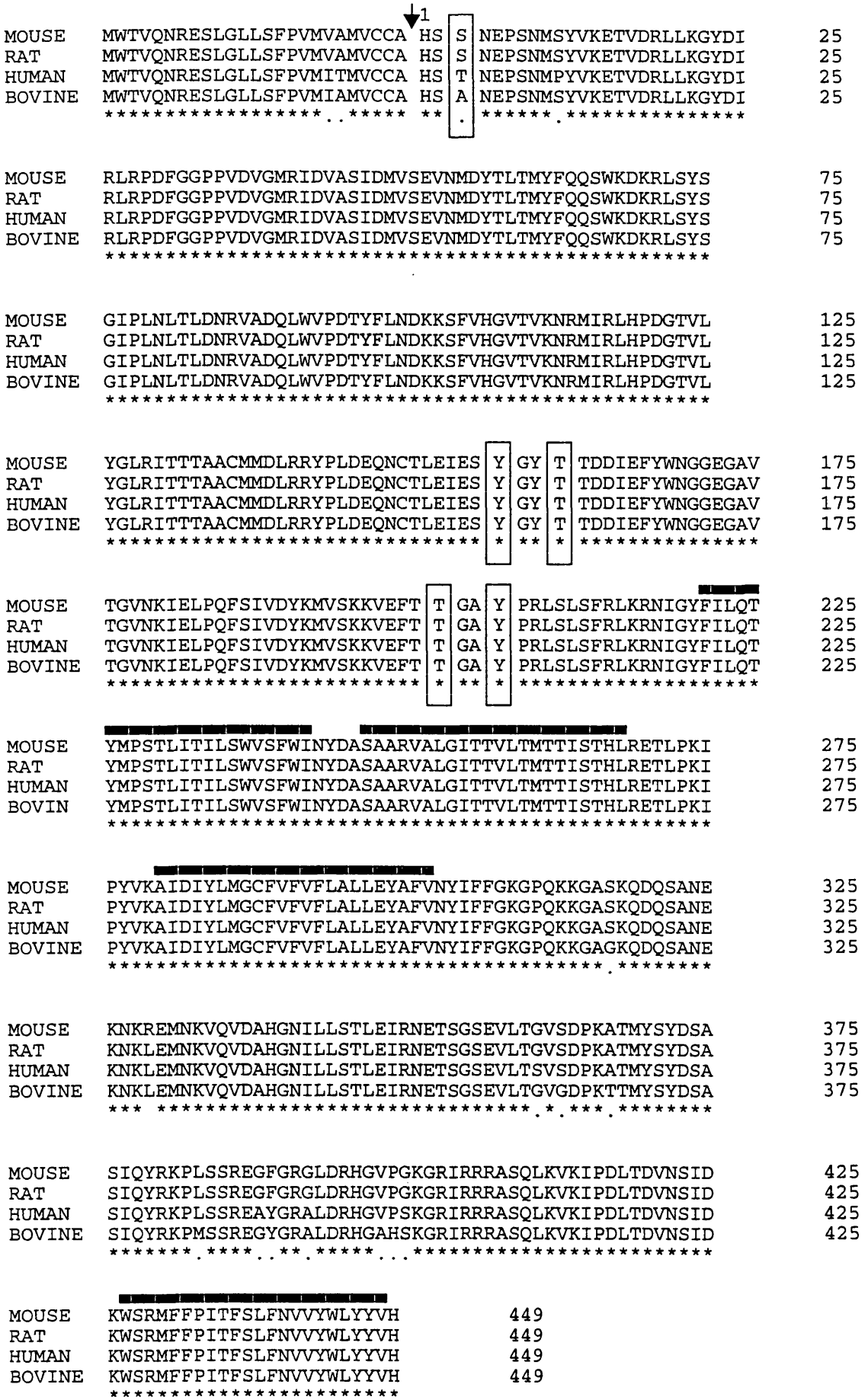
MOUSE MWTVQNRESLGLLSFPVMVAMVCCA HS S NEPSNMSYVKETVDRLLKGYDI 25
RAT MWTVQNRESLGLLSFPVMVAMVCCA HS S NEPSNMSYVKETVDRLLKGYDI 25
HUMAN MWTVQNRESLGLLSFPVMITMVCCA HS T NEPSNMPYVKETVDRLLKGYDI 25
BOVINE MWTVQNRESLGLLSFPVMIAMVCCA HS A NEPSNMSYVKETVDRLLKGYDI 25
MOUSE RLRPDFGGPPVDVGMRIDVASIDMVSEVNMDYTLTMYFQQSWKDKRLSYS 75
RAT RLRPDFGGPPVDVGMRIDVASIDMVSEVNMDYTLTMYFQQSWKDKRLSYS 75
HUMAN RLRPDFGGPPVDVGMRIDVASIDMVSEVNMDYTLTMYFQQSWKDKRLSYS 75
BOVINE RLRPDFGGPPVDVGMRIDVASIDMVSEVNMDYTLTMYFQQSWKDKRLSYS 75
MOUSE GIPLNLTLDNRVADQLWVPDTYFLNDKKSFVHGVTVKNRMIRLHPDGTVL 125
RAT GIPLNLTLDNRVADQLWVPDTYFLNDKKSFVHGVTVKNRMIRLHPDGTVL 125
HUMAN GIPLNLTLDNRVADQLWVPDTYFLNDKKSFVHGVTVKNRMIRLHPDGTVL 125
BOVINE GIPLNLTLDNRVADQLWVPDTYFLNDKKSFVHGVTVKNRMIRLHPDGTVL 125
MOUSE YGLRITTTAACMMDLRRYPLDEQNCTLEIES Y GY T TDDIEFYWNGGEGAV 175
RAT YGLRITTTAACMMDLRRYPLDEQNCTLEIES Y GY T TDDIEFYWNGGEGAV 175
HUMAN YGLRITTTAACMMDLRRYPLDEQNCTLEIES Y GY T TDDIEFYWNGGEGAV 175
BOVINE YGLRITTTAACMMDLRRYPLDEQNCTLEIES Y GY T TDDIEFYWNGGEGAV 175
MOUSE TGVNKIELPQFSIVDYKMVSKKVEFT T GA Y PRLSLSFRLKRNIGYFILQT 225
RAT TGVNKIELPQFSIVDYKMVSKKVEFT T GA Y PRLSLSFRLKRNIGYFILQT 225
HUMAN TGVNKIELPQFSIVDYKMVSKKVEFT T GA Y PRLSLSFRLKRNIGYFILQT 225
BOVINE TGVNKIELPQFSIVDYKMVSKKVEFT T GA Y PRLSLSFRLKRNIGYFILQT 225
MOUSE YMPSTLITILSWVSFWINYDASAARVALGITTVLTMTTISTHLRETLPKI 275
RAT YMPSTLITILSWVSFWINYDASAARVALGITTVLTMTTISTHLRETLPKI 275
HUMAN YMPSTLITILSWVSFWINYDASAARVALGITTVLTMTTISTHLRETLPKI 275
BOVIN YMPSTLITILSWVSFWINYDASAARVALGITTVLTMTTISTHLRETLPKI 275
MOUSE PYVKAIDIYLMGCFVFVFLALLEYAFVNYIFFGKGPQKKGASKQDQSANE 325
RAT PYVKAIDIYLMGCFVFVFLALLEYAFVNYIFFGKGPQKKGASKQDQSANE 325
HUMAN PYVKAIDIYLMGCFVFVFLALLEYAFVNYIFFGKGPQKKGASKQDQSANE 325
BOVINE PYVKAIDIYLMGCFVFVFLALLEYAFVNYIFFGKGPQKKGAGKQDQSANE 325
MOUSE KNKREMNKVQVDAHGNILLSTLEIRNETSGSEVLTGVSDPKATMYSYDSA 375
RAT KNKLEMNKVQVDAHGNILLSTLEIRNETSGSEVLTGVSDPKATMYSYDSA 375
HUMAN KNKLEMNKVQVDAHGNILLSTLEIRNETSGSEVLTSVSDPKATMYSYDSA 375
BOVINE KNKLEMNKVQVDAHGNILLSTLEIRNETSGSEVLTGVGDPKTTMYSYDSA 375
MOUSE SIQYRKPLSSREGFGRGLDRHGVPGKGRIRRRASQLKVKIPDLTDVNSID 425
RAT SIQYRKPLSSREGFGRGLDRHGVPGKGRIRRRASQLKVKIPDLTDVNSID 425
HUMAN SIQYRKPLSSREAYGRALDRHGVPSKGRIRRRASQLKVKIPDLTDVNSID 425
BOVINE SIQYRKPMSSREGYGRALDRHGAHSKGRIRRRASQLKVKIPDLTDVNSID 425
MOUSE KWSRMFFPITFSLFNVVYWLYYVH 449
RAT KWSRMFFPITFSLFNVVYWLYYVH 449
HUMAN KWSRMFFPITFSLFNVVYWLYYVH 449
BOVINE KWSRMFFPITFSLFNVVYWLYYVH 449

CHAPTER FIVE

CHARACTERISATION OF RECOMBINANT $GABA_A$ RECEPTORS WITH pH AND ZINC

CHARACTERISATION OF RECOMBINANT $GABA_A$ RECEPTORS WITH pH AND ZINC

5.1 INTRODUCTION

Increases in electrical activity of neurones, such as spike firing, have been observed to cause rapid shifts in extracellular ionic composition, including decreases in Na^+ and Ca^+ and a rise in K^+ (Nicholson, 1979; Dietzel *et al.*, 1982; Sykova, 1983). Such phenomena occur due to the flux of ions across ligand- and voltage-gated ion channels. These shifts in the concentration of extracellular ions have been associated with rapid changes in the extracellular pH (for review see Chesler, 1990). N-methyl-D-aspartate (NMDA) receptors have been shown to be selectively inhibited by protons (Tang *et al.*, 1990; Traynelis and Cull-Candy, 1990, 1991). Thus, external pH changes could have important implications for neuronal function.

In previous studies on crayfish and lobster muscle fibres it was shown that the GABA-induced chloride conductance increase was sensitive to changes in the external pH (Takeuchi and Takeuchi, 1967, Smart and Constanti, 1982). The GABA-induced response was reduced at high pH and enhanced at low pH, suggesting the existence of pH sensitive sites residing in the GABA receptor complex which might be capable of modulating the GABA response. Zinc has been shown to antagonise the GABA-evoked response on lobster muscle GABA receptors (Smart and Constanti, 1982). The binding site for zinc, in this GABA receptor, was also shown to be sensitive to pH. Reducing the external pH revealed an enhancement of the GABA-induced conductance change, but the antagonistic effect of zinc was markedly reduced (Smart and Constanti, 1982). This suggested that zinc and H^+ compete for a similar site on the lobster muscle GABA receptor. Zinc has also been shown to be a GABA antagonist on cultured embryonic neuronal $GABA_A$ receptors (Westbrook and Mayer, 1987; Smart and Constanti, 1990). Recombinant $GABA_A$ receptors

expressed in human kidney cells revealed that receptors lacking the γ subunit were inhibited by zinc and receptors possessing a γ subunit were relatively insensitive to blockade by zinc ions (Draguhn *et al.*, 1990; Smart *et al.*, 1991). However, in contrast to invertebrate muscle GABA receptors, the inhibition by zinc of the GABA-induced response was unaffected by pH in cultured embryonic neuronal $GABA_A$ receptors (Smart, 1992). This suggested that, unlike the invertebrate GABA receptors, zinc and H^+ do not compete for a similar site in mammalian $GABA_A$ receptors.

However, the effect of changing the external pH on the GABA-induced responses and the influence of this pH change on the inhibition of GABA responses by zinc has not been studied in recombinant $GABA_A$ receptors. Therefore, this study investigated the effects of pH on recombinant $GABA_A$ receptors. In addition, the pH dependence of the zinc induced inhibition of the GABA-induced responses was studied. The results demonstrate for the first time that the modulation of the GABA-induced response by pH depends on the subunit composition of the $GABA_A$ receptor. Moreover, the inhibition of the GABA response by zinc was modulated by changing the external pH in recombinant $GABA_A$ receptors. Interestingly, the zinc antagonism of the GABA-evoked responses and the modulation of this inhibition by pH was also shown to be dependent on the $GABA_A$ receptor subunit composition.

The individual pH dependent phenotypes seen in this study could prove to be a useful tool for the determination of the composition of unknown recombinant and native $GABA_A$ receptors.

5.2 RESULTS

5.2.1 pH CHARACTERISATION OF RECOMBINANT $GABA_A$ RECEPTORS

Membrane currents and conductances evoked by bath-applied GABA in Ringer solutions of different pH (4.4 to 9.4) were monitored in single *Xenopus* oocytes injected with cDNAs encoding mouse α1β1, α1β1γ2S, α1β1δ or

$\alpha 1\beta 1\gamma 2S\delta$ $GABA_A$ receptor subunits. To minimise variations in responses among oocytes, pH effects were studied on individual oocytes and normalised to the conductance change induced by 10 μM GABA at pH 7.4 obtained from the same oocyte. For all oocytes expressing any $GABA_A$ receptor construct, changes in the external pH induced a change in the resting conductance. Decreasing the pH from 7.4 to 5.4 induced a small inward current with a decrease in the resting conductance. Conversely, increasing the pH to 9.4 evoked a small outward current with an increased resting conductance (Fig. 5.1A). The pH sensitivity of the oocytes appeared to be unrelated to the cDNAs injected. In agreement, Woodward and Miledi (1992) revealed that the sensitivity of oocytes to extracellular pH was a property of native (non-injected) cells. Moreover, the same pH sensitivity was seen in defolliculated oocytes indicating the responses were activated in the oocyte itself, as opposed to enveloping follicular cells (Woodward and Miledi, 1992). The ionic basis for the pH sensitivity is thought to occur via K^+ conductance changes, with acidification of the bathing medium inducing inward currents due to reductions in membrane conductance to K^+ (Woodward and Miledi, 1992).

Under voltage clamp at a holding potential of -40 mV, oocytes injected with $\alpha 1\beta 1$ $GABA_A$ receptor constructs responded to GABA (0.1 to 500 μM) with large membrane currents at extracellular pH 7.4. On increasing the acidity of the Ringer solution to pH 5.4, the current and conductance change produced by a fixed dose of GABA (10 μM) was increased (Fig. 5.1A). Moreover, on increasing the alkalinity of the Ringer solution, the current and conductance change evoked by bath application of 10 μM GABA was decreased (Fig. 5.1A). The pH dependence of the $\alpha 1\beta 1$ $GABA_A$ receptor construct was assessed further by construction of a pH titration curve (Fig. 5.1B). From this sigmoidal relationship the pH at which the half maximal conductance increase occurred was estimated and revealed a pK_a value of approximately 6.8 (Table 5.1). Equilibrium concentration curves for this $GABA_A$ receptor construct were assembled by measuring the steady state

GABA-induced chloride conductance. These relationships revealed that on decreasing the extracellular pH from 7.4 to 5.4 the GABA-induced conductance change increased with the elevated H^+ potentiating the maximum (Fig. 5.1C). The Hill coefficients and EC_{50} values remained relatively unaffected by the decrease in extracellular pH (Table 5.1). Conversely, on increasing the extracellular pH from 7.4 to 9.4 an antagonism of the GABA-induced conductance occurred of a non-competitive type (Fig. 5.1C). The maximum conductance increase induced by saturating concentrations of GABA (500 μM) was reduced with small changes in the Hill coefficients and EC_{50}s for GABA (Table 5.1). Current-voltage (I-V) relationships for the α1β1 receptor combination were assessed during the steady-state phase of an individual GABA-induced response at pH 7.4 and 5.4. The I-Vs displayed a degree of outward rectification with no significant change in the agonist reversal potentials, -29.3 mV (pH 7.4) and -30.1 mV (pH 5.4), which are close to the Cl^- reversal potential in these cells (Fig. 5.1C; Barish, 1983; Dascal, 1987).

The pH dependence of the GABA-induced response of the mouse α1β1γ2S $GABA_A$ receptor construct revealed quite a different picture. On changing the pH of the external Ringer solution from pH 7.4 in either direction (5.4 or 9.4) the current and conductance change induced by 10 μM GABA was apparently unaffected (Fig. 5.2A). This lack of sensitivity to external pH was again observed over a broad range of pH from the pH titration curve (Fig. 5.2B). Moreover, both the equilibrium concentration response curve and I-V relation for this receptor construct were unaffected by changes in the external pH (Fig. 5.2C; Table 5.1).

The addition of a γ2S subunit to the α1β1 receptor construct rendered the $GABA_A$ receptor insensitive to external pH changes indicating a dependence of pH sensitivity on the exact composition of subunits present within the $GABA_A$ receptor complex. To further assess the dependence of pH sensitivity

on subunit composition oocytes were injected with cDNAs encoding mouse $\alpha1\beta1\delta$ $GABA_A$ subunits. The addition of the δ subunit to the $\alpha1\beta1$ receptor construct revealed a different pH profile from either $\alpha1\beta1$ or $\alpha1\beta1\gamma2S$ $GABA_A$ receptor constructs. On increasing the acidity of the external Ringer solution from pH 7.4 to pH 5.4 a greater current and conductance change was induced by 10 μM GABA (Fig. 5.3A). Conversely, the GABA-evoked response was decreased on increasing the alkalinity from pH 7.4 to 9.4 (Fig. 5.3A). Interestingly, on constructing a pH titration curve a change in the pH profile was seen between receptors comprising of $\alpha1\beta1$ subunits with and without δ subunits. Unlike the sigmoidal curve seen with $\alpha1\beta1$ $GABA_A$ receptor subunits (Fig. 5.1B), this curve could be seen to be biphasic, with a clear plateaux between pH 7.4 and 8.4 (Fig. 5.3B). The data in the titration curve provided two pK_a values of approximately 6.3 and 9.9 (Table 5.1). These two pK_a values were estimated from the titration curve by separating the two sections of the curve, with the plateaux at pH 7.4 to 8.4 either acting as the bottom or top of each curve respectively, and measuring the pH at which the half maximal conductance increase occurred in each case. Equilibrium concentration response curves were constructed and revealed that increasing the acidity of the Ringer solution from pH 7.4 to 5.4 an increase in the GABA-induced conductance change occurred (Fig. 5.3C). Conversely, increasing the alkalinity of the Ringer solution caused a depression in the maximum conductance increase induced by saturating concentrations of GABA (500 μM; Fig. 5.3C). The change in pH from 7.4 to 5.4 or 9.4 induced little change in the Hill coefficients or EC_{50} values for GABA (Table 5.1). This depression of the maximum response suggests a non-competitive mode of antagonism of the GABA-induced conductance change. I-V relationships for the $\alpha1\beta1\delta$ receptor combination were assessed during the steady-state phase of an individual GABA-induced response at pH 7.4 and 5.4. The I-Vs displayed a degree of outward rectification with no significant change in the agonist reversal potentials (Fig. 5.3C).

All three mouse $GABA_A$ receptor constructs examined so far, α1β1, α1β1γ2S and α1β1δ, revealed a different pH profile. Therefore, it was of interest to determine whether the addition of both the γ2S and the δ subunit to α1β1 $GABA_A$ receptor subunits would further influence the pH sensitivity of the $GABA_A$ receptor complex. Oocytes were injected with cDNAs encoding mouse α1β1γ2Sδ $GABA_A$ receptor subunits. Interestingly, this $GABA_A$ receptor complex revealed a pH sensitivity unlike all receptor constructs already examined. On decreasing or increasing the pH of the Ringer solution from 7.4 to 5.4 or 9.4, the current and conductance changes induced by 10 μM GABA were decreased (Fig. 5.4A). Construction of a pH titration plot revealed a symmetrical bell-shaped curve with the conductance greatest at neutral pH 7.4 to 8.4 (Fig. 5.4B). From this bell-shaped curve the pH's at which the half maximal conductance increase occurred were estimated for each symmetric side of the curve, and revealed pK_a values of approximately 5.5 and 9.6 (Table 5.1). Equilibrium concentration curves for GABA revealed that changing the external pH from 7.4 to 5.4 or 9.4 induced an antagonism of a mixed/non-competitive type revealed by a small lateral shift with a depression in the maximum (Fig. 5.4C). There was little change seen in the Hill coefficients with a small change in EC_{50}s for GABA (Table 5.1). I-V relationships for this receptor construct were constructed at pH 7.4 and 5.4 and displayed a degree of outward rectification with no significant change in the agonist reversal potentials (Fig. 5.4C).

5.2.2 COMPARISON OF THE EFFECT OF pH ON $GABA_A$ RECEPTORS FROM TWO DIFFERENT SPECIES

The difference in pH sensitivity between mouse α1β1 and α1β1γ2S $GABA_A$ receptors is intriguing. The addition of a γ2S subunit seemingly had the ability to remove the pH sensitivity of the $GABA_A$ receptor construct. Whether such an effect is related specifically to mouse $GABA_A$ receptor subunits was studied by comparison with bovine $GABA_A$ receptor subunits. Conductance

changes produced by GABA (0.1 to 250 μM) were recorded from oocytes expressing bovine α1β1 $GABA_A$ receptor subunits in Ringer solutions of varying pH (4.4 to 9.4). On increasing the alkalinity of the external solution, the conductance change evoked by a fixed concentration of GABA (10 μM) decreased along a sigmoidal curve (Fig. 5.5A) in a manner analogous to mouse α1β1 receptor constructs providing a pK_a value of approximately 6.4 (Table 5.1). The similarity of the pK_a values, mouse α1β1 6.8 and bovine 6.4, suggests the possible involvement of similar amino acid residues which may be involved in the allosteric transitions for these two receptors associated with GABA ion channel gating. Equilibrium concentration curves for GABA were also constructed for bovine α1β1 receptor constructs. This bovine receptor construct revealed that increasing the alkalinity of the Ringer solution caused a depression in the maximum conductance increase induced by saturating concentrations of GABA (250 μM) with little change in the Hill coefficients or EC_{50}s for GABA (Table 5.1), suggesting a non-competitive mode of antagonism (Fig. 5.5B). I-V relationships displayed a degree of outward rectification with no significant change in the agonist reversal potentials in Ringer solutions of pH 7.4 and 5.6 (Fig. 5.5B).

Interestingly, the addition of the bovine γ2S $GABA_A$ receptor subunit to this receptor construct, yielding receptors with α1β1γ2S subunit composition, again removed the pH sensitivity of this $GABA_A$ receptor construct. This lack of sensitivity to external pH was determined on construction of a pH titration curve (Fig. 5.6A). Moreover, both the equilibrium concentration response curve and I-V for this receptor construct were unaffected by changes in the external pH (Fig. 5.6B; Table 5.1). This lack of sensitivity to external pH was consistent with that observed for the same receptor construct with the mouse species. Therefore the addition of the γ2S subunit to α1β1 $GABA_A$ receptor constructs could lead to masking of the specific 'proton-sensitive' amino acid residues involved in influencing the $GABA_A$ receptor conductance.

5.2.3 MODULATION OF THE EFFECT OF ZINC ON RECOMBINANT $GABA_A$ RECEPTORS BY pH

The 'proton-sensitive' sites which modulated the conductance of the GABA-gated chloride channels may also be affected by other agents which could bind to these groups. Zinc has been found to be a GABA antagonist on cultured neuronal $GABA_A$ receptors (Westbrook and Mayer, 1987; Smart and Constanti, 1990). If the site at which zinc binds is also sensitive to H^+, then it should be possible to interfere with the zinc antagonism of the GABA responses by changing the pH of the external solution. Four mouse $GABA_A$ receptor subunit constructs, $\alpha1\beta1$, $\alpha1\beta1\delta$, $\alpha1\beta1\gamma2S$ and $\alpha1\beta1\gamma2S\delta$, were initially employed to assess the pH sensitivity of the antagonism of GABA responses by zinc.

GABA-induced conductances mediated by receptors comprising $\alpha1\beta1$ subunits, were inhibited by zinc (0.01 to 100 μM). The construction of a zinc inhibition curve led to the determination of the IC_{50} for zinc as 1.1 ± 0.1 μM at pH 7.4 (Fig. 5.7A; Table 5.2). On increasing the alkalinity to pH 9.4 the antagonism by zinc was only slightly affected with the IC_{50} for zinc as 1.3 ± 0.15 μM (Fig. 5.7A; Table 5.2). However, by acidifying the bathing medium and increasing the $[H^+]$ 100 fold, the blockade by zinc of the GABA-induced conductance was considerably alleviated. The IC_{50} for zinc at pH 5.4 was estimated as 55.2 ± 3.4 μM (Fig. 5.7A; Table 5.2). GABA concentration response curve analysis revealed that in the presence of 1 μM zinc at pH 7.4 a depression of the maximum response occurred. This is consistent with a non-competitive type of inhibition. There was little change seen in the Hill coefficients or EC_{50}s for GABA in the presence of zinc (Table 5.3, 5.4). On reducing the external pH to 5.4, the GABA-induced conductance change was enhanced as expected. However, the antagonistic effect of zinc was markedly reduced. As predicted from the IC_{50} value for zinc at pH 5.4, 50 μM zinc was needed to reduce the maximum GABA-induced response by approximately the same amount as

that observed with 1 μM zinc at pH 7.4 (Fig. 5.7B). This suggests that an increased H^+ binding was excluding the binding of zinc to the 'proton-sensitive' site. The equilibrium concentration curves further revealed that the antagonism produced by 50 μM zinc was of a mixed/non-competitive type. The maximum increase induced by saturating concentrations of GABA (500 μM) was reduced with little change in the Hill coefficients and a slight change in the EC_{50} for GABA (Table 5.3, 5.4). Construction of GABA equilibrium response curves at pH 9.4 revealed that on increasing the alkalinity of the external solution, the GABA-induced conductance change was decreased as expected. However, the antagonistic effect of zinc was only slightly altered from that observed at pH 7.4 as predicted from the zinc inhibition curves (Fig. 5.7B). Zinc (1 μM) inhibited the GABA-induced conductance in a mixed/non-competitive fashion with a depression of the concentration curve (Fig. 5.7B). Moreover, zinc antagonism appeared to have a greater modulatory influence at higher GABA concentrations (> 5 μM) at pH 9.4 than at lower GABA concentrations, with no antagonism of the GABA-induced response occurring at GABA concentrations less than 2.5 μM. The GABA response curves in the presence of 1 μM zinc also indicated little change in the Hill coefficients with a reduction in the EC_{50} for GABA (Table 5.3, 5.4).

The inhibition of GABA responses by zinc has been shown to depend on the composition of the $GABA_A$ receptor (Draguhn *et al.*, 1990; Smart *et al.*, 1991). The addition of a δ subunit to α1β1 $GABA_A$ receptor subunits, yielding receptors with α1β1δ subunit composition, led to a $GABA_A$ receptor with a novel zinc sensitivity. Zinc inhibition curves revealed a similar profile to α1β1 receptor constructs. Increasing the external pH from 7.4 to 9.4 had little effect on the antagonistic effect by zinc of GABA responses with IC_{50}s 14.8 ± 1.5 and 14.8 ± 1.7 μM respectively (Fig. 5.8A; Table 5.2). However, on increasing the acidity of the external solution the antagonism by zinc was considerably alleviated with an IC_{50} of 45.9 ± 3.7 μM at pH 5.4 (Fig. 5.8A; Table 5.2). Interestingly, GABA concentration response curve analyses

revealed a competitive inhibition by zinc on these α1β1δ $GABA_A$ recombinant receptors (Fig. 5.8A). Competitive inhibition has previously been seen for zinc inhibition of GABA responses on frog dorsal root ganglion cells (Akaike *et al.*, 1987; Yakushiji *et al.*, 1987). However, this is the first report of competitive inhibition for zinc on mammalian $GABA_A$ receptors. Little change occurred in the Hill coefficients but the EC_{50}s were markedly altered in the presence of 10 μM zinc (Fig. 5.8A; Table 5.3, 5.4). At a higher zinc concentration (100 μM) inhibition of the GABA-induced response remained apparently competitive (Fig. 5.8A). On reducing the external pH from 7.4 to 5.4, the GABA response was enhanced as expected but the antagonistic effect of zinc was again reduced. The antagonism however remained competitive. Zinc at a higher concentration of 50 μM was required to antagonise the $GABA_A$ receptor at pH 5.4 compared to 10 μM zinc at pH 7.4 as predicted from the IC_{50} values for zinc (Fig. 5.8B). This again suggests that increased H^+ binding excludes the binding of zinc to the 'proton-sensitive' site. Moreover, little change occurred in the Hill coefficients but the EC_{50} for GABA were markedly altered in the presence of zinc (Fig. 5.8B; Table 5.3, 5.4). Construction of GABA equilibrium response curves at pH 9.4 revealed that the GABA-induced conductance change was reduced. However, the antagonistic effect of zinc was slightly increased from that observed at pH 7.4 (Fig. 5.8B). Moreover, zinc still inhibited the GABA-induced conductance in a competitive fashion with little change in the Hill coefficients but marked changes in the EC_{50}s for GABA (Fig. 5.8B; Table 5.3, 5.4).

Zinc inhibition curves were also constructed for oocytes expressing mouse α1β1γ2S or α1β1γ2Sδ $GABA_A$ receptor subunits (Fig. 5.9A,B). The GABA-activated responses were only inhibited by high concentrations (> 100 μM) of zinc (Fig. 5.9A,B). IC_{50} values were estimated for α1β1γ2S receptors as 639.9 ± 34.9 μM and for α1β1γ2Sδ receptors as 615.4 ± 84.3 μM (Table 5.2). GABA concentration response curves for α1β1γ2S receptor constructs with and without the δ subunit revealed that low concentrations of zinc (5 to

10 μM) had no effect, but at high zinc concentrations (300 μM), the maximum conductance increase induced by saturating concentrations of GABA (500 μM) was reduced with little change in the Hill coefficients and small changes in the EC_{50} values for GABA (Fig. 5.9A,B; Table 5.3, 5.4). Both relationships revealed that the antagonism produced by 300 μM zinc was of a non-competitive type. Therefore, the addition of a δ subunit to the α1β1γ2S receptor construct did not alter the pharmacological profile of the zinc antagonism compared to the addition of the δ subunit to the α1β1 $GABA_A$ receptor construct.

5.2.4 COMPARISON OF THE EFFECT OF ZINC BY pH ON $GABA_A$ RECEPTORS FROM TWO DIFFERENT SPECIES

The pH dependence of the zinc blockade of GABA-activated responses for the murine receptor composed of α1β1 subunits was compared to that of the bovine α1β1 subunit receptor construct. Zinc inhibition curves showed a dependence on the external pH similar to that seen for the mouse receptor (Fig. 5.10A). Once again, by acidifying the bathing medium the inhibition by zinc of GABA responses could be alleviated with IC_{50} values for pH 7.4 and 6.4 as 0.73 ± 0.06 and 1.7 ± 0.1 μM respectively. Interestingly, the inhibition of GABA-induced responses by zinc was not as reduced by decreasing the pH for this bovine receptor as compared to the equivalent murine receptor with IC_{50} values increasing 50 fold (pH 7.4 to 5.4) for murine α1β1 and 2.5 fold (pH 7.4 to 6.4) for bovine α1β1 $GABA_A$ receptor constructs. By increasing the pH of the Ringer to 8.4, zinc inhibited the GABA response to a greater extent than at pH 7.4 which was reflected in the IC_{50} for zinc at pH 8.4 as 0.37 ± 0.05 μM (Fig. 5.10A; Table 5.2). GABA concentration response curve analysis revealed a similar profile as for the mouse α1β1 $GABA_A$ receptor constructs. The block induced by a low concentration of zinc (0.5 μM) at pH 7.4 or 8.4 was of a mixed/non-competitive type with a small lateral shift as well as a depression of the maximum response with small changes in the Hill

coefficients and EC_{50} values (Fig. 5.10A,B; Table 5.3, 5.4). At these pH's a higher zinc concentration (5 μM) gave virtually a complete depression of the GABA concentration-response curve (Fig. 5.10A,B). As for the mouse α1β1 receptor construct, acidifying the external Ringer significantly alleviated the blockade by zinc of the GABA responses (Fig. 5.10B). The GABA dose-conductance curves revealed that the antagonism produced by 5 μM zinc was of a mixed/non-competitive type with small changes in the Hill coefficients and EC_{50} values (Fig. 5.10B; Table 5.3, 5.4).

The addition of a γ2S subunit to this receptor construct, yielding bovine α1β1γ2S $GABA_A$ receptors, exhibited relative insensitivity to blockade by zinc ions. On construction of a zinc inhibition curve the GABA-induced responses were only inhibited at higher concentrations of zinc (> 100 μM) with the IC_{50} value determined as 616.95 ± 76.3 μM (Fig. 5.11; Table 5.2). Construction of equilibrium dose-response curves for GABA revealed that low concentrations of zinc (5 μM) had no effect on the GABA-induced responses with little changes in the EC_{50} or Hill coefficient values (Fig. 5.11; Table 5.3, 5.4). The pH and zinc profile, which is dependent on the composition of mouse $GABA_A$ receptor subunits was found to be similar for bovine $GABA_A$ receptors. The similarities in pH and zinc dependence of channel function of the $GABA_A$ receptors from the two different species suggest that the specific amino acid residues involved in the allosteric transitions are similar for these two species.

5.3 DISCUSSION

This study represents the first examination of the functional effects of changing the extracellular pH and any resultant modification in the antagonism induced by zinc ions on mammalian recombinant $GABA_A$ receptors expressed in *Xenopus* oocytes.

5.3.1 SUBUNIT DEPENDENCE OF THE pH PHENOTYPE

GABA-induced responses from oocytes expressing $GABA_A$ receptors comprising mouse α1β1 subunits were maximal at low pH's and decreased along a sigmoidal curve as the H^+ concentration decreased. Moreover, there was little effect of H^+ on the Hill coefficients and very small changes in the EC_{50} values for GABA possibly indicating that protons do not enhance this $GABA_A$ receptor by increasing its apparent binding affinity. This feature was seen with some of the other receptor constructs. The addition of the γ2 subunit to this $GABA_A$ receptor complex intriguingly rendered the receptor insensitive to external pH changes. This subunit dependence on the pH sensitivity was again seen in bovine $GABA_A$ receptors expressing the same subunit compositions. These results are unlikely to be due to pH effects on the GABA molecule, since pH minimally affects the GABA molecule over a wide pH range with 99% of GABA residing in the zwitterionic form at pH 7.6 decreasing to only 97% at pH 5.6 (Smart and Constanti, 1982). However, these results may suggest the existence of an ionizable group(s) within the α1β1 receptor construct which can modulate the conductance of the chloride channel which may become masked in these receptors when a γ2 subunit is present. The resultant pH titration curves for both mouse and bovine α1β1 receptor constructs revealed the involvement of a single group with apparent pK_a values of 6.8 and 6.4 respectively.

Interestingly, addition of the δ subunit to the α1β1 receptor construct revealed a different pH sensitivity of this α1β1δ $GABA_A$ receptor compared to the α1β1 receptor complex. $GABA_A$ receptors composed of α1β1δ subunits revealed a biphasic pH curve compared to the sigmoidal curve obtained for the α1β1 receptor complex. This suggested that the pH sensitivity of the $GABA_A$ receptor is dependent on the composition of subunits present within the construct. Moreover, this demonstrates that pH may be used as a probe to ascertain whether the δ subunit is actually expressed in a recombinant

system as part of a heterologous $GABA_A$ receptor complex. To date, the presence of a δ subunit within a functional $GABA_A$ receptor construct has not been shown. The data in the titration curve provided two pK_a values of approximately 6.3 and 9.9. Interestingly, mouse α1β1γ2Sδ $GABA_A$ receptor constructs revealed a novel bell-shaped dependence on pH. This pH profile suggests the involvement of at least two distinct chemical species participating in the determination of the GABA response, with pK_a values estimated as 5.5 and 9.6. Interestingly, a bell shaped pH titration curve has been seen for mouse nicotinic acetylcholine receptors (Landau *et al.*, 1981; Li and McNamee, 1992). This bell shaped pH titration curve for the α1β1γ2Sδ $GABA_A$ receptor suggests that there are two 'proton-sensitive' sites differentially controlling the pH sensitivity of this receptor construct compared to the one site for $GABA_A$ receptors composed of α1β1 subunits. Moreover, this pH sensitivity of the α1β1γ2δ $GABA_A$ receptor indicates that the optimum GABA-induced responses would occur at physiological pH's. Overall, pH profiling of $GABA_A$ receptors is a powerful method which could be used to broadly determine some aspects of the subunit composition of unknown recombinant and native $GABA_A$ receptors. The results clearly indicate for the first time the expression of δ subunits in heterologous $GABA_A$ receptors expressed with either α1β1 or α1β1γ2S subunit constructs.

5.3.2 pH SENSITIVE GROUPS AFFECTING THE GABA-ACTIVATED CHLORIDE CONDUCTANCE

The apparent pK_a values obtained from α1β1, α1β1δ and α1β1γ2δ $GABA_A$ receptor constructs suggested the involvement of different amino acid residues in determining the pH dependent profiles of these $GABA_A$ receptors. The groups with pK_a values of 6.4 and 6.8 on bovine and mouse α1β1 $GABA_A$ receptors respectively, and 5.5 and 6.3 for one site located on mouse α1β1γ2Sδ and α1β1δ receptors respectively, can be tentatively identified as an imidazole group in histidine residues which has a pK_a value of 6.5 (Mahler

and Cordes, 1971; Stryer, 1988; Table 5.5). Interestingly, α1, β1 γ2S and δ $GABA_A$ receptor subunits contain histidine residues in the extracellular region. Moreover, in both mouse and bovine eight histidines are extracellularly located in the α1 subunit and four histidines in the β1 subunit (Fig. 5.12/5.13). Furthermore, these histidine residues for both mouse and bovine α1 and β1 subunits are located in identical positions in the amino acid sequence (Fig. 5.12/5.13). The similarity in number and location of histidine residues present in α1β1 $GABA_A$ receptors both for the mouse and bovine species may therefore result in the similar pH profile and zinc sensitivities of these two receptors, as demonstrated by the pK_a values. The lack of both pH and zinc sensitivity on addition of the γ2 subunit to α1β1 receptor constructs is very intriguing. One histidine residue present in α1 subunits at a position close to the start of the putative first transmembrane domain (TM1), 215, is absent in the γ2S subunit (Fig. 5.14). Interestingly, the pH sensitivity is retained on addition of the δ subunit to the same α1β1 receptor construct. Unlike for the γ2S subunit, a histidine residue is present very close to TM1 in the δ subunit at position 224, which on alignment of the protein sequences corresponds to the position of the histidine residue in the α1 subunit at 215, and may account for the pK_a value of 6.3 (Fig. 5.14). It could be possible that addition of the γ2 subunit to the α1β1 receptor construct 'masks' this important histidine residue. Further identification of the amino acid residues requires the use of chimeric and site-specific mutant $GABA_A$ receptors. Alternatively, it could be possible that the conformation of the quaternary structure of the receptor protein of the α1β1 $GABA_A$ receptor could be altered by the addition of the γ2S subunit in such a way that masking occurs of the 'proton-sensitive' residues. In contrast, addition of the δ subunit to the α1β1 receptor may cause a different quaternary structure of the receptor complex to be adopted, compared to the α1β1γ2S receptor, leading to the pH sensitivities seen for δ containing $GABA_A$ receptor constructs.

The apparent values of the pK_a's for the other putative 'proton-sensitive' sites of α1β1δ and α1β1γ2Sδ of 9.9 and 9.6 respectively would suggest the involvement of tyrosine or lysine residues which both have a pK_a value of 10 (Table 5.5).

5.3.3 SUBUNIT COMPOSITION AND EXTERNAL pH AFFECTS ZINC-INDUCED INHIBITION

The inhibition of GABA responses by zinc clearly depends on the subunit composition of the $GABA_A$ receptor. Mouse and bovine α1β1 receptor constructs were sensitive to zinc inhibition with IC_{50} values of 1.1 ± 0.1 and 0.73 ± 0.06 μM respectively. This suggests a similar zinc sensitivity for α1β1 $GABA_A$ receptors from both the murine and bovine species, possibly indicating a similar binding site for zinc in these $GABA_A$ receptor constructs. Furthermore, zinc was observed to depress the equilibrium concentration curves in a mixed/non-competitive manner. Interestingly, the addition of the δ subunit yielding murine α1β1δ $GABA_A$ receptor constructs revealed that the zinc sensitivity was slightly decreased with an IC_{50} value of 14.8 ± 1.53 μM. This could possibly be due to the change in quaternary structure of the receptor complex which may reveal different binding sites for zinc on the α1β1δ $GABA_A$ receptor or alternatively the affinity of zinc for it's binding site may be altered. However, the zinc inhibition was observed to be competitive, implying that both zinc and GABA could be competing for the same binding site(s) within the α1β1δ $GABA_A$ receptor complex. Alternatively, the competitive nature of the zinc antagonism could also arise via an allosteric interaction with the $GABA_A$ receptor affecting agonist binding and/or ion channel gating.

Receptors possessing a γ2S subunit for both mouse and bovine yielding receptors of α1β1γ2S subunit constructs were relatively insensitive to blockade by zinc ions. High concentrations of zinc (300 μM) revealed a non-competitive inhibition of the GABA-induced response, irrespective of whether

the δ subunit was present in the receptor complex. Therefore, it appears that the γ2S subunit is dominant over the δ subunit in the α1β1γ2Sδ $GABA_A$ receptor complex with regard to inhibition by zinc. The similarity in the IC_{50} values for zinc for the α1β1γ2S receptor with and without the δ subunit could possibly indicate a similar zinc binding site within these receptor constructs.

pH was shown to modulate the zinc antagonism of both α1β1 and α1β1δ $GABA_A$ receptors. The antagonistic effect of zinc was reduced on decreasing the pH suggesting that H^+ and zinc were competing for a similar site in the $GABA_A$ receptor ionophore. Addition of the γ2 subunit renders this receptor insensitive to both pH and low concentrations of zinc suggesting a similar binding site for both protons and zinc ions. The 'proton-sensitive' site has been tentatively suggested to exist on imidazole groups within histidine residues. It may therefore be possible that the same residues could also be the binding site for zinc.

5.3.4 COMPARISON WITH PREVIOUS RESULTS

There have been only a few previous studies on the effect of external pH on $GABA_A$ receptors. Previous studies on crayfish and lobster muscle fibres revealed that the GABA-induced chloride conductance was increased at low pH (Takeuchi and Takeuchi, 1967, Smart and Constanti, 1982; Pasternack *et al.*, 1992). The pK_a for this effect was estimated from a titration curve to be 6.1 (Smart and Constanti, 1982). These results are compatible with the pH profile observed with both mouse and bovine α1β1 $GABA_A$ receptor constructs. However, the GABA receptor constructs found in lobster muscle may not consist of the same subunits as that seen in mammalian brain. These data provide an interesting comparison of the 'proton-sensitive' groups present in the GABA receptors in these different species. From the pK_a values obtained in this study on α1β1 $GABA_A$ receptor constructs, and that seen in lobster muscle, it is likely that similar amino acids are responsible for the proton

sensitivity of the GABA-gated chloride conductance and possibly some similarity between the ion channel modulation.

Interestingly, the effect of pH on the GABA response was studied in cultured rat spinal neurones (Gruol *et al.*, 1980) and reticulospinal vasomotor neurones (Sun and Reis, 1993). Extracellular application of H^+ by iontophoresis attenuated GABA-evoked decreases in the action potential frequency (Gruol *et al.*, 1980; Sun and Reis, 1993). Conversely, application of OH^- by iontophoresis enhanced these GABA responses (Sun and Reis, 1993). However, due to application of H^+ or OH^- by iontophoresis, the actual final pH seen by the $GABA_A$ receptors remains unknown. Moreover, it was also noted that similar results were obtained with H^+ and OH^- iontophoreses and glycine-evoked inhibition on these neurones, suggesting that H^+ modulation of the GABA-evoked inhibition may not be the result of a specific action at the GABA receptor ionophore (Sun and Reis, 1993).

The intracellular pH of the oocyte has been shown to change when the extracellular pH is altered (Sasaki *et al.*, 1992). Therefore, any intracellular pH change induced by altering the external pH could possibly influence the GABA-induced responses at different external H^+ concentrations. However, the influence on the GABA-gated chloride conductance by intracellular pH was studied in crayfish muscle fibres (Pasternack *et al.*, 1992). Large changes in the intracellular pH (range 6.4 to 8.0) did not have any detectable effects on the GABA-induced conductance changes. In the present study the intracellular pH was not monitored but any changes in the intracellular pH of the oocyte were probably of little significance as the pH profile seen was dependent on the $GABA_A$ receptor subunit composition with the GABA response of $\alpha 1\beta 1\gamma 2S$ receptor constructs being insensitive to modulation by pH.

A number of previous studies have revealed that the $GABA_A$ receptor

channels were significantly permeable to bicarbonate ions as well as chloride ions (Bormann *et al.*, 1987; Kaila and Viopio, 1987; Kaila *et al.*, 1990; Kaila *et al.*, 1992; Kaila *et al.*, 1993). Therefore, the possibility arises that bicarbonate ions could have contributed to the GABA-mediated responses observed in this study. However, current-voltage relations obtained for the studies where bicarbonate ions were shown to be permeating through the GABA ion channel revealed reversal potentials markedly more positive than E_{Cl} (by 20 mV; Kaila and Viopio, 1987; Kaila *et al.*, 1990; Kaila *et al.*, 1992; Kaila *et al.*, 1993). In this study current-voltage relations were constructed in different pH's for each $GABA_A$ receptor construct studied. The reversal potentials revealed for each receptor construct in different pH's were all close to the Cl^- reversal potential in the *Xenopus* oocyte (Barish, 1983; Dascal, 1987). Therefore, in the experimental conditions of this study it is unlikely that bicarbonate ions contributed significantly to the GABA-induced responses.

Zinc has previously been shown to be an antagonist on cultured embryonic neuronal $GABA_A$ receptors (Westbrook and Mayer, 1987; Smart and Constanti, 1990). Smart *et al.* (1991) reported that $GABA_A$ receptors lacking the $\gamma 2$ subunit were inhibited by zinc in a non-competitive manner in mouse $\alpha 1\beta 1$ $GABA_A$ receptors expressed in human embryonic kidney cells. The addition of a $\gamma 2$ subunit conversely revealed a relative insensitivity to zinc ions (Smart *et al.*, 1991). These results are entirely consistent with the zinc inhibition profile seen in $\alpha 1\beta 1$ and $\alpha 1\beta 1\gamma 2S$ $GABA_A$ receptors used in this study. It has also been noted that GABA responses from embryonic neurones are routinely sensitive to zinc (Smart and Constanti, 1990; Smart, 1990), indicating that the major type of $GABA_A$ receptor present at this stage of neural development may lack the $\gamma 2$ subunit. Therefore, adult and older postnatal forms of the $GABA_A$ receptor would then presumably contain the $\gamma 2$, or a functionally equivalent subunit, thereby rendering the receptor less sensitive to zinc. This developmental sensitivity of the $GABA_A$ receptor to zinc

was observed in adult rat superior cervical ganglia where the GABA-induced conductance change was not sensitive to blockade by zinc ions (Smart and Constanti, 1982). Interestingly, in dorsal root ganglion cells of the bullfrog, *Rana catesbeana*, the GABA-induced response was inhibited by high concentrations of zinc (1-3 mM) in a competitive manner analogous to the zinc inhibition seen in this study with $\alpha1\beta1\delta$ $GABA_A$ receptors (Akaike *et al.*, 1987; Yakushiji *et al.*, 1987). A study on embryonic neuronal $GABA_A$ receptors showed that the external pH did not affect the zinc-induced inhibition (Smart, 1992). However, only a small pH change from 7.4 to 6.18 was employed and the full pH dependent profile of the zinc inhibition, as seen in the present study with $\alpha1\beta1$ subunit containing receptors, may not have been apparent.

5.3.5 NEUROPHYSIOLOGICAL IMPLICATIONS

In several regions of the CNS, neuronal activity has been shown to cause an immediate alkalination of the extracellular space (Chesler, 1990). The alkaline shifts are rapidly observed (Chesler and Chan, 1988; Krishtal *et al.*, 1987) and can be significant in influencing excitatory transmission (Tang *et al.*, 1990; Traynelis and Cull-Candy, 1990, 1991; Vyklicky *et al.*, 1990). Moreover, the magnitude and speed of these pH shifts suggested that the underlying acid-base fluxes were mediated via postsynaptic channels (Chesler and Chan, 1988). Further evidence was obtained from the direct application of both glutamate (Chen and Chesler, 1992a,b; Chesler and Rice, 1991; Jarolimek *et al.*, 1989) or GABA (Chen and Chesler, 1990; Chen and Chesler, 1992a; Jarolimek *et al.*, 1989) which caused similar alkaline shifts independent of the presence of calcium (Chen and Chesler, 1991; Chesler and Rice, 1991).

Application of GABA to crayfish muscle caused a fall in intracellular pH associated with an alkalosis at the extracellular surface of the cell membrane. This effect could be blocked in the nominal absence of bicarbonate (Kaila and

Voipio, 1987) and in the presence of carbonic anhydrase inhibitors (Kaila *et al.*, 1990). In the vertebrate CNS, the GABA-gated ion channel has a comparable permeability to bicarbonate ions (Bormann *et al.*, 1987). Monosynaptic activation of $GABA_A$ receptors in CA1 neurones of the rat hippocampus gave rise to an extracellular alkaline shift which was abolished by picrotoxin and enhanced by pentobarbital (Kaila *et al.*, 1992; Chen and Chesler, 1992a). These results suggest that a similar mechanism for the $GABA_A$ receptor induced alkalosis occurs in rat hippocampus as observed in the crayfish muscle. Application of GABA to turtle cerebellum induced an extracellular alkaline shift which arose due to the efflux of bicarbonate across the $GABA_A$ anion channel (Chen and Chesler, 1990; Chen and Chesler, 1991; Chesler and Chen, 1992). These results suggest that synaptically evoked alkaline shifts could arise as a result of GABAergic transmission and/or activation of N-methyl-D-Aspartate (NMDA) and non-NMDA receptors (Chen and Chesler, 1992a,b; Chesler and Rice, 1991; Jarolimek *et al.*, 1989).

Interestingly, brief transient alkalinisations and acidifications of the extracellular space following stimulation of the CA1 afferents in hippocampal slices were reported to be dependent on synaptic transmission (Krishtal *et al.*, 1987). The fast acid transient was suggested to arise from either the acidic contents of transmitter vesicles or the insertion of a pump transporter, H^+-ATPase, from vesicle storage membrane into the synaptic membrane (Krishtal *et al.*, 1987). If the contents of the synaptic vesicles are appreciably acidic, this raises the intriguing possibility that the synaptic cleft will become acidified with each quantal event. The time course of acidification and/or alkalination during synaptic transmission is unknown, but it has been shown in this study, that the GABA response could be modified by pH transients and the extent and direction of modulation will be dependent on the composition of subunits present in the $GABA_A$ receptor.

5.3.6 CLINICAL IMPLICATIONS

Hypoxic and ischaemic episodes lead to decreases in the extracellular pH in neuronal tissue (Kraig *et al.*, 1983; Mutch and Handsen, 1984; Chesler, 1990), which has been suggested to contribute to neuronal damage (Siesjo, 1985; Griffith *et al.*, 1992). It could be possible that the mild decreases in extracellular pH could modulate $GABA_A$ receptors. Depending on the subunit composition present, the $GABA_A$ receptor could have a protective ($\alpha1\beta1$, $\alpha1\beta1\delta$), noxious ($\alpha1\beta1\gamma2S\delta$) or indifferent effect ($\alpha1\beta1\gamma2S$) during hypoxic or ischaemic insult due to the change in the GABA-induced conductance for each receptor with increasing H^+. However, the exact contribution of the $GABA_A$ receptor during such episodes will not only depend on the composition of the $GABA_A$ receptors present. NMDA receptor activation is thought to be an important factor in hypoxia/ischaemia-induced neuronal damage (for review see Dingledine *et al.*, 1988). NMDA receptors have also been shown to be inhibited in low pH via their proton site (Traynelis and Cull-Candy, 1990, 1991; Tang *et al.*, 1990; Giffard *et al.*, 1990). Interestingly, a number of reports have shown that reduced pH protects cultured neurones from glutamate and hypoxia-induced neuronal death (Giffard *et al.*, 1990; Kaku *et al.*, 1993; Takadera *et al.*, 1992; Tombaugh and Sapolsky, 1990). During the reperfusion period if protons are removed more rapidly than glutamate from the extracellular space then neurotoxicity may become significant. The $GABA_A$ receptor pH sensitivity may again have important implications for controlling the excitatory activity of the neuronal tissue during this time period.

Respiratory acidosis and alkalosis influence both neuronal and seizure states (Chesler, 1990). Furthermore, transient changes in pH have been reported to occur during epileptiform field discharges recorded *in vitro* (Jarolimek *et al.*, 1989) and electrographic seizures recorded *in vivo* (Balestrino and Somjen, 1988). GABAergic inhibitory mechanisms normally limit neuronal excitability

within many regions of the CNS, including both limbic and cortical structures (For review see Dingledine *et al.*, 1988). Therefore, the modulation of the GABA response by pH will be of extreme importance during such events with both physiological and clinical implications.

Figure 5.1. pH profile of mouse α1β1 $GABA_A$ receptors expressed in *Xenopus* oocytes. (A) GABA-activated membrane currents recorded at pH 7.4, 5.4 and 9.4 as indicated by the arrows. The membrane conductance was monitored throughout by repetitively applying brief hyperpolarizing voltage command steps (-10mV; 1s, 0.2Hz). Holding potential for all oocytes, -40mV. (B) pH titration curve of the GABA-induced chloride conductance evoked by 10 μM GABA and normalised with respect to the conductance obtained at pH 7.4. The solid line was drawn by eye from which the pK_a of 6.8 was determined at 50% of the maximum conductance. After each pH perturbation, the cell was always returned to pH 7.4 and control responses repeated. All points are mean ± s.e.m. obtained from 5 different oocytes. (C) The left hand plot shows GABA equilibrium concentration curves constructed in pH 7.4, 5.4 and 9.4 and normalised with respect to 10 μM GABA at pH 7.4. The points represent means ± s.e.m recorded from 3 oocytes. Curves were fitted according to the logistic model (see methods). The right hand plot indicates current-voltage relations obtained at both pH 7.4 and 5.4.

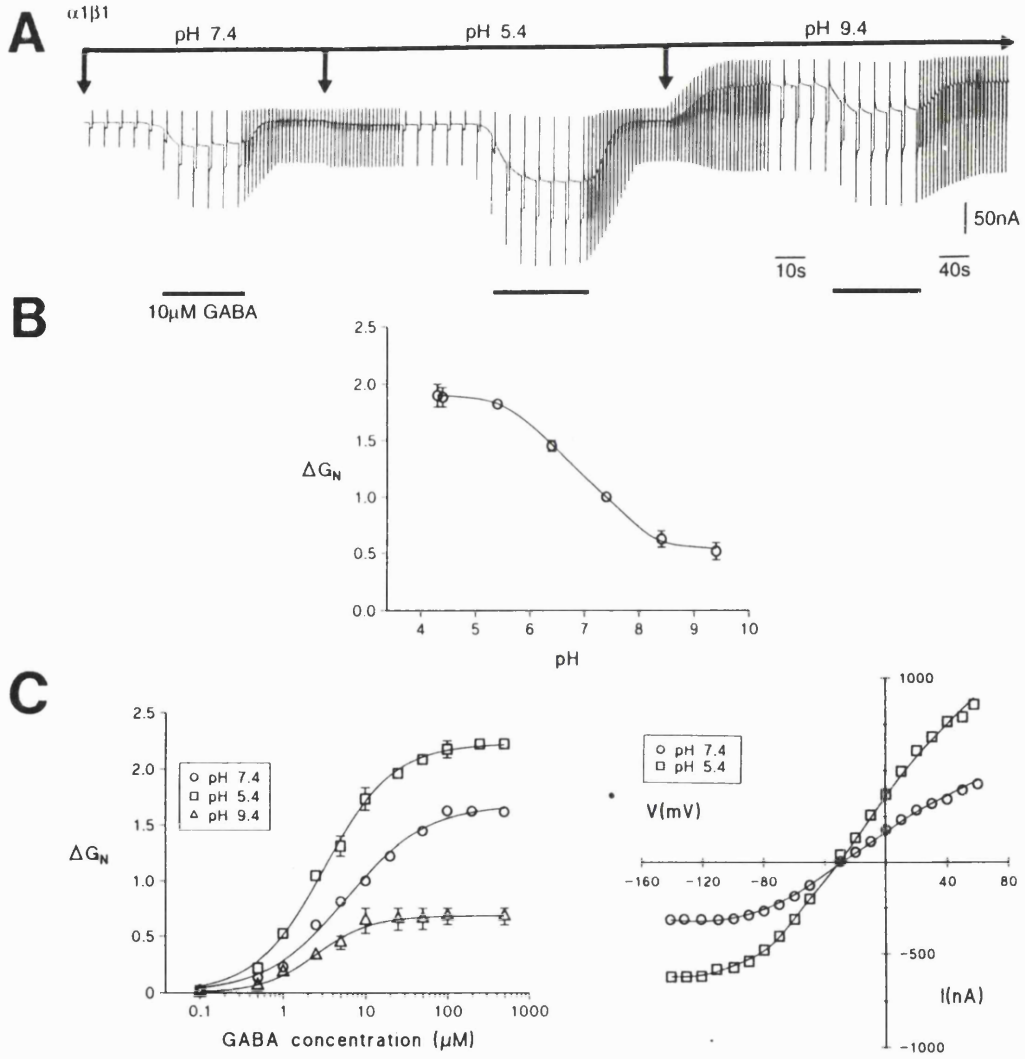
A
α1β1
pH 7.4
pH 5.4
pH 9.4
50nA
10s
40s
10μM GABA
B
ΔG_N
pH
C
ΔG_N
pH 7.4
pH 5.4
pH 9.4
GABA concentration (μM)
V(mV)
I(nA)

Figure 5.2. *Xenopus* oocytes expressing mouse α1β1γ2S $GABA_A$ receptor constructs are pH insensitive. (A) GABA-induced membrane currents recorded at pH 7.4, 5.4 and 9.4. Note, the effect of changing the external pH can still be seen on the resting conductance. (B) pH titration curve of the GABA-activated chloride conductance evoked by 10 μM GABA and normalised with respect to the conductance obtained at pH 7.4. (C) Both the GABA dose-response curve (left hand plot) and the current-voltage relation (right hand plot) reveal the insensitivity of this receptor construct to pH.

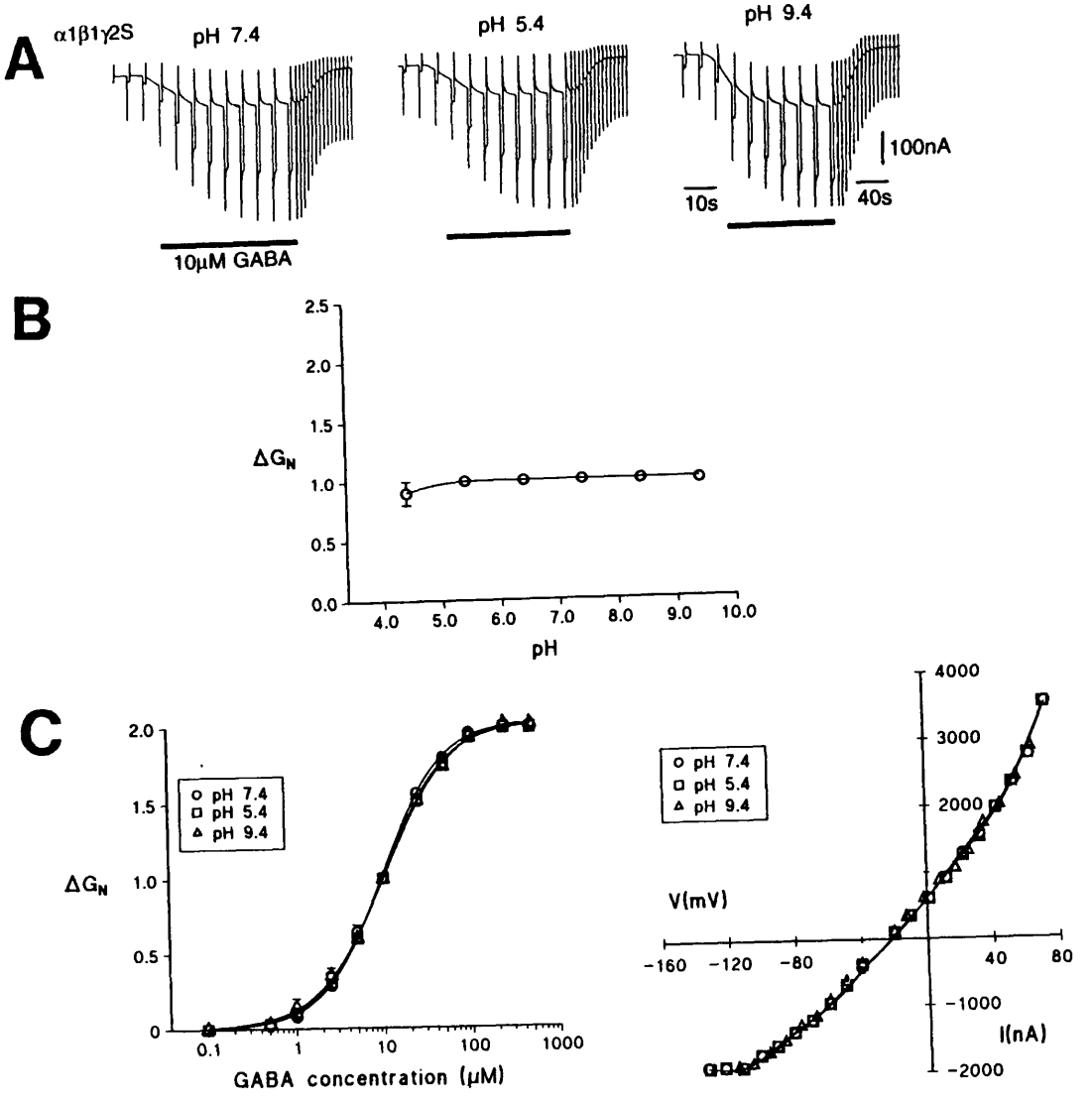
A
α1β1γ2S
pH 7.4
pH 5.4
pH 9.4
100nA
10s
40s
10μM GABA
B
ΔG_N
2.5
2.0
1.5
1.0
0.5
0.0
4.0
5.0
6.0
7.0
8.0
9.0
10.0
pH
C
ΔG_N
2.0
1.5
1.0
0.5
0
pH 7.4
pH 5.4
pH 9.4
0.1
1
10
100
1000
GABA concentration (μM)
4000
3000
2000
-1000
-2000
V(mV)
-160
-120
-80
40
80
I(nA)

Figure 5.3. GABA responses recorded from mouse $\alpha 1\beta 1\delta$ $GABA_A$ receptors are pH sensitive. (A) Application of GABA (10 μM) induces membrane current and conductance changes which are sensitive to the external pH change. (B) The pH titration plot of the GABA-induced conductance change revealed a biphasic curve. The solid line was drawn by eye and allowed an estimation of pK_a values of 6.3 and 9.9 (C) Equilibrium concentration conductance curves (left hand plot) were constructed at pH 7.4, 5.4 and 9.4 and were normalised to the conductance induced by 10 μM GABA at pH 7.4. Curves were fitted according to the logistic model (see methods). The right hand plot indicates current-voltage relations obtained at pH 5.4 and 7.4.

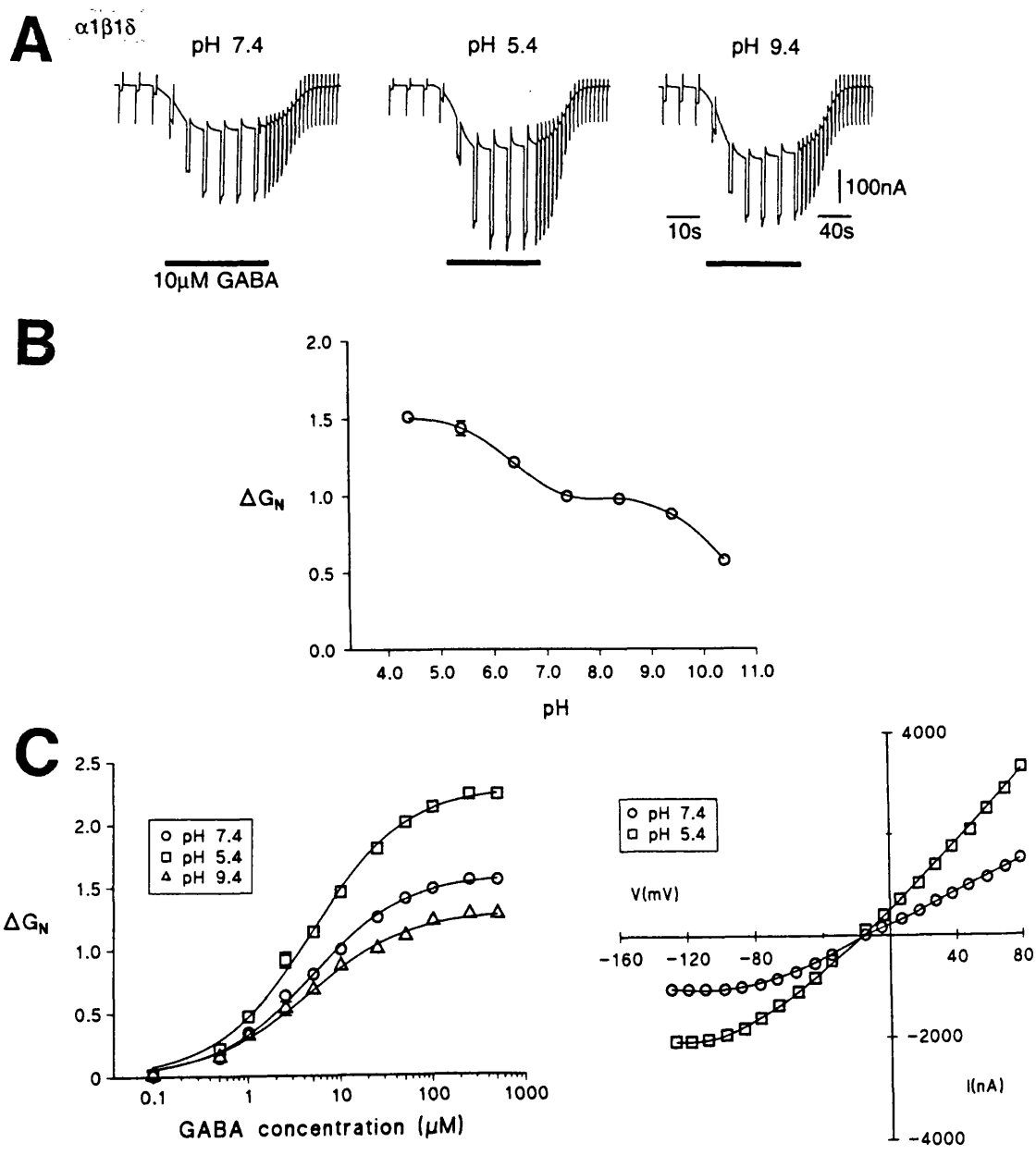
A
α1β1δ
pH 7.4
pH 5.4
pH 9.4
100nA
10s
40s
10μM GABA
B
ΔG_N
2.0
1.5
1.0
0.5
0.0
4.0 5.0 6.0 7.0 8.0 9.0 10.0 11.0
pH
C
ΔG_N
2.5
2.0
1.5
1.0
0.5
0
pH 7.4
pH 5.4
pH 9.4
0.1 1 10 100 1000
GABA concentration (μM)
4000
-2000
-4000
V(mV)
-160 -120 -80 40 80
I(nA)

Figure 5.4. pH sensitivity of α1β1γ2Sδ $GABA_A$ receptor subunits. (A) GABA-activated membrane currents recorded at pH 7.4, 5.4 and 9.4. (B) pH titration of the GABA-activated chloride conductance revealed a novel symmetrical bell-shaped curve with apparent pK_a values estimated as 5.5 and 9.6. All points were normalised with respect to the conductance induced by 10 μM GABA at pH 7.4. (C) The left hand plot shows equilibrium concentration curves obtained at pH 5.4, 7.4 and 9.4. All curves were obtained from 3-4 different oocytes and have been normalised to the conductance induced by 10μM GABA at pH 7.4. The points represent means ± s.e.m. Curves were fitted according to the logistic model (see methods). The right hand plot indicates the current-voltage relation for GABA determined at pH 7.4 and 5.4.

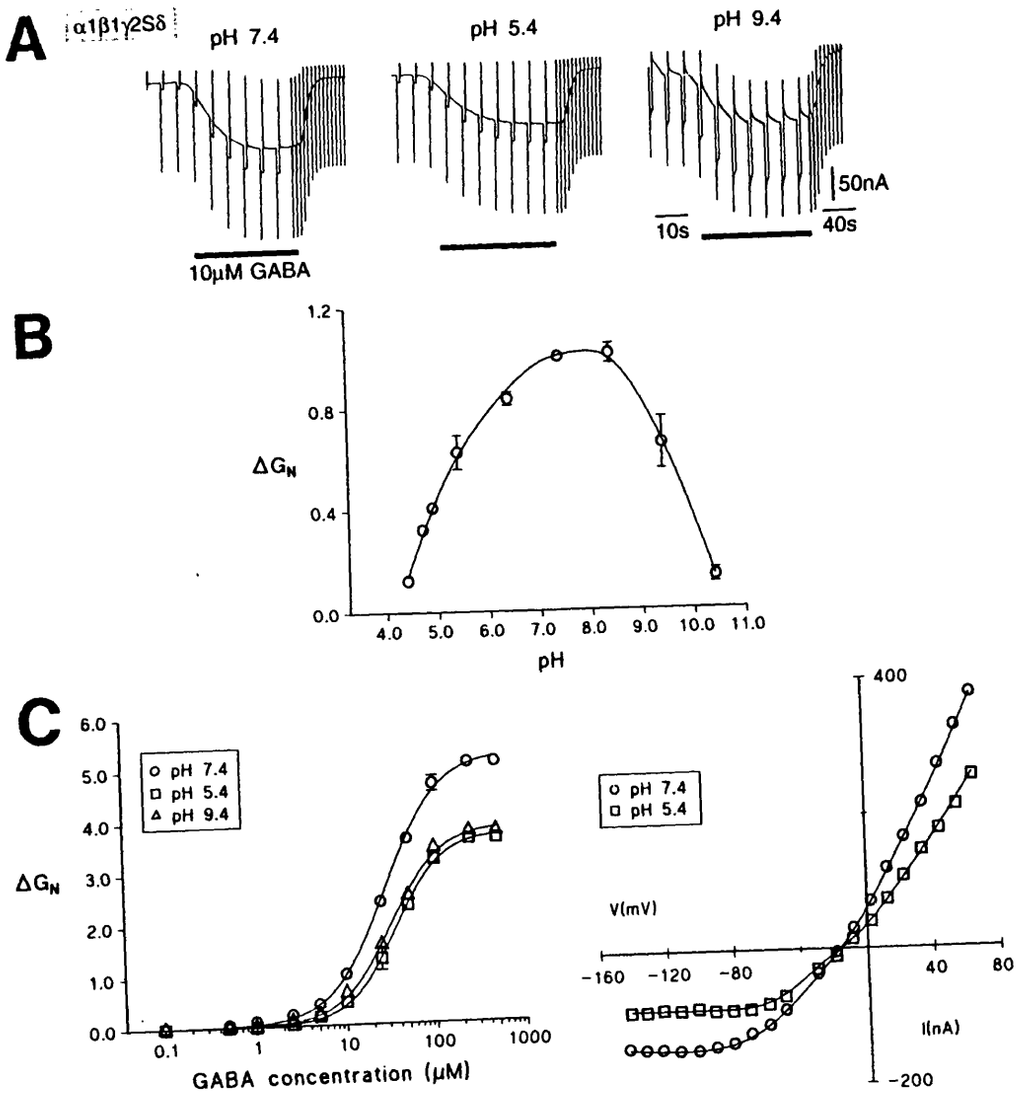
A
α1β1γ2Sδ
pH 7.4
pH 5.4
pH 9.4
50nA
10s
40s
10μM GABA
B
1.2
0.8
0.4
0.0
ΔG_N
4.0 5.0 6.0 7.0 8.0 9.0 10.0 11.0
pH
C
6.0
5.0
4.0
3.0
2.0
1.0
0.0
ΔG_N
o pH 7.4
□ pH 5.4
△ pH 9.4
0.1 1 10 100 1000
GABA concentration (μM)
400
o pH 7.4
□ pH 5.4
V(mV)
-160 -120 -80 40 80
I(nA)
-200

Figure 5.5. Effects of pH on bovine $\alpha 1\beta 1$ $GABA_A$ receptor constructs are similar to mouse $\alpha 1\beta 1$ $GABA_A$ receptors. (A) The pH titration of the GABA-induced chloride conductance revealed a sigmoidal shaped curve and pK_a value of 6.4. (B) The left hand plot indicates equilibrium concentration response curves constructed at different extracellular pH's and fitted according to the logistic model (see methods). All points represent means ± s.e.m. The right hand plot shows current-voltage relations for GABA at pH 7.4 and 5.6.

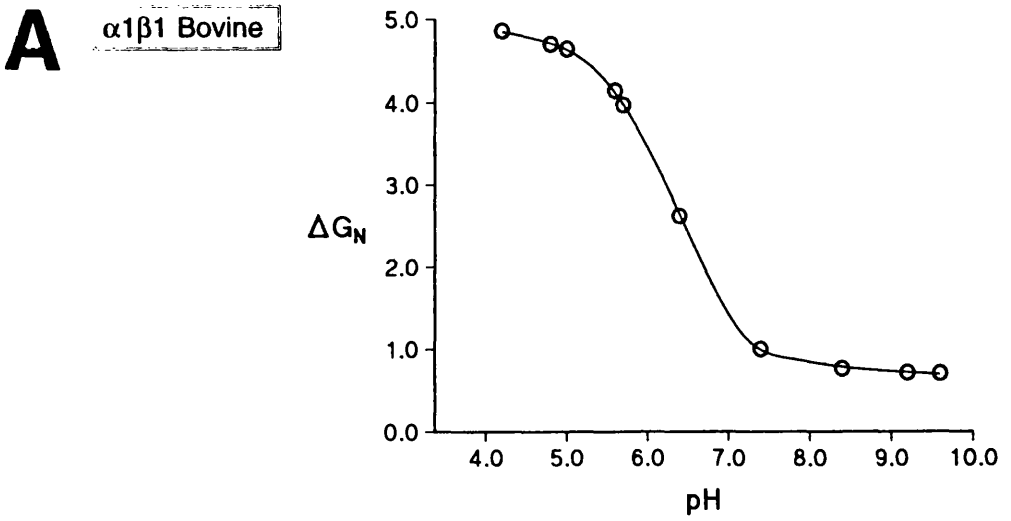
A
α1β1 Bovine
5.0
4.0
3.0
2.0
1.0
0.0
ΔG_N
4.0
5.0
6.0
7.0
8.0
9.0
10.0
pH

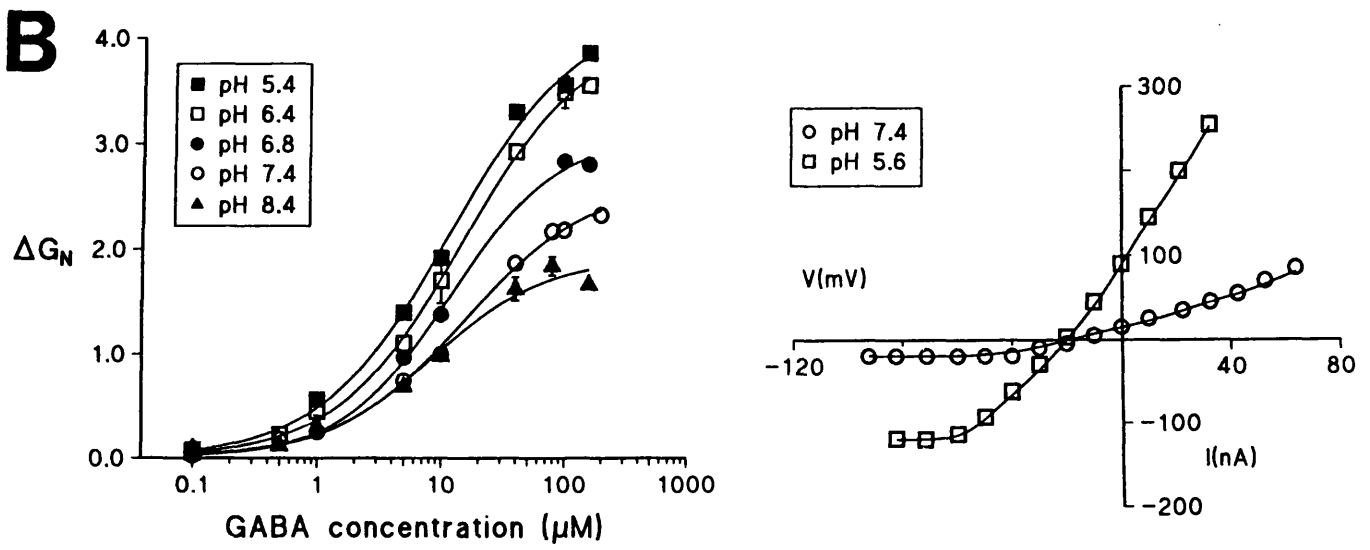
B
pH 5.4
pH 6.4
pH 6.8
pH 7.4
pH 8.4
ΔG_N
4.0
3.0
2.0
1.0
0.0
0.1
1
10
100
1000
GABA concentration (μM)
pH 7.4
pH 5.6
V(mV)
300
100
-100
-200
-120
40
80
I(nA)

Figure 5.6. Expression of bovine α1β1γ2S $GABA_A$ receptors revealed a similar pH insensitivity as seen in mouse α1β1γ2S subunit constructs. (A) pH titration curve of the GABA-induced chloride conductance evoked by 10 μM GABA and normalised with respect to the conductance obtained at pH 7.4. (B) Both the GABA dose-response curve (left hand plot) and the current-voltage relation (right hand plot) show the insensitivity of this receptor construct to pH.

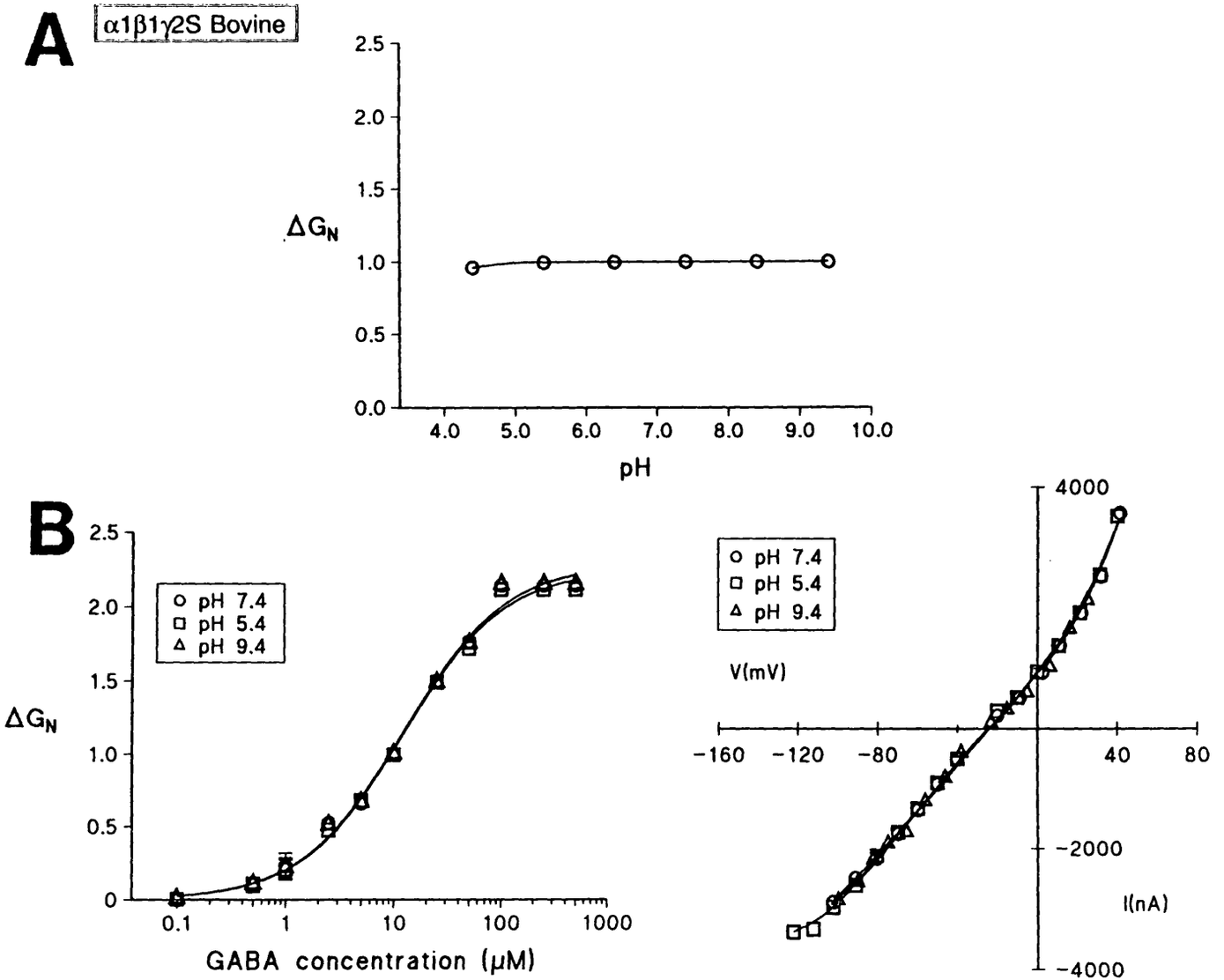
A
α1β1γ2S Bovine
ΔG_N
pH
B
pH 7.4
pH 5.4
pH 9.4
ΔG_N
GABA concentration (μM)
V(mV)
I(nA)

Figure 5.7. The inhibitory effect of zinc on GABA responses recorded from mouse $\alpha 1\beta 1$ $GABA_A$ receptors can be considerably alleviated by low pH.
(A) Zinc inhibition curves were constructed for GABA at pH 7.4, 5.4 and 9.4 (left hand plot). In this and all subsequent zinc inhibition curves the GABA-induced conductances were normalised to the response evoked by 10 μM GABA at pH 7.4 and fitted according to the antagonist inhibition model (see methods). The right hand plot indicates GABA concentration conductance curves constructed in the absence and presence of 1 μM zinc. (B) Altering the pH to 5.4 revealed a significant reversal of the inhibitory effect of zinc on the GABA-induced response. A higher concentration of zinc (50 μM) was necessary to attain a similar inhibition of the GABA-induced response at this acidic pH as seen with 1 μM zinc at pH 7.4 (left hand plot). The right hand plot revealed little change in the zinc sensitivity at pH 9.4 compared to pH 7.4.

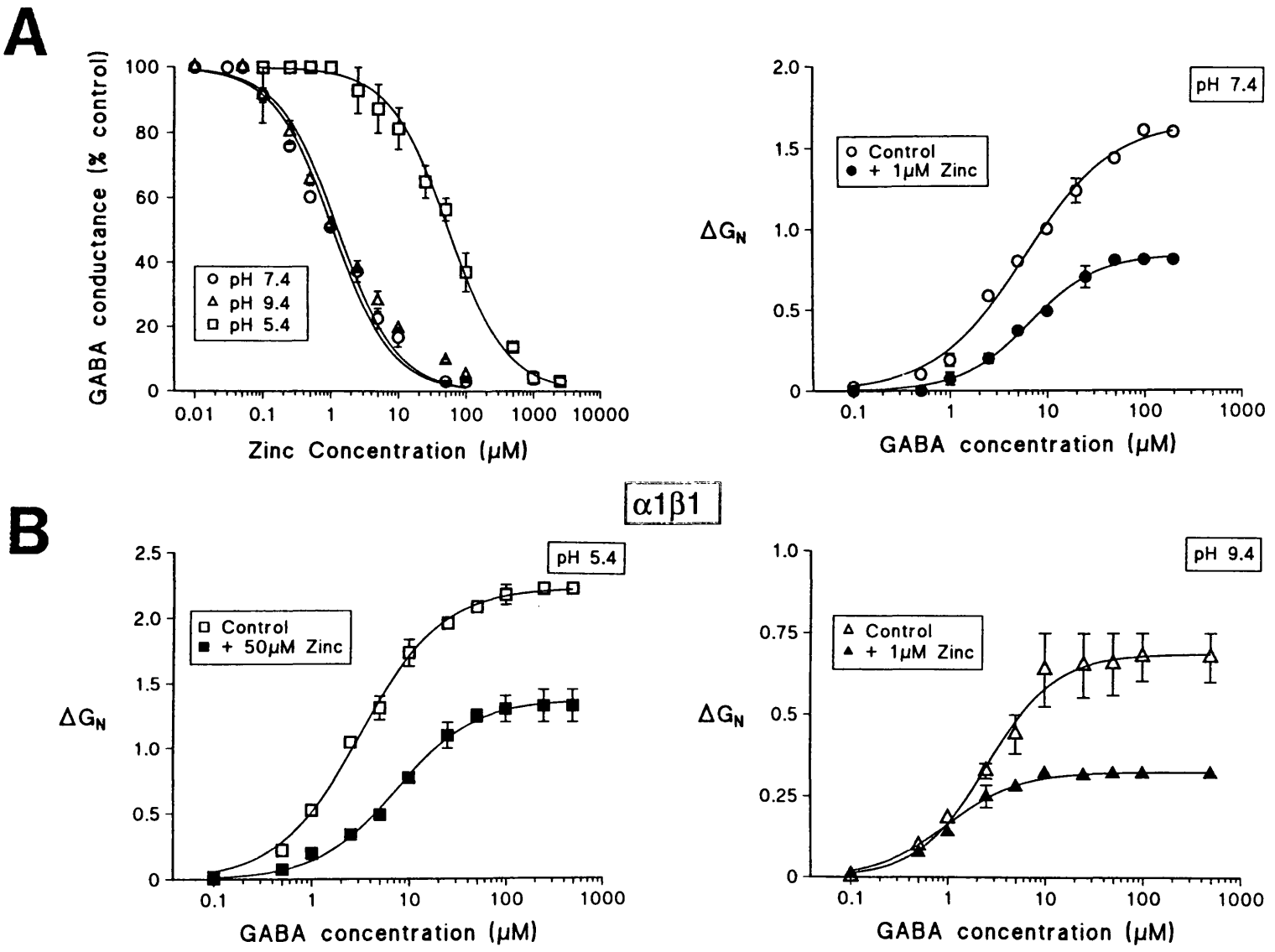
A
GABA conductance (% control)
100
80
60
40
20
0
pH 7.4
pH 9.4
pH 5.4
0.01
0.1
1
10
100
1000
10000
Zinc Concentration (μM)
2.0
1.5
1.0
0.5
0
ΔG_N
pH 7.4
Control
+ 1μM Zinc
0.1
1
10
100
1000
GABA concentration (μM)
B
α1β1
2.5
2.0
1.5
1.0
0.5
0
ΔG_N
pH 5.4
Control
+ 50μM Zinc
0.1
1
10
100
1000
GABA concentration (μM)
1.0
0.75
0.5
0.25
0
ΔG_N
pH 9.4
Control
+ 1μM Zinc
0.1
1
10
100
1000
GABA concentration (μM)

Figure 5.8. The zinc inhibition of the GABA-induced responses recorded from $GABA_A$ receptors comprising $\alpha1\beta1\delta$ subunit constructs was reduced by low pH. (A) On the left, zinc inhibition plots at pH 7.4, 5.4 and 9.4 revealed a similar profile to $\alpha1\beta1$ mouse $GABA_A$ receptor constructs. Equilibrium dose response curves were constructed in the absence and presence of zinc (10 and 100 μM) at pH 7.4. (B) The competitive nature of the zinc inhibition was seen at pH 5.4 and 9.4 (left and right hand side, respectively), with a greater protection afforded from the zinc antagonism at the low pH.

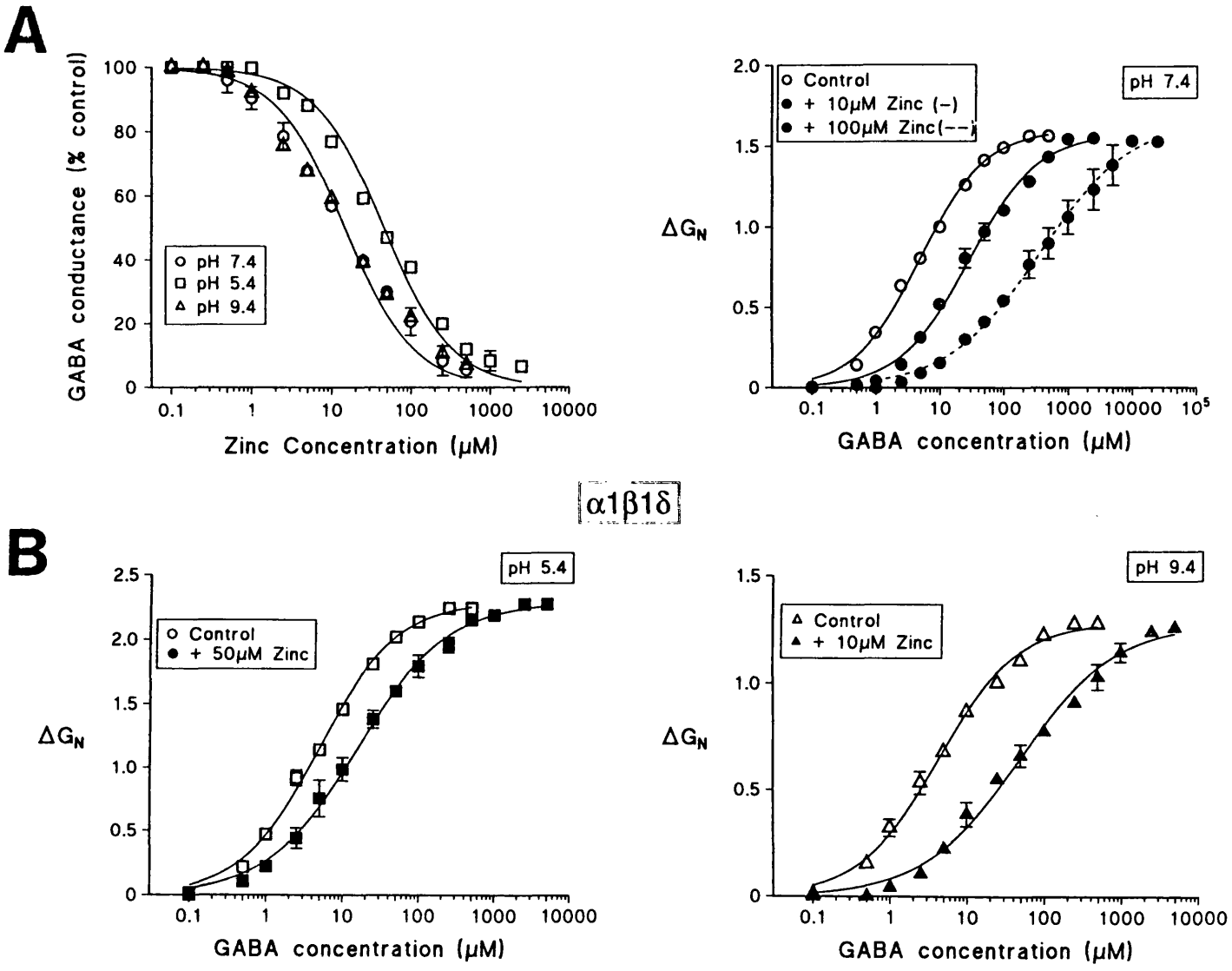
A
GABA conductance (% control)
Zinc Concentration (μM)
pH 7.4
pH 5.4
pH 9.4
ΔG_N
Control
+ 10μM Zinc (–)
+ 100μM Zinc(– –)
pH 7.4
GABA concentration (μM)
α1β1δ
B
pH 5.4
Control
+ 50μM Zinc
ΔG_N
GABA concentration (μM)
pH 9.4
Control
+ 10μM Zinc
ΔG_N
GABA concentration (μM)

Figure 5.9. GABA-induced responses show an insensitivity to zinc in $GABA_A$ receptors containing a γ2S subunit. (A) Zinc inhibition plot (left hand side) and equilibrium dose response curve in the absence and presence of zinc (5 and 300 μM; right hand side) recorded from oocytes expressing mouse α1β1γ2S $GABA_A$ receptors. (B) Similar curves were obtained from $GABA_A$ receptors consisting of mouse α1β1γ2Sδ subunits. Note the addition of the δ subunit to the α1β1γ2S receptor construct did not induce a competitive antagonism of the GABA-induced chloride conductance by zinc.

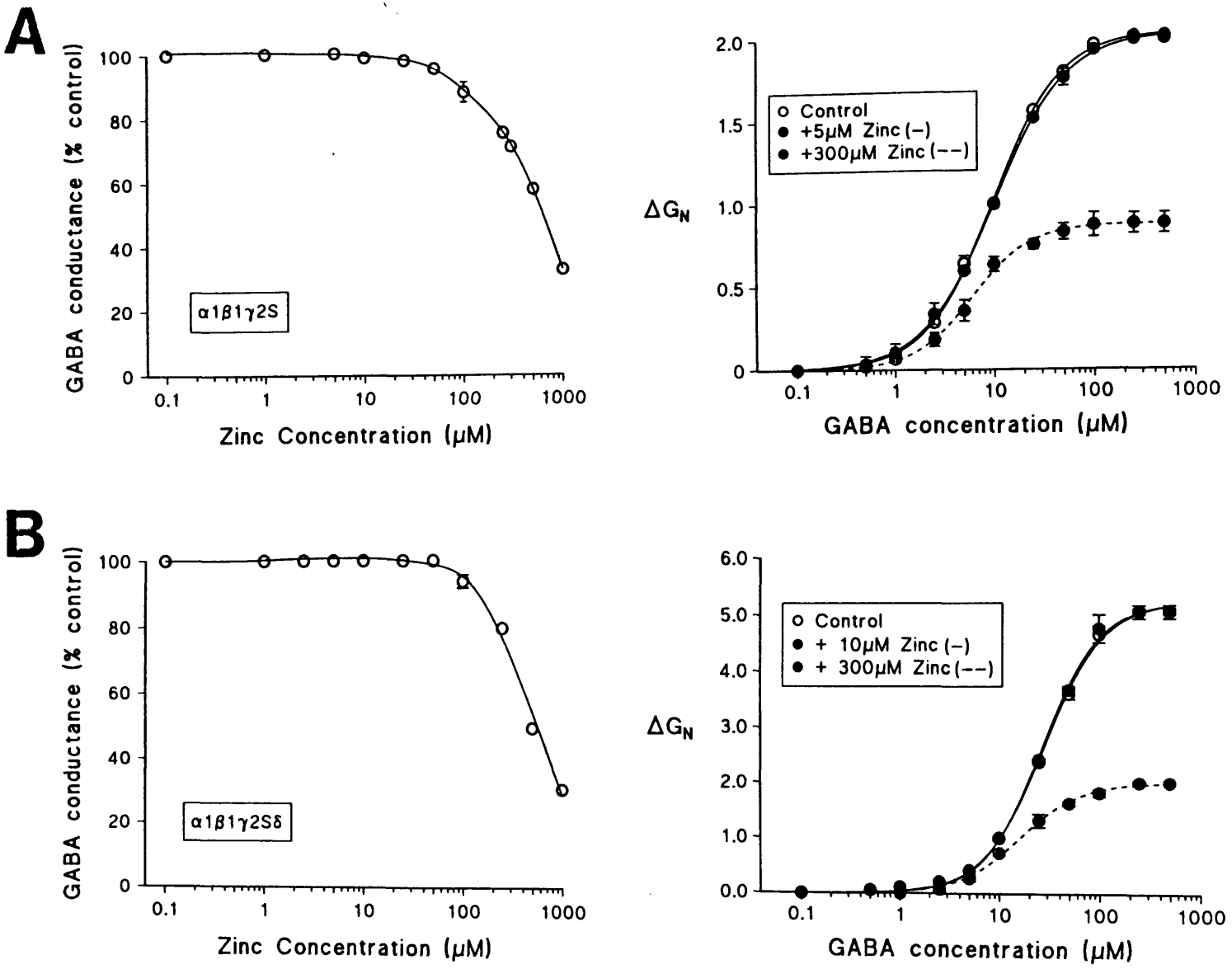
A
GABA conductance (% control)
100
80
60
40
20
0
α1β1γ2S
0.1
1
10
100
1000
Zinc Concentration (μM)
ΔG_N
2.0
1.5
1.0
0.5
0
Control
+5μM Zinc (–)
+300μM Zinc (––)
GABA concentration (μM)
B
GABA conductance (% control)
α1β1γ2Sδ
Zinc Concentration (μM)
ΔG_N
6.0
5.0
4.0
3.0
2.0
1.0
0.0
Control
+ 10μM Zinc (–)
+ 300μM Zinc (––)
GABA concentration (μM)

Figure 5.10. The antagonism of the GABA-induced responses by zinc is alleviated by low pH in bovine $\alpha 1\beta 1$ $GABA_A$ receptor constructs. (A) On the left, inhibition plot for zinc antagonism of GABA responses at pH 7.4, 6.4 and 8.4. Equilibrium dose response curves were constructed in the absence and presence of zinc (0.5 and 5 μM) at pH 7.4 (right hand side). (B) The left and right plots indicate equilibrium dose conductance curves in the absence and presence of zinc at pH 6.4 and 8.4, respectively. The increased proton concentration considerably alleviates the blockade by zinc of GABA responses.

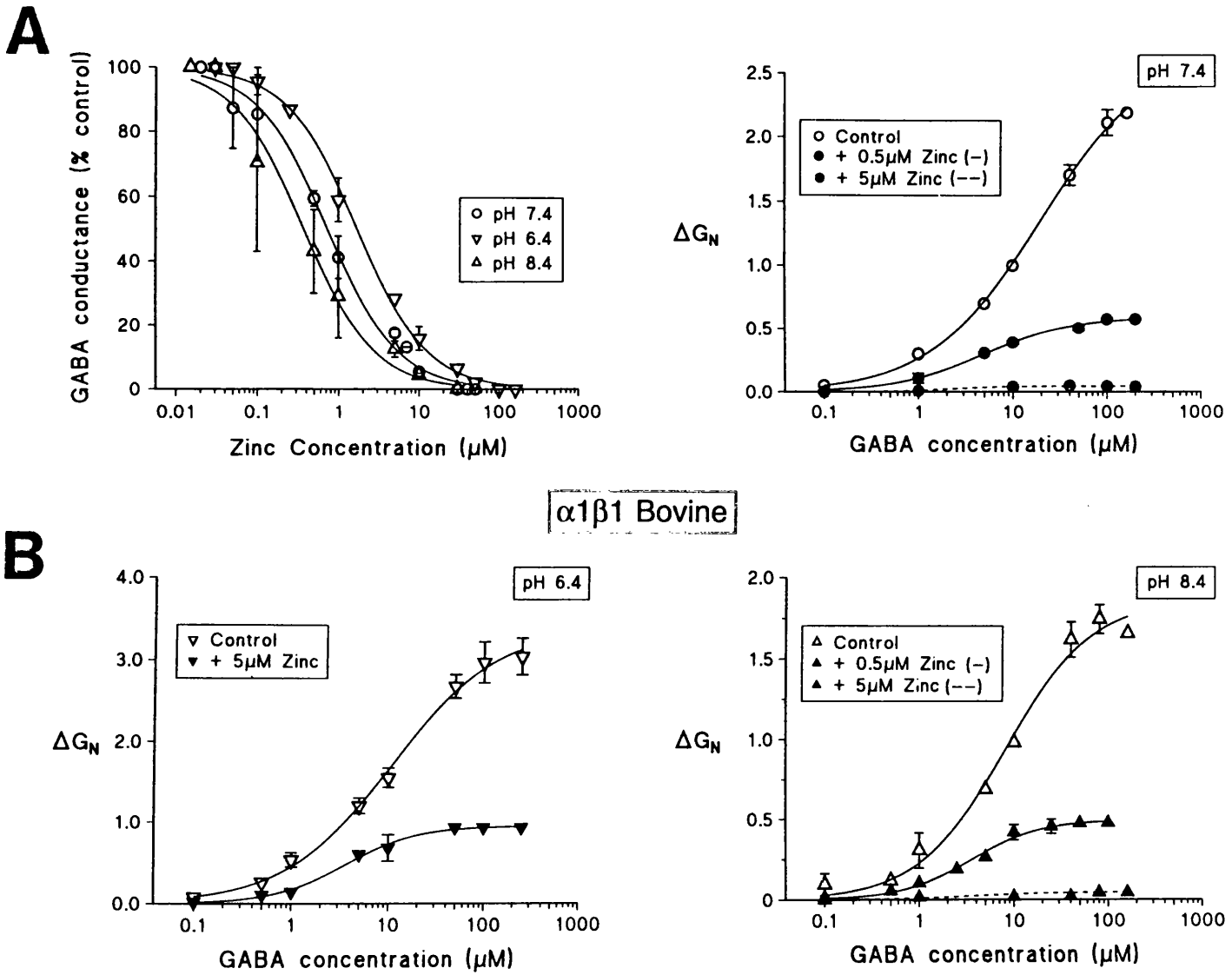
A
GABA conductance (% control)
Zinc Concentration (μM)
pH 7.4
pH 6.4
pH 8.4
ΔG_N
GABA concentration (μM)
Control
+ 0.5μM Zinc (–)
+ 5μM Zinc (––)
α1β1 Bovine
B
pH 6.4
Control
+ 5μM Zinc
pH 8.4
Control
+ 0.5μM Zinc (–)
+ 5μM Zinc (––)

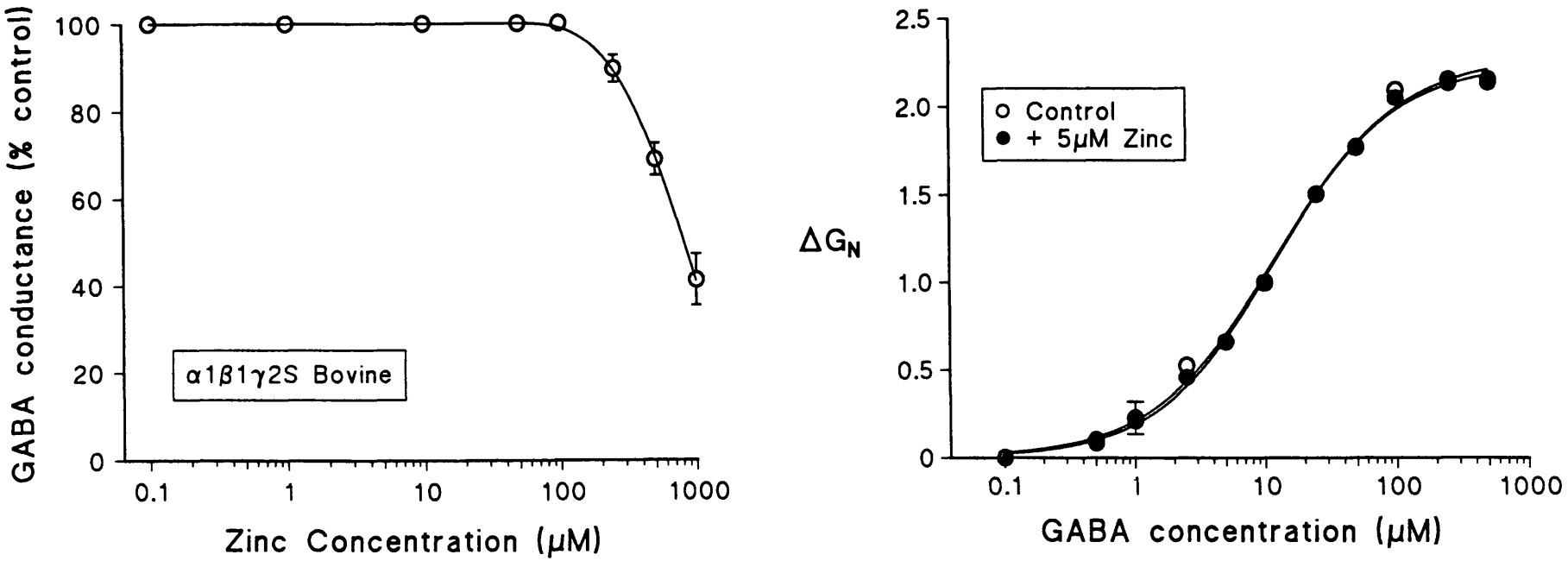

Figure 5.11. $GABA_A$ receptors comprising bovine α1β1γ2S are relatively insensitive to blockade by zinc ions. On the left, inhibition plot for zinc antagonism of GABA responses. The equilibrium dose response curve on the right were constructed in the absence and presence of 5 μM zinc.

Figure 5.12. Homologies of the predicted amino acid sequences for mouse and bovine $GABA_A$ α1 subunits. The vertical arrow indicates the proposed end of the signal sequence and the start of the mature protein, which is also where numbering starts. Numbers on the right denote amino-acid residues. Identical residues are shown by asterisks (*), a conservative change in an amino acid is indicated by a dot (.) and a non-conservative change by a space ( ). The overall sequence identity between the two $GABA_A$ α1 subunits is 99.34%. The proposed membrane-spanning hydrophobic sequences (M1-M4) are indicated by the solid bars and all extracellular histidine residues are boxed. Sequences were obtained from Wang *et al.*, 1992b (mouse) and Schofield *et al.*, 1987 (bovine) and aligned using PC/GENE version 6.6.

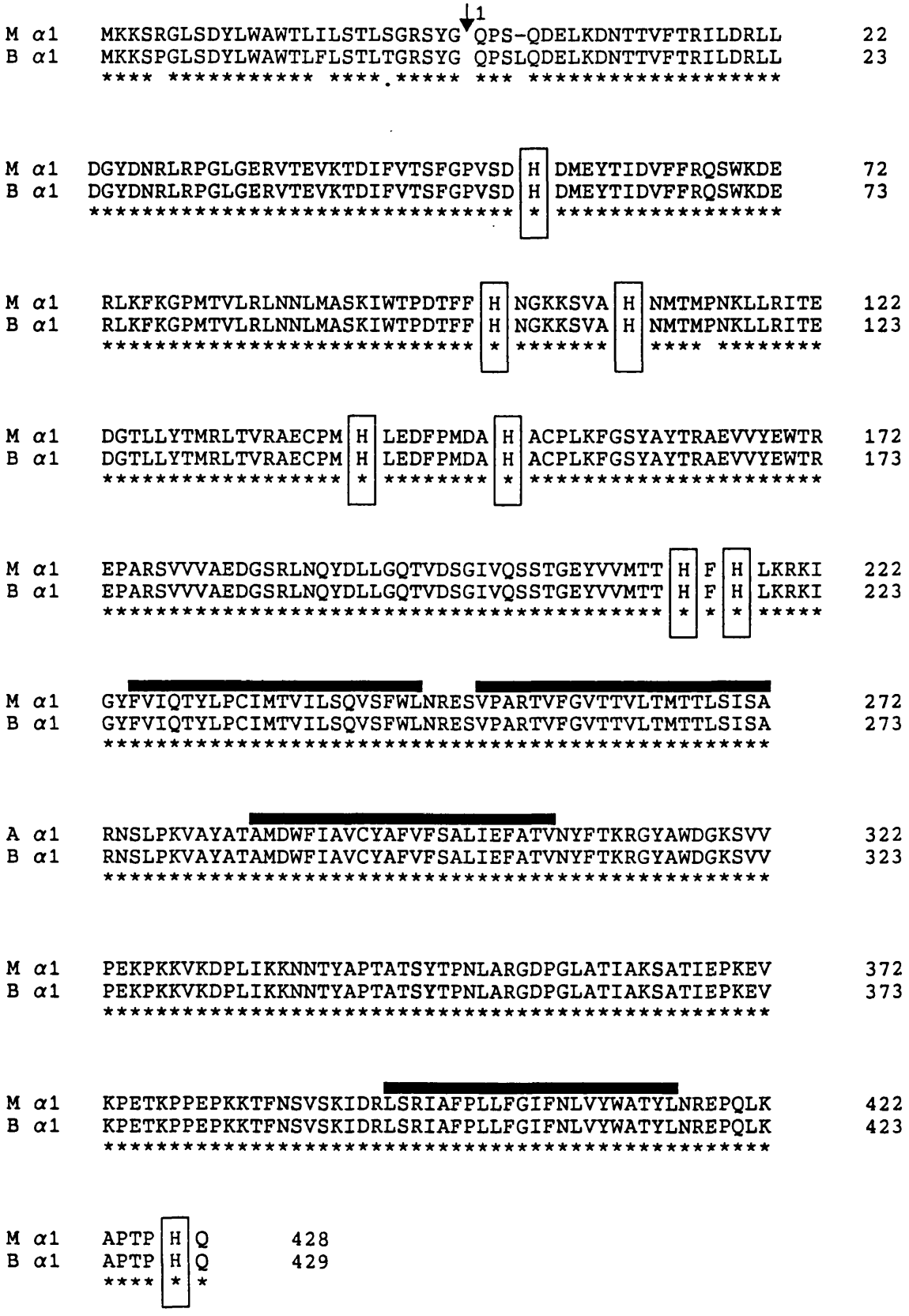
↓1
M α1 MKKSRGLSDYLWAWTLILSTLSGRSYG QPS-QDELKDNTTVFTRILDRLL 22
B α1 MKKSPGLSDYLWAWTLFLSTLTGRSYG QPSLQDELKDNTTVFTRILDRLL 23
M α1 DGYDNRLRPGLGERVTEVKTDIFVTSFGPVSD H DMEYTIDVFFRQSWKDE 72
B α1 DGYDNRLRPGLGERVTEVKTDIFVTSFGPVSD H DMEYTIDVFFRQSWKDE 73
M α1 RLKFKGPMTVLRLNNLMASKIWTPDTFF H NGKKSVA H NMTMPNKLLRITE 122
B α1 RLKFKGPMTVLRLNNLMASKIWTPDTFF H NGKKSVA H NMTMPNKLLRITE 123
M α1 DGTLLYTMRLTVRAECPM H LEDFPMDA H ACPLKFGSYAYTRAEVVYEWTR 172
B α1 DGTLLYTMRLTVRAECPM H LEDFPMDA H ACPLKFGSYAYTRAEVVYEWTR 173
M α1 EPARSVVVAEDGSRLNQYDLLGQTVDSGIVQSSTGEYVVMTT H F H LKRKI 222
B α1 EPARSVVVAEDGSRLNQYDLLGQTVDSGIVQSSTGEYVVMTT H F H LKRKI 223
M α1 GYFVIQTYLPCIMTVILSQVSFWLNRESVPARTVFGVTTVLTMTTLSISA 272
B α1 GYFVIQTYLPCIMTVILSQVSFWLNRESVPARTVFGVTTVLTMTTLSISA 273
A α1 RNSLPKVAYATAMDWFIAVCYAFVFSALIEFATVNYFTKRGYAWDGKSVV 322
B α1 RNSLPKVAYATAMDWFIAVCYAFVFSALIEFATVNYFTKRGYAWDGKSVV 323
M α1 PEKPKKVKDPLIKKNNTYAPTATSYTPNLARGDPGLATIAKSATIEPKEV 372
B α1 PEKPKKVKDPLIKKNNTYAPTATSYTPNLARGDPGLATIAKSATIEPKEV 373
M α1 KPETKPPEPKKTFNSVSKIDRLSRIAFPLLFGIFNLVYWATYLNREPQLK 422
B α1 KPETKPPEPKKTFNSVSKIDRLSRIAFPLLFGIFNLVYWATYLNREPQLK 423
M α1 APTP H Q 428
B α1 APTP H Q 429

Figure 5.13. Homologies of the predicted amino acid sequences for mouse and bovine $GABA_A$ β1 subunits. The vertical arrow indicates the proposed end of the signal sequence and the start of the mature protein, which is also where numbering starts. Numbers on the right denote amino-acid residues. Identical residues are shown by asterisks (*), a conservative change in an amino acid is indicated by a dot (.) and a non-conservative change by a space ( ). The overall sequence identity between the two $GABA_A$ β1 subunits is 97.47%. The proposed membrane-spanning hydrophobic sequences (M1-M4) are indicated by the solid bars and all extracellular histidine residues are boxed. Sequences were obtained from Dr. D. Burt, University of Maryland, Baltimore, personal communication (mouse) and Schofield *et al.*, 1987 (bovine) and aligned using PC/GENE version 6.6.

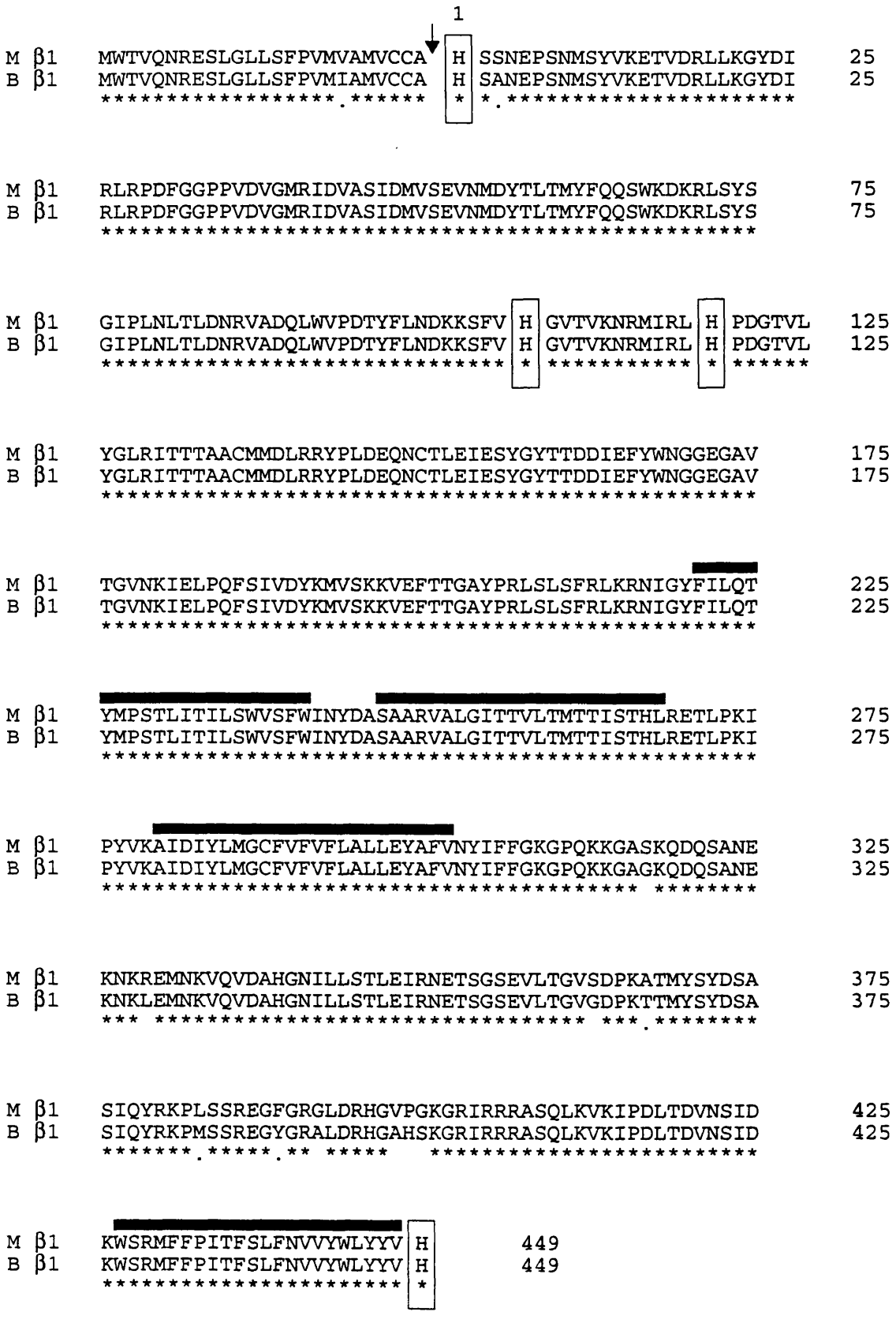
1
M β1 MWTVQNRESLGLLSFPVMVAMVCCA H SSNEPSNMSYVKETVDRLLKGYDI 25
B β1 MWTVQNRESLGLLSFPVMIAMVCCA H SANEPSNMSYVKETVDRLLKGYDI 25
M β1 RLRPDFGGPPVDVGMRIDVASIDMVSEVNMDYTLTMYFQQSWKDKRLSYS 75
B β1 RLRPDFGGPPVDVGMRIDVASIDMVSEVNMDYTLTMYFQQSWKDKRLSYS 75
M β1 GIPLNLTLDNRVADQLWVPDTYFLNDKKSFV H GVTVKNRMIRL H PDGTVL 125
B β1 GIPLNLTLDNRVADQLWVPDTYFLNDKKSFV H GVTVKNRMIRL H PDGTVL 125
M β1 YGLRITTTAACMMDLRRYPLDEQNCTLEIESYGYTTDDIEFYWNGGEGAV 175
B β1 YGLRITTTAACMMDLRRYPLDEQNCTLEIESYGYTTDDIEFYWNGGEGAV 175
M β1 TGVNKIELPQFSIVDYKMVSKKVEFTTGAYPRLSLSFRLKRNIGYFILQT 225
B β1 TGVNKIELPQFSIVDYKMVSKKVEFTTGAYPRLSLSFRLKRNIGYFILQT 225
M β1 YMPSTLITILSWVSFWINYDASAARVALGITTVLTMTTISTHLRETLPKI 275
B β1 YMPSTLITILSWVSFWINYDASAARVALGITTVLTMTTISTHLRETLPKI 275
M β1 PYVKAIDIYLMGCFVFVFLALLEYAFVNYIFFGKGPQKKGASKQDQSANE 325
B β1 PYVKAIDIYLMGCFVFVFLALLEYAFVNYIFFGKGPQKKGAGKQDQSANE 325
M β1 KNKREMNKVQVDAHGNILLSTLEIRNETSGSEVLTGVSDPKATMYSYDSA 375
B β1 KNKLEMNKVQVDAHGNILLSTLEIRNETSGSEVLTGVGDPKTTMYSYDSA 375
M β1 SIQYRKPLSSREGFGRGLDRHGVPGKGRIRRRASQLKVKIPDLTDVNSID 425
B β1 SIQYRKPMSSREGYGRALDRHGAHSKGRIRRRASQLKVKIPDLTDVNSID 425
M β1 KWSRMFFPITFSLFNVVYWLYYV H 449
B β1 KWSRMFFPITFSLFNVVYWLYYV H 449

Figure 5.14. Homologies of the predicted amino acid sequences for mouse $GABA_A$ α1, γ2S, β1 and δ subunits. Numbers on the right denote amino-acid residues after the start of the mature protein. Identical residues are shown by asterisks (*), a conservative change in an amino acid is indicated by a dot (.) and a non-conservative change by a space ( ). The overall sequence identity between the $GABA_A$ subunits is 27.7%. The proposed membrane-spanning hydrophobic sequences (M1-M4) are indicated by the solid bars and the histidine residue at position 224 in the δ subunit is boxed. Sequences were obtained from Wang *et al.*, 1992b (α1), Kofuji *et al.*, 1991 (γ2), Dr. D. Burt, University of Maryland, Baltimore, personal communication (β1) and Wang *et al.*, 1992a (δ) and aligned using PC/GENE version 6.6.

```
α1  MKKSRG-----------LSDYLWAWTLILSTLSGRSYGQPSQDELKDNTT       12
γ2  MSSPNTWSIGSSVYSPVFSQKMTLWILLLLLSLYPGFTSQKSDDDYEDYTS      12
β1  MW--------------TVQ-NRESLGLLSFPVMVAMVCCAHSSNEPSNMS       10
δ   MD--------------VLGWLLLPLLLLCTQPHHGARAMNDIGDYVGSNL       20
    *                    *.                     ..  .

α1  VFTR-------------ILDRLLDGYDNRLRPGLGERVTEVKTDIFVTSF       49
γ2  NKTWVLTPKVPEGDVTVILNNLLEGYDNKLRPDIGVKPTLIHTDMYVNSI      62
β1  YVK--ET-----------VDRLLKGYDIRLRPDFGGPPVDVGMRIDVASI      47
δ   EISWLPN-----------LDGLMEGYARNFRPGIGGAPVNVALALEVASI      59
      .                 .. *..**. ..**..*   . .   . *.*.

α1  GPVSDHDMEYTIDVFFRQSWKDERLKFKGPMTVLRLNNLMASKIWTPDTF      99
γ2  GPVNAINMEYTIDIFFAQTWYDRRLKFNSTIKVLRLNSNMVGKIWIPDTF      112
β1  DMVSEVNMDYTLTMYFQQSWKDKRLSYSGIPLNLTLDNRVADQLWVPDTY      97
δ   DHISEANMEYTMTVFLHQSWRDSRLSYNHTNETLGLDSRFVDKLWLPDTF      109
    . ... .*.**..... *.* * **...      * *..  ....* ***.

α1  FHNGKKSVAHNMTMPNKLLRITEDGTLLYTMRLTVRAECPMHLEDFPMDA      149
γ2  FRNSKKADAHWITTPNRMLRIWNDGRVLYTLRLTIDAECQLQLHNFPMDE      162
β1  FLNDKKSFVHGVTVKNRMIRLHPDGTVLYGLRITTTAACMMDLRRYPLDE      147
δ   IVNAKSAWFHDVTVENKLIRLQPDGVILYSIRITSTVACDMDLAKYPLDE      159
    . *.*..  * .*  *...*.  ** .**..*.*  ..* ..*  .*.*.

α1  HACPLKFGSYAYTRAEVVYEWTREPARSVVVAEDGSRLNQYDLLGQTVDS      199
γ2  HSCPLEFSSYGYPREEIVYQWKRSSVE--VGDTRSWRLYQFSFVGLRNTT      210
β1  QNCTLEIESYGYTTDDIEFYWN--GGEGAVTGVNKIELPQFSIVDYKMVS      195
δ   QECMLDLESYGYSSEDIVYYWS--ENQEQIHGLDRLQLAQFTITSYRFTT      207
    ..* *...**.*. .... .*.        . .      * *... .    .

α1  GIVQ-SSTGEYVVMTT H FHLKRKIGYFVIQTYLPCIMTVILSQVSFWLNR     248
γ2  EVVK-TTSGDYVVMSV Y FDLSRRMGYFTIQTYIPCTLIVVLSWVSFWINK     259
β1  KKVEF-TTGAYPRLSL S FRLKRNIGYFILQTYMPSTLITILSWVSFWINY     244
δ   ELMNFKSAGQFPRLSL H FQLRRNRGVYIIQSYMPSVLLVAMSWVSFWISQ     257
     ..  ..*..  ..     * *.*. *  ...*.*.*... . .* ****..

α1  ESVPARTVFGVTTVLTMTTLSISARNSLPKVAYATAMDWFIAVCYAFVFS      298
γ2  DAVPARTSLGITTVLTMTTLSTIARKSLPKVSYVTAMDLFVSVCFIFVFS      309
β1  DASAARVALGITTVLTMTTISTHLRETLPKIPYVKAIDIYLMGCFVFVFL      294
δ   AAVPARVSLGITTVLTMTTLMVSARSSLPRASAIKALDVYFWICYVFVFA      307
    .. .**. .*.********. .  *..**. .  .*.* .   *. ***
```

```
α1  ALIEFATVNYFTKRGYAWDGKSVVPEKPKKVKDP----LIKKNNTYAPTA      344
γ2  ALVEYGTLHYFVSNRKPSKDKD---KKKKNPLLR----MFSFKAPTIDIR      352
ß1  ALLEYAFVNYIFFGKGPQKKGASKQDQSANEKNKREMNKVQVDAHGNILL      344
δ   ALVEYAFAHFNADYRKKRKAKVKVTKPRAEMDVRNAIVLFSLSAAGVSQE      357
    **.*..  ..        .     .   .            ..

α1  TSYTPNLARGDPGL-----ATIAKSATIEPKEVKPETKPPEP--------      381
γ2  PRSATIQMNNATHL-----QERDEEYGYECLDGKDCASFFCC--------      389
ß1  STLEIRNETSGSEVLTGVSDPKATMYSYDSASIQYRKPLSSREGFGRGLD      394
δ   LAISRRQGRVPGNLMG----------SYRSVEVEAKKEGGSRPG------      375
                .         .            .    . .

α1  -------KKTFNSVSKIDR-------------LSRIAFPLLFGIFNLVYW      405
γ2  ---FEDCRTGAWRHGRIHIRIAKMDS------YARIFFPTAFCLFNLVYW      430
ß1  RHGVPGKGRIRRRASQLKVKIPDLTDVNSIDKWSRMFFPITFSLFNVVYW      444
δ   -----GPGGIRSRLKPI--------DADTIDIYARAVFPAAFAAVNIIYW      412
          .                   .        . . ..   .

α1  ATYLNR        411
γ2  VSYLYL        436
ß1  LYYV-H        449
δ   AAYT-M        417
```

Table 5.1. Analysis of the pH titration and equilibrium concentration response curves for GABA in *Xenopus laevis* oocytes injected with $GABA_A$ receptor cDNAs. The pK_a values were obtained by interpolation at 50% of the maximum responses from the pH titration curves. The EC_{50} and Hill coefficient (n) data were determined from fitting the logistic model to the normalised curves (see methods) with all values mean ± s.e.m.

Table 5.1

Subunit Composition	pKa	EC_{50} (μM)			Hill Coefficient		
		pH 7.4	pH 5.4	pH 9.4	pH 7.4	pH 5.4	pH 9.4
α1β1	6.8	5.87 ± 0.6	* 3.2 ± 0.2	* 2.6 ± 0.25	0.9 ± 0.07	1.05 ± 0.2	* 1.24 ± 0.14
α1β1γ2S	-	9.75 ± 0.3	10.06 ± 0.2	10.4 ± 0.3	1.3 ± 0.04	1.22 ± 0.04	1.25 ± 0.03
α1β1δ	6.3 and 9.9	4.9 ± 0.4	4.9 ± 0.4	4.5 ± 0.45	0.85 ± 0.05	0.86 ± 0.05	0.8 ± 0.06
α1β1γ2Sδ	5.5 and 9.6	27.7 ± 1.0	* 35.7 ± 0.98	* 31.7 ± 1.3	1.44 ± 0.06	* 1.6 ± 0.07	1.54 ± 0.08
α1β1 Bovine	6.4	15.10 ± 2.15	11.4 ± 2.2	#* 8.3 ± 2.3	0.86 ± 0.07	0.85 ± 0.1	# 0.95 ± 0.2
α1β1γ2S Bovine	-	12.06 ± 1.5	11.9 ± 1.3	12.3 ± 1.5	0.92 ± 0.08	0.94 ± 0.07	0.92 ± 0.07

(# indicates pH 8.4; * represents a significant change from control $P < 0.05$)

Table 5.2

Subunit Composition	IC_{50} (μM)		
	pH 7.4	pH 5.4	pH 9.4
α1β1	1.1 ± 0.1	55.2 ± 3.4	1.3 ± 0.15
α1β1δ	14.8 ± 1.53	45.9 ± 3.7	14.8 ± 1.7
α1β1γ2S	639.9 ± 34.9	-	-
α1β1γ2Sδ	615.4 ± 84.3	-	-
α1β1 Bovine	0.73 ± 0.06	# 1.7 ± 0.1	@ 0.37 ± 0.05
α1β1γ2S Bovine	616.95 ± 76.3	-	-

Analysis of the zinc inhibition plots for GABA in *Xenopus laevis* oocytes injected with $GABA_A$ receptor cDNAs. The IC_{50} values were obtained from fitting the antagonist inhibition model to the normalised curves (see methods) with all values mean ± s.e.m. (# and @ indicates pH 6.4 and 8.4 respectively).

Table 5.3. Analysis of the equilibrium concentration response curves for GABA in the absence and presence of zinc recorded from $GABA_A$ receptor constructs. The EC_{50} data were determined from fitting the logistic model to the normalised curves (see methods) with all values mean ± s.e.m.

Table 5.3

Subunit Composition	EC_{50} (μM)					
	pH 7.4		pH 5.4		pH 9.4	
	Control	+Zinc	Control	+Zinc	Control	+Zinc
α1β1	5.87 ± 0.7	(1) 6.6 ± 0.5	3.2 ± 0.18	(50)* 7.4 ± 0.5	2.5 ± 0.3	(1)* 1.0 ± 0.1
α1β1δ	4.9 ± 0.41	(10)* 28.4 ± 3.5 (100)* 361 ± 53.1	4.9 ± 0.4	(50)* 15.6 ± 1.2	4.3 ± 0.34	(10)* 47.8 ± 5.8
α1β1γ2S	9.7 ± 0.2	(5) 10.06 ± 0.21 (300)* 6 ± 0.3	-	-	-	-
α1β1γ2Sδ	27.7 ± 0.96	(10) 27.7 ± 0.95 (300)* 16.2 ± 1.02	-	-	-	-
α1β1 Bovine	19.5 ± 3.2	(0.5)* 4.9 ± 0.63 (5)* 2.2 ± 0.97	# 10.7 ± 1.8	#(5)* 3.7 ± 0.4	@ 8.0 ± 1.9	@(0.5)* 3.5 ± 0.4 (5)* 3.8 ± 0.5
α1β1γ2S Bovine	12.1 ± 1.2	(5) 11.9 ± 0.75	-	-	-	-

(Numbers in parentheses indicate the zinc concentration (μM); # and @ represent pH 6.4 and 8.4 respectively; * represents a significant change from control $P < 0.05$)

Table 5.4. Analysis of the equilibrium concentration response curves for GABA in the absence and presence of zinc in *Xenopus laevis* oocytes injected with $GABA_A$ receptor cDNAs. The Hill coefficient (n) data were determined from fitting the logistic model to the normalised curves (see methods) with all values mean ± s.e.m.

Table 5.4

Subunit Composition	Hill Coefficient					
	pH 7.4		pH 5.4		pH 9.4	
	Control	+Zinc	Control	+Zinc	Control	+Zinc
α1β1	0.95 ± 0.09	(1)* 1.2 ± 0.1	1.1 ± 0.06	(50) 1.1 ± 0.07	1.2 ± 0.14	(1) 1.2 ± 0.2
α1β1δ	0.85 ± 0.05	(10) 0.8± 0.06 (100)* 0.6 ± 0.03	0.86 ± 0.05	(50)* 0.75 ± 0.03	0.85 ± 0.15	(10) 0.7 ± 0.12
α1β1γ2S	1.3 ± 0.4	(5) 1.2 ± 0.03 (300) 1.5 ± 0.9	-	-	-	-
α1β1γ2Sδ	1.4 ± 0.06	(10) 1.5 ± 0.07 (300) 1.4 ± 0.1	-	-	-	-
α1β1 Bovine	0.75 ± 0.5	(0.5) 0.9 ± 0.1 (5) 1.5 ± 0.7	# 0.8 ± 0.07	#(5)* 1.2 ± 0.11	@ 0.9 ± 0.2	@ (0.5) 1.2 ± 0.15 (5) 1.0 ± 0.14
α1β1γ2S Bovine	0.9 ± 0.6	(5) 0.96 ± 0.04	-	-	-	-

(Numbers in parentheses indicate the zinc concentration (μM); # and @ represent pH 6.4 and 8.4 respectively; * represents a significant change from control $P < 0.05$)

Table 5.5

Group	Typical pK
Aspartic and glutamic acid	4.4
Histidine	6.5
Cysteine	8.5
Tyrosine	10.0
Lysine	10.0
Arginine	12.0

pK values of ionizable groups in proteins. Note the absolute values within the protein depend on temperature, ionic strength, and the microenvironment of the ionizable group. Values taken from Stryer, 1988.

CHAPTER SIX

MODULATION OF RECOMBINANT $GABA_A$ RECEPTORS BY PROTEIN KINASE C

MODULATION OF RECOMBINANT $GABA_A$ RECEPTORS BY PROTEIN KINASE C

6.1 INTRODUCTION

Expression of three $GABA_A$ receptor subunits, α, β and γ have been utilised in functional studies of $GABA_A$ receptors, either together or individually, to produce functional GABA-gated chloride channels (Schofield *et al.*, 1987; Blair *et al.*, 1988; Burt and Kamatchi, 1991). In addition to allosteric modulation by various ligands the function of ligand-gated ion channels can be regulated by covalent modification of receptor structure via phosphorylation (Swope *et al.*, 1992; Raymond *et al.*, 1993). Affinity purified preparations of the $GABA_A$ receptors have revealed a variety of protein kinase phosphorylation sites within the $GABA_A$ receptor complex (Kirkness *et al.*, 1989; Browning *et al.*, 1990). Treatment of purified porcine $GABA_A$ receptors with cyclic AMP-dependent protein kinase, protein kinase A (PKA), catalysed the phosphorylation of the β subunit of the receptor (Kirkness *et al.*, 1989). Moreover, treatment of rat purified $GABA_A$ receptors with either protein kinase C (PKC) or PKA induced the phosphorylation of the β subunits of the receptor (Browning *et al.*, 1990).

The putative large intracellular loop between transmembrane domains M3 and M4 contains potential consensus sequences for phosphorylation by PKC, PKA and protein tyrosine kinases, with the number and positions varying among the $GABA_A$ receptor subunits (Swope *et al.*, 1992). All β subunit cDNAs isolated to date (β1-4) contain a conserved consensus sequence for phosphorylation by PKA (serine 409 in the β1 subunit; Ymer *et al.*, 1989b; Swope *et al.*, 1992). Furthermore the β1 subunit has been shown to be phosphorylated by both PKA and PKC on serine 409 (Moss *et al.*, 1992a; Krishek *et al.*, 1994). This residue was also phosphorylated by calcium calmodulin dependent protein kinase II (CaM kinase II) and cyclic guanosine monophosphate (cGMP) - dependent protein kinase (MacDonald and Moss.,

1994; cf Browning *et al.*, 1990). In addition, recent studies have revealed that two differently spliced forms of the γ2 subunit exist, termed short (γ2S) and long (γ2L), which differ by an insertion of 8 amino acids in the major intracellular loop (Whiting *et al.*, 1990; Kofuji *et al.*, 1991). Both the short and the long form of the γ2 subunit contain a consensus sequence for phosphorylation by PKC, with phosphorylation occurring on serine 327 (Whiting *et al.*, 1990; Moss *et al.*, 1992a). The long form of the γ2 subunit contains an additional consensus sequence for phosphorylation by PKC, on serine 343 (Whiting *et al.*, 1990; Moss *et al.*, 1992a). Interestingly, patterns of temporal and spatial expression in the brain differ between the mRNAs encoding these two forms of the γ2 subunit (Glencorse *et al.*, 1992). This suggests that alternative splicing of the γ2 subunit provides a novel role for phosphorylation in the regulation of $GABA_A$ receptor function. Furthermore, both γ1 and γ2 $GABA_A$ receptor subunits contain consensus sites for protein tyrosine phosphorylation (Pritchett *et al.*, 1989; Swope *et al.*, 1992). A serine protein kinase, yet to be identified, has been reported to phosphorylate the α subunit of the $GABA_A$ receptor (Sweetnam *et al.*, 1988).

Functional effects of phosphorylation in native neurones and cell expression systems have been found to be complex. For example phosphorylation has been shown to inhibit GABA-activated responses (Porter *et al.*, 1990; Moss *et al.*, 1992b) whereas a continuous rundown of the GABA response amplitude in dissociated hippocampal and chick sensory neurones was prevented by agents known to promote phosphorylation (Stelzer *et al.*, 1988; Gyenes *et al.*, 1988; Stelzer, 1992). These different effects of phosphorylation could be due to heterogeneity of the $GABA_A$ receptor complex, however interpretations are often complicated by the non-specific activity of many drugs used to modulate kinase activity (Leidenheimer *et al.*, 1991).

PKC was discovered in 1977 and characterised as a calcium/phospholipid-dependent protein kinase activated by diacylglycerol or phorbol esters (for

review see Huang, 1989, Nishizuka, 1992). Recent studies have identified 8 subtypes of the PKC enzyme which are unequally distributed and show individual enzymatic properties, including activation by diacylglycerol, sensitivity to calcium, arachidonic acid and lipoxin A (Nishizuka, 1988). Knowledge of the PKC subtype is important if functional effects of PKC-induced phosphorylation are to be compared between different cell types. This study utilises recombinant $GABA_A$ receptors expressed in the *Xenopus* oocyte where the endogenous PKC isoform, identified by kinetic properties, is very similar to an isoform of the rat α-PKC (Sahara *et al.*, 1992). The endogenous PKC was activated by phorbol esters and specific point mutations of the likely phosphoacceptor amino acid residues have been made on relevant $GABA_A$ receptor subunits to assess the functional consequences of phosphorylation. The results demonstrate that PKC-induced phosphorylation leads to differential effects depending on the $GABA_A$ receptor subunit composition and the number of phosphorylation sites present within these subunits.
All cDNAs were kindly supplied by Dr. S.J. Moss, University College.

6.2 RESULTS

6.2.1 EFFECT OF PKC-INDUCED PHOSPHORYLATION ON GABA-ACTIVATED MEMBRANE CURRENTS

Heteromeric $GABA_A$ receptors incorporating combinations of α1, β1, γ2S and γ2L subunits were expressed in *Xenopus* oocytes. Recording from cells expressing α1β1, α1β1γ2S or α1βγ2L receptor subunits, membrane currents evoked by bath-applied GABA to single *Xenopus* oocytes were monitored. At holding potentials of -40 to -60 mV under voltage-clamp the GABA-activated responses had consistent membrane currents which were maintained over recording periods of up to 240 min. The effect of phosphorylation by PKC on $GABA_A$ receptor function was addressed by the application of active, β, and inactive α, phorbol esters. Bath-application of the active phorbol ester,

250 nM phorbol 12-myristate 13-acetate (PMA), resulted in a small transient enhancement (within 3-5 min; shown in Fig. 6.1D) which decayed to a gradual decrease in the GABA-activated response (Fig. 6.1A,B). This response profile was observed with α1β1, α1β1γ2S and α1β1γ2L subunit combinations after PMA treatment.

The specificity of action of the phorbol esters for PKC was ascertained by either using a phorbol ester which does not activate PKC, 4α-phorbol 12,13 didecanoate (α-PDD), or by recording from cells expressing mutant forms of the $GABA_A$ receptor subunits where serine (S) residues, previously demonstrated to be substrates for PKC (Moss *et al.*, 1992a), on β1 (S409), γ2S (S327) and γ2L (S327/S343) were replaced by alanine (A) residues. The action of PMA was further analysed by using a PKC inhibitory peptide (PKCI). Bath application of 500 nM α-PDD to oocytes expressing α1β1, α1β1γ2S and α1β1γ2L (Fig. 6.1C) often resulted in an initial small transient enhancement (not shown) after which the amplitude of the GABA-induced current and conductance were unaffected. This suggested that the inhibitory action of PMA was mediated by activation of PKC and that the initial transient enhancement was not associated with the activation of PKC.

Biochemical studies have previously demonstrated a number of serine residues within the $GABA_A$ receptor that are substrates for PKC-induced phosphorylation (Moss *et al.*, 1992a; Krishek *et al.*, 1994). Site directed mutagenesis revealed serine residues located on the β1 (S409), γ2S (S327) and γ2L (S327/S343) subunits to be the sites for PKC phosphorylation (Moss *et al.*, 1992a,b; Krishek *et al.*, 1994). Point mutation of these serine residues to alanine residues removed the ability of PKC to phosphorylate the $GABA_A$ receptor (Moss *et al.*, 1992a,b; Krishek *et al.*, 1994). In order to assess whether these serine residues were the functional targets for PKC-induced phosphorylation the following $GABA_A$ receptors were constructed: α1β1(S409A), α1β1(S409A)γ2S(S327A) and α1β1(S409A)γ2L(S327A/S343A). Recordings from oocytes expressing these mutant constructs exhibited

consistent responses to GABA over 120 min allowing the effect on the GABA-induced response by PKC activation to be studied. Bath application of PMA to each mutant receptor, occasionally induced small transient enhancements followed by a reduction back to control GABA-induced response amplitudes (Fig. 6.1D). These results therefore gave further support for the conclusion that the transient enhancements seen in the presence of PMA was not associated with the activation of PKC.

Further analysis of the specificity of the action of PMA on the PKC enzyme was obtained using a protein kinase C inhibitor peptide (PKCI, 19-36; House and Kemp, 1987). Oocytes expressing $\alpha1\beta1\gamma2S$ were microinjected with PKCI (500 ng per oocyte) 90 min before PMA application. Inhibition of the GABA-induced currents and conductances by 250 nM PMA was significantly but not completely antagonised by PKCI ($P < 0.01$; Fig. 6.2).

6.2.2 EQUILIBRIUM-CONCENTRATION RESPONSE RELATIONSHIPS

Equilibrium concentration response curves for GABA were constructed by measuring the steady state GABA-induced chloride conductance for oocytes expressing $\alpha1\beta1$, $\alpha1\beta1\gamma2S$ and $\alpha1\beta1\gamma2L$ subunit combinations. The time course for the effect of PMA on the amplitude of the GABA-induced conductance for these receptor constructs was ascertained and the concentration response curves were measured only after the effect of 250 nM PMA had attained a steady state 30 to 50 mins following application (Fig. 6.1E). These relationships demonstrated that the antagonism produced by prior exposure to 250 nM PMA induced a small lateral shift to the right of the control curve with a depression in the maximum response (Fig. 6.3A) indicative of a mixed/non-competitive type of inhibition (Smart and Constanti, 1986). Moreover, the antagonism was not found to be reversible after the removal of PMA from the bath solution. The maximum conductance increase induced by saturating concentrations of GABA (100 to 1000 μM) was reduced with little change in the EC_{50}s or Hill coefficients for GABA after exposure to

PMA (Table 6.1). The degree of inhibition induced by PMA at each GABA concentration was ascertained from the equilibrium concentration response curves (Fig. 6.4A). Percentage inhibition plots revealed that the degree of depression of the GABA-induced responses was partly dependent on the agonist concentration and on the subunit composition of the $GABA_A$ receptors (Fig. 6.4A). The PMA-induced inhibition was more effective with γ2 subunit containing $GABA_A$ receptors, however the sensitivity difference between receptors containing the short and the long forms of the γ2 subunit appeared to be smaller. Overall, the rank order of inhibitory potency for 250 nM PMA was:

$$\alpha1\beta1\gamma2L > \alpha1\beta1\gamma2S >> \alpha1\beta1.$$

Application of 250 nM PMA did not affect the GABA concentration-response relationships for the mutant $GABA_A$ receptors (Fig. 6.3B, Table 6.1). This demonstrated that the PKC-induced phosphorylation by PMA was most likely being mediated via the β1 or γ2 subunits or both at the serine residues previously identified from biochemical analyses (Moss *et al.*, 1992a; Krishek *et al.*, 1994).

6.2.3 CURRENT-VOLTAGE RELATIONSHIPS

Current-voltage (I-V) relationships for α1β1, α1β1γ2S and α1β1γ2L receptor combinations were assessed during the steady-state phase of an individual GABA-induced response. The I-Vs for the wild-type $GABA_A$ receptor subunit combinations displayed a degree of outward rectification with reversal potentials of -17 mV (α1β1), -21 mV (α1β1γ2S) and -22 mV (α1β1γ2L) which are close to the Cl^- reversal potential in these cells (Fig. 6.5A; Barish, 1983; Dascal, 1987). Application of 250 nM PMA (30 to 50 min) reduced the chord conductances of the I-V relationship at +40 and -100 mV without any significant change in the agonist reversal potential. This type of depression in the I-V relation is consistent with a voltage insensitive mechanism of inhibition. I-Vs for α1β1(S409A), α1β1(S409A)γ2S(S327A) and

α1β1(S409A)γ2L(S327A/S343A) $GABA_A$ receptor constructs were unaffected by PMA (Fig. 6.5B). The chord conductances at +40 and -100 mV were used to calculate a rectification ratio (G_R) in the absence and presence of PMA ($G_R = G_{+40} / G_{-100}$; Table 6.1). Interestingly, the I-V relationships for the mutant $GABA_A$ receptor constructs generally displayed a greater degree of outward rectification ($G_R > 1$) compared to the wild-type $GABA_A$ receptors.

6.2.4 PKC-INDUCED PHOSPHORYLATION: DEPENDENCE ON RECEPTOR COMPOSITION

Whether phosphorylation at each of the 3 serine residues (S409 in β, S327 in γ2S and S327/S343 in γ2L) was functionally equivalent was studied using site directed mutagenesis to sequentially replace each serine residue with an alanine residue. Four new $GABA_A$ receptor constructs were assembled. The functional effect of phosphorylating the two serine residues (S327 and S343) in γ2L were initially studied in $GABA_A$ receptors comprising of α1β1(S409A)γ2L subunits. The GABA concentration response curve was inhibited by 250 nM PMA in a non-competitive fashion with no significant change in the Hill coefficient or EC_{50} values (Fig. 6.6A; Table 6.1). The I-V relationship for this mutant $GABA_A$ receptor was relatively voltage independent in the presence of PMA with marked outward rectification (Fig. 6.7A; Table 6.1). To compare the relative contribution of phosphorylation in the β1 subunit for $GABA_A$ receptors comprising α1β1γ2L, both S327 and S343 were replaced in the γ2L subunit with alanines and a wild-type β1 subunit was used, forming the mutant $GABA_A$ receptor construct α1β1γ2L(S327A/S343A). This receptor mediated GABA-induced currents which were inhibited by PMA in a non-competitive fashion with a depression in the concentration response curve with little lateral shift (Fig. 6.6A). Moreover, there was little change in the EC_{50} or Hill coefficient values (Table 6.1). The I-V relationship for this mutant receptor was relatively voltage insensitive in the presence of PMA with marked outward rectification (Fig.

6.7B; Table 6.1). The type of depression of the equilibrium response curve for α1β1γ2L(S327A/S343A) in the presence of PMA was consistent with that observed with phorbol esters and wild-type receptors comprising of only α1β1 subunits.

The functional effects of phosphorylation at S327 and S343 residues were compared by constructing α1β1(S409A)γ2L(S327A) and α1β1(S409A)γ2L(S343A) receptors, where the former construct removed the serine residue normally present in both γ2S and γ2L whilst retaining the serine residue in the alternatively spliced section of the γ2L subunit. The latter construct removed the serine in the alternatively spliced region of γ2L and retained the serine normally present in γ2S. Expression of these mutant $GABA_A$ receptor constructs resulted in functional receptors with GABA-induced currents and conductances inhibited by 250 nM PMA. The degree of inhibition decreased with increasing agonist concentration and at GABA concentrations above 10 μM membrane currents and conductances mediated by the α1β1(S409A)γ2L(S327A) receptor constructs were more inhibited compared to responses mediated by α1β1(S409A)γ2L(S343A) (Fig. 6.4B/6.6B). The equilibrium response curves for the two forms of the γ2L subunit in the presence of PMA both exhibited a small lateral shift and a depression of the maximum response (Fig. 6.6B). This type of inhibition is consistent with a complex mode of antagonism suggesting a mixed type of inhibition (Smart and Constanti, 1986). For the $GABA_A$ receptor construct α1β1(S409A)γ2L(S327A) there was no significant change in the EC_{50} or Hill coefficient values obtained after treatment with PMA (Table 6.1). For the receptor construct α1β1(S409A)γ2L(S343A) a significant change in the EC_{50} and Hill coefficient values was seen after PKC-induced phosphorylation (Table 6.1). It is possible that the point mutations present in this receptor construct could have changed the quaternary structure of this receptor which could lead to an alteration in the GABA binding site. However, any structural change must have been slight as this receptor construct retained a

pharmacological profile typical of the equivalent wild-type receptor, α1β1γ2L, with bicuculline and picrotoxin inhibiting and both pentobarbitone and flurazepam potentiating the GABA-induced response (not shown). Overall, phosphorylation of the serine 343 in γ2L appeared to have a greater modulatory influence than the serine 327 in γ2S or 409 in β1 at GABA concentrations higher than 10 μM (Fig. 6.4B). As the PKC-induced inhibition of the GABA concentration response curve mediated via α1β1(S409A)γ2L was only slightly greater than that observed with α1β1(S409A)γ2L(S327A), phosphorylation at both S327 and S343 did not produce an additive depression (Fig. 6.6B). Therefore the function of the two sites on the γ2L subunit may be mutually exclusive. The inhibition exerted by phosphorylation of the $GABA_A$ receptor β1 and γ2 subunits appears to be saturable as the maximum depressions of the GABA concentration response curves achieved after application of PMA to receptors comprising α1β1γ2L in comparison to α1β1(S409A)γ2L were similar.

6.3 DISCUSSION

6.3.1 MODULATION OF $GABA_A$ RECEPTOR FUNCTION BY PKC PHOSPHORYLATION

This study demonstrated that PKC phosphorylation induced by PMA negatively modulates $GABA_A$ receptor function. Phorbol esters also induced a transient enhancement in the GABA-activated responses. However, this latter response was reproduced by the inactive phorbol, α-PDD, and also observed on application of PMA to mutated $GABA_A$ receptors which were devoid of PKC phosphorylation. Overall these data revealed that this transient enhancement is probably not occurring by direct phosphorylation of the $GABA_A$ receptor by PKC. This conclusion was supported by the reduced amplitudes of the GABA-activated currents and conductances in addition to the mixed/non-competitive depression of the GABA equilibrium concentration

response curves after treatment with PMA. The depression of the GABA-induced responses occurred at least 15 to 30 mins after the application of PMA which is consistent with second messenger mediation. It is also possible that the phorbol ester penetration into the folliculated oocyte could require some length of time, although the exact time-period remains unknown. Mutation of the phosphoacceptor serine residues to alanine by site-directed mutagenesis in β1, γ2S and γ2L $GABA_A$ receptor subunits abolished these effects of PMA. PKCI, a potent antagonist of PKC, significantly antagonised the PKC-induced phosphorylation by PMA. Therefore the decrease in the GABA-induced responses seen after the application of PMA probably was likely to be occurring via PKC-activated phosphorylation. A complete antagonism of the PKC enzyme by PKCI was not achieved. This could be due to the inability of the PKCI to physically reach all the PKC present within the *Xenopus* oocyte, partly due to the large size of the cell and due to the compartmentalisation of the PKC within the oocyte. I-V relationships revealed that the mechanism of PMA reduction of the GABA-induced responses was relatively voltage insensitive and the reversal potentials of the GABA-induced current were not significantly changed. Interestingly, mutant $GABA_A$ receptors showed a greater degree of outward rectification than wild-type receptors. It is possible that substitution of a serine residue containing an aliphatic hydroxyl group with a non-polar alanine residue confers a conformational change in the $GABA_A$ receptor which results in a greater voltage sensitivity at hyperpolarising membrane potentials.

Responses recorded from *Xenopus* oocytes expressing α1β1γ2S and α1β1γ2L $GABA_A$ receptor subunits revealed that phosphorylation at any one of these sites, all studied separately, produced a negative modulation of receptor function. Moreover, phosphorylation at S343 contained in the 8 amino acid insert in the alternatively spliced long version of γ2 (Whiting *et al.*, 1990; Kofuji *et al.*, 1991) produced the largest effect suggesting that the sites of phosphorylation are not functionally equivalent. The conformation of the large

intracellular loop between transmembrane domains M3 and M4 may be altered by the insertion of the alternatively spliced region in the γ2L subunit producing a more profound effect when phosphorylation occurs. Interestingly, this additional phosphorylation site in the γ2L subunit of the $GABA_A$ receptor was shown to be necessary for ethanol potentiation of receptor function (Wafford *et al.*, 1991; Wafford and Whiting, 1992). A point mutation of the serine residue 343 to alanine in the γ2L subunit eliminated potentiation of the $GABA_A$ receptor by ethanol (Wafford and Whiting, 1992). It was postulated that phosphorylation may underlie the mechanism by which ethanol potentiates $GABA_A$ receptor mediated chloride conductance. In contrast, Sigel and colleagues found no differential ethanol sensitivity between the γ2S and γ2L subunits (Sigel *et al.*, 1993). The reason for the discrepancy in the stimulatory effect of ethanol on the GABA-induced response in previous studies is unclear. It is unlikely to be due to a species difference as Wafford and colleagues expressed both bovine and mouse $GABA_A$ receptors and revealed the requirement of the extra 8 amino acids contained in the γ2L subunit for ethanol sensitivity (Wafford *et al.*, 1991; Wafford and Whiting, 1992). The differences are not due to the expression system *per se* as all studies utilised the *Xenopus* oocyte, the only possibility could be subtle differences in the experimental conditions.

Activation of PKC inhibited GABA-gated chloride currents but also enhanced the ability of diazepam and pentobarbital to potentiate GABA responses on recombinant human α1β1γ2L $GABA_A$ receptors expressed in *Xenopus* oocytes. Moreover, enhancement of the benzodiazepine responses by PMA-induced phosphorylation was not dependent on which PKC phosphorylation site in the γ2 subunit was present (Leidenheimer *et al.*, 1993). These results suggest that protein phosphorylation may alter the coupling between the allosteric modulatory sites within the $GABA_A$ receptor construct but the exact mechanism of this effect remains elusive.

Phosphorylation at S409 in the β1 subunit in addition to the γ2 subunit did not produce a further significant reduction in the GABA-activated responses suggesting the functional effects of phosphorylation at the three PKC serine acceptor sites do not sum linearly. The type of inhibition of the GABA concentration response curves also revealed another difference between the three sites of phosphorylation. A small lateral shift in the curve in addition to a depression in the maximum occurred when PMA was applied to $GABA_A$ receptors expressing a γ2 subunit. This mixed inhibition was not seen with wild-type $GABA_A$ receptors expressing α1β1 subunits or when both S327 and S343 in the γ2L subunit were mutated to alanines in α1β1γ2L(S327A/S343A). This shift could be interpreted as an effect of phosphorylation on agonist affinity and/or steps leading up to ion channel activation. Attempts to express $GABA_A$ receptors devoid of β subunits (α1γ2S or α1γ2L) failed to produce functional channels (cf Angelotti *et al.*, 1993).

Previous studies of the functional effect of PKC-induced phosphorylation on $GABA_A$ receptors have reported a variety of results. A reduction of GABA-activated currents after application of phorbol ester was observed in *Xenopus* oocytes expressing chick whole-brain mRNA (Sigel and Baur, 1988) and rat whole-brain mRNA (Moran and Dascal, 1989; Vaello *et al.*, 1994). In accordance with these results inhibition of responses to GABA was also evident on recombinant $GABA_A$ receptors comprising rat α5β2γ2S subunits (Sigel *et al.*, 1991). It was observed that the GABA-induced currents were depressed more strongly by PMA at lower GABA concentrations than compared to a saturating GABA concentration. This type of depression is consistent with a mixed-type of inhibition for phosphorylation as seen in this study for γ2 subunit containing receptors. However, application of PMA to *Xenopus* oocytes expressing mouse whole-brain $GABA_A$ receptors induced an inhibition of the GABA responses in a non-competitive manner (Leidenheimer *et al.*, 1992). Independence of inhibition on the GABA concentration was also seen in this study in $GABA_A$ receptors comprising α1β1 subunits. Sigel *et al.*

(1991) compared the inhibitory effect of PMA on $GABA_A$ receptors containing either γ2S or γ2L. The results revealed that there was no observable difference in the response to phosphorylation between the two types of γ2 subunits. However, in the present study a difference was observable between γ2S and γ2L subunit containing receptors but only after construction of full equilibrium concentration response curves and was not evident at lower concentrations of GABA producing responses of 5-40% of the maximum and would not therefore have been seen by Sigel and colleagues (1991). Functional effects of PKC-induced phosphorylation following activation by PMA was blocked by mutating the serine residues in β1 and γ2 subunits to alanines. Curiously, in a recent study by Kellenberger *et al.* (1992) these mutations did not completely inhibit the depression of responses by phorbol esters in $GABA_A$ receptors comprising α1β2(S410A)γ2S(S327A). In the rat β2 subunit the phosphoacceptor serine residue at position 410 is equivalent to that found at position 409 in the mouse β1 subunit. Responses mediated by wild-type $GABA_A$ receptors were reduced to a larger extent after only 1.5 min exposure to PMA when compared to the mutant $GABA_A$ receptors. However, after incubation for 10 to 15 min, both the receptor constructs exhibited responses that seemed equally reduced by PMA (Kellenberger *et al.*, 1992). From biochemical studies of β1 and γ2 subunits, mutation of serine residues to alanines resulted in insignificant levels of phosphorylation (Moss *et al.*, 1992a). Thus, it would be expected that the functional effect of PKC-activation by PMA would be clearly affected by these mutations.

In comparison to studies expressing recombinant $GABA_A$ receptors, PKC-induced phosphorylation has been studied in a variety of native neuronal $GABA_A$ receptors. An inhibition of GABA-induced currents by phorbol-12,13-dibutyrate (PDBu) was observed in acutely isolated guinea-pig hippocampal neurones (Stelzer *et al.*, 1992); however, the biologically inactive α-analogue of PDBu had no effect (Stelzer, 1992). Similar results were observed in cultured sympathetic neurones where PDBu inhibited the GABA-activated

responses (Krishek *et al.*, 1994). Leidenheimer *et al.* (1992) observed that application of PMA to cortical or cerebellar microsacs reduced muscimol activated $^{36}Cl^-$ flux (Leidenheimer *et al.*, 1992). Furthermore, Rapallino and colleagues revealed an inhibition of the stimulation of Cl^- permeation by GABA in the presence of PDBu on the plasma membranes of Dieters' neurones. Moreover, application of the inactive phorbol ester, α-PDD, did not reproduce this effect (Rapallino *et al.*, 1993). In contrast, exposure of mouse spinal neurones to PDBu did not affect GABA-induced $^{36}Cl^-$ flux (Ticku and Mehta, 1990). It is possible that these results may differ due to receptor heterogeneity or different PKC species present within the preparation under study. Also the efficiency of the kinase to phosphorylate the $GABA_A$ receptor proteins, as well as a possible existence of compartmentalisation within some neurones of PKC and $GABA_A$ receptors, may have a role in the different responses of PKC-induced phosphorylation observed.

6.3.2 PHYSIOLOGICAL SIGNIFICANCE OF PKC-INDUCED PHOSPHORYLATION

The complex regulation of $GABA_A$ receptors by phosphorylation suggests that different susceptibilities could be conferred by altering the expression of receptor subunit constructs. Phosphorylation could have a profound effect on the long-term modulation of $GABA_A$ receptor function. It is not known at present whether all types of PKA and PKC can induce functional changes by phosphorylating $GABA_A$ receptors. In neurones, the functional importance of phosphorylation remains to be shown. If this phenomenon occurs at the level of the synapse the negative modulation of the $GABA_A$ receptor by PKC could have a significant effect on neuronal excitability. Specifically, in some synapses GABA has been observed to co-localise with other neurotransmitters (dopamine, Everitt *et al.*, 1986; serotonin, Belin *et al.*, 1983). On release the co-transmitter could act at the postsynaptic membrane through protein kinase stimulation providing a mechanism of limiting excessive effects of GABA. This

modulation could be important, providing a control mechanism for GABAergic transmission. Another intriguing facet of PKC-induced phosphorylation is the possible role in the maintenance of long-term potentiation (LTP). LTP of synaptic transmission is believed to be a primary mechanism for learning and memory in vertebrates. Although extensive studies of LTP have concentrated on the hippocampus, similar phenomena have been observed in other limbic structures and the neocortex (for review see Linden and Routtenberg, 1989; Bliss and Collingridge, 1993; Colley and Routtenberg, 1993). Interestingly, a recent study revealed an impairment of $GABA_A$ receptor function during the maintenance of LTP in the hippocampus although the role of PKC in this decrease in receptor function was not ascertained (Stelzer *et al.*, 1994). It will be of interest to determine the involvement of PKC in this reduction of synaptic inhibition and therefore the importance of PKC modulation of the $GABA_A$ receptor function during LTP.

Figure 6.1. GABA-activated membrane currents recorded from *Xenopus laevis* oocytes injected with, (A) α1β1; (B & C) α1β1γ2L and (D) α1β1(S409A)γ2L(S327A,S343A) $GABA_A$ receptor constructs. These receptors were exposed to bath-applied 250 nM PMA (A,B and D) or 500 nM α-PDD (C). Records were recorded at various times after exposure to the phorbol esters (t, min). The membrane conductance was monitored throughout by repetitively applying brief hyperpolarizing voltage command steps (-10mV; 1s, 0.2Hz). Holding potential for all oocytes, -40mV. The 50 nA calibration applies to A and C. (E) Time course plot for the relative membrane conductance (control, 100%) induced by 10 μM GABA on $GABA_A$ receptor constructs, α1β1, α1β1γ2L and α1β1(S409A)γ2L(S327A,S343A). 250 nM PMA or 500 nM α-PDD were applied at 0 min. All points are mean ± s.e.m. obtained from 15 different oocytes.

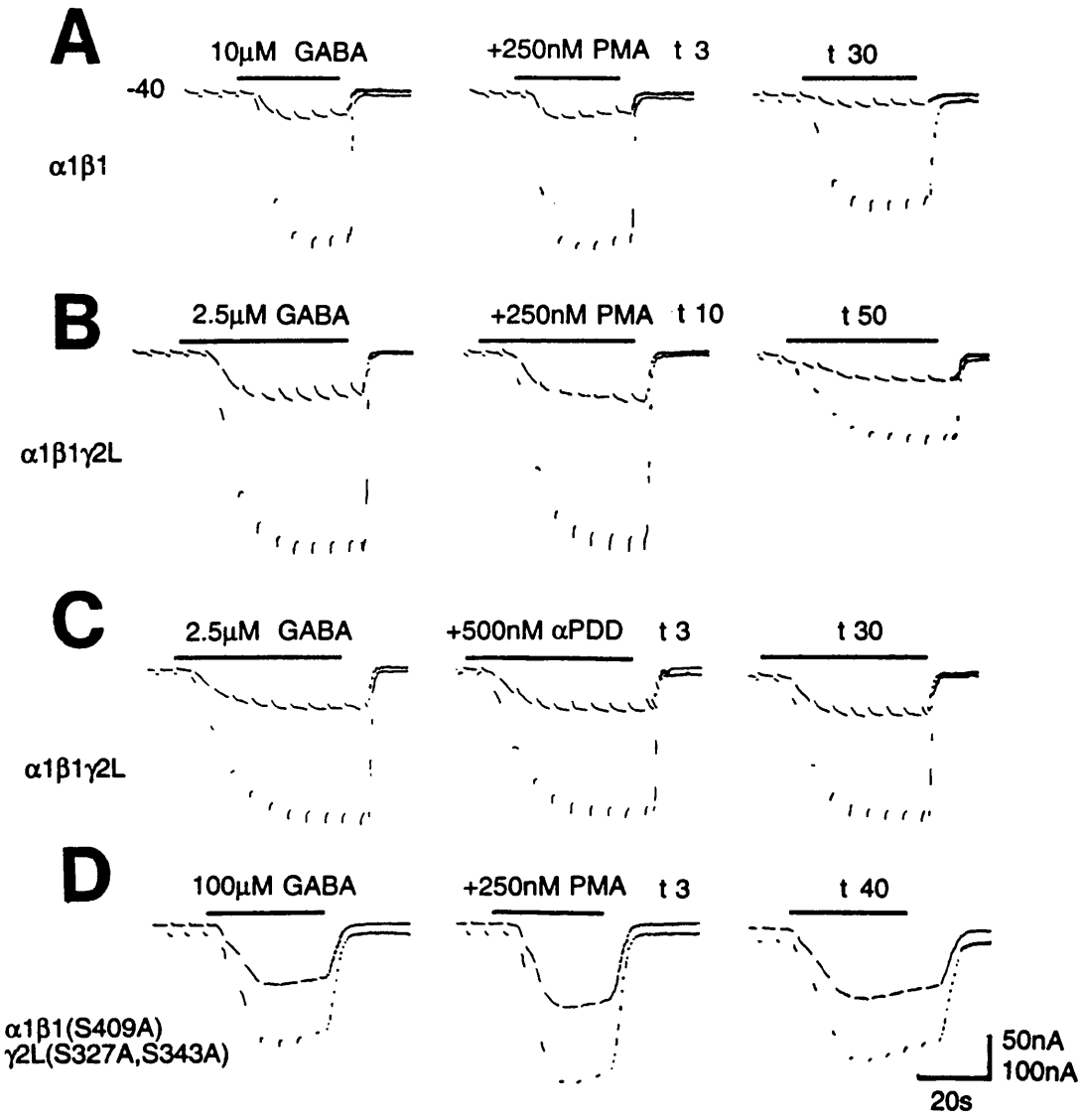
A
10μM GABA
+250nM PMA t 3
t 30
-40
α1β1
B
2.5μM GABA
+250nM PMA t 10
t 50
α1β1γ2L
C
2.5μM GABA
+500nM αPDD t 3
t 30
α1β1γ2L
D
100μM GABA
+250nM PMA t 3
t 40
α1β1(S409A)
γ2L(S327A,S343A)
50nA
100nA
20s

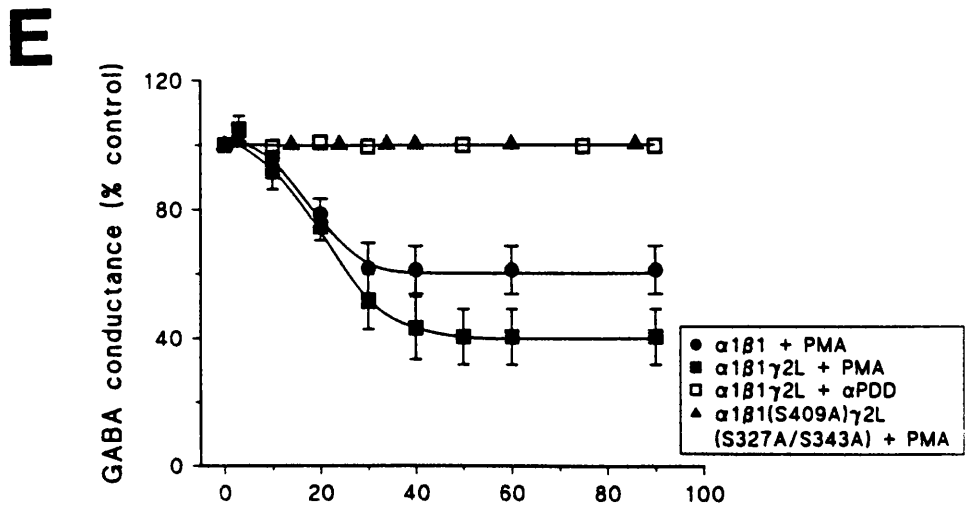
E
GABA conductance (% control)
120
80
40
0
0
20
40
60
80
100
α1β1 + PMA
α1β1γ2L + PMA
α1β1γ2L + αPDD
α1β1(S409A)γ2L
(S327A/S343A) + PMA

Figure 6.2. GABA-activated membrane currents recorded from *Xenopus laevis* oocytes injected with $\alpha 1\beta\gamma 2S$ $GABA_A$ receptor subunits and PKCI peptide. PMA (250 nM) was bath-applied to these receptors in the absence (A) and presence of PKCI peptide, microinjected (500 ng per oocyte) 90 min before PMA application (B). The membrane conductance was monitored as in Fig. 6.1. Holding potential -40mV. (C) Histogram of PKC-induced phosphorylation by PMA on GABA-induced conductances (control, 100%) in the absence (open bar) and presence (hatched bar) of PKCI. PMA plus PKCI is significantly different from PMA alone ($P < 0.01$, paired t test).

A
Control
250nM PMA
t10
t30
t50
B
10μM GABA
+PKCI
10s
40s
50nA
C
GABA conductance (% control)
0
20
40
60
80
100
PMA
PMA + PKCI

Figure 6.3. Equilibrium concentration response curves for GABA-induced membrane conductance (ΔG_N; see methods) recorded from oocytes expressing wild-type receptors (A) or mutant receptors (B). All curves (control, open symbols; + 250 nM PMA, closed symbols) were obtained from 3-7 different oocytes for each receptor construct and have been normalised to the conductance induced by 10μM GABA in control Ringer. The points represent means ± s.e.m. Curves were fitted according to the logistic model (see methods). The concentration response curves were measured after the effect of PMA had attained a steady state, usually after 30 mins following application. Response curves for the mutant receptors were also measured after 30 mins exposure to PMA.

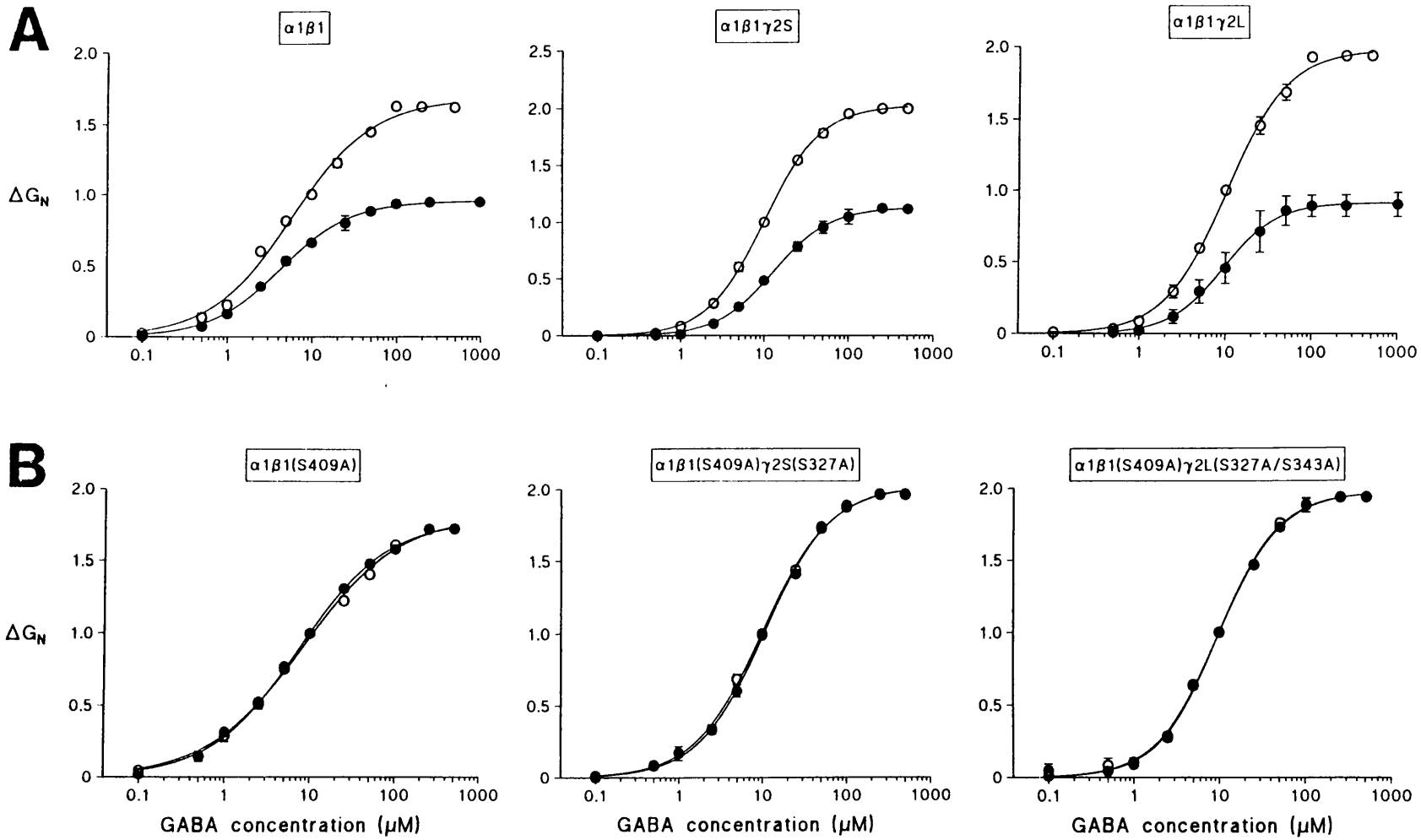
A
α1β1
α1β1γ2S
α1β1γ2L
ΔG_N
2.0
1.5
1.0
0.5
0
2.5
0.1
1
10
100
1000
B
α1β1(S409A)
α1β1(S409A)γ2S(S327A)
α1β1(S409A)γ2L(S327A/S343A)
GABA concentration (μM)

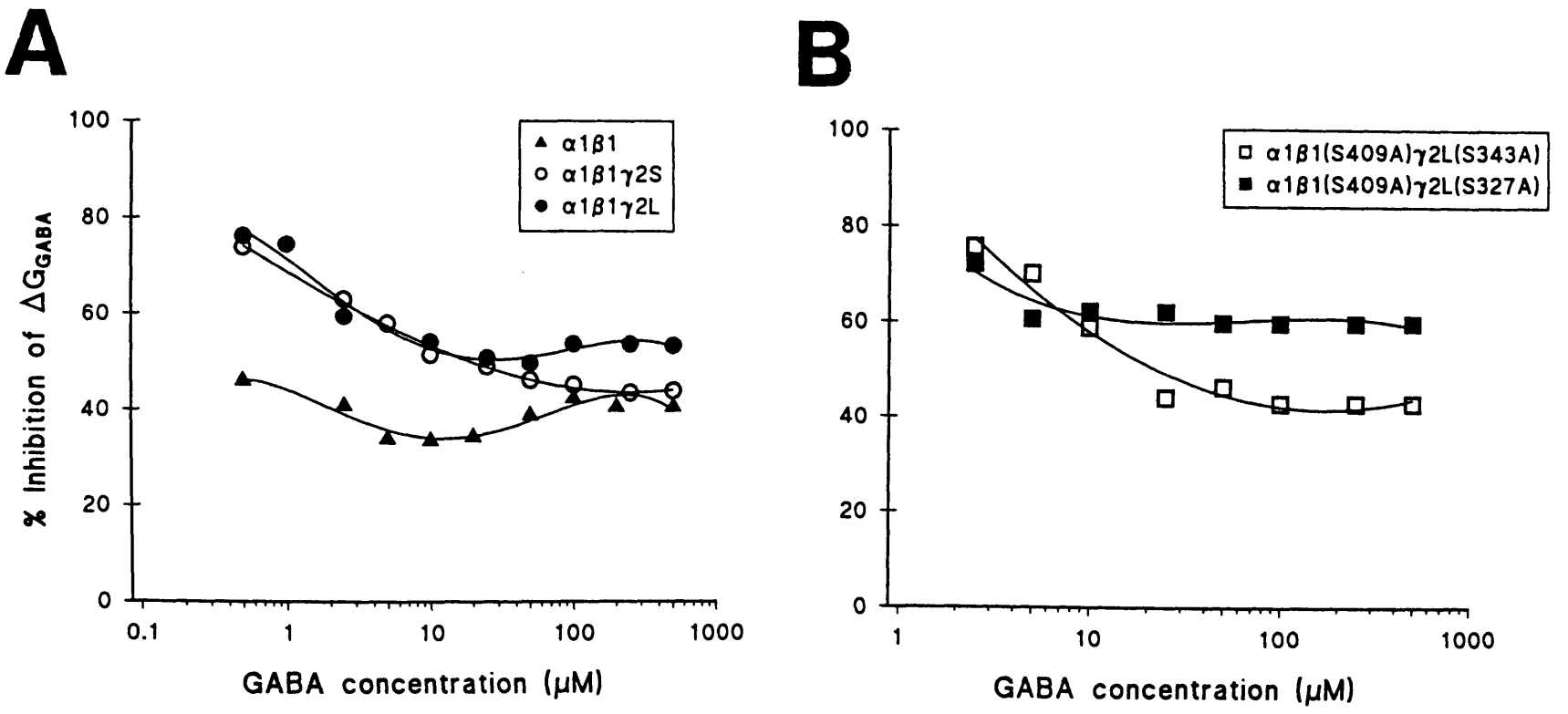

Figure 6.4. Plot of the percentage inhibition in the GABA-induced conductance after treatment with 250 nM PMA for wild-type receptors (A) and selected mutant receptors (B). The points have been calculated from the data in figures 6.3 and 6.6 and the curves were generated using 3rd. or 4th. order polynomials.

Figure 6.5. Current-voltage relationships for GABA recorded from oocytes expressing wild-type receptors (A) or selected mutant receptors (B). The GABA response was determined before (open symbols) and after (closed symbols) application of 250 nM PMA. Note the increased outward rectification in the mutant $GABA_A$ receptor constructs.

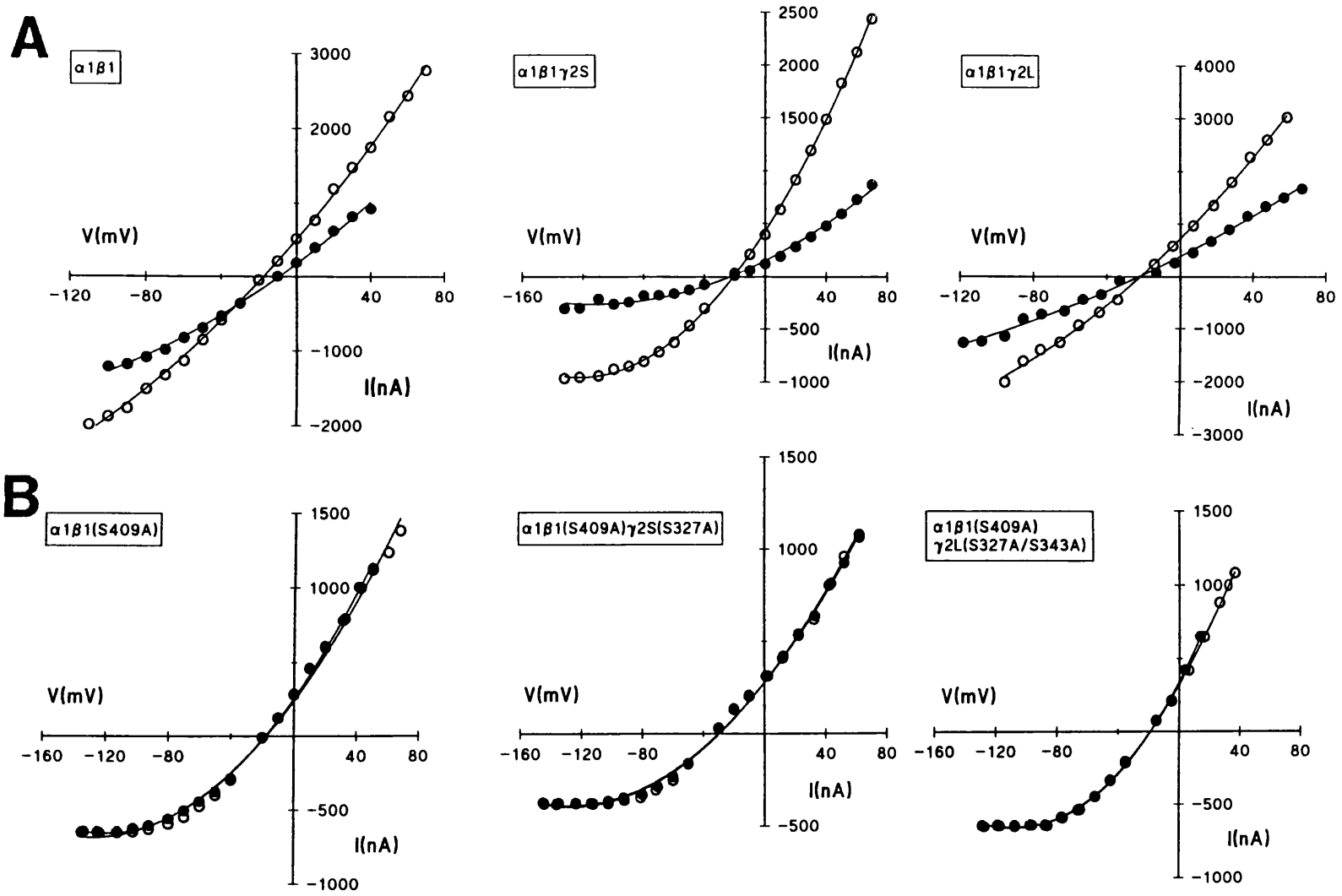
A
α1β1
3000
2000
V(mV)
-120
-80
40
80
-1000
I(nA)
-2000
α1β1γ2S
2500
2000
1500
V(mV)
-160
40
80
-500
I(nA)
-1000
α1β1γ2L
4000
3000
V(mV)
-120
-80
40
80
-1000
-2000
I(nA)
-3000
B
α1β1(S409A)
1500
1000
V(mV)
-160
-120
-80
40
80
-500
I(nA)
-1000
α1β1(S409A)γ2S(S327A)
1500
1000
V(mV)
-160
-120
-80
40
80
I(nA)
-500
α1β1(S409A)
γ2L(S327A/S343A)
1500
1000
V(mV)
-160
-120
-80
40
80
-500
I(nA)
-1000

Figure 6.6. Equilibrium concentration response curves for GABA-induced membrane conductance recorded in *Xenopus* oocytes from $GABA_A$ receptors comprising selected mutations in the β1 and γ2L subunits in the absence (open symbols) and presence (closed symbols) of 250 nM PMA.
(A) Comparison of the effect of mutating S409 in β1 with S327 and S343 in γ2L. The broken line indicates the position of the curve for α1β1(S409A)γ2L.
(B) Comparison of the two serines in γ2L by selectively mutating S327 or S343 whilst S409 in β1 remains mutated to an alanine. The broken line indicates the position of the α1β1(S409A)γ2L(S343A) curve. The curves are normalised as described in figure 6.3. All points are mean ± s.e.m. and are fitted with the logistic model (see methods). Data were obtained from 3-8 oocytes per curve.

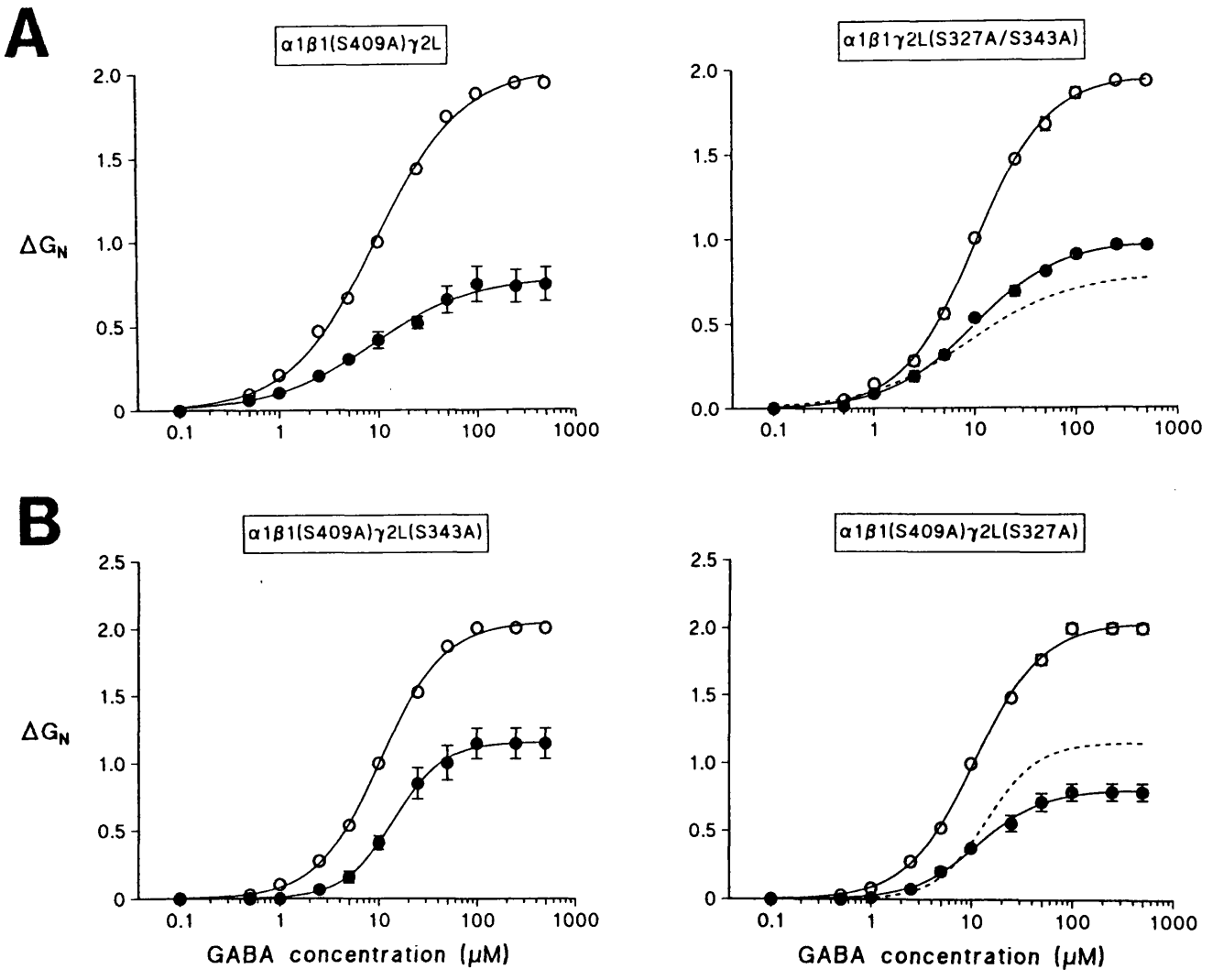
A
α1β1(S409A)γ2L
α1β1γ2L(S327A/S343A)
ΔG_N
2.0
1.5
1.0
0.5
0
0.0
0.1
1
10
100
1000
B
α1β1(S409A)γ2L(S343A)
α1β1(S409A)γ2L(S327A)
2.5
GABA concentration (μM)

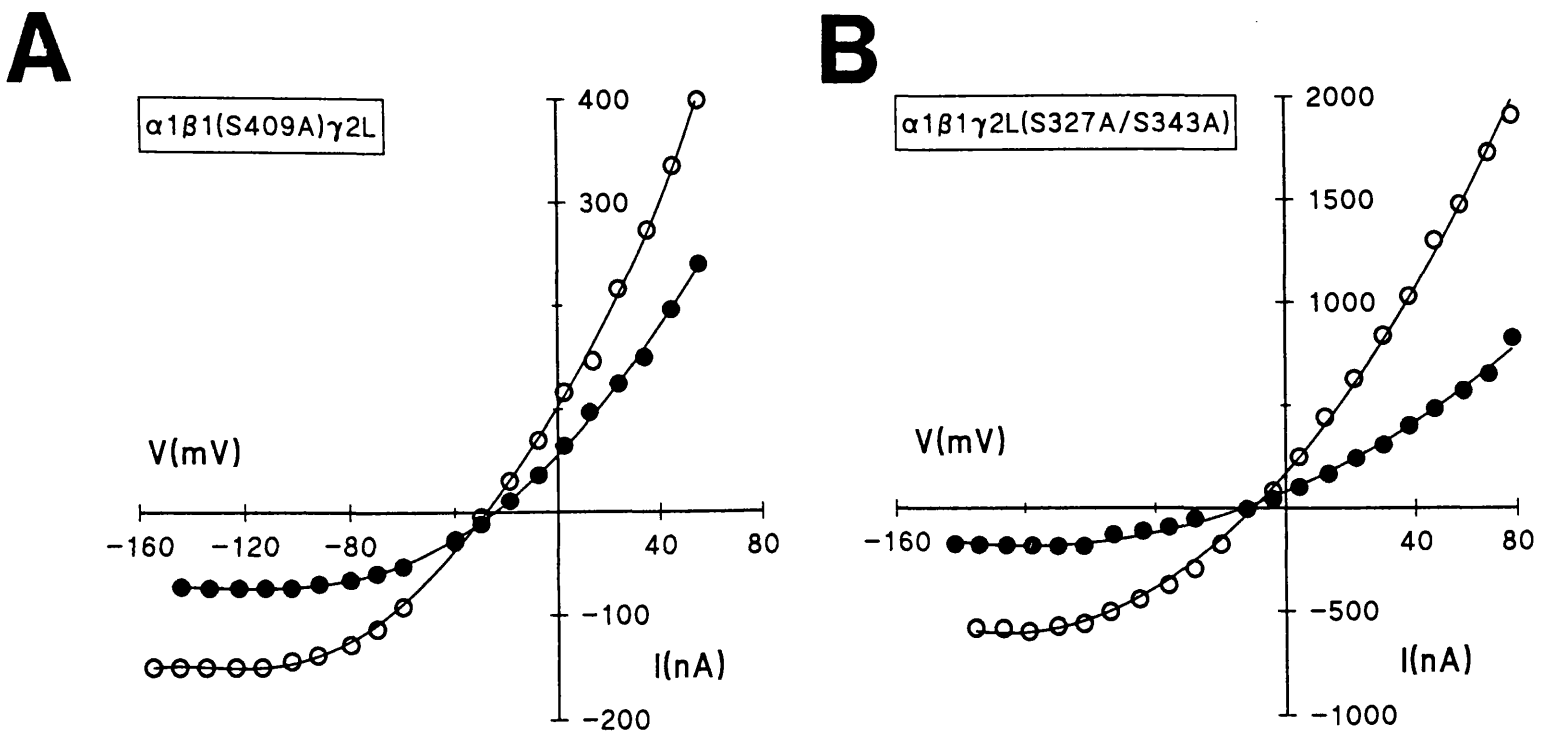

Figure 6.7. Current-voltage (I-V) relationships for GABA recorded from oocytes expressing $GABA_A$ receptors comprising selected mutations in the β1 and γ2L subunits. The effect of mutating S409 in β1 (A) or S327/S343 in γ2L was measured in the absence (open symbols) and presence (closed symbols) of 250 nM PMA.

Table 6.1. Analysis of the equilibrium concentration response curves for GABA in *Xenopus laevis* oocytes injected with $GABA_A$ receptor cDNAs. The EC_{50} and Hill coefficient (n) data were determined from fitting the logistic model to the normalised curves (see methods) with all values mean ± s.e.m. The rectification ratio G_R was calculated from the current-voltage relationships in Figs 6.5 and 6.7 using the chord conductances at +40 and -100 mV ($G_R = G_{+40} / G_{-100}$) in the absence and presence of PMA. The significance of the PMA treatment on the EC_{50} and Hill coefficient values was determined using Instat (version 2).

Table 6.1

Subunit Composition	EC_{50} (μM)		n		G_R (G^{+40}/G^{-100})	
	Control	+ PMA	Control	+ PMA	Control	+ PMA
α1β1	5.88±0.6	*4.27±0.2	0.91±0.07	*1.05±0.05	1.35	1.43
α1β1γ2S	10.03±0.21	*13.01±0.41	1.30±0.03	1.32±0.04	2.11	2.34
α1β1γ2L	10.20±0.47	9.43±0.47	1.22±0.06	*1.41±0.08	1.41	1.40
α1β1(S409A)	8.30±0.77	7.40±0.37	0.77±0.04	0.83±0.03	1.96	2.08
α1β1(S409A)γ2S(S327A)	10.06±0.38	10.65±0.45	1.07±0.04	1.10±0.04	2.20	2.28
α1β1(S409A)γ2L(S327A/S343A)	9.73±0.35	9.75±0.35	1.24±0.05	1.20±0.04	2.55	2.63
α1β1γ2L(S327A/S343A)	10.13±0.34	9.74±0.65	1.22±0.04	*1.04±0.06	2.24	2.58
α1β1(S409A)γ2L	9.58±0.60	8.78±1.07	1.00±0.05	0.87±0.07	2.23	2.87
α1β1(S409A)γ2L(S327A)	10.93±0.47	11.82±0.72	1.29±0.06	1.34±0.09	ND	ND
α1β1(S409A)γ2L(S343A)	10.46±0.39	*14.14±0.45	1.35±0.06	*1.71±0.07	ND	ND

(* represents a significant change from control $P < 0.05$)

CHAPTER SEVEN

GENERAL DISCUSSION

GENERAL DISCUSSION

In the present study, the *Xenopus laevis* oocyte provided a useful model cell in which recombinant $GABA_A$ receptors were transiently expressed following microinjection of cRNAs or cDNAs encoding a variety of $GABA_A$ receptor subunits. The data presented provides a basis for comparing the functional properties of $GABA_A$ receptors consisting of a variety of distinct subunit combinations. The actual subunit stoichiometry of the functional channels assembled and expressed in the *Xenopus* oocyte is unknown. This is also the position regarding 'native' $GABA_A$ receptors expressed in neurones. Therefore the possibility that some subunits may affect receptor assembly or processing without actually becoming part of the structure cannot be ruled out. However, this study has revealed that many subunit combinations possess a unique pharmacological signature. Therefore, the most likely explanation for these results is that subunit structure determines, at least in part, the functional characteristics of the $GABA_A$ receptor.

HETEROGENEITY OF $GABA_A$ RECEPTORS

Theoretically there is an immense number of possible ways to build distinct $GABA_A$ receptors based on the number of subunits and their isoforms. It is probable that only a small percentage of this potential variability manifests itself in native $GABA_A$ receptors (Wisden and Seeburg, 1992; Angelotti *et al.*, 1993). The present results suggest that assembly of $GABA_A$ receptors from constituent subunits does not proceed along a random pathway, but that certain subunit assemblies are distinctly preferred. The structural heterogeneity of the $GABA_A$ receptor has turned out to be of paramount importance since the functional properties depends directly on the distinct subunit combinations (Sigel *et al.*, 1990; Verdoorn *et al.*, 1990).

There is much evidence indicating considerable regional differences in the distribution of $GABA_A$ receptor subunits in the mammalian brain and the

possibility exists that heterogenous populations of $GABA_A$ receptors may be expressed in individual neurones or glial cells (Wisden *et al.*, 1988; Olsen and Tobin, 1990). Further complexity arises due to changes in subunit expression during development (Laurie et al., 1992; Poulter *et al.*, 1993). Interestingly, the δ subunit was found to be associated with the α1, α3, β2/3 and γ2S subunits using immunoaffinity chromatography (Mertens *et al.*, 1993). Therefore, this suggests that both the γ2S and δ subunits can co-localise within $GABA_A$ receptors. The functional role of the δ subunit has previously remained unknown. Therefore, the knowledge of the co-expression of δ with other subunits from the $GABA_A$ receptor complex provoked the investigation of the function of this novel subunit.

FUNCTIONAL PROPERTIES OF β, γ AND δ SUBUNITS

The presence of β1 subunits was required for the functional expression of heteromeric receptors with α1γ2S subunits not forming functional $GABA_A$ receptors. Therefore the β1 subunit may well be an essential structural component of the $GABA_A$ receptor. Expression of homomeric murine β1 subunits revealed channels that were not gated by GABA but were inhibited by picrotoxin and zinc. Interestingly, such picrotoxin responses have also been observed for rat α1β1γ2 heteromeric $GABA_A$ receptors expressed in *Xenopus* oocytes (Malherbe *et al.*, 1990b), although these responses only amounted to less than 0.5% of the maximum current obtained (Malherbe *et al.*, 1990b). This could indicate that a minor fraction of channels from heteromeric $GABA_A$ receptors are open in the absence of added GABA or that these open channels could be representative of the expression of a small amount of homomeric β1 $GABA_A$ receptors. It is clear that the combination of β1 with both α1 and γ2 subunits virtually abolished the open channel observed with the homomeric β1 subunit. Therefore, it is probable that heteromeric $GABA_A$ receptors adopt more stable closed channel conformations compared to the homomeric β1 subunit. Interestingly, spontaneous openings of $GABA_A$ chloride channels

have been shown to occur in neurones (Jackson *et al.*, 1982). A GABA binding site was however present on bovine β1 subunits indicating the possibility that β1 subunits could have important implications for the formation of GABA binding domains in heteromeric $GABA_A$ receptors. Furthermore, a recent study indicated that the $GABA_A$ receptor required two domains present in the β-subunit for activation by GABA (Amin and Weiss, 1993). Therefore microinjection of α1γ2S subunits could have lead to the formation of $GABA_A$ receptors but without the presence of the β1 subunit there may not have been a GABA binding domain. Another possibility is that the β1 subunit could be important for transporting the protein subunits to the membrane of the cell.

Unlike the β1 subunit, the γ2 subunit was not necessary for the expression of functional $GABA_A$ receptors. However, the addition of γ2 subunits conferred a benzodiazepine sensitivity to α1β1 $GABA_A$ receptors (Pritchett *et al.*, 1989; cf Malherbe *et al.*, 1990a). Furthermore, the ability of zinc to antagonise the GABA response on α1β1 receptors was considerably diminished by the addition of a γ2 subunit. Previous work on lobster muscle fibres revealed that lowering external pH antagonised the zinc blockade of GABA responses suggesting that H^+ and zinc could also bind to the same site, possibly a histidine residue as indicated by pH titration of the GABA-evoked conductance (Smart and Constanti, 1982). Interestingly, there appears to be a high degree of homology between some vertebrate and invertebrate subunits which was exemplified by coexpression studies where molluscan β subunits were capable of replacing mammalian β subunits forming chimeric GABA-gated ion channels with mammalian α subunits (Harvey *et al.*, 1991; Darlison, 1992). Therefore, a logical extension of the lobster muscle study was to investigate the effect of pH on recombinant $GABA_A$ receptors and establish whether H^+ and zinc could bind to the same site in these mammalian receptors. Interestingly, each receptor construct that was studied had a unique pH sensitivity profile. Moreover, the δ subunit appeared to play a pivotal role in defining the pH sensitivity of $GABA_A$ receptors. Previous

studies have revealed that the $GABA_A$ antagonistic action of zinc is non-competitive (Smart and Constanti, 1982; Smart and Constanti, 1990; Legendre and Westbrook, 1991). Intriguingly, in dorsal root ganglion cells of the bullfrog, *Rana catesbeana*, the GABA-induced response was inhibited by zinc in a *competitive* manner (Akaike *et al.*, 1987; Yakushiji *et al.*, 1987). The present study revealed for the first time that the zinc inhibition of GABA responses was competitive for $\alpha1\beta1\delta$ $GABA_A$ receptors. Moreover, as for the invertebrate GABA receptor, H^+ and zinc appeared to compete for a binding site on both $\alpha1\beta1$ and $\alpha1\beta1\delta$ recombinant mammalian $GABA_A$ receptors. Furthermore, for $\alpha1\beta1\gamma2S$ $GABA_A$ receptors, the common binding site for zinc and H^+ was absent rendering this receptor virtually insensitive to zinc blockade and external pH changes.

Neurones and glial cells are likely to perform different posttranslational processing on their respective $GABA_A$ receptors, presumably affecting receptor function and pharmacology. Therefore, for one subunit composition the appearance of receptors with different properties could be possible. The best studied posttranslational modification of $GABA_A$ receptors is phosphorylation, which is thought to be involved in dynamic regulation of function (Huganir and Greengard, 1990; Leidenheimer *et al.*, 1991; Levitan, 1994). Both β and $\gamma2$ subunits contain potential consensus sequences for phosphorylation by PKC, PKA and protein tyrosine kinases in the putative large intracellular loops between transmembrane domains M3 and M4 (Swope *et al.*, 1992). The present study identified the functional effect of PKC-induced phosphorylation to be a negative modulation of the GABA response. Each potential phosphorylation site, S409 in $\beta1$, S327 in $\gamma2S$ and S327/S343 in $\gamma2L$, was shown to exert functional effects when phosphorylated individually. The extent of PKC-induced phosphorylation on the $GABA_A$ receptor function was also clearly dependent on the number of consensus sites present and therefore on the receptor subunit composition. The modulatory role of phosphorylation on the $GABA_A$ receptor function could therefore vary, (1) in different regions

of the CNS where the expression of $GABA_A$ receptor subunits also varies (Malherbe *et al.*, 1990b), and (2) with different subunit expression during development (Laurie *et al.*, 1992; Poulter *et al.*, 1993).

FUTURE DIRECTIONS

Functional studies are necessary for the provision of information concerning the extent and possible significance of $GABA_A$ receptor subunit diversity. The pharmacological and physiological properties of recombinant $GABA_A$ receptors of various subunits expressed in *Xenopus* oocytes and other recombinant systems can be compared to the properties of $GABA_A$ receptors in brain slices (Edwards *et al.*, 1989). These studies performed in parallel will greatly facilitate classification of native $GABA_A$ receptors. Furthermore, both functional studies and biochemical techniques and/or immunocytochemistry will be combined and ultimately lead to the structure of native $GABA_A$ receptors in different regions of the CNS.

As more information becomes available on the functional properties of individual $GABA_A$ subunits located within the receptor the possibility arises that new subunit-selective drugs will be discovered for both clinical and experimental pharmacological use. Drugs currently in use, such as barbiturates and benzodiazepines, will then hopefully be superceeded with newer more selective compounds with more discrete effects on behaviour. The recombinant systems will be invaluable tools for the screening of such compounds. Furthermore, by utilising the plethora of techniques currently available including the use of pharmacological tools to the application and analysis of *in vitro* mutagenesis, a better understanding of the structural domains for drug binding on individual subunits will be obtained permitting custom design of more selective compounds. These compounds could then be put to good use in defining subunit distribution and function in the CNS.

The $GABA_A$ receptor quest has now entered a new phase. With the introduction of molecular biological techniques there has been an explosion in the number of subunit isoforms, with the function of many such polypeptides waiting to be studied. Such techniques have produced a working model for the structure of the $GABA_A$ receptor. The way forward now is to consolidate and advance on all the available information from both biochemical and functional studies in order to determine the exact *in vivo* composition of $GABA_A$ receptors found in all areas of the CNS.

In summary, this study has provided evidence that individual subunits within the $GABA_A$ receptor have distinct functional role(s). For the very first time a novel pharmacology for δ subunit containing receptors was revealed. Furthermore, two novel sites on the $GABA_A$ receptor have been uncovered which can modulate receptor function. These sites are sensitive to H^+ or PKC-induced phosphorylation and may be significant in affecting the pharmacological and physiological profile of the $GABA_A$ receptor.

ACKNOWLEDGEMENTS

I would like to express my gratitude to my supervisor, Dr. Trevor G. Smart, for his unstinting guidance and encouragement throughout my PhD. In addition, I am indebted to him for the detailed reading of the manuscript of this thesis.

I wish to thank Dr. Steve Moss at the Institute for Molecular Cell Biology, University College, London for the provision of all murine cRNAs and cDNAs and all the work on producing the mutant polypeptide sequences. In addition, I would like to thank Professor Eric Barnard at the Molecular Neurobiology Unit, Royal Free Hospital School of Medicine, London and Dr. Alan Bateson at the Department of Pharmacology, University of Alberta, Canada for their kind provision of bovine cRNAs and cDNAs.

I am grateful to the Medical Research Council for financial support and Professor Norman Bowery for allowing me to work in his department.

This study would not have been achieved without the help of the technical expertise in the Department: Chris Courtice (electronics), Dave Tulett (workshop), Steve Coppard, Donna Howell and Dave Zeraschi (Animal House), Derek King, Annie Cavanagh and Dave McCarthy (photography), Dave Khan (teaching technician), Graham Withers (Laboratory Superintendent) and Angela Tregaskes (secretary).

I am particularly grateful for the help and friendship of Dr. Xinmin Xie, Dr. Daniel Eugene, Dr. Mike Poulter, Dave Langley, Paul Britton, Renzo Carletti, Dr. Vincenzo Libri, Munaf Alam, Dr. Noel Harris, Dr. Brian Pierce, Dr. Mike Starr, Dr. Andy Constanti and Dr. Miroslav Cik; a special thanks to Jacqui Miller. I would also like to thank Professor Mike Simmonds for his helpful advice and discussion.

I owe very much to Marc Krishek, my husband, for all his love, encouragement and understanding. I would also like to say a special thanks to my parents, Hilary and Keith Barnett and my brother Grant for their wholehearted support at all times.

Without the help of all these kind people, and others too numerous to mention, this thesis would never have been completed.

REFERENCES

Adrian R.H. (1956) The effect of internal and external potassium concentration on the membrane potential of frog muscle. *J. Physiol.*, **133**, 631-658.

Agin D.P. (1969) Electrochemical properties of glass microelectrodes in *Glass Microelectrodes*, (Lavellee M., Schanne O.F. and Herbert N.C. eds), pp 62-75, John Wiley & Sons, New York.

Agin D.P. and Holtzmann D. (1966) Glass microelectrodes: origin and elimination of tip potentials. *Nature*, **211**, 1194-1195.

Akaike N., Inoue M. and Krishtal O.A. (1986) "Concentration-clamp" study of γ-aminobutyric-acid-induced chloride current kinetics in frog sensory neurones. *J. Physiol.*, **379**, 171-185.

Akaike N., Yakushiji T., Tokutomi N. and Carpenter D.O. (1987) Multiple mechanisms of antagonism of γ-aminobutyric acid (GABA) responses. *Cell. Mol. Neurobiol.*, **7**, 97-103.

Allan R.D., Evans R.H. and Johnston G.A.R. (1980) γ-Aminobutyric acid agonists: an *in vivo* comparison between depression of spinal synaptic activity and depolarisation of spinal root fibres in the rat. *Br. J. Pharmacol.*, **70**, 609-615.

Amin J., Dickerson I.M. and Weiss D.S. (1994) The agonist binding site of the γ-aminobutyric acid type A channel is not formed by the extracellular cysteine loop. *Mol. Pharmacol.*, **45**, 317-323.

Amin J. and Weiss D.S. (1993) $GABA_A$ receptor needs two homologous domains of the β-subunit for activation by GABA but not by pentobarbital. *Nature*, **366**, 565-569.

Angelotti, T.P. and Macdonald, R.L. (1993) Assembly of $GABA_A$ receptor subunits: α1β1 and α1β1γ2S subunits produce simple unique ion channel with dissimilar single-channel properties. *J. Neurosci.*, **13**, 1429-1440.

Angelotti, T., Uhler, M.D. and Macdonald, R. (1993) Assembly of $GABA_A$ receptor subunits: Analysis of transient single-cell expression utilizing a fluorescent substrate/marker gene technique. *J. Neurosci.*, **13**, 1418-1428.

Araki T., Kiyama H. and Tohyama M. (1992) $GABA_A$ receptor subunit messenger RNAs show differential expression during cortical development in the rat brain. *Neuroscience*, **51**, 583-591.

Arunlakshana O. and Schild H.O. (1959) Some quantitative uses of drug antagonists. *Br. J. Pharmacol. Chemother.*, **14**, 48-58.

Balestrino M. and Somjen G.G. (1988) Concentration of carbon dioxide, interstitial pH and synaptic transmission in hippocampal formation of the rat. *J. Physiol.*,**396**, 247-266.

Barish M.E. (1983) A transient calcium-dependent chloride current in the immature *Xenopus* oocyte. *J. Physiol. (Lond.)*, **342**, 309-325.

Barnard E.A., Darlison M.G. and Seeburg P. (1987) Molecular biology of the $GABA_A$ receptor: the receptor/channel superfamily. *Trends Neurosci.*, **10**, 502-509.

Barnard E.A., Miledi R., and Sumikawa K. (1982) Translation of exogenous messenger RNA coding for nicotinic acetylcholine receptors produces functional receptors in *Xenopus* oocytes. *Proc. Roy. Soc. Lond. B*, **215**, 241-246.

Bassford P., Beckwith J., Bermann M., Brickman E., Casadaban M., Guarente L., Saint-Girons I., Sarthy A., Schwartz M., Shuman H. and Silhavy T. (1978) Genetic fusions of the *lac* operon: a new approach to the study of biological processes, in *The Operon*, (Miller J.H. and Reznikoff W.S. eds), pp 245-262, Cold Spring Harbour Laboratory, Cold Spring Harbour, New York.

Bateson A.N., Harvey R.J., Bloks C.C.M. and Darlison M.G. (1990) Sequence of the chicken $GABA_A$ receptor β3-subunit cDNA. *Nucleic Acids Res.*, **18**, 5557.

Bateson A.N., Harvey R.J., Wisden W., Glencorse T.A., Hicks A.A., Hunt S.P., Barnard E.A. and Darlison M.G. (1991a) The chicken $GABA_A$ receptor α1 subunit: cDNA sequence and localisation of the corresponding mRNA. *Mol. Brain Res.*, **9**, 333-339.

Bateson A.N., Lasham A., and Darlison M.G. (1991b) γ-Aminobutyric $acid_A$ receptor heterogeneity is increased by alternative splicing of a novel β-subunit gene transcript. J. Neurochem., **56**, 1437-1440.

Belin M.F., Nanopoulos D., Didier M., Aguera M., Steinbusch H., Verhofstad A., Maitre M. and Pujol J.F. (1983) Immunohistochemical evidence for the presence of γ-aminobutyric acid and serotonin in one nerve cell. A study on the raphe nuclei of the rat using antibodies to glutamate decarboxylase and serotonin. *Brain Res.*, **275**, 329-339.

Benke D., Mertens S., Trzeciak A., Gillessen D. and Mohler H. (1991) Identification and immunohistochemical mapping of $GABA_A$ receptor subtypes containing the δ-subunit in rat brain. *FEBS Letts.*, **283**, 145-149.

Bertrand D., Cooper E., Valera S., Runger D. and Ballivet M. (1991) Electrophysiology of neuronal nicotinic acetylcholine receptors expressed in *Xenopus* oocytes following nuclear injection of genes or cDNAs. *Methods in Neurosci.,* **4**, 174-193.

Blair, L.A.C., Levitan, E.S., Marshall, J., Dionne, V.E. and Barnard, E.A. (1988) Single subunits of the $GABA_A$ receptor form ion channels with properties of the native receptor. *Science*, **242**, 577-579.

Bliss T.V.P. and Collingridge G.L. (1993) A synaptic model of memory: long-term potentiation in the hippocampus. *Nature.*, **361**, 31-39.

Bormann J. (1988) Electrophysiology of $GABA_A$ and $GABA_B$ receptor subtypes. *Trends Neurosci.*, **11**, 112-116.

Bormann J. and Clapham D.E. (1985) γ-Aminobutyric acid receptors in adrenal chromaffin cells: a patch clamp study. *Proc. Natl. Acad. Sci. USA*, **82**, 2168-2172.

Bormann J., Hamill O.P. and Sakmann B. (1987) Mechanism of anion permeation through channels gated by glycine and γ-aminobutyric acid in mouse cultured spinal neurones. *J. Physiol.*, **385**, 243-286.

Boulter J., Connolly J., Deneris E., Goldman D., Heinemann S. and Patrick J. (1987) Functional expression of two neuronal nicotinic acetylcholine receptors from cDNA clones identifies a gene family. *Proc. Natl. Acad. Sci. USA*, **84**, 7763-7767.

Bovolin P., Santi M.-R., Memo M., Costa E. and Grayson D.R. (1992) Distinct developmental patterns of expression of rat α1, α5, γ2S, and γ2L γ-aminobutyric $acid_A$ receptor subunit mRNAs in vivo and in vitro. *J. Neurochem.*, **59**, 62-72.

Bowery N.G. (1993) $GABA_B$ receptor pharmacology. *Annu. Rev. Pharmacol. Toxicol.*, **33**, 109-147.

Bowery N.G., Collins J.F., Hudson A.L. and Neal M.J. (1978) Isoguvacine, isonipecotic acid, muscimol and N-methyl isoguvacine on the GABA receptor in rat sympathetic ganglia. *Experimentia.*, **34**, 1193-1195.

Bowie D. and Smart T.G. (1993) Interplay between expressed non-NMDA receptors and endogenous calcium-activated chloride currents in *Xenopus laevis* oocytes. *Neurosci. Letts.*, **151**, 4-8.

Braestrup C. and Nielsen M. (1981) [^{3}H]Propyl β-carboline-3-carboxylate as a selective radioligand for the BZ_1 benzodiazepine receptor subclass. *J. Neurochem.*, **37**, 333-341.

Browning, M.D., Bureau, M., Dudek, E.M. and Olsen, R.W. (1990) Protein kinase C and cAMP-dependent protein kinase phosphorylate the β subunit of the purified γ-aminobutyric acid A receptor. *Proc. Natl. Acad. Sci. USA,* **87**, 1315-1318.

Buller A.L. and White M.M. (1989) Functional acetylcholine receptors expressed in *Xenopus* oocytes after injection of *Torpedo* β, γ, and δ subunit RNAs are a consequence of endogenous oocyte gene expression. *Mol. Pharmacol.*, **37**, 423-428.

Bureau M. and Olsen R.W. (1990) Multiple distinct subunits of the γ-aminobutyric acid-A receptor protein show different ligand-binding affinities. *Mol. Pharmacol.*, **37**, 497-502.

Burmeister M. and Soreq H. (1984) Production and analysis of radioactivity labelled translation products in microinjected *Xenopus* oocytes, in *Molecular biology approach to neurosciences,* (Soreq H. ed), pp 195-203, Weily, London.

Burt, D.R. and Kamatchi, G.L. (1991) $GABA_A$ receptor subtypes: from pharmacology to molecular biology. *FASEB J.*, **5**, 2916-2923.

Casalotti S.O., Stephenson F.A. and Barnard E.A. (1986) Separate subunits for agonist and benzodiazepine binding in the γ-aminobutyric $acid_A$ receptor oligomer. *J. Biol. Chem.*, **261**, 15013-15016.

Change L.R. and Barnard E.A. (1982) The benzodiazepine/GABA receptor complex: molecular size in brain synaptic membranes and in solution. *J. Neurochem.*, **39**, 1507-1518.

Chen J.C. and Chesler M. (1990) A bicarbonate-dependent increase in extracellular pH mediated by GABA-A receptors in turtle cerebellum. *Neurosci. Lett.*, **116**, 130-135.

Chen J.C.T. and Chesler M. (1991) Extracellular alkalinization evoked by GABA and its relationship to activity-dependent pH shifts in turtle cerebellum. *J. Physiol.*, **442**, 431-446.

Chen J.C.T and Chesler M. (1992a) Modulation of extracellular pH by glutamate and GABA in rat hippocampal slices. *J. Neurophysiol.*, **67**, 29-36.

Chen J.C.T and Chesler M. (1992b) Extracellular alkaline shifts in rat hippocampal slice are mediated by NMDA and non-NMDA receptors. *J. Neurophysiol.*, **68**, 342-344.

Chesler M. (1990) The regulation and modulation of pH in the nervous system. *Prog. Neurobiol.*, **34**, 401-427.

Chesler M. and Chan C.Y. (1988) Stimulus-induced extracellular pH transients in the *in vivo* turtle cerebellum. *Neuroscience.*, **27**, 941-948.

Chesler M. and Chen J.C.T. (1992) Alkaline extracellular pH shifts generated by two transmitter-dependent mechanisms. *Can J. Physiol.*, **70**, S286-S292.

Chesler M. and Rice M.E. (1991) Extracellular alkaline-acid pH shifts evoked by iontophoresis of glutamate and aspartate in turtle cerebellum. *Neuroscience.*, **41**, 257-267.

Chow P. and Mathers D. (1986) Convulsant doses of penicillin shorten the lifetime of GABA-induced channels in cultured central neurones. *Br. J. Pharmacol.*, **88**, 541-547.

Colley P.A. and Routtenberg A. (1993) Long-term potentiation as synaptic dialogue. *Brain Res. Rev.*, **18**, 115-122.

Colman A. (1984) Translation of eukaryotic messenger RNA in *Xenopus* oocytes, in *Transcription and translation a practical approach*, (Hames B.D. and Higgins S.J. eds.), pp. 271-302, IRL Press, Oxford.

Colman A. and Drummond D. (1986) The stability and movement of mRNA in *Xenopus* oocytes and embryos. *J. Embryol.Exp. Morphol.*, **97** suppl, 197-209.

Contreras R., Cheroutre H. and Fiers W. (1981) A simple apparatus for injection of nanolitre quantities into *Xenopus* oocytes. *Anal. Biochem.*, **113**, 185-187.

Cutting G.R., Lu L., O'Hara B., Kasch L.M., Donovan D., Shimada S., Antonarakis S.E., Guggino W.B., Uhl G.R. and Kazazian H.H. (1991) Cloning of the GABA ρ1 cDNA: a novel GABA subunit highly expressed in the retina. *Proc. Natl. Acad. Sci. USA*, **88**, 2673-2677.

Darlison M.G. (1992) Invertebrate GABA and glutamate receptors: molecular biology reveals predictable structures but some unusual pharmacologies. *Trends Neurosci.*, **15**, 469-474.

Dascal N. (1987) The use of *Xenopus* oocytes for the study of ion-channels. *CRC Crit. Rev. Biochem.*, **22**, 317-387.

Dietzel I., Heinemann U., Hofmeier G. and Lux H.D. (1982) Stimulus-induced changes in extracellular Na^+ and Cl^- concentration in relation to changes in the size of the extracellular space. *Exp. Brain Res.*, **46**, 73-84.

Dingledine R., Boland L.M., Chamberlin N.L., Kawasaki K., Kleckner N.W., Traynelis S.F. and Verdoorn T.A. (1988) Amino acid receptors and uptake systems in the mammalian central nervous system. *CRC Critical Rev. Neurobiol.*, **4**, 1-96.

Doble A. and Martin I.L. (1992) Multiple benzodiazepine receptors: no reason for anxiety. *Trend Pharmacol. Sci.*, **13**, 76-81.

Draguhn A., Verdoorn T.A., Ewert M., Seeburg P,H. and Sakmann B. (1990) Functional and molecular distinction between recombinant rat $GABA_A$ receptor subtypes by Zn^{2+}. *Neuron*, **5**, 781-788.

Dumont J.N. (1972) Oogenesis in *Xenopus* laevis (Daudin), 1. Stages of oocyte development in laboratory maintained animals. *J. Morph.*, **136**, 153-180.

Dumont J.N. and Brummett A.R. (1978) Oogenesis in *Xenopus laevis* (Daudin). Relationships between developing oocytes and their investing follicular tissues. *J. Morphol.*, **155**, 73-98.

Edwards F.A., Konnerth A., Sakmann B. and Takahashi T. (1989) A thin slice preparation for patch clamp recordings from neurones of the mammalian central nervous system. *Pflugers Arch.*, **414**, 600-612.

Everitt B., Meister m., Hokfelt T., Melander T., Terenius L., Rokaeus A., Theodorsson-Norheim E., Dockray G., Edwardson J., Cuello A.C., Elde R., Goldstein M., Hemmings H., Ouimet C., Walaas I., Greengard P., Vale W., Weber E. and Wu J.-Y. (1986) The hypothalamic arcuate nucleus-median eminence complex: immunohistochemistry of transmitters, peptides and DARPP-32 with special reference to coexistence in dopamine neurones. *Brain Res. Rev.*, **11**, 97-155.

Finkel A.S. and Gage P.W. (1985) Conventional voltage clamping with two intracellular microelectrodes in *Voltage and patch clamping with microelectrodes*, (Smith T.G., Lecar H., Redman S.J. and Gage P.W. eds), Chapter 4, American Physiological Society, Bethesda, Maryland.

Ffrench-Constant R.H., Rocheleau T.A., Steichen J.C. and Chalmers A.E. (1993) A point mutation in a *Drosophila* GABA receptor confers insecticide resistance. *Nature*, **363**, 449-451.

Fuchs K., Adamiker D. and Sieghart W. (1990) Identification of α2- and α3-subunits of the $GABA_A$-benzodiazepine receptor complex purified from brains of young rats. *FEBS Letts.*, **261**, 52-54.

Fuchs K., Mohler H. and Sieghart W. (1988) Various proteins from rat brain, specifically and irreversibly labeled by [^{3}H]flunitrazepam, are distinct α-subunits of the GABA-benzodiazepine receptor complex. *Neurosci. Letts.*, **90**, 314-319.

Fuchs K. and Sieghart W. (1989) Evidence for the existence of several α- and β-subunits of the GABA/benzodiazepine receptor complex from rat brain. *Neurosci. Letts.*, **97**, 329-333.

Galzi J.-L., Devillers-Thiery A., Hussy N., Bertrand S., Changeux J.-P. and Bertrand D. (1992) Mutations in the channel domain of a neuronal nicotinic receptor convert ion selectivity from cationic to anionic. *Nature*, **359**, 500-505.

Giffard R.G., Monyer H., Christine C.W. and Choi D.W. (1990) Acidosis reduces NMDA receptor activation, glutamate neurotoxicity, and oxygen-glucose deprivation neuronal injury in cortical cultures. *Brain Res.*, **506**, 339-342.

Glencorse T. A., Bateson A.N. and Darlison M. G. (1990) Sequence of the chicken $GABA_A$ receptor γ2-subunit cDNA. *Nucleic Acids Res.*, **18**, 7157.

Glencorse, T.A., Bateson, A.N. and Darlison, M.G. (1992) Differential localization of two alternatively spliced $GABA_A$ receptor γ2-subunit mRNAs in the chick brain. *Eur. J. Neurosci.*, **4**, 271-277.

Grenningloh G., Rienitz A., Schmitt B., Methfessel C., Zensen M., Beyreuther K., Gundelfinger D.E. and Betz H. (1987) The strychnine-binding subunit of the glycine receptor shows homology with nicotinic acetylcholine receptors. *Nature*, **328**, 215-220.

Griffith J.K., Cordisco B.R., Lin C.-W. and LaManna J.C. (1992) Distribution of intracellular pH in rat brain cortex after global ischemia as measured by color film histophotometry of neutral red. *Brian Res.*, **573**, 1-7.

Gruol D.L., Barker J.L., Huang L.-Y.M., MacDonald F. and Smith T.G. (1980) Hydrogen ions have multiple effects on the excitability of cultured mammalian neurones. *Brain Res.*, **183**, 247-252.

Gundersen C.B., Miledi R., and Parker I. (1984) Messenger RNA from human brain induces drug- and voltage-operated channels in *Xenopus* oocytes. *Nature*, **308**, 421-424.

Gurdon J.B. (1974) *The control of gene expression in animal development.*, Harvard Univeristy Press, Cambridge, MA.

Gurdon J.B., Lane C.D., Woodland H.R., and Marbaix G. (1971) Use of frog eggs and oocytes for the study of messenger RNA and its translation in living cells. *Nature* (Lond.), **233**, 177-182.

Gyenes, M., Farrant, M. and Farb, D.H. (1988) "Run-down" of γ-aminobutyric $acid_A$ receptor function during whole-cell recording: A possible role for phosphorylation. *Mol. Pharmac.*, **34**, 719-723.

Hadingham K.L., Harkness P.C., McKernan M.R., Quirk K., Le Bourdelles B., Horne A.L., Kemp J.A., Barnard E.A., Ragan C.I. and Whiting P.J. (1992) Stable expression of mammalian type A γ-aminobutyric acid receptors in mouse cells: demonstration of functional assembly of benzodiazepine-responsive sites. *Proc. Natl. Acad. Sci. USA*, **89**, 6378-6382.

Hales T.G. and Lambert J.J. (1991) The actions of propofol on the inhibitory amino acid receptors of bovine adrenomedullary chromaffin cells and rodent central neurones. *Br. J. Pharmacol.*, **104**, 619-628.

Hales T.G. and Lambert J.J. (1992) Modulation of $GABA_A$ and glycine receptors by chlormethiazole. *Eur. J. Pharmacol.*, **210**, 239-246.

Halliwell J.V. and Whitaker M.J. (1987) Using microelectrodes in *Microelectrode Techniques: the Plymouth Workshop Handbook*, (Standen N.B., Gray P.T.A. and Whitaker M.J. eds.), Chapter 1, The Company of Biologists Limited, Cambridge.

Haring P., Stahli C., Schoch P., Takacs B., Staehelin T. and Mohler H. (1985) Monoclonal antibodies reveal structural homogeneity of gamma-aminobutyric acid/benzodiazepine receptors in different brain areas. *Proc. Natl. Acad. Sci. USA*, **82**, 4837-4841.

Harrison N.L. and Simmonds M.A. (1983) Two distinct interactions of barbiturates and chlormethiazole with the $GABA_A$ receptor complex in rat cuneate nucleus *in vitro*. *Br. J. Pharmacol.*, **80**, 387-394.

Harvey R.J., Chinchetru M.A. and Darlison M.G. (1994) Alternative splicing of a 51-nucleotide exon that encodes a putative protein kinase C phosphorylation site generates two forms of the chicken γ-aminobutyric $acid_A$ receptor β2 subunit. *J. Neurochem.*, **62**, 10-16.

Harvey R.J., Kim H.-C. and Darlison M.G. (1993) Molecular cloning reveals the existence of a fourth γ subunit of the vertebrate brain $GABA_A$ receptor. *FEBS Letts.*, **331**, 211-216.

Harvey R.J., Vreugdenhil E., Zaman S.H., Bhandal N.S., Usherwood P.N.R., Barnard E.A. and Darlison M.G. (1991) Sequence of a functional invertebrate $GABA_A$ receptor subunit which can form a chimeric receptor with a vertebrate α subunit. *EMBO J.*, **10**, 3239-3245.

Hitchcock M.J.M., Ginns E.I. and Marcus-Sekura C.J. (1987) Microinjection into *Xenopus* oocytes, in *Methods in Enzymology.*, pp 276-288, Academic Press, San Diego.

Horne A.L., Hadingham K.L., Macaulay A.J., Whiting P. and Kemp J.A. (1992) The pharmacology of recombinant $GABA_A$ receptors containing bovine α1, β1, γ2L sub-units stably transfected into mouse fibroblast L-cells. *Br. J. Pharmacol.*, **107**, 732-737.

Horne A.L., Harkness P.C., Hadingham K.L., Whiting P. and Kemp J.A. (1993) The influence of the γ2L subunit on the modulation of responses to $GABA_A$ receptor activation. *Br. J. Pharmacol.*, **108**, 711-716.

Houamed K.M. (1988) Electrophysiological characterization of some ion channels synthesized following microinjection of brain-derived messenger ribonucleic acid in *Xenopus laevis* oocytes. PhD Thesis, pp 220-221, University of London.

Houamed K.M., Bilbe G., Smart T.G., Constanti A, Brown D.A., Barnard E.A., and Richards B.M. (1984) Expression of functional GABA, glycine and glutamate receptors in *Xenopus* oocytes injected with rat brain mRNA. *Nature*, **310**, 318-321.

House C. and Kemp B.E. (1987) Protein kinase C contains a pseudosubstrate prototope in its regulatory domain. *Science*, **238**, 1726-1728.

Huang K.-P. (1989) The mechanism of protein kinase C activation. *Trends Neurosci.*, **12**, 425-432.

Huganir R.L. and Greengard P. (1990) Regulation of neurotransmitter receptor desensitization by protein phosphorylation. *Neuron.*, **5**, 555-567.

Jackson M.B., Lecar H., Mathers D.A. and Barker J.L. (1982) Single channel currents activated by γ-aminobutyric acid, muscimol, and (-)-pentobarbital in cultured mouse spinal neurones. *J. Neurosci.*, **2**, 889-894.

Jarolimek W., Misgeld U. and Lux H.D. (1989) Activity dependent alkaline and acid transients in guinea pig hippocampal slices. *Brain Res.*, **505**, 225-232.

Jenkinson D. (1991) How we describe competitive antagonists: three questions of usage. *Trends Pharmacol. Sci.*, **12**, 53-54.

Jenkinson D. and Abbott A. (1990) Are molecular and electrophysiological data refining models of antagonism?. *Trends Pharmacol. Sci.*, **11**, 91-94.

Johnston G.A.R. (1986) Multiplicity of GABA receptors in *Benzodiazepine/GABA receptors and chloride channels. Receptor biochemistry and methodology* (Olsen R.W. and Venter J.C., eds), **5**, pp 57-71, Alan R. Liss, New York.

Johnston G.A.R., Kennedy S.M.E. and Lodge D. (1978) Muscimol uptake, release and binding in rat brain slices. *J. Neurochem.*, **31**, 1519-1523.

Jones S.W. (1990) Whole-cell and microelectrode voltage clamp in *Neuromethods, Neurophysiological techniques: basic methods and concepts*, (Boulton A.A., Baker G.B. and Vanderwolf C.H. eds), Humana Press, New Jersey, **14**, 143-192.

Kaila K., Paalasmaa P., Taira T. and Voipio J. (1992) pH transients due to monosynaptic activation of $GABA_A$ receptors in rat hippocampal slices. *Neuroreport.*, **3**, 105-108.

Kaila K., Saarikoski J. and Voipio J. (1990) Mechanism of action of GABA on intracellular pH and on surface pH in crayfish muscle fibres. *J. Physiol.*, **427**, 241-260.

Kaila K. and Voipio J. (1987) Postsynaptic fall in intracellular pH induced by GABA-activated bicarbonate conductance. *Nature*, **330**, 163-165.

Kaila K., Voipio J., Paalasmaa P., Pasternack M. and Deisz R.A. (1993) The role of bicarbonate in $GABA_A$ receptor-mediated IPSPs of rat neocortical neurones. *J. Physiol.*, **464**, 273-289.

Kaku D.A., Giffard R.G. and Choi D.W. (1993) Neuroprotective effects of glutamate antagonists and extracellular acidity. *Science*, **260**, 1516-1518.

Katayama N., Tokutomi N., Nabekura J. and Akaike N. (1992) Penicillin-induced triphasic modulation of $GABA_A$ receptor-operated chloride current in frog sensory neuron. *Brain Res.*, **595**, 249-255.

Keir W.J., Kozak C.A., Chakraborti A., Dietrich R.A. and Sikela J.M. (1991) The cDNA sequence and chromosomal localization of the murine $GABA_A$ α_1 receptor gene. *Genomics*, **9**, 390-395.

Kellenberger, S., Malherbe, P. and Sigel, E. (1992) Function of the $\alpha 1\beta 2\gamma 2S$ γ-aminobutyric acid type A receptor is modulated by protein kinase C via multiple phosphorylation sites. *J. Biol. Chem.*, **267**, 25660-25663.

Kemp J.A., Marshall G.R. and Woodruff G.N. (1986) Quantitative evaluation of the potencies of GABA-receptor agonists and antagonists using the rat hippocampal slice preparation. *Br. J. Pharmacol.*, **87**, 677-684.

Khrestchatisky M., MacLennan A.J., Chiang M.-Y., Xu W., Jackson M.B., Brecha N., Sternini C., Olsen R.W. and Tobin A.J. (1989) A novel α subunit in rat brain $GABA_A$ receptors. *Neurone*, **3**, 745-753.

Khrestchatisky M., MacLennan A.J., Tillakaratne N.J.K., Chiang M.-Y. and Tobin A. J. (1991) Sequence and regional distribution of the mRNA encoding the α2 polypeptide of rat γ-aminobutyric $acid_A$ receptors. *J. Neurochem.*, **56**, 1717-1722.

Kirkness, E.F., Bovenkerk, C.F., Ueda, T. and Turner, A.J. (1989) Phosphorylation of γ-aminobutyrate (GABA)/benzodiazepine receptors by cyclic AMP-dependent protein kinase. *Biochem J.*, **259**, 613-616.

Kofuji, P., Wang, J.B., Moss, S.J., Huganir, R.L. and Burt, R.D. (1991) Generation of two forms of the γ-aminobutyric $acid_A$ receptor γ2-subunit in mice by alternative splicing. *J. Neurochem.*, **56**, 713-715.

Korpi E.A., Kleingoor C., Kettenmann H. and Seeburg P.H. (1993) Benzodiazepine-induced motor impairment linked to point mutation in cerebellar $GABA_A$ receptor. *Nature*, **361**, 356-359.

Krafte D.S. and Lester H.A. (1989) Expression of functional sodium channels in stage II-III *Xenopus* oocytes. *J. Neurosci. Meth.*, **26**, 211-215.

Kraig R.P., Ferreira-Filho C.R. and Nicholson C. (1983) Alkaline and acid transients in cerebellar microenvironment. *J. Neurophysiol.*, **49**, 831-850.

Kressmann A., Clarkson S.G., Telford J.L. and Birnsteil M.L. (1977) Transcription of *Xenopus* $tDNA_1^{met}$ and sea urchin histone. DNA injected into the *Xenopus* oocyte nucleus. *Cold Spring Harbor Symp. Biol.*, **42**, 1077-1082.

Krishek B.J., Xie X., Blackstone C., Huganir R.L., Moss S.J. and Smart T.G. (1994) Regulation of $GABA_A$ receptor function by protein kinase C phosphorylation. *Neuron*, **12**, 1081-1095.

Krishtal O.A., Osipchuk Y.V., Shelest T.N. and Smirnoff S.V. (1987) Rapid extracellular pH transients related to synaptic transmission in rat hippocampal slices. *Brain Res.*, **436**, 352-356.

Landau E.M., Gavish B., Nachshen D.A. and Lotan I. (1981) pH dependence of the acetylcholine receptor channel. *J. Gen. Physiol.*, **77**, 647-666.

Lane C.D. (1983) The fate of genes, messengers, and proteins introduced into *Xenopus* oocytes, in *Current Topics in Developmental Biology*, Vol. **18**, pp. 89-116, Academic Press, New York.

Lasham A., Vreugdenhil E., Bateson A.N., Barnard E.A. and Darlison M.G. (1991) Conserved organisation of γ-aminobutyric acid$_A$ receptor genes: cloning and analysis of the chicken β4-subunit gene. *J. Neurochem.*, **57**, 352-355.

Laurie D.J., Wisden W. and Seeburg P.H. (1992) The distribution of thirteen GABA$_A$ receptor subunit mRNAs in the rat brain. III. Embryonic and postnatal development. *J. Neurosci.*, **12**, 4151-4172.

Leeb-Lundberg L.M.F. and Olsen R.W. (1983) Heterogeneity of benzodiazepine receptor interactions with GABA and barbiturate receptors. *Mol. Pharmacol.*, **23**, 315-325.

Legendre P. and Westbrook G.L. (1991) Noncompetitive inhibition of gamma-aminobutyric acidA channels by zinc. *Mol. Pharmacol.*, **39**, 267-274.

Leidenheimer, N.J., Browning, M.D. and Aldron Harris, R. (1991) GABA$_A$ receptor phosphorylation: multiple sites, actions and artifacts. *Trends in Pharmacol. Sci.*, **12**, 84-87.

Leidenheimer, N.J., McQuilkin, S.J., Hahner, L.D., Whiting, P. and Adron Harris, R. (1992) Activation of protein kinase C selectively inhibits the γ-aminobutyric acid$_A$ receptor: Role of desensitization. *Mol Pharmac.*, **41**, 1116-1123.

Leidenheimer, N.J., Whiting P.J. and Aldron Harris, R. (1993) Activation of calcium-phospholipid-dependent protein kinase enhances benzodiazepine and barbiturate potentiation of the GABA$_A$ receptor. *J. Neurochem.*, **60**, 1972-1975.

Levitan I.B. (1994) Modulation of ion channels by protein phosphorylation and dephosphorylation. *Annu. Rev. Physiol.*, **56**, 193-212.

Levitan E.S., Schofield P.R., Burt D.R., Rhee L.M., Wisden W., Kohler M., Fujita N., Rodriguez H.F., Stephenson A., Darlison M.G., Barnard E.A. and Seeburg P.H. (1988) Structural and functional basis for GABA$_A$ receptor heterogeneity. *Nature*, **335**, 76-79.

Li L. and McNamee M.G. (1992) Modulation of nicotinic acetylcholine receptor channel by pH: a difference in pH sensitivity of *Torpedo* and mouse receptors expressed in *Xenopus* oocytes. *Cell. Mol. Neurobiol.*, **12**, 83-93.

Linden D.J. and Routtenberg A. (1989) The role of protein kinase C in long-term potentiation: a testable model. *Brain Res. Rev.*, **14**, 279-296.

Lolait S.J., O'Carroll A.-M., Kusano K., Muller J.-M., Brownstein M.J. and Mahan L.C. (1989a) Cloning and expression of a novel rat $GABA_A$ receptor. *FEBS Letts.*, **246**, 145-148.

Luddens H., Pritchett D. B., Kohler M., Killisch I., Keinanen K., Monyer H., Sprengel R., and Seeburg P. H. (1990) Cerebellar $GABA_A$ receptor selective for a behavioral alcohol antagonist. *Nature*, **346**, 648-651.

MacDonald B.J. and Moss S.J. (1994) Differential phosphorylation of intracellular domains of γ-aminobutyric acid type A receptor subunits by calcium/calmodulin type 2-dependent protein kinase and cGMP-dependent protein kinase. *J. Biol. Chem.*, **269**, 18111-18117.

Mahler H.R. and Cordes E.H. (1971) *Biological chemistry* (2^{nd} edn), pp 44, Harper & Row, New York.

Malherbe P., Draguhn A., Multhaup G., Beyreuther K. and Mohler H. (1990a) $GABA_A$-receptor expressed from rat brain α- and β-subunit cDNAs displays potentiation by benzodiazepine receptor ligands. *Mol. Brain Res.*, **8**, 199-208.

Malherbe P., Sigel E., Baur R., Persohn E., Richards J.G. and Mohler H. (1990b) Functional characteristics and sites of gene expression of the α1,β1,γ2-isoform of the rat $GABA_A$ receptor. *J. Neurosci.*, **10**, 2330-2337.

Malherbe P., Sigel E., Baur R., Persohn E., Richards J.G. and Mohler H. (1990c) Functional expression and sites of gene expression of a novel α subunit of the rat $GABA_A$ receptor in rat brain. *FEBS Letts.*, **260**, 261-265.

Mertens S., Benke D. and Mohler H. (1993) $GABA_A$ receptor populations with novel subunit combinations and drug binding profiles identified in brain by α5- and δ-subunit-specific immunopurification. *J. Biol. Chem.*, **268**, 5965-5973.

Mertz J.E. and Gurdon J.B. (1977) Purified DNAs are transcribed after microinjection into *Xenopus* oocytes. *Proc. Natl. Acad. Sci. USA*, **74**, 1502-1506.

Miledi R., Parker I., and Sumikawa K. (1982) Synthesis of chick brain GABA receptors by frog oocytes. *Proc. Roy. Soc. Lond. B*, **216**, 509-515.

Mohler H., Battersby M.K. and Richards J.G. (1980) Benzodiazepine receptor protein identified and visualised in brain tissue by a photoaffinity label. *Proc. Natl. Acad. Sci. USA*, **77**, 1666-1670.

Moran, O. and Dascal, N. (1989) Protein kinase C modulates neurotransmitter responses in *Xenopus* oocytes injected with rat brain mRNA. *Mol. Brain Res.*, **5**, 193-202.

Moss, S.J., Doherty, C.A. and Huganir, R.L. (1992a) Identification of the cAMP-dependent protein kinase and protein kinase C phosphorylation sites within the major intracellular domains of the β1, γ2S, and γ2L subunits of the γ-aminobutyric acid type A receptor. *J. Biol. Chem.*, **267**, 14470-14476.

Moss, S.J., Smart, T.G., Blackstone, C.D. and Huganir, R.L. (1992b) Functional modulation of $GABA_A$ receptors by cAMP-dependent protein phosphorylation. *Science,* **257**, 661-665.

Moss, S.J., Smart, T.G., Porter N.M., Nayeem N., Devine J., Stephenson F.A., Macdonald R.L. and Barnard E.A. (1990) Cloned GABA receptors are maintained in a stable cell line: allosteric and channel properties. *Eur. J. Pharmacol.*, **189**, 77-88.

Mutch W.A.C. and Hansen A.J. (1984) Extracellular pH changes during spreading depression and cerebral ischemia: mechanisms of brain pH regulation. *J. Cerebral Blood Flow and Metabolism*, **4**, 17-27.

Nayeem N., Green T.P., Martin I.L. and Barnard E.A. (1994) Quaternary structure of the native $GABA_A$ receptor determined by electron microscopic image analysis. *J. Neurochem.*, **62**, 815-818.

Nicholson C. (1979) Brain-cell microenvironment as a communication channel, in *The neurosciences fourth study program.,* (Schmitt F.O. and Warden F.G. eds), pp 457-476, Cambridge, Mass.

Nishizuka Y. (1988) The molecular heterogeneity of protein kinase C and its implications for cellular regulation. *Nature*, **334**, 661-665.

Nishizuka Y. (1992) Intracellular signalling by hydrolysis of phospholipids and activation of protein kinase C. *Science*, **258**, 607-614.

Nistri A. and Sivilotti L. (1985) An unusual effect of γ-aminobutyric acid on synaptic transmission of frog tectal neurons *in vitro*. *Br. J. Pharmacol.*, **85**, 917-921.

Olsen R.W. (1982) Drug interactions at the GABA receptor-ionophore complex. Ann. Rev. Pharmacol. Toxicol., **22**, 245-277.

Olsen R.W. and Tobin A.J. (1990) Molecular biology of the $GABA_A$ receptor. *FASEB J.*, **4**, 1469-1480.

Olsen R.W. and Venter J.C., eds (1986) *Benzodiazepine / GABA receptors and chloride channels. Receptor biochemistry and methodology* (Olsen R.W. and Venter J.C., eds), **5**, Alan R. Liss, New York.

Parker I., Gundersen C.B. and Miledi R. (1986) Actions of pentobarbital on rat brain receptors expressed in *Xenopus* oocytes. *J. Neurochem.*, **6**, 2290-2297.

Pasternack M., Bountra C., Voipio J. and Kaila K. (1992) Influence of extracellular and intracellular pH on GABA-gated chloride conductance in crayfish muscle fibres. *Neuroscience.*, **47**, 921-929.

Pickles H.G. and Simmonds M.A. (1980) Antagonism by penicillin of γ-aminobutyric acid depolarizations at presynaptic sites in rat olfactory cortex and cuneate nucleus *in vitro*. *Neuropharmacol.*, **19**, 35-38.

Polenzani L., Woodward R.M. and Miledi R. (1991) Expression of mammalian γ-aminobutyric acid receptors with distinct pharmacology in *Xenopus* oocytes. *Proc. Natl. Acad. Sci. USA*, **88**, 4318-4322.

Porter, N.M., Twyman, R.E., Uhler, M.D. and Macdonald, R.L. (1990) Cyclic AMP-dependent protein kinase decreases $GABA_A$ receptor current in mouse spinal neurons. *Neuron,* **5**, 789-796.

Poulter M.O., Barker J.L., O'Carroll A.-M., Lolait S.J. and Mahan L.C. (1993). Co-existent expression of $GABA_A$ receptor β2, β3 and γ2 subunit messenger RNAs during embryogenesis and early postnatal development of the rat central nervous system. *Neuroscience*, **53**, 1019-1033.

Prince R.J. and Simmonds M.A. (1992) Propofol potentiates the binding of [^{3}H]flunitrazepam to the $GABA_A$ receptor complex. *Brain Res.*, **596**, 238-242.

Pritchett D.B. and Seeburg P.H. (1990) γ-aminobutyric $acid_A$ receptor α5-subunit creates novel type II benzodiazepine receptor pharmacology. *J. Neurochem.*, **54**, 1802-1804.

Pritchett D.B., Sontheimer H., Gorman C.M., Kettenmann H., Seeburg P.H. and Schofield P.R. (1988) Transient expression shows ligand gating and allosteric potentiation of $GABA_A$ receptor subunits. *Science*, **242**, 1306-1308.

Pritchett, D.B., Sontheimer, H., Shivers, B.D., Ymer, S., Kettenmann, H., Schofield, P.R. and Seeburg, P.H. (1989) Importance of a novel $GABA_A$ receptor subunit for benzodiazepine pharmacology. *Nature*, **338**, 582-585.

Rapallino M.V., Cupello A. and Hyden H. (1993) The increase in Cl^- permeation across the Dieters' neuron membrane by GABA on its cytoplasmic side is abolished by protein kinase C (PKC) activators. *Cell. Mol. Neurobiol.*, **13**, 547-558.

Raymond, L.A., Blackstone, C.D. and Huganir, R.L. (1993) Phosphorylation of amino acid neurotransmitter receptors in synaptic plasticity. *Trends in Neurosci.*, **16**, 147-153.

Rungger D. and Turler H. (1978) DNAs of simian virus 40 and polyoma direct the synthesis of viral tumor antigens and capsid proteins in *Xenopus* oocytes. *Proc. Natl. Acad. Sci. USA,* **75**, 6073-6077.

Sahara S., Sato K.-I., Aoto M., Ohnishi T., Kaise H., Koide H., Ogita K and Fukami Y. (1992) Characterization of protein kinase C in *Xenopus* oocytes. *Biochem. Biophys. Res. Comm.*, **182**, 105-114.

Sasaki S., Ishibashi K., Nagai T. and Marumo F. (1992) Regulation mechanisms of intracellular pH of *Xenopus laevis* oocyte. *Biochim. et Biophys. Acta.*, **1137**, 45-51.

Schmeiden V., Kuhse J. and Betz H. (1993) Mutation of glycine receptor subunit creates β-alanine receptor responsive to GABA. *Science*, **262**, 256-258.

Schoch P., Richards J.G., Haring P., Takacs B., Stahli C., Staehelin T., Haefely W. and Mohler H. (1985) Co-localization of $GABA_A$ receptors and benzodiazepine receptors in the brain shown by monoclonal antibodies. *Nature*, **314**, 168-171.

Schofield, P.R. (1989) The $GABA_A$ receptor: molecular biology reveals a complex picture. *Trends. Pharmacol. Sci.*, **10**, 476-478.

Schofield, P.R., Darlison, M.G., Fujita, N., Burt, D.R., Stephenson, F.A., Rodriguez, H., Rhee, L.M., Ramachandran, J., Reale, V., Glencorse, T.A., Seeburg, P.H. and Barnard, E.A. (1987) Sequence and functional expression of the $GABA_A$ receptor shows a ligand-gated receptor super-family. *Nature,* **328**, 221-227.

Schofield, P.R., Pritchett D.B., Sontheimer H., Kettenmann H. and Seeburg P.H. (1989) Sequence and expression of human $GABA_A$ α1 and β1 subunits. *FEBS Letts.*, **244**, 361-364.

Sequier J.M., Richards J.G., Malherbe P., Price G.W., Mathews S. and Mohler H. (1988) Mapping of brain areas containing RNA homologous to cDNAs encoding the alpha and beta subunits of the rat $GABA_A$ γ-aminobutyrate receptor. *Proc. Natl. Acad. Sci. USA*, **85**, 7815-7819.

Shingai R., Sutherland M.L. and Barnard E.A. (1991) Effects of subunit types of the cloned $GABA_A$ receptor on the response to a neurosteroid. *Eur. J. Pharmacol.*, **206**, 77-80.

Shivers B.D., Killisch I., Sprengel R., Sontheimer H., Kohler M., Schofield P.R. and Seeburg P.H. (1989) Two novel $GABA_A$ receptor subunits exist in distinct neuronal subpopulations. *Neuron*, **3**, 327-337.

Siegel R.E. (1988) The mRNA encoding GABA-A/benzodiazepine receptor subunits are localised in different cell populations of the bovine cerebellum. *Neuron.*, **1**, 579-584.

Sieghart W. (1989) Multiplicity of $GABA_A$-benzodiazepine receptors. *Trend Pharmacol. Sci.*, **10**, 407-411.

Sieghart W. and Karobath M. (1980) Molecular heterogeneity of benzodiazepine receptors. *Nature*, **286**, 285-287.

Siesjo B.K. (1985) Acid-base homeostasis in the brain: physiology, chemistry, and neurochemical pathology. *Prog. Brain Res.*, **63**, 121-154.

Sigel E. (1990) Use of *Xenopus* oocytes for the functional expression of plasma membrane proteins. *J. Membrane Biol.*, **117**, 201-221.

Sigel E. and Barnard E.A. (1984) A γ-aminobutyric acid/benzodiazepine receptor complex from bovine cerebral cortex: improved purification with preservation of regulatory sites and their interactions. *J. Biol. Chem.*, **259**, 7219-7223.

Sigel, E. and Baur, R. (1988) Activation of protein kinase C differentially modulates neuronal Na^+, Ca^{2+}, and γ-aminobutyrate type A channels. *Proc. Natl. Acad. Sci. USA.*, **85**, 6192-6196.

Sigel E., Baur R., Kellenberger S. and Malherbe P. (1992) Point mutations affecting antagonist affinity and agonist dependent gating of $GABA_A$ receptor channels. *EMBO J.*, **11**, 2017-2023.

Sigel, E., Baur, R. and Malherbe, P. (1991) Activation of protein kinase C results in down-modulation of different recombinant $GABA_A$-channels. *FEBS Letts.*, **291**, 150-152.

Sigel, E., Baur, R. and Malherbe, P. (1993) Recombinant $GABA_A$ receptor function and ethanol. *FEBS Letts.*, **324**, 140-142.

Sigel E., Baur R., Malherbe P. and Mohler H. (1989) The rat β_1-subunit of the $GABA_A$ receptor forms a picrotoxin-sensitive anion channel open in the absence of GABA. *FEBS Letts.*, **257**, 377-379.

Sigel E., Baur R., Trude G., Mohler H. and Malherbe P. (1990) The effect of subunit composition of rat brain $GABA_A$ receptors on channel function. *Neuron.*, **5**, 703-711.

Sigel E., Stephenson F.A., Mamalaki C. and Barnard E.A. (1983) A γ-aminobutyric acid/benzodiazepine receptor complex of bovine cerebral cortex: purification and partial characterization. *J. Biol. Chem.*, **258**, 6965-6971.

Simmonds M.A. (1982) Classification of some GABA antagonists with regard to site of action and potency in slices of rat cuneate nucleus. *Eur. J. Pharmacol.*, **80**, 347-358.

Sivilotti L. and Nistri A. (1991) GABA receptor mechanisms in the central nervous system. *Prog. Neurobiol.*, **36**, 35-92.

Smart T.G. (1990) Uncultured lobster muscle, cultured neurones and brain slices: the neurophysiology of zinc. *J. Pharm. Pharmacol.*, **42**,377-387.

Smart T.G. (1992) A novel modulatory binding site for zinc on the $GABA_A$ receptor complex in cultured rat neurones. *J. Physiol.*, **447**, 587-625.

Smart T.G. and Constanti A. (1982) A novel effect of zinc on the lobster muscle GABA receptor. *Proc. R. Soc. Lond. B*, **215**, 327-341.

Smart, T.G. and Constanti, A. (1986) Studies on the mechanism of action of picrotoxinin and other convulsants at the crustacean muscle GABA receptor. *Proc. Roy. Soc. Lond. B,* **227**, 191-216.

Smart T.G. and Constanti A. (1990) Differential effect of zinc on the vertebrate $GABA_A$-receptor complex. *Br. J. Pharmacol.*, **199**, 643-654.

Smart T.G., Constanti A., Bilbe G., Brown D.A., and Barnard E.A. (1983) Synthesis of functional chick brain GABA-benzodiazepine-barbiturate/receptor complexes in mRNA-injected *Xenopus* oocytes. *Neurosci. Lett.*, **40**, 55-59.

Smart T.G., Houamed M.K., Van Renterghem C. and Constanti A. (1987) mRNA-directed synthesis and insertion of functional amino acid receptors in *Xenopus laevis* oocytes. *Biochem. Soc. Trans.*, **15**, 117-122.

Smart T.G. and Krishek B.J. (1994) *Xenopus* oocyte microinjection and ion channel expression in *Neuromethods, Patch Clamp Techniques and Protocols*, (Boulton A.A., Baker G.B. and Walz W. eds), (In Press) Humana Press, New Jersey.

Smart T.G., Moss S.J., Xie X. and Huganir R.L. (1991) $GABA_A$ receptors are differentially sensitive to zinc: dependence on subunit composition. *Br. J. Pharmacol.*, **103**, 1837-1839.

Smith S.M., Zorec R. and Mcburney (1989) Conductance states activated by glycine and GABA in rat cultured spinal neurones. *J. Membr. Biol.*, **180**, 45-52.

Snutch T.P. (1988) The use of *Xenopus* oocytes to probe synaptic communication. *Trends in Neurosci.*, **11**, 250-256.

Soreq H. (1985) The biosynthesis of biologically active proteins in mRNA-microinjected *Xenopus* oocytes. *CRC Crit. Rev. in Biochem.*, **18**, 199-238.

Squires R.F., Benson D.I., Braestrup C., Coupet J., Klepner C.A., Myers V. and Beer B. (1979) Some properties of brain specific benzodiazepine receptors: new evidence for multiple receptors. *Pharmacol. Biochem. Behav.*, **10**, 825-830.

Stelzer, A. (1992) Intracellular regulation of $GABA_A$-receptor function, in *Ion Channels* vol. **3**. (T. Narahashi, ed.), Plenum Press, New York, pp. 83-136.

Stelzer, A., Kay, A.R. and Wong, R.K.S. (1988) $GABA_A$-receptor function in hippocampal cells is maintained by phosphorylation factors. *Science.*, **241**, 339-341.

Stelzer, A., Simon G., Kovacs G. and Rai R. (1994) Synaptic disinhibition during maintenance of long-term potentiation in the CA1 hippocampal subfield. *Proc. Natl. Acad. Sci. USA*, **91**, 3058-3062.

Stryer L. (1988) Protein structure and function in *Biochemistry* (third edition), pp 21, W.H.Freeman and company, New York.

Sumikawa K., Houghton M., Emtage J.S., Richards B.M., and Barnard E.A. (1981) Active multisubunit ACh receptor assembled by translation of heterologous mRNA in *Xenopus* oocytes. *Nature* (Lond.), **292**, 862-864.

Sumikawa K., Parker I., and Miledi R. (1986) *Xenopus* oocytes as a tool for molecular cloning of the genes coding for neurotransmitter receptors and voltage-operated channels. *Fortschritte der Zoologie*, Band 33: Membrane control, pp. 127-139, Gustav Fischer Verlag, Stuttgart.

Sumikawa K., Parker I. and Miledi R. (1988) Effect of tunicamycin on the expression of functional brain neurotransmitter receptors and voltage-operated channels in *Xenopus* oocytes. *Mol. Brain. Res.*, **4**, 191-199.

Sun M.-K. and Reis D.J. (1993) Extracellular H^+ iontophoresis modifies responses to γ-aminobutyric acid and cyanide of reticulospinal vasomotor neurons in rats. *Eur. J. Pharmacol.*, **236**, 305-313.

Sweetnam, P.M., Lloyd, J., Gallombardo, P., Madison, R.T., Gallagher, D.W., Tallman, J.F. and Nestler, E.J. (1988) Phosphorylation of the $GABA_A$/benzodiazepine receptor α subunit by a receptor associated protein kinase. *J. Neurochem.*, **51**, 1274-1284.

Swope, S.L., Moss, S.J., Blackstone, C.D. and Huganir, R.L. (1992) Phosphorylation of ligand-gated ion channels: a possible mode of synaptic plasticity. *FASEB J.*, **6**, 2514-2523.

Sykova E. (1983) Extracellular K^+ accumulation in the central nervous system. *Prog. Biophy. Mol. Biol.*, **42**, 135-189.

Takadera T., Shimada Y. and Mohri T. (1992) Extracellular pH modulates N-methyl-D-aspartate receptor-mediated neurotoxicity and calcium accumulation in rat cortical cultures. *Brain Res.*, **572**, 126-131.

Takeuchi A. and Takeuchi N. (1967) Anion permeability of the inhibitory postsynaptic membrane of the crayfish neuromuscular junction. *J. Physiol., Lond.*, **191**, 575-590.

Taleb O. and Betz H. (1994) Expression of the human glycine receptor α1 subunit in *Xenopus* oocytes: apparent affinities of agonists increase at high receptor density. *EMBO J.*, **13**, 1318-1324.

Tang C.-M., Dichter M. and Morad M. (1990) Modulation of N-methyl-D-aspartate channels by extracellular H^+. *Proc. Natl. Acad. Sci. USA*, **87**, 6445-6559.

Ticku, M.K. and Mehta, A.K. (1990) γ-aminobutyric $acid_A$ receptor desensitization in mice spinal cord cultured neurones: Lack of involvement of protein kinases A and C. *Mol. Pharmac.*, **38**, 719-724.

Tombaugh G.C. and Sapolsky R.M. (1990) Mild acidosis protects neurones from injury induced by oxygen and glucose deprivation. *Brain Res.*, **506**, 343-345.

Toyoshima C. and Unwin N. (1990) Three-dimensional structure of the acetylcholine receptor by cryoelectron microscopy and helical image reconstruction. *J. Cell Biol.*, **111**, 2623-2635.

Traynelis S.F. and Cull-Candy S.G. (1990) Proton inhibition of N-methyl-D-aspartate receptors in cerebellar neurones. *Nature*, **345**, 347-350.

Traynelis S.F. and Cull-Candy S.G. (1991). Pharmacological properties and sensitivity of excitatory amino acid receptor channels in rat cerebellar granule neurones. *J. Physiol.*, **433**, 727-763.

Twyman R.E., Green R.M. and Macdonald R.L. (1992) Kinetics of open channel block by penicillin of single $GABA_A$ receptor channels from mouse spinal cord neurones in culture. *J. Physiol.*, **445**, 97-127.

Vaello M.-L., Ruiz-Gomez A., Lerma J and Mayor Jn. F. (1994) Modulation of inhibitory glycine receptors by phosphorylation by protein kinase C and cAMP-dependent protein kinase. *J. Biol. Chem.*, **269**, 2002-2008.

Valerio A., Tinti C., Spano P. and Memo M. (1992) Rat pituitary cells selectively express mRNA encoding the short isoform of the γ2 $GABA_A$ receptor subunit. *Mol. Brain Res.*, **13**, 145-150.

Verdoorn T.A., Draguhn A., Ymer S., Seeburg P.H. and Sakmann B. (1990) Functional properties of recombinant rat $GABA_A$ receptors depend upon subunit composition. *Neuron.*, **4**, 919-928.

Verhoeff-de Fremery R. and Griffin J. (1987) Anurans (frogs and toads) in *The care and management of laboratory animals*, (Poole T. ed.), 6th. ed., pp.773-783.

Vyklicky L., Vlachova V. and Krusek J. (1990) The effect of external pH changes on responses to excitatory amino acids in mouse hippocampal neurones. *J. Physiol.*, **430**, 497-517.

Wafford, K.A., Burnett, D.M., Leidenheimer, N.J., Burt, D.R., Wang, J.B., Kofuji, P., Dunwiddie, T.V., Harris, R.A. and Sikela, J. (1991) Ethanol sensitivity of the $GABA_A$ receptor expressed in *Xenopus* oocytes requires 8 amino acids contained in the γ2L subunit. *Neuron,* **7**, 27-33.

Wafford, K.A. and Whiting, P.J. (1992) Ethanol potentiation of $GABA_A$ receptors requires phosphorylation of the alternatively spliced variant of the γ2 subunit. *FEBS Letts.*, **313**, 113-117.

Wafford K.A., Whiting P.J. and Kemp J.A. (1992) Differences in affinity and efficacy of benzodiazepine receptor ligands at recombinant γ-aminobutyric acid receptor subtypes. *Mol. Pharmacol.*, **43**, 240-244.

Wang J.B., Kofuji P. and Burt D.R. (1992a) Strain comparisons and developmental profile of the delta subunit of the murine $GABA_A$ receptor. *Brain Res. Bulletin*, **29**, 119-123.

Wang J.B., Kofuji P., Fernando J.C., Moss S.J., Huganir R.L. and Burt D.R. (1992b) The alpha 1, alpha 2, and alpha 3 subunits of $GABA_A$ receptors: comparison in seizure-prone and -resistant mice during development. *J. Mol. Neurosci.*, **3**, 177-184.

Westbrook G.L. and Mayer M.L. (1987) Micromolar concentrations of Zn^{2+} antagonise NMDA and GABA responses of hippocampal neurones. *Nature*, **328**, 640-643.

Whiting, P., McKernan, R.M. and Iversen, L.L. (1990) Another mechanism for creating diversity in γ-aminobutyrate type A receptors: RNA splicing directs expression of two forms of γ2 subunit, one of which contains a protein kinase C phosphorylation site. *Proc. Natl. Acad. Sci. USA*, **87**, 9966-9970.

Wisden W., Herb A., Wieland H., Keinanen K., Luddens H. and Seeburg P.H. (1991) Cloning, pharmacological characteristics and expression pattern of the rat $GABA_A$ receptor α4 subunit. *FEBS Letts.*, **289**, 227-230.

Wisden W., Laurie D.J., Monyer H. and Seeburg P.H. (1992) The distribution of 13 $GABA_A$ receptor subunit mRNAs in the rat brain. I. Telencephalon, diencephalon, mesencephalon. *J. Neurosci.*, **12**, 1040-1062.

Wisden W., Morris B.J., Darlison M.G., Hunt S.P. and Barnard E.A. (1988) Distinct $GABA_A$ receptor α subunit mRNAs show differential patterns of expression in bovine brain. *Neuron*, **1**, 937-947.

Wisden W. and Seeburg P.H. (1992) $GABA_A$ receptor channels: from subunits to functional entities. *Current opinions in Neurobiol.*, **2**, 263-269.

Wilson-Shaw D., Robinson M., Gambarana C., Siegel R. E., and Sikela J. M. (1991) A novel γ subunit of the $GABA_A$ receptor identified using the polymerase chain reaction. *FEBS Letts.*, **284**, 211-215.

Woodward R.M. and Miledi R. (1992) Sensitivity of *Xenopus* oocytes to changes in extracellular pH: possible relevance to proposed expression of atypical mammalian $GABA_B$ receptors. *Mol. Brain Res.*, **16**, 204-210.

Yakushiji T., Tokutomi N., Akaike N. and Carpenter D.O. (1987) Antagonists of GABA responses, studied using internally perfused frog dorsal root ganglion neurones. *Neuroscience*, **22**, 1123-1133.

Ymer, S., Draguhn, A., Kohler, M., Schofield, P.R. and Seeburg, P.H. (1989a) Sequence and expression of a novel $GABA_A$ receptor α subunit. *FEBS Letts.*, **258**, 119-122.

Ymer S., Draguhn A., Wisden W., Werner P., Keinanen K., Schofield P.R., Sprengel R., Pritchett D.B. and Seeburg P.H. (1990) Structural and functional characterization of the γ1 subunit of the $GABA_A$/benzodiazepine receptors. *EMBO J.*, **9**, 3261-3267.

Ymer, S., Schofield, P.R., Draguhn, A., Werner, P., Kohler, M. and Seeburg, P.H. (1989b) $GABA_A$ receptor β subunit heterogeneity: functional expression of cloned cDNAs. *EMBO J.*, **8**, 1665-1670.

Zamin S.H., Shingai R., Harvey R.J., Darlison M.G. and Barnard E.A. (1992) Effects of subunit types of the recombinant $GABA_A$ receptor on the response to a neurosteroid. *Eur. J. Pharmacol.*, **225**, 321-330.